The role of diet and gut microbiota in lipid metabolism: Implications for health outcomes using a mouse model

by

Isaac Ampong

Submitted for the Degree of Doctor of Philosophy

(Biochemistry & Physiology)

School of Biosciences and Medicine
Faculty of Health and Medical Sciences
University of Surrey

Supervisors: Professor Helen Griffiths

Dr Jorge Gutierrez

Declaration

This thesis and the work to which it refers are the results of my own efforts. Any ideas, data, images or text resulting from the work of others (whether published or unpublished) are fully identified as such within the work and attributed to their originator in the text, bibliography or in footnotes. This thesis has not been submitted in whole or in part for any other academic degree or professional qualification. I agree that the University has the right to submit my work to the plagiarism detection service Turnitin UK for originality checks. Whether or not drafts have been so-assessed, the University reserves the right to require an electronic version of the final document (as submitted) for assessment as above.

Signature:

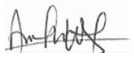

Date: 20/01/2020

Summary

The prevalence of non-Alcoholic Fatty Liver Disease (NAFLD) has now reached epidemic proportions, but the role of gene-lifestyle interactions in its pathogenesis remains poorly understood. While evidence for an inverse association between odd-chain length fatty acids (OCFA) and cardiometabolic diseases, suggests a possible link between OCFAs and NAFLD, little is known about the impact of diet, gut microbiota and peroxisomal biogenesis on the metabolism of OCFAs. We hypothesized that suboptimal diet, altered gut microbiota and peroxisomal biogenesis could promote the development of NAFLD by impairing the metabolism of OCFAs. This thesis aimed to understand the effect of dietary fat/protein on the genetic and metabolic regulation of lipids and OCFAs in relation to NAFLD, using a high fat diet (HFD) model, well established in the literature for inducing obesity and insulin resistance in mice within 4 weeks, and a low protein diet (LPD) model, known to promote NAFLD. Under specific pathogen free or normal husbandry conditions, a HFD reduced serum OCFA in mice after 4 and 12 weeks of feeding, and down-regulated the activity of several key enzymes in fatty acid metabolism (desaturases, lyase, elongase). Liver histology also showed deposition of lipid droplets and higher expression of peroxin 14 protein in HFD fed mice (Chapter 3). The characterisation of gut microbiota revealed an alteration in propionate-producing bacteria, Lachnospiraceae and Clostridiales, in HFD fed mice (Chapter 4). Mice fed with carbohydrate rich-LPD for 7 weeks resulted in lower levels of serum OCFA, increased CD36 mRNA and peroxin 14 expressions. However, OCFA did not change in the reduced and quality carbohydrate-LPD after 8 weeks (Chapter 5). In conclusion, these findings provide evidence that HFD and carbohydrate rich-LPD reduced OCFA via changes in gut microbiota and peroxisomal biogenesis in the liver and increases our understanding of how suboptimal diets contributes to NAFLD.

Key words: Protein malnutrition, High fat diet, Odd chain fatty acid, Lipid metabolism, Gut microbiota, NAFLD

Dedication

Dedicated to my lovely wife, Mrs Beatrice Ampong and son, Henry B. Ampong;

To my parents, Mr Robert K. Ampong and Mrs Hannah Kyerewaa; to my In-laws, Mr Kingsley Danso & Mrs Agartha Dadzie

& to my siblings:

Mercy Ampong

Lawrence Ampong

Florence Owusu

Rebecca Ampong

Simon Agyenim Boateng

Francis Owusu Ampong

John Ampong

Acknowledgements

I would like to express my heartfelt appreciation to Professor Helen Griffiths for the opportunity to pursue my PhD under her supervision and guidance. Due to her support in designing a research proposal, I was successfully awarded a commonwealth PhD scholarship for my PhD research. I am also grateful for her tremendous help, encouragement, patience and providing me the opportunity to collaborate extensively with researchers in UK and internationally.

I would like to thank my second supervisor, Dr Jorge Gutierrez, who supported me in diverse ways especially providing advice on microbiology component of the project and ordering of consumables.

Special thanks go to Dr Adam Watkins, who was my second supervisor when I started my PhD in Aston University. He provided the tissues for the low protein diet study, guided me on qPCR and donated analytical algorithm for gene expression analyses, showed me how to perform anatomical dissection and continued to provide advice upon my transfer to University of Surrey. Thank you, Adam. I am grateful to Dr Dan Gao for her collaboration in the high fat diet study and for her kind support when I worked with her during my visit to Xi'an Jiaotong University, China. Many thanks to Dr Barbara Fielding for the numerous advice and allowing me to use their GC-MS lab for my fatty acid study in Surrey. I would like to acknowledge Professor Clifford Bailey, who also provided me with advice and support during my first-year transfer report preparation. Thank you also to the VSM pathology team led by Katherine Walker who supported in the IHC staining and preparing the slides to enable me to carry out the microscopy work. I would like to thank the Novogene Company Ltd, Cambridge, UK for their services in microbial sequencing and bioinformatics. Also, thanks to Dr Augusto Coppi for advice on histology.

I would like to express my gratitude to all technical staff including Dr Nicola Jackson, Dr Fariba Shojaee-Moradie, Anuska Mann, John Elliot for their technical assistance and support. Special thanks also go to all former Lab 358 members in Aston University.

A big thank you to the Commonwealth Scholarships Commission, UK for providing financial support to enable me to study in the UK for my PhD degree.

Finally, I would like to thank my wife, my parents, my siblings and in-laws for being a source of motivation. They have shown love, support, encouragement and above all prayed for me over the years. Thanks to all friends and loved ones whom I have shared my research challenges and concerns.

Publications, Conferences and Awards

Publications

Ampong I, Watkins A, Gutierrez-Merino J, Ikwuobe J, Griffiths HR. Dietary protein insufficiency–an important consideration in fatty liver disease? British Journal of Nutrition. 2019 Nov 29:1-29.

Morgan HL, **Ampong I**, Eid N, Rouillon C, Griffiths HR, Watkins AJ. Low protein diet and methyl-donor supplements modify testicular physiology in mice. Reproduction. 2020 May 1;159(5):627-41.

Conferences/ presentations

Isaac Ampong, Adam Watkins, Helen R Griffiths, A comprehensive study of plasma and liver odd-chain saturated fatty acids by GC-MS in mice fed a low protein diet (Oral presentation) Presented on November 2019, The North America Metabolomics conference, Atlanta, USA

Isaac Ampong, Adam Watkins, Jorge Gutierrez-Merino, Helen R Griffiths, Methyl donor supplementation reverses the risk of diabetes induced by dietary low protein intake. (Poster) Presented at September 2018 The Europhysiology conference 2019, London

Isaac Ampong, Adam Watkins, Jorge Gutierrez-Merino, Helen Griffiths. Methyl donor supplementation reverses effects of a low protein diet on fatty acid metabolism in mice (oral presentation), Presented at Nutrition society Irish section 27th Annual postgraduate meeting, Belfast, Northern Ireland

Isaac Ampong. Attended but not presented January at annual Biochemistry society conference, Aston University, Birmingham, UK

Scholarships/Awards

Commonwealth PhD scholarship, Commonwealth Scholarships Commission, UK, 2016-2019

Travel grant award for scientific training in Belarus, 2018, European Society of Endocrinology

Travel grant award for Europhysiology conference, September 2018, Physiological Society, UK

Travel grant award for MANA conference, November 2019, The Physiology Society, UK

Travel grant award for MANA conference, November 2019, The Nutrition Society, UK

Abbreviations

ABC	Avidin-biotin peroxidase complex
Acadm	Acyl-CoA dehydrogenase
ACBP	Acyl-CoA-binding protein
ACC	Acetyl-CoA carboxylase
Acox	Acyl-coenzyme A oxidase
ALP	Alkaline phosphatase
ALT	Alanine aminotransferase
AST	Aspartate aminotransferase
ATF	Activating transcription factor
AXOS	Arabinoxylan oligo-saccharides
BAC	Blood alcohol concentration
BCAAs	B ranched-chain amino acids
BCFAs	Branched-chain fatty acids
BCKAs	Branched-chain alpha-keto acids
BCKDHA	Branched chain ketoacid dehydrogenase E1, alpha polypeptide
BMP	Binding mixture pellet
C16:0	Palmitic acid
C18:0	Stearic acid
CAT	Carnitine translocase
CAT	Catalase
CD	Control diet
CD36	Cluster of differentiation 36
CDD	Choline deficient diets
cDNA	complementary DNA
CH_2	Methylene
ChREBP	Carbohydrate regulatory element-binding protein
CPT1	Carnitine palmitoyltransferase 1
CPT2	Carnitine palmitoyltransferase 2
CV	Coefficient of variation

CV	Conventional
CVD	Cardiovascular disease
DHA	Docosahexaenoic acid
DNL	*de novo* lipogenesis
ECFA	Even-chain saturated fatty acid
Echs1	Enoyl-CoA hydratase 1
ELOVL6	Long chain fatty acid elongase 6
EPA	Eicosapentaenoic acid
ER	Endoplasmic reticulum
FA	Fatty acids
FABP1	Fatty acid binding protein 1
FACS	Fatty acyl-CoA synthase
FADS2	Fatty acid desaturase 2
FAMEs	Fatty acid methyl esters
FASN	Fatty acid synthase
FAT	Fatty acid translocase
FATP	Fatty acid transporter proteins
FFA	Free fatty acids
FFAR	Fatty Acid Receptors
GC	Gas Chromatography
GF	Germ free
GGT	Gamma-glutamyl transferase
GPAT	Glycerol-3-phosphate acyltransferase
GPx	Glutathione peroxidase
GSR	Glutathione reductase
GSSG	Glutathione disulfide
H&E	Haematoxylin and eosin
HA	Heptadecanoic acid
HACL1	Hydroxyacyl-CoA lyase 1
Hadh	Hydroxyacyl-coenzyme A dehydrogenase

HCC	Hepatocellular carcinoma
HF-C	Coconut oil based high fat diet
HFD	High fat diet
HF-F	Fish oil-based high fat diet
HF-L	Lard based-high fat diet
IGN	Intestinal gluconeogenesis
IHC	Immunohistochemistry
IHTG	Intrahepatic triglyceride
IL	Interleukin (IL)
IR	Insulin receptor
LC	Liquid chromatography
LC-PUFA	Long-chain polyunsaturated fatty acids
LDA	Linear discrimination analysis
LHFD	Lard based-high fat diet
LPD	Low protein diet
LXRα	Liver X receptor α
MCDD	Methionine and choline deficient dietary
MCP-1	Monocyte chemoattractant protein-1
MD-LPD	LPD supplemented with methyl donors
MetS	Metabolic syndrome
MLYCD	Malonyl-CoA decarboxylase
mRNA	messenger RNA
MTTP	Microsomal triglyceride transfer protein
MUFA	Monounsaturated fatty acid
NAFL	Non-alcoholic fatty liver
NAFLD	Non-alcoholic fatty liver disease
NASH	N on-alcoholic steatohepatitis
NF-Kb	Nuclear factor kappa
NGS	Next-generation sequencing
NHC	Normal husbandry condition

OCFA	Odd chain fatty acids
OTU	Operational taxonomic unit
OXPHOS	Oxidative phosphorylation
PA	Peak areas
PCCA	Propionyl-CoA carboxylase
PCM	Protein-calorie malnutrition
PCoA	Principal coordinate analyses
PCR	Polymerase chain reaction
PGK1	Phosphoglycerate kinase *1*
PGs	Prostaglandins
PI3K	Phosphoinositide 3-kinase
PK	Proteinase kinase
PMP70	Peroxisomal membrane protein 70
Pnpla2	Patatin-like phospholipase domain containing 2
PUFAs	Polyunsaturated fatty acids
RNA	Ribonucleic acid
ROS	Reactive oxygen species (ROS)
RT	Retention time
RTqPCR	Real time quantitative PCR
SAM	S-adenosyl methionine
SC	Standard rodent chow
SCFA	Short-chain fatty acid
SCOT	Support-coated open tubular
SFAs	Saturated fatty acids
SPF	Specific pathogen free
SREBP1c	Sterol regulatory element-binding protein 1c
TBP	*TATA-box binding protein*
TEC	Total energy consumption
TNF	Tumour necrosis factor
TBS	Tris-Buffered Saline

TRX	Thioredoxin
WAT	White adipose tissue
WCOT	Wall-coated open tubular

Contents page

List of tables

List of figures

Chapter 1

1 Introduction

1.1 Non-alcoholic fatty liver disease

1.1.1 Clinical features

Non-alcoholic fatty liver disease (NAFLD) is a condition characterized by excessive fat build-up in the liver with insulin resistance due to causes other than alcohol use, Ipsen et al (2018). NAFLD is classified into a broad clinical spectrum ranging from non-alcoholic fatty liver to non-alcoholic steatohepatitis (NASH), advanced fibrosis, cirrhosis, and hepatocellular carcinoma (HCC), Perumpail et al (2017). NAFLD is commonly associated with metabolic comorbidities, including obesity, type II diabetes, dyslipidaemia, and metabolic syndrome, Paschos & Paletas (2009). It has been reported that >90% of obese, 60% of diabetic and up to 20% normal-weight people develop the condition, Younossi (2018). NAFLD is diagnosed by elevated levels of serum alanine aminotransferase (ALT), aspartate aminotransferase (AST), alkaline phosphatase (ALP) with ALT/AST ratio >1. Apart from biochemical test, NAFLD can be diagnosed by ultrasound or magnetic resonance imaging and magnetic resonance elastography of the liver as well as invasive liver biopsy, Sattar et al (2014).

Global prevalence is estimated to 25.25%, Araújo et al (2018). Whilst NAFLD has become a global health concern, the incidence of this metabolic disorder is becoming more challenging in developing countries particularly in the Middle East where the prevalence rate is reported to be highest followed by South America and Africa, respectively, Younossi et al (2016). The risk factors of NAFLD include overweight or obesity, insulin resistance, dyslipidemia, type 2 diabetes and having one or more traits of metabolic syndrome (MetS), Salt (2004); Anstee et al (2013). Studies have reported that excessive consumption of carbohydrates, particularly refined carbohydrates, fats, saturated fats and protein from meat are associated with NAFLD as well as higher intakes of soft drinks, Mirmiran et al (2017). An association between dysbiosis of the gut microbiota and liver diseases, particularly NAFLD has been reported, Sharpton et al

(2019). Treatment guidelines for NAFLD are mainly based on lifestyle changes and dietary modifications, Nseir et al (2014).

1.1.2 NAFLD subtypes

Generally, there are two subtypes of NAFLD: non-alcoholic fatty liver (NAFL) and non-alcoholic steatohepatitis (NASH). NASH is distinguished from steatosis by the presence of inflammation and hepatocyte injury, Lindenmeyer & McCullough (2017). A recent study has reported that about 25% of individuals with NAFL progress to NASH and out of those patients who develop NASH, 25% progress to cirrhosis, of whom at least 1%-2% per year develop hepatocellular carcinoma (HCC), Mato et al (2019). It is clinically important to differentiate patients with the NASH subtype, as most NAFLD patients have steatosis without necroinflammation or fibrosis and do not require medical therapy, Lindenmeyer & McCullough (2017).

1.1.3 Genetic causes of NAFLD

Apart from environmental factors that cause NAFLD, previous studies have identified a link between genetic changes with the pathogenesis of NAFLD and NASH. For instance, variation in the PNPLA3 and TM6SF2 genes have been shown to correlate with NAFLD presence and severity, Wong et al (2018). Studies indicate that the activity (expression) of the PNPLA3 gene decreases during fasting and increases postprandially, suggesting that the amount of adiponutrin protein produced is regulated as needed to help process and store dietary fats, Bruschi et al (2017).

1.2 Nutrient metabolism in metabolic organs

After digestion of macronutrients including carbohydrate, proteins and fats, the end products of digestion including glucose, amino acids, free fatty acids (FFA), TG and monoacylglycerols are released and metabolised or stored in the muscle, adipose tissue and liver according to energy needs. These organs work together to maintain glucose and lipid homeostasis.

Muscle

The muscle utilizes glucose, fatty acids, and ketone bodies as its major fuel. Muscle has a large store of glycogen which is readily converted into glucose 6-phosphate for use within muscle cells. However, in the resting state, fatty acids are the major source of fuel, forming 85% of its energy demands. Fatty acids are also the major source of energy for heart muscle, in addition to ketone bodies and lactate.

Adipose tissue

The adipose tissues are traditionally known to be the major sites for storage of surplus energy. When fuels are abundant, the adipose tissue receives triglyceride (TG) from chylomicrons-TG released from the intestinal mucosa cells or very-low density lipoprotein-TG (VLDL-TG) from the liver released into circulation. TGs cannot be taken directly by adipocytes but are first hydrolysed by an extracellular lipoprotein lipase for uptake. The lipase is stimulated by processes initiated by insulin. Upon entry of fatty acids into the cell, the adipose cells activate these FFAs into acyl-CoA before they are shuttled via acyl-CoA-binding protein (ACBP) to mitochondria or peroxisomes for β-oxidation (and formation of energy as ATP and heat) or to endoplasmic reticulum for esterification to different classes of lipid. The resulting CoA derivatives is transferd glycerol in the form of glycerol 3-phosphate via glycerophosphate acyltransferase. This essential intermediate in lipid biosynthesis originates from the reduction of the glycolytic intermediate dihydroxyacetone phosphate. Hence, adipose cells require

glucose for the synthesis of TG. TG in adipose cells are hydrolysed by intracellular lipase particularly when food is scarce, or energy expenditure requirements increase. The triglycerides are hydrolysed into glycerol and fatty acids within adipocytes before being transported in the blood to the liver and muscle where they are used in fatty acid oxidation, Sethi & Vidal-Puig (2007).

Liver

The liver plays an important role in metabolism of glucose and lipids, hence is essential for providing fuel to the brain, muscle, and other peripheral organs. The liver is involved in production of glucose by breaking down glycogen and by carrying out gluconeogenesis. In gluconeogenesis, the main precursors are lactate and alanine obtained from muscle, glycerol from adipose tissue and glucogenic amino acids (e.g. methionine) derived from diet. In humans, the liver is the major site of fatty acid synthesis. The process of fatty acid regulation by the liver involves the digestion of dietary lipids to release free fatty acids (FFA) and monoacylglycerols after absorption into the small intestine. In the intestinal mucosa cells, FFA are re-esterified to TG, before being transported via lymphatic vessels into the circulatory system as part of chylomicrons. In the circulation, fatty acids are transported bound to albumin or as part of lipoproteins. FFA are taken up into hepatocytes mainly by protein transporters in the plasma membrane and are transported intracellularly via fatty acid-binding proteins (FABP). FFA are subsequently activated (acyl-CoA) before they are shuttled via acyl-CoA-binding protein (ACBP) to mitochondria or peroxisomes for β-oxidation (and formation of energy as ATP and heat) or to endoplasmic reticulum for esterification to different classes of lipid, Hellerstein (1999). Glucose may be converted to fatty acids (lipogenesis) if there is an extra of glucose/energy in the cells, Rustan, & Drevon (2005). The pathway of lipid metabolism in muscle, adipose tissue and liver following dietary intake is summarised in figure 1.1.

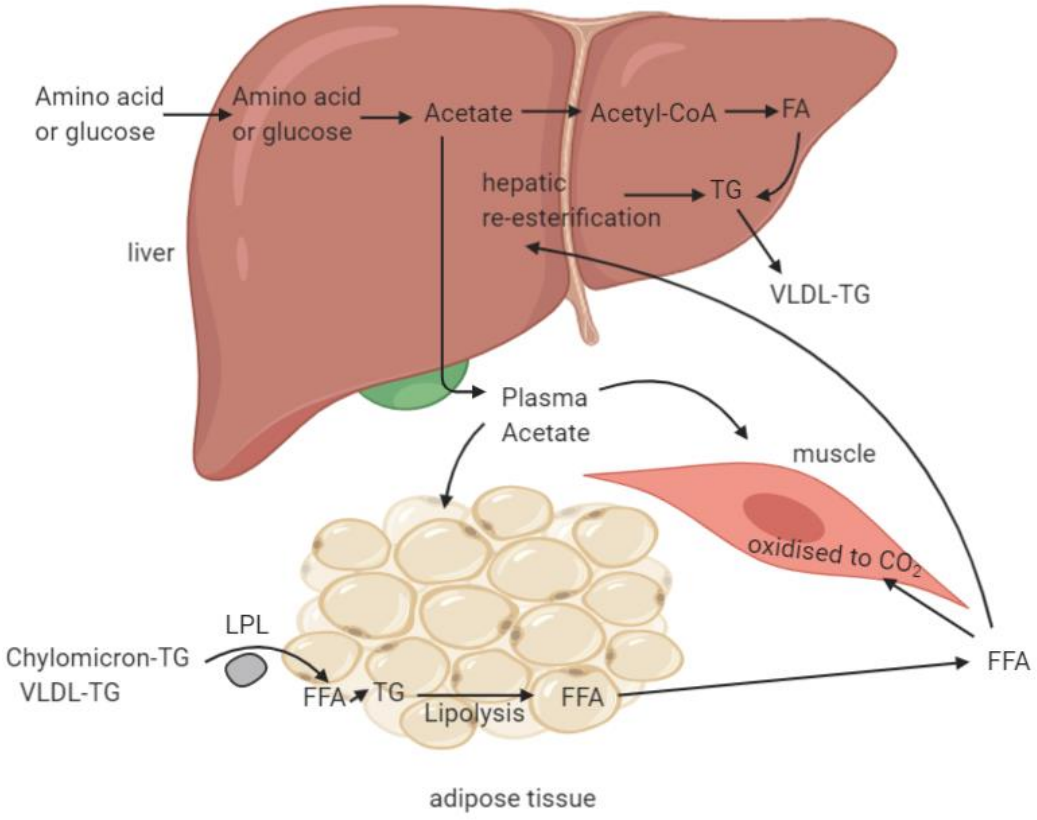

Figure 1.1: Metabolic pathways of lipid metabolism in response to consumption of carbohydrate or protein (Diagram adapted from Hellerstein (1999)).

Abbreviations: TG, triglyceride: FFA, free fatty acid: LPL, Lipoprotein lipase: VLDL, very low-density lipoprotein: CO_2, carbon dioxide

1.3 The role of fatty acids in NAFLD

1.3.1 Lipids

Lipids comprise a large group of chemically heterogeneous compounds, De Carvalho & Caramujo (2018). Lipids are grouped on the basis of their solubility in organic solvents; each has contrasting functional roles. Fatty acids are the "building blocks" of lipids, as they are components of many complex classes called complex lipids. These include acyl glycerols (glycerides) and sphingolipids in which the fatty acids have been esterified into alcohol or amino groups, respectively. Simple lipids that do not contain fatty acids comprise a much smaller group, with cholesterol and other sterols being the major representatives. Lipids can also be classified into two groups based on polarity: polar lipids such as phospholipids play a

major structural role and neutral lipids are mainly responsible for storage of energy in the form of TGs and other storage components including sterol esters, Fahy et al (2011).

1.3.2 Fatty acids

Fatty acids (FAs) are important fraction of lipids and may either circulate in blood or constitute a basic structural component of a more complex lipids. They are incorporated into phospholipids and glycolipids of biological membranes and form triglyceride, Mika et al (2016). FAs play key roles in metabolism including metabolic fuel (storage of energy in the adipose tissue and skeletal muscles, and transport of energy via TG), as essential components of all membranes via phospholipid, and as gene regulators, Rustan & Drevon (2001). Almost all fatty acids play a role in energy provision and as structural components, but some specific fatty acids have key roles in control and regulation of metabolism, Beenakkers et al (1981).

1.3.3 Fatty acid structure

The basic structure of FAs consists of a long aliphatic chain with a carboxyl at one end and a methyl group at the other end. The hydrocarbon chain can be "saturated" thus, all carbon bonds are saturated with hydrogen, or "unsaturated" containing one or more carbon-carbon double bonds. Fatty acid such as C16:0 represents a saturated fatty acid containing a 16-carbon aliphatic chain with no double bonds and C18:1n9 denotes a monounsaturated fatty acid (MUFA) with an 18-carbon aliphatic chain with a single cis double- bond nine carbons from the methyl group. Polyunsaturated fatty acids (PUFAs) contain two or more double bonds and are most commonly separated by methylene (CH2) groups. For instance, C22:6n3 is a 22-carbon containing six double bonds with the first positioned three carbons from the methylene group. A typical fatty acid consists carboxyl group, the carbon atom next to this group is called the α-carbon, and the subsequent one is the β carbon. The letter n is often used instead of the Greek ω to show the position of the double bond closest to the methyl end (figure 1.2).

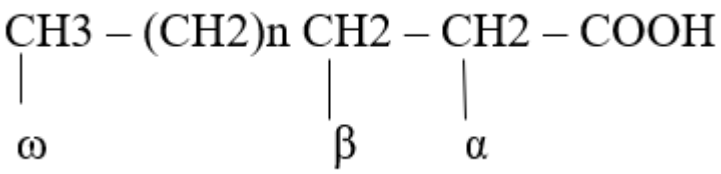

Figure 1.2: Structure of a typical fatty acid

(a) Saturated fatty acids (SFAs)

Saturated fatty acids are mostly straight hydrocarbon chains with an even number of carbon atoms e.g. palmitic acid (C16:0), stearic acid (C18:0). The most common fatty acids contain 12–22 carbon atoms. Saturated fatty acids are grouped into either short-chain containing 4–12 carbon chains, mid-chain containing 13–16 carbon long chains and long-chain fatty acids of 17–26 carbon chains, Grundy (2003). Dietary sources including tropical oils (i.e., palm oil, palm kernel oil and coconut oil) are high in SFA (30% of total FA) from plants, Zevenbergen et al (2009). Other saturated dietary fats are heterogeneous. For instance, coconut oil is high in lauric acid (12:0), whereas palm oil mainly consists of palmitic acid (16:0) and oleic acid (18:1n-9). Generally, most the common dietary SFA are C16:0 and stearic acid (18:0), present in animal fat as well as in plants, Iggman and Risérus (2011). Apart from dietary sources of SFA, these fatty acids can also be synthesized endogenously, Mozaffarian (2004); Carta et al (2017). It has been reported that long-chain saturated fatty acids (SFAs) particularly palmitate (C16:0) and stearate (C18:0), which are abundant in animal fat and dairy products and produced in the liver from dietary sugar, may be harmful to hepatocytes in NAFLD, Yu et al (2016). Increased dietary intake of saturated fatty acids increases intrahepatic triglyceride and insulin resistance, Luukkonen et al (2018). A previous study reported that palmitate, a saturated fatty acid, induced mild liver fibrosis, however, restricting palmitate intake improved NAFLD pathogenesis, Ogawa et al (2018).

(b) Odd chain fatty acids (OCFA)

OCFA may be saturated fatty acids with odd chain carbon number e.g. pentadecanoic acid (C15:0) and heptadecanoic acid (C17:0). Odd-chain saturated fatty acids constitute less than 1% of total fatty acids in human plasma, Weitkunat et al (2017). It has long been assumed that OCFAs are not synthesized endogenously by mammals and therefore reflect dietary habits, Sun et al (2007). Observational studies have demonstrated an association between plasma OCFAs and the consumption of dairy products, particularly milk fat, Weitkunat et al (2017). It is also known that in ruminants, OCFAs can derive from *de novo* synthesis via propionyl-CoA instead of acetyl-CoA for fatty acid synthesis, Massart-Leën et al (1983). Furthermore, another study reported that OCFAs originate from dairy fat as they are synthesized in relatively high levels by rumen microbial fermentation and microbial *de-novo* lipogenesis, Vlaeminck et al (2016). Many cohort and case-control studies have found an inverse association between plasma OCFA concentration (C15:0, C17:0, or both combined) and the risk of cardiometabolic diseases, Hodge et al (2007); Santaren et al (2014); Huang et al (2019). Serum levels of C15:0 and C17:0 have also been negatively correlated with NAFLD, Yoo et al (2017). In a previous study, mice treated with C15:0-supplemented methionine- and choline-deficient diet (MCD) diet showed reduced serum AST levels and hepatic infiltration of ceroid-laden macrophages compared to MCD-treated mice, which suggests that C15:0 deficiency may contribute to liver injury in NASH, Yoo et al (2017).

(c) Monounsaturated fatty acids

MUFAs are fatty acid classes with only one double bond. The most common MUFAs are palmitoleic acid (16:1 n−7), cis-vaccenic acid (18:1 n−7) and oleic acid (18:1 n−9). Just like other fatty acids, MUFA are almost completely absorbed in the intestine and are oxidized for energy production, converted into other fatty acids, or incorporated into tissue lipids,

Schwingshackl & Hoffmann (2012). MUFA can be found in olive oil, in canola oil, in olives, avocadoes as well as oleaginous plants, Bressan et al (2009). A study has shown that oleic acid contained in olive oil (from 55 to 85%) can account for from 60 to 80% of the entire daily dietary intake of oleic acid, Oi-Kano et al (2007). The role of MUFAs in metabolic diseases are still not clearly defined as contrasting evidence exists. For instance, MUFA has been associated with lower risk of CVD, Roche (2005). The American Heart Association recommend MUFA intake to be <15% of total energy consumption (TEC). However, the American Dietetic Association proposed the corresponding value to be set to <20%, Schwingshackl et al (2011). MUFA have been suggested to play a protective role against increases in intrahepatic triglyceride (IHTG). Diets high in MUFA have been shown to improve serum lipid profiles associated with NAFLD, Garg (1998). A clinical trial of MUFA showed decreased abdominal fat deposition and improved insulin sensitivity, which are both conditions associated with NAFLD, Paniagua et al (2007). However, another study revealed a higher MUFA consumption in patients with NAFLD, Cortez-Pinto et al (2006). Moreover, dietary intake in 1128 NAFLD patients showed an association with the Fatty Liver Index (FLI; derived from BMI, waist circumference, triglycerides and gamma-glutamyl transferase [GGT]). MUFA consumption and total fat intake were positively associated with a higher FLI score Rietman et al (2018). Similarly, in the Rotterdam Cohort, MUFA consumption was not associated with beneficial effect in NAFLD, Perdomo et al (2019).

(d) Polyunsaturated fatty acids

PUFAs have two or more double bonds. PUFAs can be further subdivided based on the location of the first double bond relative to the methyl end group of the chain. For instance, n-3 and n-6 FAs are two of the most important PUFA classes and have their first double bond on either the third or sixth carbon from the chain end group, respectively. The final carbon in the FA chain is also termed as the omega carbon, hence the common reference to these FAs as omega-

3 or omega-6 PUFAs, Ander et al (2003). Aquatic species that have been shown to have long chain n-3 PUFA include fishes, shrimps, prawns, crabs, shellfishes, leafy green vegetables, nuts and seeds (e.g. sesame, hummus), oils (linseed/flaxseed), soya bean and algae, Abedi & Sahari (2014); Shefer-Weinberg et al (2007). Fats and oils, meat and poultry, cereal-based products and cereals, vegetables, and nuts and seeds are reported to be important sources of n−6 PUFA, Meyer et al (2003). Long-chain n-3 and n-6 PUFAs (LC-PUFAs) are synthesized from the essential FAs alpha-linolenic acid (ALA) and linoleic acid, respectively. These two essential fatty acids cannot be synthesized by the body and can only be obtained via dietary sources. The most common LC-PUFAs are EPA (eicosapentaenoic acid, 20:5n-3), DHA (docosahexaenoic acid, 22:6n-3) and ARA (arachidonic acid, 20:4n-6), Zárate et al (2017). Animals and humans have the capacity to metabolize essential fatty acids into long-chain derivatives, Kaur et al (2014). It is generally thought that n-3 PUFAs are antithrombotic, anti-inflammatory, and vasodilating whilst n-6 PUFAs are relatively prothrombotic, proinflammatory, and vasoconstricting, Sacks & Campos (2006).

The role of polyunsaturated fatty acids (PUFAs) in inflammation is attributed to eicosanoid production, which are mediators and regulators of inflammation. It is well known that arachidonic acid is usually the major precursor for eicosanoid synthesis. Previous studies suggest that modestly increased intake of arachidonic acid results in incorporation of arachidonic acid into cells involved in inflammatory responses, Thies et al (2001). Eicosanoids include prostaglandins (PGs), thromboxanes, leukotrienes (LTs), and other oxidized derivatives, Calder (2006). The role of arachidonic acid as a substrate for the synthesis of eicosanoids indicates the potential for dietary n–6 PUFAs (linoleic or arachidonic acid) to influence inflammatory processes. Studies have reported that both n-6 and n-3 pathways compete with one another for enzyme activity, hence the ratio of n-6 to n-3 PUFAs is crucial to human health, Ander et al (2003). This means that increased consumption of long-chain n−3

PUFAs results in less substrate availability for synthesis of eicosanoids from arachidonic acid, Calder (2006) and is therefore protective against inflammation. Studies suggest that optimal ratio of n-6 PUFA to n-3 PUFA in the diet is 4 to 1, He et al (2016). Previous studies have reported that consumption of large amount of dietary fish oil results in decreased leukocyte chemotaxis, decreased output of ROS and proinflammatory cytokines, as well as decreased adhesion molecule expression, Calder (2006). Maresin 1 (MAR1), derived from docosahexaenoic acid (DHA) is known to protect against inflammation and insulin resistance, Jung et al (2018).

Polyunsaturated fatty acids (n-3 PUFAs and n-6 PUFAs) also influence lipid accumulation in the liver. In human studies, dietary patterns of patients with NAFLD compared to controls have reported that individuals with NAFLD show lower omega-3 polyunsaturated fatty acid (n-3 PUFA) intake and higher n-6/n-3 PUFA intake ratio, Araya et al (2004). Moreover, supplementation of n-3 polyunsaturated fatty acids (n-3 PUFAs) is known to improve NAFLD, Oya et al (2010); Valenzuela et al (2019); Jeyakumar & Vajreswari (2019). In animal studies, n-3 PUFAs have been shown to reduce hepatic lipogenesis and inflammation, Putti et al (2016).

(e) Branched-chain fatty acids

Branched-chain fatty acids (BCFAs) are normally saturated fatty acids having one or more methyl branches on the carbon chain, Ran-Ressler et al (2008). BCFA are prominent components of bacterial membranes across many genera and species and in humans are synthesized in sebaceous and meibomian glands of human skin, Dingess et al (2016). They include *iso* tetradecanoic acid, *iso* C14:0; 13-methyltetradecanoic acid, *iso* C15:0; 12 methyltetradecanoic acid, *anteiso* C15:0; *iso* hexadecanoic acid, *iso* C16:0; 15-methylhexadecanoic acid, *iso* C17:0; 14-methylhexadecanoic acid, *anteiso* C17:0 and heptadecenoic acid, *cis*-9 C17:1, and are only in trace amounts, Fievez et al (2003). Human milk contains BCFAs, Nicolaides et al (1965); Adamska & Rutkowska (2014). These FAs can

also be found in tissues of ruminants and marine organisms however constitute only about 1% to 2% of total FA content in mammals, Adamska & Rutkowska (2014). Just like OCFAs, BCFAs exert a significant effect on human health. A study reported that obesity was associated with a decrease in serum iso-BCFA level. A study found a strong association between serum concentrations of FAs between OCFAs and BCFAs which suggested that both FAs may, at least partially, originate from the same source, perhaps, ruminant fat and milk, Mika et al (2016). Interestingly, the role of branched-chain fatty acids on hepatic lipid accumulation has not been studied. However, the role of branched chain amino acids in NAFLD has been explored. NAFLD is well known to be associated with elevated plasma branched-chain amino acids (BCAAs), Koliaki et al (2015); van den Berg et al (2019). Branched-chain fatty acids can be biosynthesized using either branched-chain amino acids (BCAAs) or branched-chain alpha-keto acids (BCKAs), or combination of both as precursor, Hirosuke et al (1994). We can therefore infer from this to hypothesize that BCFAs may be implicated in the pathogenesis of NAFLD.

Table 1.1: Summary of current evidence on effect of dietary fatty acids on circulating fatty acids in mouse and humans.

Dietary FA	Experimental model	Metabolic effect/pathway
Saturated	*in vivo* humans	High intake of SFA increased IHTG: (Rosqvist et al (2014), Bjermo et al (2012), Hodson et al (2020), Sevastianova et al (2012). Luukkonen et al (2018)
	in vivo humans	High intake of SFA inhibit lipolysis: Wueest et al (2016)
MUFA	*in vivo* humans	Hiigh intake of MUFA reduced IHTG: Bozzetto et al (2012), Ryan et al (2013)
OCFA	*in vivo* humans	Decrease OCFA was associated with increased NAFLD risk (Kratz et al (2014)
n-3 PUFA	*in vivo* mice	Increased n-3 PUFA intake decreased IHTG: Pachikian et al (2008),
	in vivo humans	Scorletti et al (2014)
	in vivo humans	Evidence support n-3 PUFA supplements containing DHA as treatment strategy for NAFLD Jump et al (2018).
n-6 PUFA	*in vivo* humans	Increased n-6 PUFA reduced IHTG: Bjermo et al (2012), Rosqvist et al (2014)

IHTG, Intrahepatic triglyceride

1.3.4 Mechanisms of fatty acid metabolism

The processes involved in fatty acid metabolism in the liver include fatty acid uptake from the blood and chylomicron remnant uptake, *de novo* lipogenesis and fatty acid oxidation, Wagenmakers et al (2006); Jump (2011). Each of these pathways is highly regulated hence,

their contribution to the total liver FA pool is variable, Mashek (2013). Changes in any of these pathways has potential to influence both hepatic and whole-body energy metabolism and can contribute to pathogenesis of diseases including NAFLD.

(a) Fatty acid uptake by the liver

The liver plays a role in the uptake of fatty acids from the blood, Mashek (2013). In human stable isotopic studies, evidence suggests that uptake of exogenous FFA is the single largest source of FA in stored hepatic TG and this contribution is further increased during fasting and NAFLD, Donnelly et al (2005). Clearance of chylomicron-remnant TG also contributes to the hepatic FA pool. Chylomicrons are formed in the intestine and are involved in the transport of dietary triglyceride to peripheral tissues and the liver. Chylomicron remnants are formed as a result of hydrolysis of chylomicron TG by the enzyme lipoprotein lipase, with apolipoprotein (apo)C-I1 as a co-factor. In humans, studies suggest that chylomicron remnant uptake accounts for 15% of the liver FA pool during fasting and 25% during the fed state, Barrows & Parks (2006), and this decreases with meal feeding compared with continuous feeding, Barrows et al (2005).

The main plasma membrane transporters of FFA into the liver post-prandially and during obesity are fatty acid transporter proteins (FATP), caveolins, fatty acid translocase (FAT)/cluster of differentiation 36 (CD36), and fatty acid binding protein (FABP). Of the six member family, only FATP2 and FATP5 are highly expressed in the liver, Ipsen et al (2018). Knockdown of FATP2 in mice decreased the uptake of FFA and ameliorated hepatic steatosis induced by a high fat diet, Falcon et al (2010). Similarly, FATP5 knockout mice are resistant to diet-induced obesity and hepatic TG accumulation, Doege et al (2006) highlighting the significant role played by FATP in liver lipid accumulation. The second family of lipid transporters, caveolins, have three members namely caveolins 1, 2, and 3, and play an important

role in the formation of lipid droplets. Caveolin 1 is increased in the liver of mice with NAFLD, mainly in the centrilobular zone 3, where the steatosis tends to be severe; zone 3 predominant hepatic steatosis has been reported in adult NAFLD patients. Whole-body caveolin 1 knockout (cav1−/−) reduced hepatic steatosis in high fat fed mice in response to 24 h of fasting whereas, unexpectedly, liver-specific caveolin 1 knockout had no effect on hepatic fat content, Ipsen et al (2018). FAT/CD36 accelerates FFA uptake via facilitated diffusion. Elevated hepatic expression of CD36 has been observed in NAFLD and is associated with enhanced uptake of FFA, Miquilena-Colina et al (2011). High fat diet-fed mice develop hepatic steatosis alongside increased mRNA and protein expression of CD36, Wilson et al (2015), which appears to suggest a positive feed-forward loop for FFA removal. After uptake, the cytosolic fatty acid binding protein (FABP)s facilitate intracellular transport of FFAs. Targeted deletion of the liver isoform, LFABP in mice results in NAFLD-like pathology in female mice, Martin et al (2015).

(b) *De novo* lipogenesis

De novo lipogenesis (DNL) is a metabolic pathway that consisting of glycolysis (conversion of glucose to acetyl-CoA), biosynthesis of saturated fatty acid followed by desaturation, and the formation of TG. DNL has been suggested to be abnormally increased in and contribute to the pathogenesis of non-alcoholic fatty liver disease (NAFLD), Donnelly et al (2005). At first, acetyl-CoA is converted to malonyl-CoA by acetyl-CoA carboxylase (ACC) and malonyl-CoA is then converted to palmitate by fatty acid synthase (FASN). Newly formed fatty acids may then undergo desaturation, elongation or esterification steps before ultimately being stored as triglycerides or exported as VLDL particles. Enzymes involved in the pathway include glucokinase and liver-type pyruvate kinase in the glycolysis, ACC and fatty acid synthase (FAS) in the fatty acid synthesis, long chain fatty acid elongase 6 (ELOVL6) and stearoyl-CoA desaturase (SCD) in the formation of MUFAs, and glycerol-3-phosphate acyltransferase (GPAT), lipins, and acyl-CoA: diacylglycerol acyltransferase (DGAT) in the formation of TG,

Koo (2013). In NAFLD, these key enzymes are upregulated, Mitsuyoshi et al (2009). A study showed that liver-directed inhibition of ACC in rats caused a significant reduction in hepatic DNL and triglycerides after just a week of high-fructose (60%) feeding, Goedeke et al (2018). The transcriptional regulation of DNL is mainly orchestrated by two key transcription factors: sterol regulatory element-binding protein 1c (SREBP1c), which is activated by insulin and liver X receptor α, and carbohydrate regulatory element-binding protein (ChREBP), which is activated by carbohydrates, Sanders & Griffin (2016). SREBP-1c is regulated by insulin through a phosphoinositide 3-kinase (PI3K)-dependent mechanism that involves the liver X receptor α (LXRα) (figure 1.3). LXRα promotes the expression of SREBP-1c and targets genes such as fatty acid synthase (FAS), acetyl CoA carboxylase (ACC), stearoyl-CoA desaturase (SCD1) and lipin, Ferre & Foufelle (2010).

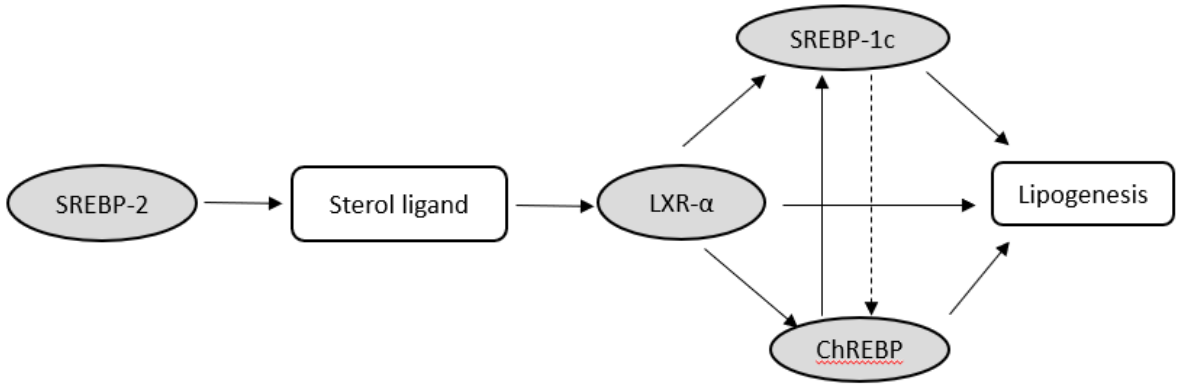

Figure 1.3 Transcriptional regulation of lipogenesis.

SREBP1c expression is enhanced in NAFLD and is consistent with its lipogenic role. A study reported higher levels of hepatic triglyceride in transgenic mice overexpressing SREBP1c while SREBP1c knockout mice showed a decrease in expression of lipogenic enzymes, Ipsen et al (2018). The activity of SREBP-1c can also be activated by mammalian target of rapamycin (mTOR) pathway and can be inhibited by PKA, AMP-activated protein kinase (AMPK), and salt inducible kinases (SIKs), Porstmann et al (2008).

ELOVL6 catalyzes the elongation of palmitate (C16:0) to stearate (C18:0) fatty acids and has been shown to promote NASH, Muir et al (2013). Increased ELOVL6 mRNA expression has been observed in NASH animal models, such as low-density lipoprotein receptor knockout animals fed a western type diet or a fructose diet, Muir et al (2013); Imajo et al (2013). SCD1 is a microsomal enzyme that catalyses the synthesis of MUFAs from saturated fatty acyl-CoAs. The preferred substrates for SCD1 are palmitoyl- (16:0) and stearoyl-CoA (18:0), which are then converted to palmitoleoyl- (16:1 n-7) and oleoyl- (18:1 n-9) CoA respectively. Hepatic SCD1 activity was correlated negatively with liver fat in a human study, Stefan et al (2008).

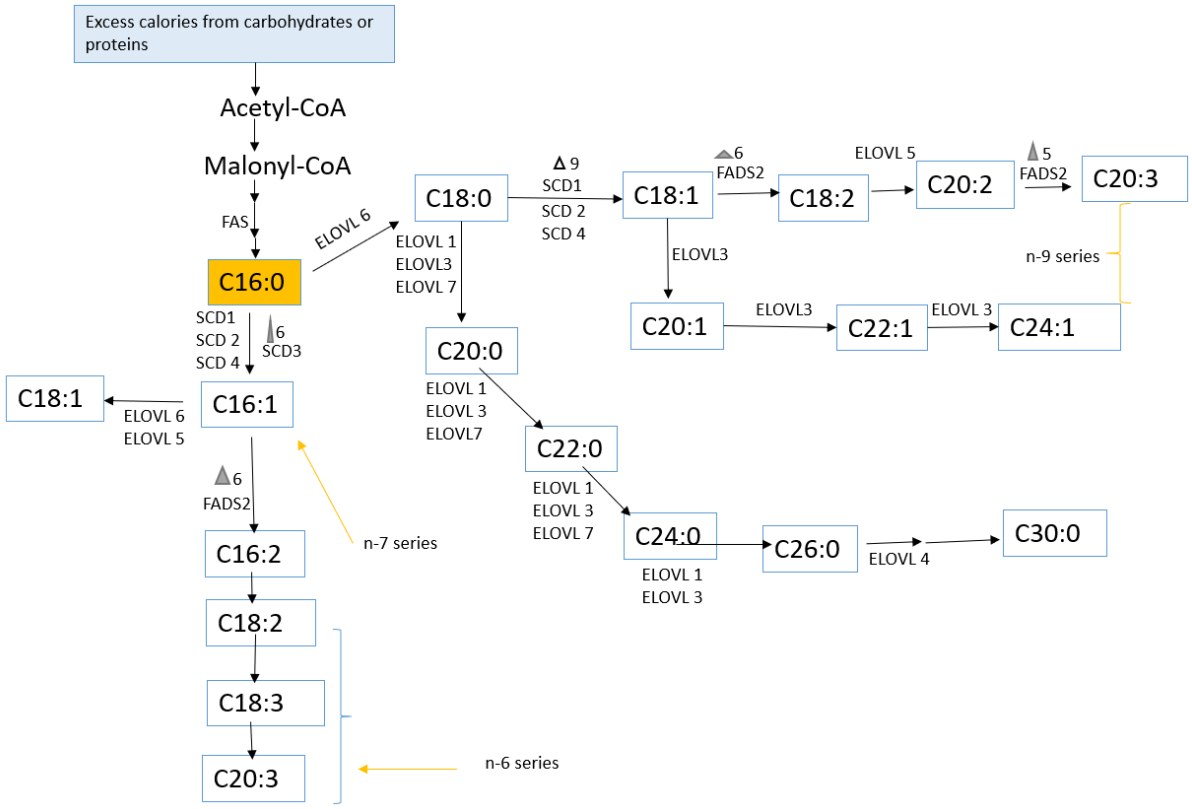

Figure 1.4: *De novo* synthesis of fatty acids, elongation and desaturation

The product of carbohydrate or protein breakdown, Acetyl-CoA, is carboxylated with bicarbonate to generate malonyl-CoA via the activity of acetyl-CoA carboxylase (ACC). The malonyl-CoA combines with further acetyl-CoA units with fatty acid synthase enzyme complex (FAS) and further units are added to produce C16 saturated fatty acid palmitate, Ratnayake & Galli (2009). Palmitate produced then undergoes elongation and desaturation processes to generate new fatty acids. Elovl6 elongates fatty acids ranging from 12-16 carbons to a length of 18-carbons, Zadravec et al (2010). Stearate (C18:0) can be elongated by ELOVL 1, ELOVL 3 and ELOVL 7 to produce arachidic acid (C20:0) with these enzymes capable of

further elongation up towards very long chain fatty acids >C20:0. Desaturation occurs at the n-7 (Δ7) position of the carbon chain of palmitate or at the n-9 (Δ9) position of palmitate or stearate generating palmitoleate (C16:1) and oleate (C18:1) respectively by Δ9 desaturase, also known as stearoyl-CoA desaturase 1 (SCD-1). The n-7 fatty acids can be subjected to elongation by ELOVL6 and ELOVL 5. The n-9 fatty acids are subject to elongation by elovl3 generating cis-11-eicosenoic acid ethyl ester (C20:1), erucic acid (C22:1) and nervonic acid (C24:1), the final reaction being terminal in the production of monounsaturated fatty acids. In the absence of n-3 and n-6 fatty acids which cannot be synthesized and are required in the diet, oleic acid can undergo desaturation by Δ6 desaturase to produce the n-9 family of polyunsaturates, Zadravec et al (2010).

In odd-chain saturated fatty acids, *de novo* synthesis of these fatty acids is achieved by repeated condensation of malonyl-coenzyme A (CoA) with propionyl-CoA, instead of acetyl-CoA as primer, Kaneda (1991). It is reported that straight-chain fatty acid synthetase accepts both acetyl-CoA and propionyl-CoA and the balance to which extent acetyl-CoA and propionyl-CoA are used may be in part a function of the relative availability of both primers, rather than a reflection of an altered specificity of the fatty acid synthetase, Fulco, 1983; Vlaeminck et al (2016).

Insulin signalling and *de novo* lipogenesis

Insulin signalling in the liver is mediated by the hepatic insulin receptor (IR), which signals through the downstream kinase, protein kinase B/Akt, to coordinate hepatic metabolism. Akt signals through multiple downstream pathways, including those involved in mechanistic target of rapamycin (mTorc1) and the Foxo family of transcription factors. Studies suggest activation of mTorc1 by Akt is required but not sufficient for insulin-induced activation of DNL, Wan et al (2011).

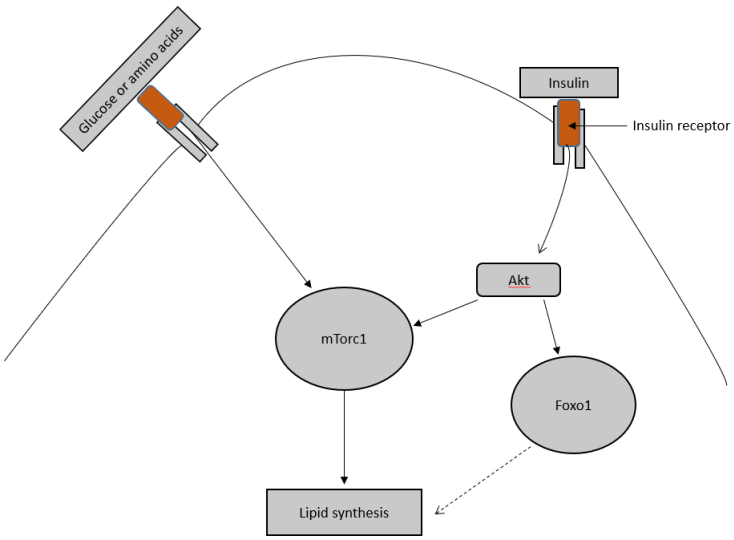

Figure 1.5: Nutrient and insulin signalling pathway.
Amino acids (e.g. isoleucine) and glucose activate mTorc1, resulting in the induction of lipid synthesis. Insulin activates mTorc1 and Foxo1 via the Akt resulting in lipid synthesis.

The role of Foxo1 in liver lipid metabolism is not fully understood, as some studies suggest Foxo1 can contribute directly to regulation of lipogenic gene expression by insulin and DNL in liver while other studies suggest it requires the presence of other proteins such as Akt to induce lipogenesis, Titchenell et al (2016). Foxo1 regulated carbohydrate metabolism in the liver as demonstrated by liver-specific Foxo1 deletion leading to sufficient normalization of hyperglycemia and whole-body insulin sensitivity in mice lacking the hepatic IR, IR substrates, or the two Akt isoforms expressed in liver, Akt1 and Akt2, Titchenell et al (2016).

VLDL secretion and TG transport

Very low-density lipoprotein (VLDL) is responsible for endogenous lipid transport, Feingold & Grunfeld (2018). VLDL is assembled within the liver from TGs, cholesterol esters, and apolipoproteins (apoB). The assembly of VLDL in the endoplasmic reticulum (ER) requires the crucial interaction between apoB and microsomal triglyceride transfer protein (MTP) which facilitates the secretion of the lipoprotein particle. Insulin plays an important role in the regulation of VLDL assembly and secretion. VLDL particle is stabilized by a single molecule

of apolipoprotein B 100 (apoB 100). ApoB 100 is a long polypeptide that is lipidated with triglycerides within the lumen of endoplasmic reticulum (ER) while it is being translated and translocated across the ER membrane. Lipidation of apoB 100 is facilitated by microsomal triglyceride transfer protein (MTP), an ER resident protein that has both apoB 100 binding and lipid transfer domains. Hypertriglycedaemia and hepatic steatosis have been observed in NAFLD patients, Choi & Ginsberg (2011). Impaired VLDL assembly and secretion result in excessive hepatic lipid accumulation.

(c) Fatty acid oxidation

Mitochondria play a central role in energy generation. Fatty acids primarily enter a cell through fatty acid protein transporters on the cell surface. Inside the cell, a CoA group is added to the fatty acid by fatty acyl-CoA synthase (FACS), forming long-chain acyl-CoA. Carnitine palmitoyltransferase 1 (CPT1) conversion of the long-chain acyl-CoA to long-chain acylcarnitine facilitates the fatty acid moiety to be transported across the inner mitochondrial membrane via carnitine translocase (CAT), which exchanges long-chain acylcarnitines for carnitine. An inner mitochondrial membrane CPT2 then converts the long-chain acylcarnitine back to long-chain acyl-CoA. The long-chain acyl-CoA enters the fatty acid β-oxidation pathway, which results in the production of one acetyl-CoA from each cycle of fatty acid β-oxidation (figure 1.6), Gumpen & Norum (1973).

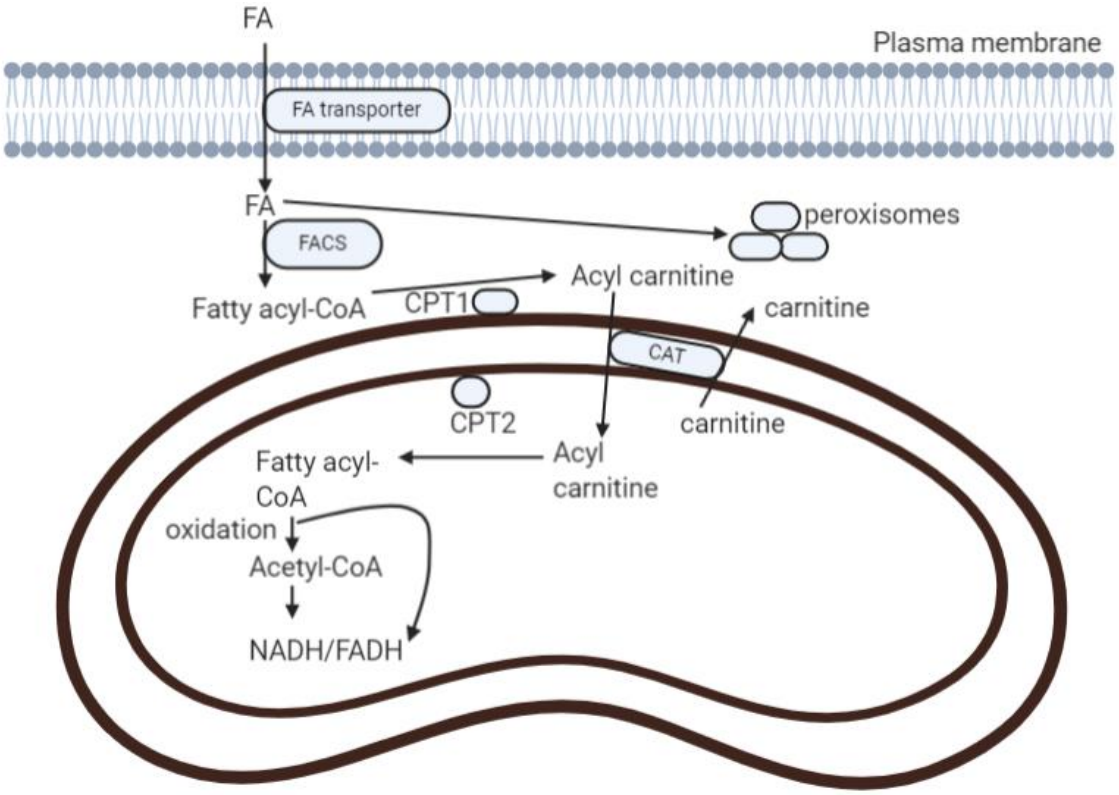

Figure 1.6 Fatty acid β-oxidation pathway (diagram adapted from Fillmore et al (2011)).

Peroxisome proliferator-activated receptors (PPARs) are ligand-induced transcription factors that regulate the transcription of target genes in response to specific ligands, both synthetic and endogenous. There are three isoforms that have been discovered PPAR-α (NR1C1), PPAR-β /-δ (NR1C2) and PPAR-γ (NR1C3). PPAR-α plays a central role in the transcriptional regulation of lipid and glucose metabolism genes in the liver, Mandard et al (2004). Hepatic PPAR- α expression was substantially reduced at 16-week after obese mice fed a high-fat (HF) diet made up of 60% of energy as lipids. PPAR- α regulates mitochondrial beta-oxidation of fatty acids. When PPAR-α expression in the liver is inhibited, the transcription of its target gene, carnitine palmitoyl transferase-1 (CPT-1), is impaired resulting in accumulation of excessive fatty acids in the form of triglycerides, Yu et al (1998).

Peroxisomes and mitochondria role in fatty acid oxidation

Peroxisomes and mitochondria are cellular organelles involved in various liver metabolic functions including lipid metabolism and energy production. Changes in these organelles are associated with disorders affecting the liver such as Zellweger syndrome and non-alcoholic fatty liver disease, Begriche et al (2013).

Peroxisomes are single bound membrane and play important role in bile acid synthesis, β-oxidation chain shortening of long-chain and very-long-chain fatty acyl-coenzyme (CoAs), long-chain dicarboxylyl-CoAs, alpha oxidation of branched-chain fatty acids and cellular redox homeostasis, Reddy & Hashimoto (2001); Smith & Aitchison (2013). They are also involved in the maintenance of normal mitochondrial function, Schrader et al (2013). Mitochondria are essential for aerobic ATP production, fatty acid β-oxidation (acyl-chain length of ⩽C20), ketogenesis and gluconeogenesis from pyruvate and tricarboxylic acid (TCA) cycle intermediates. It is well established in the literature that mitochondrial dysfunction contributes to the pathogenesis of NAFLD partly because it affects liver lipid homeostasis, promotes ROS production and lipid peroxidation, cytokine release and cell death, Nassir & Ibdah (2014).

Beta-oxidation of very long chain fatty acids

Beta-oxidation is primarily handled by the mitochondrial *beta*-oxidation pathway and there is very little contribution from the peroxisomal system. However, certain very long-chain fatty acids (VLCFAs), including C22:0, C24:0 and C26:0 can only be oxidized in peroxisomes and not in mitochondria. This is because VLCFAs are not suitable substrates for carnitine palmitoyltransferase 1 (CPT1) which is essential for their entry into mitochondria. Peroxisomes are known to lack a citric acid cycle and respiratory chain, hence the end products of *beta*-oxidation in peroxisomes including acetyl-CoA, propionyl-CoA and other acyl-CoAs, and

NADH are then shuttled from peroxisomes to mitochondria for complete oxidation to CO_2 and H_2O in case of acetyl-CoA, propionyl-CoA and the other acyl-CoAs and re-oxidation of NADH back to NAD, Wanders (2014). Acyl-coenzyme A oxidase (Acox) 1, a rate-limiting enzyme in peroxisomal fatty acid β-oxidation, regulates metabolism, spontaneous hepatic steatosis, and hepatocellular damage over time. Twelve-week-old, chow diet–fed, $Acox1^{Lampe1}$ mice showed increased energy expenditure, degradation of TGs stored in the white adipose tissue (WAT) degraded and released as fatty acids, via the process of lipolysis, to be used by brown adipose tissue (BAT). Moreover, this observation was in agreement with WAT mRNA expression of lipase E, hormone sensitive type *(Lipe)*, PPAR-γ, and patatin-like phospholipase domain containing 2 *(Pnpla2)*, which are genes associated with lipolysis, and was increased in $Acox1^{Lampe1}$ mice compared with wild type controls, Moreno-Fernandez et al (2018).

Alpha-oxidation pathway

Branch-chain fatty acids including 3-methyl branched-chain fatty acids cannot undergo beta-oxidation due to the location of the methyl-group at position 3. Moreover, even-numbered hydroxylated very-long-chain FAs and other even-chain fatty acids may undergo an alternative oxidation pathway, Vlaeminck & Fievez (2006); Pfeuffer & Jaudszus (2016). These FAs undergo alpha-oxidation by removing the terminal carbon to generate a 2-methyl FA before entering into beta-oxidation pathway. For instance, phytanic acid which is a 3-methyl branched chain fatty acid in humans undergoes alpha-oxidation beginning with formation of phytanoyl-CoA, followed by hydroxylation to produce 2-hydroxyphytanoyl-CoA, a reaction catalyzed by the enzyme phytanoyl-CoA 2-hydroxylase. Subsequently, 2-hydroxyphytanoyl-CoA is lysed by the enzyme 2-hydroxyacyl-CoA lyase (HACL) to pristanal and formyl-CoA and then hydrolyzed into formic acid and CoASH. Pristanal is oxidized to pristanic acid (2, 6, 10, 14-tetramethylpentadecanoic acid) as catalyzed by a yet undefined peroxisomal aldehyde dehydrogenase. Finally, after activation to its CoA-ester, pristanoyl-CoA undergoes three

cycles of beta-oxidation in peroxisomes before the end-products are transported to mitochondria for complete oxidation, Wanders (2014).

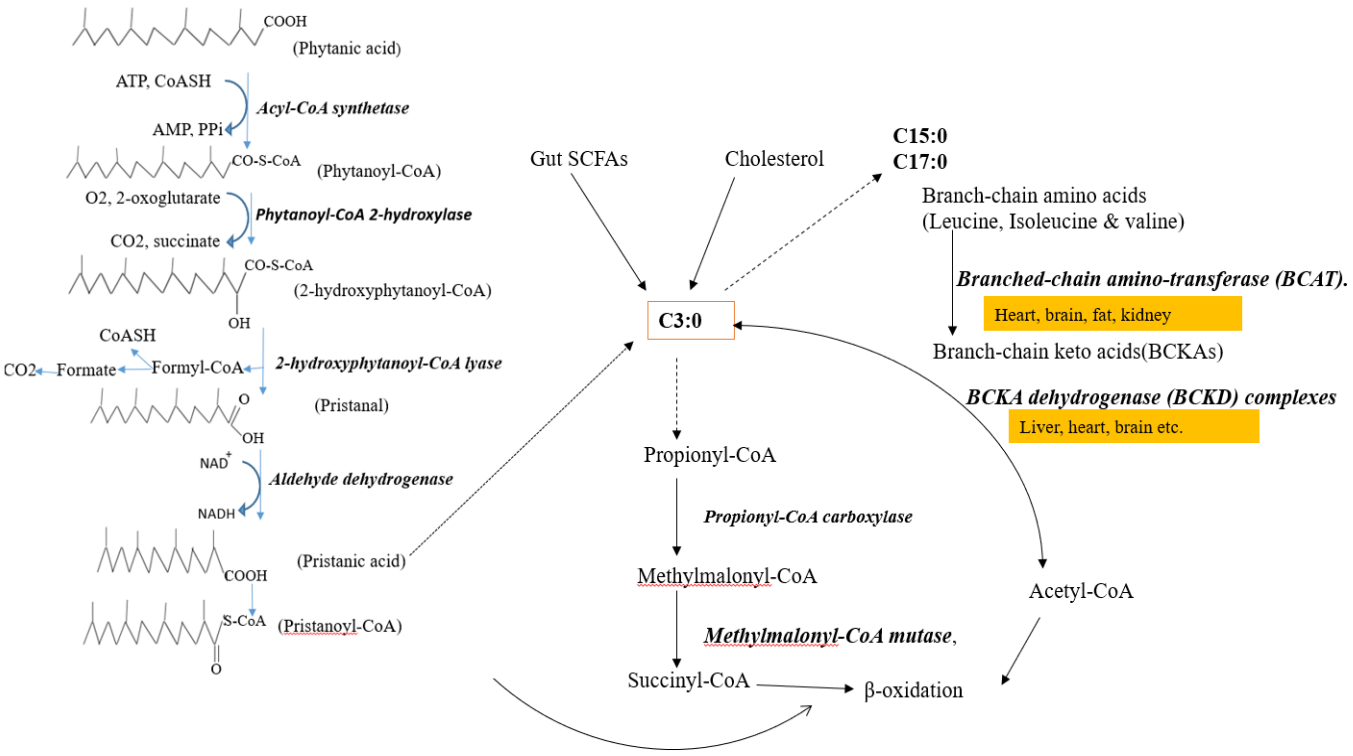

Figure 1.7: Pathways for C15:0 & C17:0 biosynthesis and alpha oxidation of branched-chain fatty acid, phytanic acid.

Pentadecanoic acid (C15:0) and heptadecanoic acid (C17:0) can be synthesized from short chain fatty acid, propionic acid (C3:0). Propionic acid can be generated via colonic bacterial fermentation of dietary fibre; breakdown of amino acids such as methionine valine, isoleucine, and threonine; peroxisomal oxidation of cholesterol side chain as well as α-oxidation of phytanic acid followed by successive β-oxidative degradation pathway. Aside chain lengthening of short-chain fatty acid (SCFA) to produce long OCFA, very long even-chain fatty acids can also undergo α-oxidation partial peroxisomal β-oxidation to yield C15:0 and C17:0, Pfeuffer & Jaudszus (2016).

1.3.5 Peroxisomal and mitochondrial dysfunction and NAFLD

As mitochondria and peroxisomes play important roles in fatty acid oxidation, changes in the biogenesis and functions of these organelles lead to impairment of lipid metabolism in the liver. Mitochondrial and peroxisome dysfunction has been implicated in the pathogenesis of NAFLD, Begriche et al (2006); Koliaki et al (2015). Moreover, impaired hepatic mitochondrial function has been reported in type 2 diabetes and steatohepatitis, Schmid et al (2011); Pérez-

Carreras et al (2003). A review study conducted by Nassir & Ibdah (2014) demonstrated a link between mitochondrial dysfunction and NAFLD. Another review has furthered our understanding of how mitochondria-derived oxidative stress leads to progression of NAFLD, Simões et al (2018).

In dietary protein restriction, impairment of hepatic lipid metabolism result in consequential changes in peroxisome numbers and functions. A study by van Zutphen (2016) et al showed diminished hepatic peroxisome content and impaired peroxisomal function following a 4-week low protein diet (LPD). It was explained that a possible cause of hepatic steatosis was due to the loss or dysfunction of the organelles involved in lipid oxidation. Electron microscopic analyses revealed a near absence of peroxisomes in the periportal area of livers of LPD-fed animals compared to controls as shown by decreased immunofluorescence staining of peroxisomal membrane protein PEX14. Moreover, protein levels of peroxisomal membrane protein 70 (PMP70) and matrix protein catalase were decreased after 4 weeks of LPD, van Zutphen et al (2016). Proteins required for mitochondrial assembly and stability of complex I, oxidative phosphorylation (OXPHOS) complex I activity and level of NADH dehydrogenase (ubiquinone) activity 8 (Ndufb8) were reduced in the dietary challenged mice livers. Also, Complex IV activity and protein levels of subunit 1 were decreased in the LPD group. Proteomic analysis showed a decreased mitochondrial fatty acid oxidation enzyme such as medium-chain specific acyl-CoA dehydrogenase (Acadm), medium and short-chain L-3-hydroxyacyl-coenzyme A dehydrogenase (Hadh) and enoyl-CoA hydratase (Echs1), Zutphen et al (2016).

1.4 The role of diet in NAFLD

1.4.1 Dietary fat and NAFLD risk

1.4.1.1 Dietary fat and hepatic lipid accumulation

Dietary fat is an important component of the human diet, although excessive fat or an imbalance of the type of fat can have detrimental effects on health. Over consumption of excess calories have been known to increase the risks of cardiometabolic diseases including type 2 diabetes, obesity and NAFLD, Jump (2011). A high-fat diet can influence free fatty acid concentration in circulation, Raatz et al (2001). In animal studies, rats fed HFD (60% energy as fat) diets showed significantly increased both serum TG and FFA composition from predominantly MUFA to predominantly PUFA. More importantly, linoleic acid and arachidonic acid, predominantly accounted for the increased percentage of PUFA in the serum TG (72% and 15% of the PUFA were linoleic acid and arachidonic acid, respectively) and serum FFA (83% and 4%, respectively), Liu et al (2015). Moreover, consumption of high fat diet compared with a low-fat diet showed significantly greater percentages of plasma phospholipid total PUFA, total (n-6) fatty acids, and 18:2(n-6), Raatz et al (2001).

Previous studies have demonstrated that triglycerides and FA are elevated in the liver of mice fed a HFD, Eisinger et al (2014). Feeding male C57BL/6 mice with a high-fat diet for 14 weeks resulted in decreased liver n-6 PUFA linoleic acid and n-3 PUFA α-linolenic acid with no effect on n-6/n-3 PUFA ratio compared to the control group. Moreover, the MUFA/SFA ratio was elevated and PUFA/SFA ratio was decreased in the fatty liver showing altered desaturation of FAs, Eisinger et al (2014). When the researchers performed analyses of SCD1 mRNA expression, which is involved in the conversion of palmitate and stearate to palmitoleate and oleate, they observed no changes in mice with the fatty liver (i.e HFD-fed group), Eisinger et al (2014).

1.4.1.2 High fat diet and lipid metabolism in the liver

A variety of "high-fat" and "control" diet formulations have been used in rodent studies investigating their effect on lipogenesis. These have produced different effects on lipogenesis pathways depending on the type or source of fat used in diet formulation. It has been reported that high fat diet increases lipogenic gene expression, Lin et al (2005); Sampath et al (2007). In these studies, the high fat diet contained high amount of saturated fatty acids. Despite upregulation of lipogenic gene expression including acetyl CoA carboxylase (*ACC), SCD1*, this does not always correlate with *de novo* lipogenesis. For instance, increases in lipogenic genes did not result in a significant induction of *de novo* lipogenesis in mice, Oosterveer et al (2009). A relative decrease in the contribution of *de novo* lipogenesis to hepatic TG has also been reported in rats fed a high-fat diet, Delgado et al (2009). In human studies, *de novo* lipogenesis was not induced upon a short-term dietary fat challenge in human subjects, Schwarz et al (1995); Hudgins et al (1996). Buettner et al (2006) performed studies on different high-fat diets (fat content 42% of energy) based on lard (HF-L), olive oil (HF-O), coconut oil (HF-C) and fish oil (HF-F) on genes of lipid synthesis compared to rats fed a standard rodent chow (SC, fat content 11% of energy) for 12 weeks. They reported that the genes encoding fatty acid synthase or SCD1 were upregulated in HF-L, HF-O and HF-C, with the effect being quantitatively strongest in HF-O. Moreover, they reported that in HF-F animals, some liposynthetic genes, such as SCD1, were also upregulated, but, in general, there was no significant change to SCD1. When they analysed key enzymes of fatty acid oxidation, such as *CPT1* or enoyl-CoA hydratase, these were downregulated in HF-L, HF-O and HF-C, but were not changed in HF-F. Moreover, transcriptional regulator of hepatic fatty acid synthesis, SREBP1c, was consistently upregulated in all diet groups, whereas PPARα, a key regulator of fatty acid oxidation, was upregulated only in HF-F, Buettner et al (2006).

1.4.2 Dietary protein intake and risk for NAFLD

1.4.2.1 Protein malnutrition in developing economies

Diets that favour high carbohydrate with a low protein intake are typical in developing countries and this may be a major risk factor for the increase prevalence of NAFLD. A comprehensive review by Kearney, 2010 showed that typical food intake in developing countries consist of a carbohydrate-rich staples (including cereals, roots, tubers), vegetable oils and sugar. In developing countries such as in Africa and parts of Asia, cereals can contribute more than 70 per cent of energy intake, Alexandratos 2006. The cereals consumed are mostly rice, wheat, sorghum and maize. This potentially deprives intake of other macronutrients such as proteins. Consumption trends for roots and tubers (including cassava, potatoes, yams, taro and plantain) have not seen a significant decline particularly in China and sub-Saharan Africa. For instance, 19 countries within sub-Saharan Africa depend on these products for at least 20 per cent of their food consumption in terms of calories, Alexandratos 2006. Sugar, as well as vegetable oils, has seen marked increases in consumption among developing countries, most notably in Asia, India and to a lesser extent in Latin America and Africa. Whilst Diet and Nutrition data is scarce in most developing countries, one review of dietary surveys conducted on adult South African population from 2000 to 2015 revealed that out of the total energy intake of men and women, the % energy from protein ranges from 10.9% to 18.3%; fat from 17% to 37.1%; and carbohydrate from 47.0% to 69%, Mchiza et al (2015).

1.4.2.2 Dietary proteins and hepatic lipid accumulation

Emerging evidence has shown that dietary protein insufficiency affects lipid content of the liver. Both human and animal studies have shown that a low protein diet (below 9% of total energy) causes an increase hepatic lipid accumulation. In human studies, a diet generally low in protein and high in carbohydrates, often seen in the elderly and typical of all ages in

developing countries, has been shown to cause liver lipid accumulation, Mayneris-Perxachs et al (2016). Moreover, children presenting with severe malnutrition were found to show several metabolic disturbances including increased oxidative stress and hepatic steatosis.

In animal models, feeding Wistar rats for 4 weeks with a 3% isocaloric low protein diet, in which reduced dietary caloric intake of protein was replaced with higher sucrose consumption and a lower protein consumption per g/100g but no significant differences regarding carbohydrates, minerals, vitamins and fat per g/100g energy resulted in increased hepatic triglyceride accumulation, Kuwahata et al (2011). Moreover, feeding Sprague-Dawley male rats for 4 weeks with an 8% isocaloric low protein diet with energy intake reduced via protein deficiency replaced by sucrose also led to hepatic triglyceride accumulation which was associated with down-regulation of hepatic microsomal triglyceride transfer protein and increased expression of *ACC*, Kang et al (2011). Further, Kwon et al reported that an 8% low protein diet resulted in steatohepatitis with severe steatosis in lactating female Sprague-Dawley rats, Kwon et al (2012). Despite the emerging evidence from animal models, there is a potential of confounding in the interpretation of the data; e.g. a low protein diet in mice for 16 weeks led to increased body weight, adiposity and fatty liver, Huang et al (2013) but the lack of dietary protein was substituted with a high carbohydrate content in the diet. Whether the development of fatty liver in this model was due to low protein or high carbohydrate or a combination of both has been addressed in part by dietary supplementation studies where the effect of protein extract or amino acids have been explored on low protein-induced NAFLD.

1.4.2.3 Effect of amino acid supplementation on low protein induced-NAFLD

Studies in animal models have reported a low protein diet supplemented with specific amino acids e.g. methionine, to moderate fat accumulation in major metabolic tissues such as the liver, muscle and subcutaneous adipose tissue. The amino acid derivative, betaine (trimethyl

glycine), occurs naturally in most living organisms. It is synthesized during the oxidation of choline, Ueland (2011). Betaine and choline are methylating agents and methyl donors are important for regulating DNA methylation and downstream gene expression. Choline is directed to maintain the S-adenosyl methionine (SAM) cycle; both choline deficient diets (CDD) and methionine and choline deficient dietary MCDD models may be useful for understanding the role of dietary amino acids for human NAFLD partly due to their histological similarity with these diseases, Kulinski et al (2004); Lyall et al (2017). A study by Madeira et al demonstrated that betaine and arginine supplementation, either individually or combined, with reduced protein diets (160 g kg−1 versus 130 g kg−1 of crude protein) decreased plasma total lipids and total cholesterol that had been induced by low protein diets in lean pigs, Madeira et al (2018). In the presence of either betaine or arginine supplementation, except for FAS which was down-regulated by protein reduction, no effects on hepatic FA composition and gene expression levels of lipid-sensitive factors were induced by the protein restricted diet, Madeira et al (2018). Another study showed that supplementation with fish derived protein was hepatoprotective during a low protein diet, Bjørndal et al (2013). Together these studies indicate that in animals receiving low protein diets, the associated development of fatty liver may be prevented by simple amino acid supplementation. The beneficial effects of supplementing with methyl donors that are absent during protein malnutrition may be explained, at least in part, by epigenetic regulation of hepatic metabolic gene expression. Conversely, it has been demonstrated in rat pups from dams previously fed low protein diets during lactation; hypomethylation of PGC1-α was observed in the offspring, decreased metabolic gene expression and subsequently impaired mitochondrial fatty acid oxidation, Pooya et al (2002). It is not known whether a similar pattern of gene promotor hypomethylation may be induced by protein malnutrition in human liver.

1.4.2.4 Dietary protein and hepatic lipid metabolism

Dietary protein is known to affect hepatic lipogenesis, Schwarz et al (2012). In an animal study, dietary protein restriction increased the expression of *ACC* in the liver of rats, Kang et al (2011). ACC is known to be a major lipogenic enzyme. A previous study reported a positive correlation between ACC protein levels and its enzymatic activity in rat liver, Atkinson et al (2002). Studies of specific amino acid deficiency have also provided evidence of their effects in altering lipid metabolism. It has been reported that the response to amino acid deprivation in mammals is thought to be characterized by upregulation of lipid synthesis, Guo & Cavener (2007). GCN2 eIF2α kinase, is a sensor of amino acid deficiency and plays a key role in mammals in modulating amino acid metabolism as part of adaptation to nutrient deprivation, Guo & Cavener (2007); Laeger et al (2016). The GCN2 kinase is well established as the amino acid monitoring mechanism for the activating transcription factor (ATF) 4 pathway, Kilberg et al (2012). A study found that lipid synthesis was upregulated in the livers of Gcn2−/− mice during prolonged leucine deprivation resulting in severe liver steatosis, Guo & Cavener (2007). The same study reported that this was due to persistent increased expression of SREBP-1c and its downstream transcriptional targets underlying FA and TG synthesis. Leucine deprivation had marked increased on expression level of mRNAs encoding the transcription factor of Pparα, Aco, Lcad, and Mcad mRNA in the livers of Gcn2−/− mice.

1.5 The role of inflammation and antioxidants in NAFLD

1.5.1 Pro-inflammatory cytokines

Inflammation is involved in almost all acute and chronic liver disorders including fatty liver disorders including NAFLD, Niederreiter & Tilg (2018). After prolonged lipid infiltration in the liver, progression to hepatocellular inflammation and fibrosis may occur, McCullough (2006). It has been reported that the amount of inflammation affects long-term outcomes of

liver disease including evolution of liver fibrosis, cirrhosis and hepatocellular carcinoma. Pro-inflammatory cytokines have been implicated in the pathogenesis of non-alcoholic fatty liver disease, Kumar et al (2012). Among the various cytokines, the pro-inflammatory interleukin (IL)-1-type cytokines and tumour necrosis factor (TNF)-α have emerged as key factors that play an important role in various stages of liver diseases mediating fundamental aspects of those diseases including acute phase protein synthesis, lipid metabolism, cholestasis and degree of fibrosis, Niederreiter & Tilg (2018).

TNF-α

TNF-α was identified as the first inflammatory molecule linking obesity with insulin resistance, Lang et al (1992); Hotamisligil et al (1993). TNF-α is composed of three 17-kDa polypeptides forming a compact trimer, Jones et al (1989). TNF- α is produced by a variety of cell types including monocyte/macrophages, neutrophils, and T-cells, as well as many other tissues, such as the endothelium, adipose tissue, or neuronal tissue. In the liver, TNF-α is secreted directly by hepatocytes and Kupffer cells or indirectly by abdominal fat, Braunersreuther et al (2012). The TNF-α trimer may activate inflammatory responses by binding to normally two distinct cell surface receptors of 55 kDa (TNFR-I) and 75 kDa (TNFR-II), Tartaglia & Goeddel (1992). Several clinical and animal studies have demonstrated TNF-α as a key factor in the development of NAFLD and NASH, Braunersreuther et al (2012); Seo et al (2013). Moreover, TNFα levels were increased in adult and paediatric NASH subjects relative to controls, Wigg et al (2001); Engstler et al (2016). In another clinical study, TNF-α levels were found to be significantly higher in NAFLD patients relative to control patients, however there was no significant difference in TNF-α levels between patients with NAFLD and those with NASH via liver biopsy diagnosis. Moreover, another cross-sectional study of patients with NASH, NAFLD, and control patients showed serum TNF-α and soluble TNF receptor 1 to be significantly higher in patients with NASH relative to patients with NAFLD and controls, Seo

et al (2013). In an animal study, mice treated thalidomide which prevents TNF-α production resulted in improvements in the hepatic alterations mediated by a high-fat diet, de Fraia et al (2010). This study was also confirmed in rats, where the use of anti-TNF-α antibodies in an experimental model of NASH decreased inflammation, necrosis, and fibrosis in rats, Koca et al (2008). The role for TNF-α in obesity and related metabolic dysregulation has been studied, Kern et al (1995). TNF-α expression was increased in obesity and levels decreased after weight loss, Dandona et al (1998). Moreover, TNF-α was overexpressed in white adipose tissue of obese rodent models, Xu et al (2002). Furthermore, it was observed that obese individuals with insulin resistance displayed a higher adipose TNF-α mRNA level compared to lean patients, Arner (2003), suggesting that TNF-α may play a role in the pathophysiology of insulin resistance.

Interleukins (IL)

Apart from tumor necrosis factor (TNF)-α, other pro-inflammatory interleukin (IL) type cytokines have found to play a role in pathogenesis of fatty liver diseases and in various aspects of liver diseases. Two pro-inflammatory interleukins, IL-1 and IL-6, have been extensively studied with the later emerged as key factor in fatty liver diseases, Niederreiter & Tilg (2018). IL-1 was the first cytokine identified and is recognised by receptors on virtually all cells and organs in the body, Dinarello (2009). IL-1 triggers inflammation via IL-1 receptors (IL-1Rs), Boraschi et al (2018). Previous studies have shown that inflammatory cytokines, particularly, IL-1 family (IL-1F) members, are implicated in the regulation of insulin resistance, adipose tissue inflammation and atherosclerosis, which all share common characteristics of NAFLD, Tilg & Moschen (2008); Hotamisligil (2017). Within the IL-1 family, IL-1R antagonist (IL-1Ra) and IL-37 are known to block the actions of IL-1 cytokines specifically at the receptor level and protect against liver inflammation. A previous study has reported that IL-1Ra anti-inflammatory mediator is present in the healthy liver, Matsukawa et al (1997). On the contrary,

IL-family members IL-1α, IL-1β, IL-18 are pro-inflammatory and are increased following lipid accumulation in hepatocytes contributing to inflammation, hepatic insulin resistance and fibrosis, Kamari et al (2011); Niederreiter & Tilg (2018).

Another pro-inflammatory interleukin that has been studied extensively in NAFLD is interleukin-6 (IL-6). Despite the interest in this cytokine, the role of IL-6 in liver pathology is very complex, and its involvement in the pathogenesis of NAFLD has not been fully understood, Braunersreuther et al (2012). IL-6 is known to activate several cells, including immune cells, hepatocytes, hematopoietic stem cells, and osteoclasts, Kishimoto (2010). Previous studies have reported that serum IL-6 levels were higher in animal models and patients with NAFLD, Cai et al (2005); Haukeland et al (2006). In humans with NASH, an association between IL-6 expression in hepatocytes and the severity of NAFLD has been reported, Wieckowska et al (2008). Blocking IL-6 in mice prevented liver damage but enhanced liver steatosis, Yamaguchi et al (2010). The link between insulin resistance which is a key feature of NAFLD and IL6 have been well defined. IL-6 produced by white adipose tissue (WAT) was found to contribute to insulin resistance observed in obese humans, Bastard et al (2002). Moreover, IL-6-deficient mice developed mature onset obesity and associated insulin resistance, Wallenius et al (2002).

1.5.1.1 Effect of diet on pro-inflammatory cytokines

Non-alcoholic fatty liver disease is strongly associated with obesity. Excess fat causes insulin resistance and inflammatory cytokine secretion, Tack et al (2012). Previous studies showed that poor diets are implicated in the activation of inflammation in various cells and tissues. Here we define a poor diet as any diet which either deficient or excessive in macronutrients such as protein, fat or carbohydrate. A study reported that protein malnutrition (5 g/kg) for 3 weeks increased LPS-induced NF-κB activation as well as transcription levels of its

downstream genes IL-1β and TNF-α compared to control mice (150 g/kg), Li et al. (2002). A study in mice compared the effect of long-term (8-weeks) high carbohydrate (HC, 64% carbohydrate, 19% protein, and 11% fat)) or high-fat (HF, 45% carbohydrate, 17% protein, and 38% fat) and standard rodent (chow) diet on secretion of TNF-α and monocyte chemoattractant protein-1 (MCP-1) inflammatory cytokines by the liver. This study reported increased plasma concentrations of TNF-α and MCP-1. Moreover, in the liver both diets (HC and HF) increased MCP-1 levels compared to control. However, the HC diet, but not the HF diet, increased TNF-α concentration in the liver suggesting that the influence on the type of proinflammatory cytokines may depend on the nature of nutrients consumed, Ferreira et al (1992). Another high fat study in male C57BL/6J mice showed significantly elevated serum TNF-α levels, Qiao et al (2019).

1.5.2 Oxidative stress and antioxidant activity

Oxidative stress is a key mediator of hepatic damage and a major contributor to the progression from simple steatosis to steatohepatitis, Sumida et al (2013). Oxidative stress is defined as an imbalance between the excessive formation of pro-oxidants (including ROS and/or reactive nitrogen species, (RNS) and antioxidant levels, Gornicka et al (2011); Ferramosca et al (2017); Sies et al (2017). Cellular regulation of oxidative stress is extremely important in maintaining cell homeostasis which can be achieved via the antioxidant system, by controlling the formation of ROS or RNS and repairing oxidative damage to cells Valko et al (2007); Simioni et al (2018). Previous studies have classified antioxidants into enzymatic or non-enzymatic antioxidants. Most common endogenous enzymatic antioxidants include superoxide dismutase (SOD), catalase (CAT), glutathione peroxidase (GPx), glutathione reductase (GSR). Other physiologically important non-enzymatic antioxidants include ascorbate, glutathione, α-tocopherol (vitamin E), ubiquinone, thioredoxin (TRX), bilirubin, Ore et al (2019). For the purpose of this thesis, GSR and TRX antioxidants are discussed.

Controlling ROS via GSR and TRX

Activation of nuclear factor E2-related factor 2 (Nrf2; Nfe2l2 gene name) is critical in counteracting the detrimental effects of ROS and electrophiles on cells. Nrf2 is known to play an important role in regulating the expression of many antioxidant enzymes including glutathione (GSH) and TRX antioxidant system, Tonelli et al (2018). Glutathione reductase catalyses the reduction of glutathione disulfide (GSSG) to the sulfhydryl form GSH, a critical molecule in resisting oxidative stress and maintaining the reducing environment of cells, Deponte (2013). A previous study has reported that only two cytosolic enzymes can channel reducing power from NADPH into disulfide reduction reactions and these are thioredoxin reductase-1 (TrxR1) and glutathione reductase (Gsr). The thioredoxin system, composed of the selenoenzyme thioredoxin reductase (TrxR), thioredoxin (Trx), and NADPH, plays a key role in redox regulation and is involved in many signaling pathways, Fang & Holmgren (2006). TrxR1 reduces the active site disulfide in oxidized thioredoxin-1 (Trx1) into a dithiol whilst Gsr reduces glutathione disulfide (GSSG) into 2GSH, which can reduce oxidized glutaredoxins (Grxs), Prigge et al (2017). Moreover, Prigge et al showed that show that liver-specific co-disruption of the genes encoding Trx1, TrxR1, and Gsr (triplenull) causes dramatic hepatocyte hyperproliferation, Prigge et al (2017). In a previous study, a 13-week HFD-induced insulin-resistant mouse model (HFD composed of 50% fat, 36% carbohydrate and 14% protein), it was reported that liver Trx and TrxR expression were significantly decreased compared to control (composed of 12% fat, 62% carbohydrate and 26% protein) suggesting impairment of lipid metabolism via induction of oxidative stress, Qin et al (2014).

1.6 Gut microbiota and NAFLD

1.6.1 Gut microbiota community

Animals and humans have a collection of diverse micro-organisms living in their gut. These groups of microbes that mutually inhabit their hosts are popularly referred to as microbiota, microflora or normal flora, Neish (2009). This community of microbes among others includes viruses, archaea and bacteria which have received increasing attention in the past few years. The gut harbours the largest number of bacteria, consisting of more than 150-fold of their eukaryotic nuclear genome, Qin et al (2010). More than 10^{14} bacteria are said to colonise the human gut. This figure is 10 times more than the overall number of human cell in our bodies. Moreover, there are over 1000 distinct species of bacteria inhabiting the human intestinal tract, which collectively constitute over 100 trillion organisms. Again, the gastrointestinal tract which is the major coloniser organ has about 70% of entire human microbes inhabit in the colon alone, Ley et al (2006). The availability of molecules in the gut that can be used by bacteria as nutrients for the makes it the preferred site for colonization; Schloss and Handelsman (2004) showed that despite the over 50 bacterial phyla described so far, only two major of them dominate the human gut microbiota Bacteroidetes and the Firmicutes, in relation to Proteobacteria, Verrucomicrobia, Actinobacteria, Fusobacteria, and Cyanobacteria that constitute minor populations, Eckburg et al (2005). The phylum Firmicutes consist of a diverse group that comprises Gram-positive bacteria from more than 200 different genera such as *Catenibacterium*, *Clostridium*, *Eubacterium*, *Dorea*, *Faecalibacterium*, *Lactobacillus*, *Roseburia*, *Ruminococcus* and *Veillonella*. The phylum Bacteroidetes comprises mainly Gram-negative bacteria from ∼20 genera including *Bacteroides*, *Odoribacter*, *Prevotella* and *Tannerella*, Tremaroli & Backhed (2012). Apart from these two major phyla, there are other common but less abundant gut microbiota such as Actinobacteria (*Bifidobacterium*,

Collinsella), Proteobacteria (*Bilophila*, *Desulfovibrio*, *Escherichia*) and Verrucomicrobia (*Akkermansia*), Eckburg et al (2005).

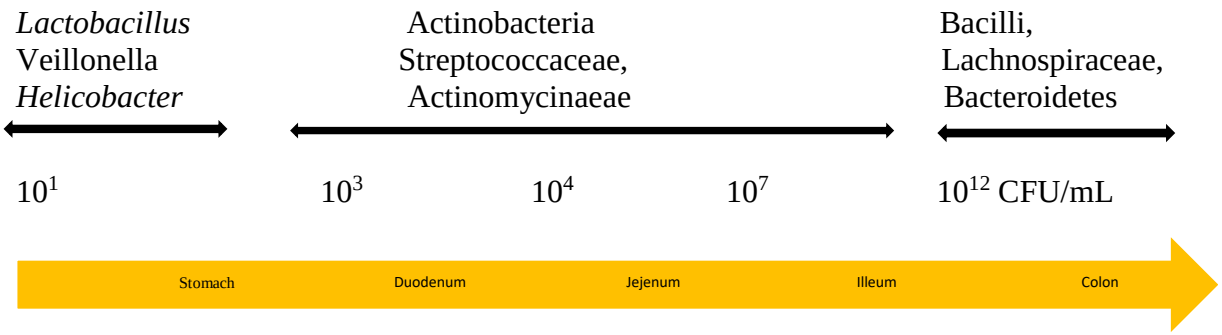

Figure 1.8: Increasing numbers and diversity of microbiota in the GI tract

The above figure shows that the intestinal microbiota is not evenly distributed. The amount of bacterial cells present in the mammalian gut increases from 10^1 to 10^3 bacteria per gram of contents in the stomach and duodenum, this is further increased to 10^4 to 10^7 bacteria per gram in the jejunum and ileum and progressing to 10^{11} to 10^{12} cells per gram in the colon.

1.6.2 Formation of the gut microbiome

The development of the gut microbiota begins after birth where the host genotype, mode of delivery and early feeding influence which microbes colonize the infant gastrointestinal tract, Lozupone et al (2012). The initial establishment of the human gut microbiota is believed to occur immediately after birth, which is dominated by key gut commensal bacteria genus *Bifidobacteria* known to be generally acquired from the mother, Turroni et al (2020). The early gut microbiota composition in vaginally delivered infants is similar to the vaginal microbiota of the mother which is mainly Lactobacillus and Prevotella species. In comparison, infants delivered through caesarean section have early gut microbiota that resemble that of the mothers' skin, mostly *Staphylococcus* species, Dominguez-Bello et al (2010). Again, depending on whether infants are breast or formula fed could determine the early microbial inhabitants, Azad et al (2013). Within the first 3 years of life, the diversity of the gut microbiota increases till it reaches a level comparable to that of the adult, Yatsunenko et al (2012).

According to Faith et al (2013) generally, there is stability of the individual's gut microbiota, however, the relative abundance of bacterial species varies depending on an adults' individual's physiological state. This has been demonstrated by a number of studies including altered gut microbiota in pregnancy, obesity, type 2 diabetes, Koren et al (2012); Turnbaugh et al (2009) & Kalsson et al (2013).

1.6.3 Functions of the gut microbiota

The gut microbial community performs different physiological functions, including gut protection and metabolic regulation such as playing an active role in glucose and lipid metabolism, Prakash et al (2011). Recent studies implicate gut microbiota in the development of insulin resistance and obesity, Ley et al (2005); Ley et al (2006); Myers-Morales et al (2013); Bäckhed et al (2004), suggesting gut microbiota may play a role NAFLD. The close anatomical and functional relationship between gut and liver, through portal circulation may favour bidirectional influences, Compare et al (2012). For example, the liver receives about 70% of its blood supply from the intestine, representing the first line of defence against gut-derived antigens, Compare et al (2012). Thus, the gut microbiome may be critical in the maintenance of gut-liver axis health and in NAFLD pathogenesis.

The gut microbiota plays an integral role in human metabolism by contributing enzymes that are not encoded by the human genome, for instance, for the breakdown of polysaccharides, polyphenols and vitamin synthesis. Evidence for the role of the microbiota in metabolism of dietary components and for its effect on health have been derived from comparative studies in germ-free and conventional microbiota, or human microbiota-associated animals, and from in vitro studies using human faecal incubations or more complex continuous culture gut models. Also, observational studies where faecal microbiota of healthy subjects are compared with those of patients have strongly suggested that the gut microbiota plays a significant role in the

cause and/or development of a wide range of gastrointestinal diseases and conditions including inflammatory bowel disease, irritable bowel syndrome, colon cancer, and antibiotic-associated diarrhoea. In recent times, evidence has been accumulating that seem to suggest that microbiota may also be involved in obesity and diabetes, Greenblum et al (2012): Marchesi et al (2016).

1.6.3.1 The role of gut microbiota in specific metabolic pathways

Several mechanisms have been proposed on how gut microbiota contribute to the pathogenesis of NAFLD and other metabolic disorders. These include the gut microbiota role in increasing production and absorption of gut short-chain fatty acids (SCFAs), altered dietary choline metabolism as well as bile acid pools changes, increased delivery of microbiota-derived ethanol to liver; changes in gut permeability and release of endotoxin; and interaction between specific diet and microbiota, Yu et al (2016).

Turnbaugh et al showed that the cecum of ob/ob mice has an increased concentration of SCFAs and that transplantation of germ-free mice with the gut microbiome from ob/ob mice caused greater fat gain than transplants from lean animals, Turnbaugh et al (2006). Studies in humans also revealed an increased production of SCFAs by the gut microbiota in overweight and obese people compared to lean subjects, Schwiertz et al (2010). SCFAs account for a large part of caloric intake of the host, and they enhance intestinal absorption through activation of GLP-2 signaling, Zhu et al (2014). Alterations to gut microbiota affect signaling pathways of host energy metabolism, Cani & Delzenne (2009). Further, microbial metabolites and cell components are also involved in the development of hepatic steatosis and inflammation. Altered gut microbiota in ob/ob mice, Ley et al (2005) and obese patients, (Ley et al (2006)) exhibited a reduced abundance of Bacteroidetes and proportionally increased abundance of Firmicutes.

Dietary choline is necessary for VLDL synthesis and hepatic lipid export. Dietary choline-deficiency caused increased hepatic steatosis which could be reversed by choline supplementation, Buchman et al (1995). In hepatocytes, bile acids are synthesized from cholesterol via enzymatic pathways and then conjugated with either glycine or taurine before secretion into bile and released into the small intestine. The role of conjugated bile acids includes supporting lipid absorption and transport as well as acting as nuclear receptor binders and to have a putative role in altering the microbiome, Russell (2003). Activation of bile acid receptors with a receptor agonist was reported to improve NAFLD histology in an obese mouse model, McMahan et al (2013).

Endogenous alcohol, ethanol, is produced naturally in all living humans. The resulting blood alcohol concentration is generally low. The concentrations of endogenous ethanol in the peripheral venous blood of healthy patients and those suffering from metabolic disorders such as diabetes, cirrhosis, or hepatitis ranged from 0 to 0.08 mg/dl captured in a study by Bukong et al (2016). Zhu et al observed that NASH patients exhibited significantly elevated blood ethanol levels. Similar blood ethanol concentrations levels were observed between healthy subjects and obese non-NASH patients, Zhu et al (2013).

The gut microbiota help maintain the integrity of the intestinal barrier and therefore alterations in the composition of microbiota may lead to increased intestinal permeability and subsequent overflow of harmful bacterial by-products to the liver which can then trigger hepatic inflammation and metabolic disorders. Endotoxemia readily induces steatohepatitis in obese rats and mice, Yang et al (1997). Murine NAFLD models of bacterial overgrowth develop compositional changes of the gut microbiota and increased intestinal permeability, whilst the expression of tight junction proteins was reduced, Miele et al (2009). Similarly, studies in humans have reported a disruption in the intestinal barrier of biopsy-proven NAFLD patients in addition to increased rate of small bowel bacteria overgrowth which means that changes in

the microbiome may contribute to disturbance of gut barrier integrity, Miele et al (2009). Evidence suggests that excess fructose consumption results in pathogenesis of NAFLD via upregulation of de novo lipogenesis and inhibition fatty acid β-oxidation, Lim et al (2010). A study using fructose-induced NAFLD mouse model revealed fructose to significantly decrease *Bifidobacterium* and *Lactobacillus* and increase endotoxemia, Jin et al (2014). Probiotic bacterial strains of *Lactobacillus* attenuated high-fructose-induced NAFLD in rats, Hsieh et al (2013).

1.6.4 Gut microbiota metabolism of carbohydrates and SCFA synthesis

A previous study has reported changes in the composition of the gut microbiota in response to the total quantity of carbohydrate intake in obese people. Thus, *Bifidobacteria* showed a significant reduction with decreased carbohydrate intake and some Clostridium subgroups (*Roseburia* and *Eubacterium rectale*), which correlated strongly with the reduction in stool butyrate levels, Duncan et al (2007). To survive in the large intestine, bacteria rely on substrates that are undigested in the upper digestive tract. Some bacteria such as Saccharolytic bacterial fermentation products are generally beneficial metabolites, whereas if there is limited carbohydrate, bacteria tend to rely on an alternative energy sources leading to the secretion of other metabolites that may be more harmful to human health, Boyd et al (2013). The major products of bacterial fermentation following the fermentation of dietary carbohydrates are SCFAs and gases. It is known that in the gut, there is high concentration of bacteria in the colonic lumen (90–95%) and this is because of the increased availability of faecal SCFA concentrations in the colon which create a favorable niche for these bacteria, Venegas et al (2019). Changing the carbohydrate content of the diet can also alter the faecal SCFA profile by affecting the bacterial composition. Reducing the carbohydrate content of the diet significantly reduced both faecal butyrate concentrations and numbers of the Roseburia/E. rectale group in human studies, Duncan et al (2007), while wheat bran supplementation

(consisting of >70% arabinoxylan oligo-saccharides; AXOS) raised the abundance of all three predominant SCFAs and thus also total SCFA concentrations, François et al (2012). However, it is probable that the indiscriminate increases in faecal SCFA concentrations observed in studies where the fibre content of the diet is increased are at least partly caused by the increased faecal bulking and reduced transit time resulting in decreased colonic absorption of SCFAs.

Short chain fatty acids

Acetate, propionate, and butyrate are the three most abundant SCFAs normally present in faecal samples in molar ratios which range from 3:1:1 to 10:2:1. These ratios have been shown to be consistent with values detected within the intestine in early sudden death victims, Macfarlane et al (1992). These three main short chain fatty acids (SCFA) perform very different but important roles in the human body. Butyrate is arguably the most important SCFA for human health. It constitutes the main energy source for human colonocytes and also has potential anti-cancer activity through the ability to induce apoptosis of colon cancer cells and its ability to regulate gene expression by inhibiting histone deacetylases, Steliou et al (2012). There is also evidence that butyrate can activate intestinal gluconeogenesis (IGN) via a cAMP-dependent mechanism with beneficial effects on glucose and energy homeostasis, De Vadder et al (2014). Propionate is an energy source for the epithelial cells but is also transferred to the liver where it also plays a role in gluconeogenesis. Propionate is increasingly thought to be an important molecule in satiety signalling as it interacts with the gut receptors (G protein-coupled receptor, GPR) GPR 41 and GPR 43, and in turn activate intestinal gluconeogenesis, Brown et al (2003). The conversion of propionate to glucose in intestinal gluconeogenesis directly promotes energy homeostasis by reducing the production of hepatic glucose, and consequently reduces adiposity, De Vadder et al (2014).

Acetate is the most abundant SCFA and is an essential co-factor/metabolite for the growth of other bacteria. For example, *Faecalibacterium prausnitzii* will not grow in pure culture in the absence of acetate, Duncan et al (2004). Within the human body, acetate is transported to the peripheral tissues and used in cholesterol metabolism and lipogenesis, and recent evidence from studies in mice indicates that it also plays a significant role in central appetite regulation, Frost et al (2014).

While many bacteria produce acetate, other specific bacteria tend to produce propionate and butyrate, Luis et al (2017); Reichardt et al (2014). Within the environment of the gut, the predominant butyrate producers are Firmicutes including some Lachnospiraceae and also *Faecalibacterium prausnitzii*, whilst propionate is produced by *Bacteroides* species, Negativicutes, and also some *Clostridium* species. Metagenomic screening of over 3000 sequenced bacterial genomes identified many other species containing butyrate production pathways, with no consistency within families, Vital et al (2014). Since the production of SCFA is not defined by bacterial phylogeny, diverse techniques which target key genes are needed to enumerate bacteria with specific metabolic activities. Louis and co-workers identified two major routes of butyrate production, Louis et al (2004) and three pathways for propionate production, Reichardt et al (2014) amongst the colonic microbiota. The primers designed against key metabolic genes in these pathways can provide help to enumerate functional groups of bacteria in different cohorts. They suggested that this approach may prove more useful than the current focus on the 16S rRNA gene, which gives information about the bacterial composition but does not indicate anything about fluctuations in metabolic activities.

It is relevant to note that propionate and butyrate can also be formed from peptide and amino-acid fermentation by certain Bacteroidetes and Firmicutes species Louis & Flint (2016). In

vitro studies have shown that aspartate, alanine, threonine, and methionine are the main sources of propionate, whereas butyrate is predominantly resulted from fermentation of glutamate, lysine, histidine, cysteine, serine, and methionine, Louis & Flint (2017). A targeted gene approach revealed that most bacteria either had the ability to synthesize propionate or butyrate but very few had genetic capacity to produce both, Reichardt et al (2014). However, some bacteria can alter their fermentation and produce different SCFA in the presence of different, substrate-dependent, growth conditions. *Roseburia inulinivorans* is a butyrate producer, but during growth on fucose, it is able to completely change its gene expression pattern, switching on a set of genes capable of using fucose as a source of energy, and synthesizing propionate and propanol via a propanediol utilization pathway, Scott et al (2006). *Ruminococcus obeum* produces acetate, formate, and lactate during growth on glucose on pure culture, but in addition produces propionate during growth on fucose using the propanediol utilization pathway, Reichardt et al (2014). Fucose is a particularly important alternative dietary substrate, since many of the epithelial glycoconjugates are fucosylated. The ability of a bacterium to flick a metabolic switch and change its metabolism, and metabolic products, may give the bacterium a competitive advantage during times of low substrate availability. In *Bacteroides thetaiotaomicron*, the presence of fucose as a growth substrate not only stimulates expression of genes involved in fucose metabolism, but intracellular fucose levels are also important in activating a signalling mechanism to the host, upregulating synthesis of fucosylated glycans and thus ensuring a continued supply of substrate to the bacterium, Hooper et al (1999). This whole alternative metabolism is increased during periods of nutrient depletion, and it may also be relevant in early colonization events in the infant gut, El Aidy et al (2013).

1.6.5 Protein degradation by gut microbiota

A previous study based on culture techniques identified *Bacteroides* and *Propionibacterium* species as the predominant proteolytic species in faecal samples, with proteolysis common also amongst *Clostridia*, *Streptococci*, *Staphylococci*, and *Bacillus* species. Furthermore, Gibson et al showed that the proteolytic activity of the faecal microbiota differed, both in quantity and quality of protein breakdown, from that in the ileum, Gibson et al (1989). Aromatic amino acids such as phenylalanine, tyrosine, and tryptophan can be fermented to phenylpropanoid metabolites, phenylacetic acid, and 4-hydroxyphenyl-acetic acid, which are abundant in faeces, Russell et al (2013). The organisms involved include several species of *Bacteroides*, *Eubacterium hallii*, and *Clostridium barlettii*. Interestingly, these phenolic compounds are the same as those generated by microbial breakdown of plant polyphenols.

1.6.6 The effect of diet on gut microbiota

Microbiota composition can be modified by changing dietary composition. A Western-type of diet (high fat) or low protein diet can change the microbiota unfavourably, resulting in increased Firmicutes and decreased Bacteriodetes, Chen et al (2015). Phylum-level changes have been identified in faecal microbiota affected by dietary composition and duration of feeding. It is possible that the metabolic effect of poor diet intake can be modulated by specific gut microbiota. Protein deficient diet alters the gut microbiota at different taxonomic level. Evidence of effect of diet on gut microbiota are summarized in the table 1

Table 1.2 Dietary fat/protein alters gut microbiota resulting inflammatory effect associated with NAFLD

Diet	Experimental model	Effect on gut microbiota	Metabolic or inflammatory effect
High fat (35% energy from fat)	*in vivo* in rats	Decrease of genera within the class Clostridia in the ileum. Increase Bacteroidales in large intestine, Hamilton et al (2015)	Increase lipopolysaccharides (LPS), pro-inflammatory cytokines (Toll-like receptors (TLRs), nuclear factor kappa (NF-kB), Baothman et al (2016).
	in vivo in mice	Increase Firmicutes to Bacteriodetes ratio, Kim et al (2012).	
	in vivo in rats	And increased Enterobecteriaceae, Chen et al (2015)	
	in vivo in rats	Increase Bacteroidales, Clostridiales and Enterobacteriales, de La Serre et al (2010)	
High protein (>20% of total energy from protein)	*in vivo* in humans	Increased levels of *Clostridium spp*. and *Bacteroides spp*., Houghton et al (2016).	Low butyrate production; increased endotoxemia; impaired mucus barrier function; decreased insulin sensitivity, Cani et al (2007).
	in vivo in humans	Decreased level of *Bifidobacterium spp*., *Roseburia spp*., and *Eubacterium spp*., Russell et al (2011)	
Normal protein (20% total energy from protein)	*in vivo* in mice	Bacteroidetes and Firmicutes decreased whilst Verrucomicrobia, Tenericutes, and Proteobacteria increased after 14 days (postweaning mice). Verrucomicrobia, Tenericutes decreased after further 10 days whilst Firmicutes and Proteobacteria increased this time, Mayneris-Perxachs et al (2016).	
Protein deficient (2% of total energy from protein)	*in vivo* in mice	Post weaning increased in Verrucomicrobia. No decrease in Bacteroidetes but post weaning loss of Firmicutes observed, Mayneris-Perxachs et al (2016).	Increased lipocalin-2 and myeloperoxidase in the stool (inflammatory markers),
(13% of LPD)	*in vivo* in pigs	Increased in genera of Prevotella and Coprococcus (in the caecum) as well as Sarcina, Subdoligranulum, Coprococcus, and Mogibacterium (in the colon) but decreased genera abundance of Lactobacillus (in the caecum) and Streptococcus in the colon of pigs, Zhou et al (2016).	Mayneris-Perxachs et al (2016). Decreased in isobutyrate, isovalerate and branch chain proportion (BCP)

1.7 Models of NAFLD

Animal models have played a critical role in elucidating the pathophysiological mechanisms of NAFLD and continue to do so. However, it is important to note that translation of results obtained in an animal model to a human population has repeatedly failed, Hebbard et al (2011). Therefore, selecting the right animal model for preclinical study is critical in order to be useful to study human disease and draw important conclusions. In NAFLD and related diseases, mice and rats have been used most frequently for modelling human NAFLD. The C57BL/6 strain in mice and Wistar and Sprague Dawley strains in rats are considered to be ideal preclinical animal model for studying human metabolic diseases since they are cheap, easy to handle and above all susceptible to develop obesity, type 2 diabetes and NAFLD, Kohli & Feldstein (2011). In our current study, male C57BL/6 mice were used in all experiments since they are easy to handle and comparatively cheaper than rats. Previous studies have reported that, wild type C57BL/6 male mice fed a high fat diet (HFD, 60% calories as fat [91% lard; 9% soybean oil, Research Diets)] or a high fat-high cholesterol diet [HFHC, 54% calories as fat + cholesterol (0.5 % w/w)] become obese and develop glucose intolerance (diabetes), hepatosteatosis and mild hepatic inflammation (Jump, 2016). In this thesis, we used (HFD, 60% calories as fat [91% lard; 9% soybean oil, Research Diets)] for the dietary fat studies.

Germ free and specific pathogen free models are good strategies to avoid the frustration with the presence of disease or infection as an unwanted variable in experiments, however, translation in human trials is often a challenge since the gut microbiota do not depict that of the "normal" environment, Lane-Petter (1962). The SPF methods are in direct contrast to breeding conventional healthy animals (sometimes called 'dirty' animals) in open cages in a controlled, health-monitored and more natural environment of antigenic exposures and indigenous gut flora. However, the conventional animals are more prone to diseases or infection which could affect the overall goal of the experiment. Given the variations in existing animal models, and

the difficulty associated with obtaining a model that perfectly satisfies all the criteria for an ideal animal model, in this thesis, SPF mice were used to investigate the role of gut microbiota in lipid metabolism as this was relatively cheaper than using germ free mice, Dobson et al (2019).

1.8 Rationale and hypothesis of this thesis

Non-alcoholic fatty liver disease remains a global health challenge as there is already high prevalence of the condition in the Western world. In recent times the frequency of this condition has been growing in the developing countries particularly in Africa, South America and the middle East. OCFAs (C15:0 &C17:0) have emerged as biomarkers for predicting metabolic diseases including NAFLD. Therefore, determining the factors that affect their levels will be important to understand the aetiology of NAFLD and could provide a mechanistic insight into their possible treatment route. It is thought that gut microbiota can influence lipid metabolism. Therefore, we wanted to understand how gut microbiota affect lipid metabolism in the state of high fat feeding. Moreover, there is the need to better understand on the effect of dietary protein is on lipid metabolism; thereafter the effect of decreased dietary protein on lipid metabolism was studied. Overall, we hypothesized that low protein or high fat diets alter the gut microbiota and impair odd-chain fatty acid metabolism leading to the pathogenesis of NAFLD.

1.9 Study aim and objectives

1.9.1 Study aims

The main aim of this study was to investigate the effect of dietary fat/protein on lipid metabolism and gut microbiota in mice. The specific aims were to:

1. characterize the differences in serum & liver FAs of male mice with protein-deficient diets/following high fat diets compared to those from control
2. investigate the differences in gut microbiota in male mice following high fat diets compared to control
3. elucidate the hepatic transcript expression related to specific fatty acid changes in the liver/serum in mice on protein deficient diets/high fat diets
4. determine gene and protein expression of hepatic lipid metabolism in mice following protein deficient diets/high fat diets.

1.9.2 Objectives

1. Serum and liver FA analyses of protein and fat diet studies were performed with either GC-FID or GC-MS
2. Hepatic transcript expression related to specific fatty acid changes in the liver/serum of dietary fat/protein study were characterized using qPCR
3. Basic liver histological technique, H&E staining was used to investigate hepatic lipid accumulation.
4. Peroxisome biogenesis protein expressions in fixed liver tissue were performed using immunohistochemistry technique.
5. The gut microbiota of the high fat diet model were characterized by 16S rRNA sequencing platform

Chapter 2

2 Materials and methods

2.1 Animals and treatment

2.1.1 Housing and environmental conditions

Male C57BL/6 males either maintained in normal husbandry or specific pathogen free (SPF) facility were used for the experiments in this thesis. Normal husbandry facility has no barrier or microbiota restrictions. Animals were housed either singly per cage or grouped depending on the experimental type under controlled conditions of light (12/12 h light-dark cycle) and temperature (20-22°C), with *ad libitum* access to chow and water. After five days of acclimatisation, the mice were used for the experiments. In this thesis, three high fat and two low protein dietary models were used. The LPD (Aston and Nottingham) models which were carried out in facilities in UK and the HFD (4-week SPF, 4-weeks normal husbandry and 12-week normal husbandry) models which were carried out in facilities in China. All animal experiments in the protein study were carried out in strict accordance with the UK Home Office guidelines and the Animal Scientific Procedures Act (1986) under the project licence number PPL30/3253. The high fat diet experimental procedures were conducted under the State Council of the People's Republic of China (Decree No. 2 of the State Science and Technology Commission) October 31, 1988. Amendment Regulations and approval of the local ethics committee for use effective March 1, 2017.

2.1.2 Low Protein dietary treatments

In this thesis, two different low protein dietary models were studied. One was set up in Aston University's Biomedical Research Unit and the other was set up at the University of Nottingham medical school facility. The procedures for dietary treatment in both models were similar. Briefly, eight (8) week old C57BL/6 males were maintained at Aston University's Biomedical Research Unit or University of Nottingham medical school's facility on a 07:00–19:00 light-dark cycle at a temperature of 20–22°C with *ad libitum* access to chow and water

for 5 days. In the Aston cohort, following acclimatisation, weight matched male mice were housed singly and fed one of three different diets either control normal protein diet (18 % casein; n = 8) isocaloric low protein diet (LPD) (9% casein; n = 8) or LPD supplemented with/without methyl donors (5 g/kg diet choline chloride, 15 g/kg diet betaine, 7.5 g/kg diet methionine, 15 mg/kg diet folic acid, 1.5 mg/kg diet vitamin B12; termed MD-LPD). Similarly, in the Nottingham group, mice were housed singly and fed either normal protein diet with methyl donors (MD-NPD), a low protein diet without methyl donor component, (LPD) and a low protein diet with methyl donor (MD-LPD) isocaloric with LPD (Special Dietary Services Ltd, UK, Table 2.1 and 2.2, respectively). Here, we housed the mice singly based on the fact that in experiments involving food intake and/or energy expenditure, social housing often is not feasible especially when individual intakes are the critical measures to ensure reproducibility of each sample, Robertson & Rowland (2005). Furthermore, mice are notoriously known to eat their faeces. All diets were given *ad libitum* for at least 7 weeks for Aston and 8 weeks for Nottingham group prior to culling via cervical dislocation for the collection of tissues. In both models, blood samples were collected via heart puncture and allowed to clot on ice before centrifugation at 10,000 rpm, 4 °C for 10 minutes. Isolated serum was aliquoted, snap frozen and stored at -80 °C. Samples of liver, kidneys, heart, lungs, testes, and gonadal fat were removed, weighed, snap frozen and stored at -80 °C. Moreover, in the case of Nottingham samples faecal samples were collected and stored in -80 °C freezer.

Table 2.1: Dietary composition of Aston low protein diet

Diet Type (w/w)	NPD (18% Casein w/w)	LPD (9% Casein w/w)	MD-LPD (9% Casein w/w)
Starch (%)	42.5	48.50	48.50
Sucrose (%)	21.30	24.30	24.30
Casein (%)	18.00	9.00	9.00
Corn Oil (%)	10.00	10.00	10.00
Cellulose (%)	5.00	5.00	5.00
Minerals (%)	2.00	2.00	2.00
DL-methionine (%)	0.50	0.50	0.50
Vitamins (%)	0.50	0.50	0.50
Choline chloride (%)	0.20	0.20	0.20
Extra choline chloride (g/kg)	-	-	5.00
Betain (g/kg)	-	-	15.00
Extra methionine (g/kg)	-	-	7.50
Folic acid (mg/kg)	-	-	15.00
Vitamin B12(mg/kg)	-	-	1.50

Note: Protein energy loss in LPD was compensated for by only carbohydrate

Table 2.2: Dietary composition of Nottingham low protein diet

g / kg	MD-NPD (16.5% kcal^{-1} protein)	LPD (9% kcal^{-1} protein)	MD-LPD (9% kcal^{-1} protein)
Casein	175.2	98.9	96.0
Corn starch	413.6	467.0	453.3
Fibre	48.7	54.9	53.3
Sucrose	207.3	234.1	227.2
Choline chloride	1.9	2.2	2.1
DL-Methionine	4.9	5.5	5.3
AIN-76 mineral mix	19.5	22.0	21.3
AIN-76 vitamin mix	4.9	5.5	5.3
Corn oil (gm/kl)	97.3	109.9	106.7
Choline chloride	4.9	0	5
Betaine	14.6	0	16
Methionine	7.3	0	8
Folic acid	0.0146	0.000	0.016
Vitamin B12	0.0015	0.000	0.002
Weight (g)	1000.0	1000	1000

Note: Protein loss in LPD group were compensated for by nutrient balance of all dietary composition including fibre, fat, minerals.

Glucose tolerance test of Nottingham low protein diet

A glucose tolerance was determined at the end of 8 weeks of feeding. The mice were fasted overnight, with access to water *ad libitum*, and weighed immediately prior to glucose tolerance testing (GTT). Following weight measurement, fasting blood glucose levels were determined in a sample collected from the tail vein using a hand-held glucometer (Freestyle Optium, UK). Subsequently, glucose bolus (2g/kg body weight in PBS) was administered via intraperitoneal injection. Blood samples were collected from the tail vein at 15, 30, 60 and120 minutes post-bolus for determination of glucose concentration (figure 2.1). MD-LPD blood glucose concentration was higher at baseline (0), 15 and 30 minutes (area under the curve, AUC;

p<0.001, p=0.001 and p<0.001, respectively) compared to MD-LPD. However, from an hour time this difference disappeared. In terms of methyl donor effect on blood glucose, LPD mice displayed high glucose concentration from baseline to 15 minutes (AUC; p<0.001 and p=0.006, respectively) until this difference disappeared to the end of glucose tolerance test (GTT).

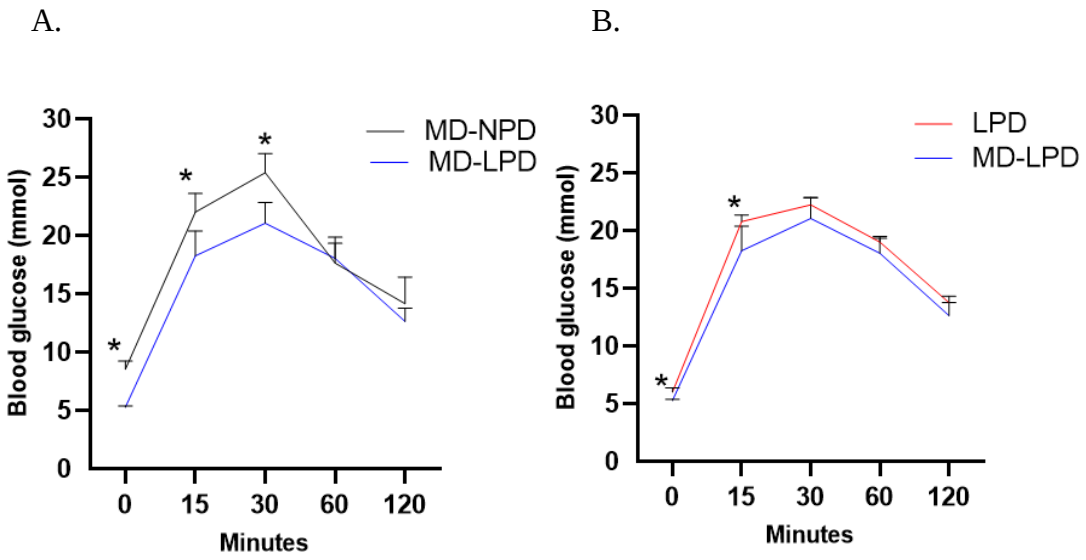

Figure 2.1: Glucose tolerance test.

Data represent mean ± SEM. Male mice with MD-NPD; 16.5% kcal^{-1} protein, n=8, LPD; 9% 16.5% kcal^{-1} protein, n=8 and male mice fed with MD-LPD, 16.5% kcal^{-1} protein, n=8. There were no significant changes at the end of GTT between MD-NPD vs MD-LPD or LPD vs MD-LPD of feeding (week 8)

Table 2.3: Fatty acid composition of both models (Aston and Nottingham)

	NPD		LPD	
Fatty acid	g/kg diet	%	g/kg diet	%
C12:0	0.02	0.25	0.01	0.13
C14:0	0.02	0.25	0.01	0.13
C14 1	0.01	0.12	0.01	0.13
C16:0	1.01	12.56	0.99	12.44
C16 :1	0.01	0.12	0.01	0.13
C18:0	0.22	2.74	0.21	2.63
C18 :1n9	2.37	29.48	2.35	29.52
C18 :2n6	4.3	53.48	4.29	53.89
C18 :3n3	0.08	1.00	0.08	1.00
C20 :4n6	0	0	0	0
C22 :5n3	0	0	0	0
Total	8.04	100.0	7.96	100.0
SFA		15.80		15.33
MUFA		29.72		29.78
PUFA		54.48		54.89

Dietary fat compositions. Both Aston and Nottingham diets had same FA composition

2.1.3 High fat dietary treatment

Four (4) week old C57BL/6 male mice (n=20) were maintained in Nanjing- China SPF animal facility on a 07.00-19.00 day/light cycle at 20-22°C with food and water ad libitum. They were housed 4 in a cage and fed either chow or HFD ad libitum for 4 weeks. The body weight of the mice was taken every week. In another HFD feeding experiment, 20 male mice were maintained in normal husbandry for either 4 or 12 weeks on similar conditions as the SPF raised mice (n = 5-10/group, table 2.4). The animals in the high fat diet (HFD) treated group were fed a 60% fat, 20% carbohydrate and 20% protein per kcal% while the animals in the

control (CD)-treated group received a 10% fat, 70% carbohydrate and 20% protein per kcal% (table 2.5). At the end of their respective periods of feeding mice were culled through cervical dislocation for tissue collection. Isolated serum was aliquoted, snap frozen and stored at -80°C freezer. Liver, kidneys, heart, lungs, testes, and gonadal fat were removed, and with systematic sampling part of the tissues were snap frozen and stored at -80 °C whilst others were fixed in 4% formaldehyde for histological analyses. Faecal samples were also collected and stored in -80 °C freezer. The growth rate of the mice fed high fat diet in an SPF facility is shown below (figure 2.4).

Table 2.4: Details of the different high fat diet feeding experiments.

Condition	**SPF**	**SPF**	**Normal husbandry**	**Normal husbandry**	**Normal husbandry**	**Normal husbandry**
Treatments &	CD	HFD	CD	HFD	CD	HFD
Period (week)	4	4	4	4	12	12
Sample size	10	10	5	5	5	5

Table 2.5: Dietary composition of high fat diet used for both SPF and normal husbandry conditions

	Control Diet		**HFD**	
	% by weight	% of energy	% by weight	% of energy
Protein	19.2	20	26.2	20
CHO	67.3	70	26.3	20
Fat	4.3	10	34.9	60
Total		100		100
kcal/g	3.85		5.24	

	Control Diet		**HFD**	
	G	Kcal	g	Kcal
Sucrose	350	1400	68.8	275.2
Soybean oil	25	225	25	225
Lard	20	180	245	2205
Total	1055	4057	774	4057

Diets compositions. Data from Research Diet Inc. website: g-grams (http://www.researchdiets.com/opensource-diets/stock-diets/dio-series-diets)

Table 2.6: Fatty acid composition of SPF and normal husbandry conditions dietary fat

	Control Diet (D12450B)		**HFD (D12492)**	
Fatty acid	g/kg diet	% by weight	g/kg diet	% by weight
16:0	6.5	15.1	49.9	20.3
16:1	0.3	0.7	3.4	1.4
18:0	3.1	7.2	26.9	10.9
18:1n9	12.6	29.2	86.6	35.2
18:2n6	18.3	42.5	73.1	29.7
18:3n3	2.2	5.1	5.2	2.1
20:4n6	0.1	0.2	0.7	0.3
Total	43.1	100.0	246.0	100.0
SFA		22.0		31.0
MUFA		30.0		37.0
PUFA		48.0		32.0

Fatty acid profile of the diets. Data from Research Diet Inc. website (http://www.researchdiets.com/opensource-diets/stock-diets/dio-series-diets).

2.1.4 Dissection of liver tissues

At the study end, the animals were sacrificed by rapid cervical dislocation for liver histology, fatty acid and gene expression analyses. Using a fine scalpel, the liver tissues were dissected out and weighed. In some experiments, half were dissected out and fixed in 4% formaldehyde for histological analyses. The rest of the liver tissue was snap frozen in liquid nitrogen and stored at -80ºC prior to fatty acid and gene expression analysis.

2.2 GC-FID/MS-based FA analyses

Metabolomics refers to the comprehensive measurement of all metabolites and low-molecular-weight molecules in a biological specimen Clish (2015). Gas Chromatography (GC), is a technique that is used to separate, detect, and quantify small volatile compounds in the gas

phase. This thesis utilised GC coupled with mass spectrometer (MS) or flame ionization detector (FID) based detection following chromatography for lipid profiling in the blood and liver. In GC analyses, the analyte is either a gas or a liquid that is vaporized in an injection port. Typically, the compounds analysed in GC are less than 1,000 Da. For larger, aqueous, or polar molecules that are difficult to vaporize, liquid chromatography (LC) is considered as a useful alternative. In a typical GC experiment, a solution of a biological sample in an injection port is vaporized and carried by an inert gas (mobile phase). In this thesis, the mobile phase for the gas chromatography was helium and was selected because of its low molecular weight and being chemically inert. Pressure then builds up and the mobile phase moves the analyte through a long, thin column. The analyte separation is accomplished using a column coated with a stationary phase (Omegawax 250, a bonded polyethylene glycol-based phase was used for the GC-FID sample analyses in this thesis). A typical gas chromatography consists of sample injection port, carrier gas, oven column and detector described below (figure 2.2).

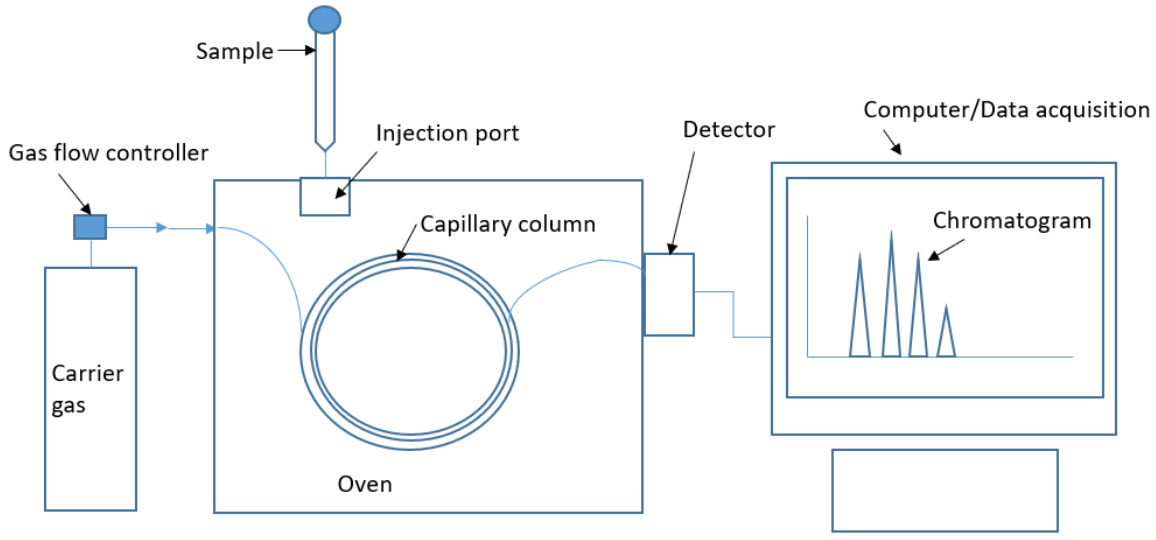

Figure 2.2: Schematic operation of a typical gas chromatography.

The GCMS platform sample is injected into the port which carried by a carrier gas. Then passes through and interact with the capillary column where samples are separated before entering the detector and finally data acquired are recorded on a computer system.

Sample Injection port

A sample port is where the samples to be analysed are injected into the head of the column. These are often heated sample ports through which the sample can be injected and vaporized in a near simultaneous fashion. Using a calibrated Hamilton blunt tipped syringe a small amount of sample can be injected via a rubber septum into the vaporization chamber. In most cases, separations require only a small fraction of the initial sample volume and a sample splitter is used to direct excess sample to waste. The vaporization chamber is typically heated 50 °C above the lowest boiling point of the sample and subsequently mixed with the carrier gas to transport the sample into the column.

Carrier gas

In GC techniques, generally the carrier gas must be dry, free of oxygen and chemically inert. Mostly, helium is commonly used as it is thought to be safer than, but comparable to hydrogen in efficiency, and has a larger range of flow rates vis-a-vis compatible with many detectors. In this thesis, helium was used for the GC-FID. Mass spectrometer detector uses nitrogen and this turns to improve vacuum pump efficiency due to its higher molecular weights compared to helium or hydrogen.

Oven

The thermostatic oven controls the temperature of the column. The temperature of the column can be set constant throughout the entire separation (isothermal) or programmed at specific set of temperatures. Isothermal programming works best only if the boiling point range of the sample is narrow. Rates of 5-7 °C/minute are usually typical for temperature programming separations.

Column

There are two basic forms of capillary columns- a wall-coated open tubular (WCOT) column or a support-coated open tubular (SCOT) column. WCOT columns are capillary tubes that have a thin layer of the stationary phase coated along the column walls. Different types of columns can be applied for different fields.

Detector

The detector device is located at the end of the column and provides a quantitative measurement of the components of the mixture as they elute in combination with the carrier gas. An ideal detector should have adequate sensitivity to provide a high-resolution signal for all components in the mixture. In addition, it should be reliable, predictable and easy to operate.

Mass spectrometry detector: In a GC-MS system, the mass spectrometer scans the masses continuously throughout the separation. When the sample leaves the chromatography column, it passes through a transfer line into the inlet of the mass spectrometer. The sample then ionises and fragments via an electron-impact ion source. The sample is bombarded by electrons which ionize the molecule by causing them to lose an electron due to electrostatic repulsion. Further bombardment causes the ions to fragment. The ions then pass into a mass analyser where the ions are sorted according to their mass per charge (m/z) value, or ratio. Most ions are only singly charged. The chromatogram shows the retention times and analysing the mass spectra of the peaks to compare to existing libraries each kind of molecule in the mixture can be identified (figure 2.3).

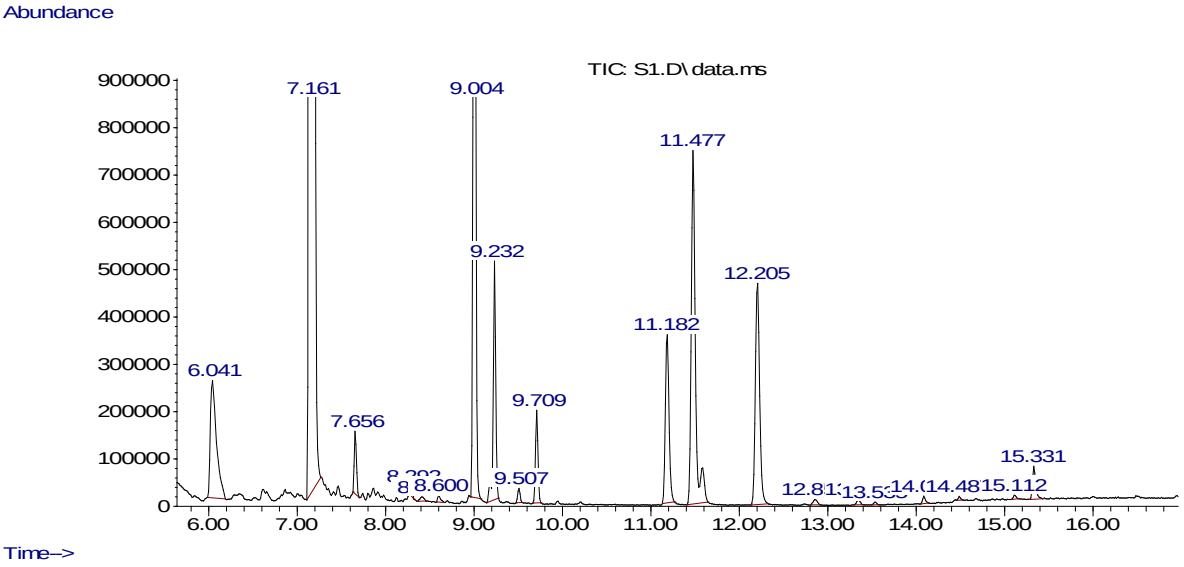

Figure 2.3: Chromatogram of fatty acid peaks in a mouse plasma sample.

Chromatogram was acquired using Agilent 5975 Inert XL MSD & 5973 network MSD GCMS's with Chemstation software.

Flame ionization detector (FID): These are the most generally applicable and widely used detectors. In a FID, the sample is directed at an air-hydrogen flame after exiting the column. At the high temperature of the air-hydrogen flame, the sample undergoes pyrolysis, or chemical decomposition via intense heating. Pyrolized hydrocarbons release ions and electrons that carry current. A high-impedance picoammeter measures this current to monitor the sample elution. FID is useful because the detector is unaffected by flow rate, non-combustible gases and water. These properties allow FID to have high sensitivity and low noise. The unit is both reliable and relatively easy to use. However, this technique does require flammable gas and can also destroys the sample.

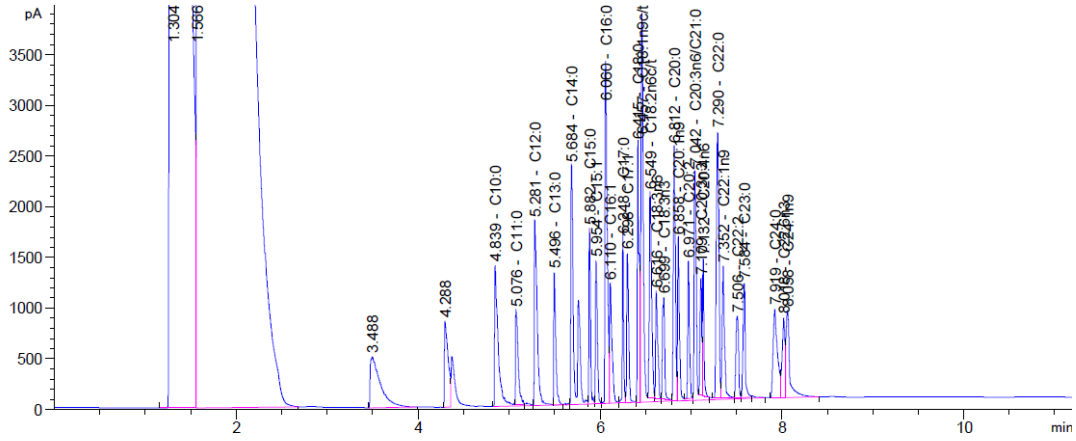

Figure 2.4: Chromatogram of fatty acid peaks in a mouse plasma sample.

Chromatogram was acquired using Agilent 7820A GC with flame ionization detector system.

In general, the main stages of GC-FID/MS-based metabolomics include sample extraction, preparation of fatty acid methyl esters (FAMEs), gas chromatographic analysis, metabolite identification, and data analysis and interpretation (figure 2.5). Salimon et al (2017).

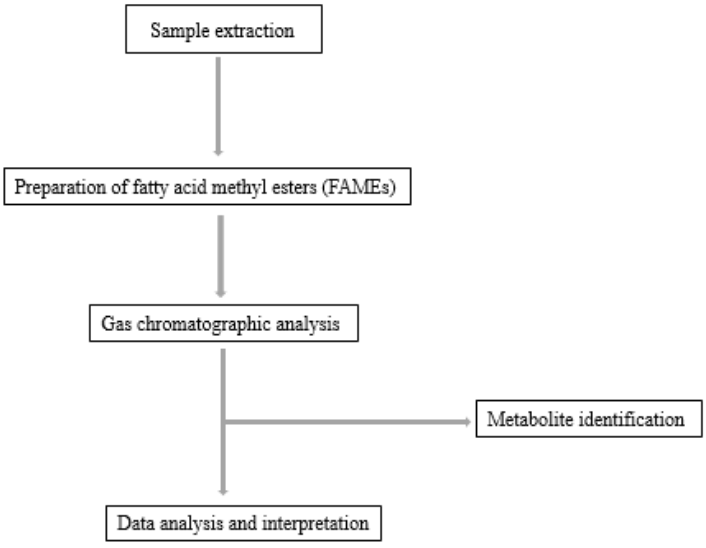

Figure 2.5: Typical GC-FID/MS FA analysis workflow.

The workflow consists of sample extraction, preparation of fatty acid methyl esters (FAMEs), gas chromatographic analysis, metabolite identification, and data analysis and interpretation.

The sample preparation is an important step and requires the use of suitable solvents that that dissolve fatty acids (e.g. chloroform, methanol). Extraction is followed by methylation to make samples suitable for GC analyses. Free online reference spectra such as NIST/EPA/NIH Mass Spectral Library (Peterson & Hayes, (1978) are available to compare their mass spectra with the sample spectra. The spectral data can then be analysed statistically. A major challenge associated with gas chromatography has to do with overlapping/co-eluting peaks, where different metabolites may peak at the same time. Also, if peak tops are broad and several local maxima are present, a component may be identified more than once. However, this challenge can be reduced in severity by using reverse matching logic (ignoring mass spectral peaks not in the library spectrum), but this can also increase false positive risks significantly. The GC-FID/MS workflow employed in this thesis are discussed in greater detail below.

2.2.1 Serum preparation for fatty acid extraction

The frozen serum samples were thawed and lipid was extracted using chloroform-methanol mixture (2:1, v/v). The extraction procedure used was based on that described by Folch *et al.* (1957), but with some minor modifications. In brief, the frozen samples were allowed to thaw. after vortexing, 50µl of mouse serum, 450µl of PBS (Thermo-Fisher, UK) and 2.63µg/ml internal standard, undecanoic acid (C11:0) were mixed with 1.5ml of 2:1 Chloroform-methanol (Sigma, UK) containing 0.01% tert-butylated hydroxytoluene (Sigma, UK). The mixture was then centrifuged at 200 x g for 10 min at 4°C. Following centrifugation, the bottom phase (chloroform) is collected with glass pasteur pipette into a new glass tube.

2.2.2 Preparation of liver extracts for fatty acid extraction

The frozen liver samples were retrieved and put on wet ice. Following the same extraction procedure as described above (see 2.2.1), about 50mg of liver tissue samples was weighed before being homogenised in 80µL of normal saline (sodium chloride). Homogenates were

kept on ice and 2.63µg/ml C11:0, 1.5ml of 2:1 chloroform-methanol (Sigma, UK) containing 0.01% tert-butylated hydroxytoluene (Sigma, UK) added. The mixture was then centrifuged at 200 x g for 10 min at 4°C. The bottom layer containing the lipid was collected into a new tube.

2.2.3 Preparation of fatty acid methyl esters (FAMEs)

Following Folch lipid extraction, the chloroform layer was dried under nitrogen gas and FAs were methylated using 200 µl toluene (Thermo-Fisher, UK), 1.5 mL methanol and 0.3 mL of 6.3% HCl in methanol at 35°C or 100 °C for 10 minutes or ~1 hour respectively, in PTFE-sealed glass vials. The FA methyl esters (FAMEs) were subsequently extracted with 1 mL of hexane and 1 mL of water, evaporated under nitrogen and resuspended in 20 -150 µl of hexane (depending on GC detector used) prior to analyses by gas chromatography (GC)

2.2.4 Gas chromatographic analysis

2.2.4.1 GC-FID

One microlitre volume of each sample was manually injected into GC equipped with FID for separation and quantification of the FAMEs. The analysis was carried out using OMEGAWAX 250 polyethylene glycol-based capillary column (30m x 0.25mm ID x 0.25µm film thickness, (Sigma-Aldrich, UK). The separation was achieved under an optimised temperature programme as follows: initial column temperature 50°C held for 2 minutes, then programmed to increase at a rate of 1 °C min $^{-1}$ up to 260°C. This temperature was maintained for 5 min. The injector temperature was 250°C. Helium was used as the carrier gas at a flow rate of 1 mL min^{-1} with no split ratio. All GC-FID analyses were done in School of Life and Health Sciences laboratory, Aston University, Birmingham.

2.2.4.2 GC-MS

In the GC-MS analyses, 0.2µl was injected by the autosampler of the GC equipped with MSD for separation and quantification of the FAMEs. The analysis was carried out using a Restek

FAMEWAX 250 polyethylene glycol-based capillary column (30m x 250µm ID x 0.25µm film thickness, Fisher Scientific, UK). The separation was achieved under an optimised temperature programme as follows: initial column temperature 100°C with 3 minutes hold time, programmed to increase at a rate of 25°Cmin^{-1} up to 200°C before holding for 6 minutes and ramped again at 25°Cmin $^{-1}$ up to 240°C. This temperature was maintained for 5 minutes. The injector temperature was at 250°C. Helium was used as the carrier gas at a flow rate of 1.3mL min^{-1} and was in splitless mode. All GC-MS analyses were done at the Centre for Diabetes and Metabolic Research Laboratory, Leggett Building, Faculty of Health and Medical Sciences, University of Surrey, Guildford.

2.2.5 Identification of fatty acids

A commercial fatty acid standard mix consisting of 37 FA Components (i.e 37 FAME Standard) purchased from Sigma-Aldrich, UK was submitted to a similar procedure, as previously described and (1 µL) was injected in the GC under the same conditions used for analysing the samples. FAMEs in plasma or liver samples were accurately identified by conducting a comparison of similar peak retention times (Rt) using the 37 FAME standard as well as reference library NIST 2011 (in the case of GC-MS analytes) which include mass spectra of methyl esters of all analysed FAs.

An internal standard, undecanoic acid 2.63µg/mL which was not present in the lipid extracts, was used for quantitative purposes.

In the GC-MS analyses, in addition to the internal standard (IS), calibration curve was constructed for heptadecanoic acid (C17:0) against C11:0. A calibration plot of C17:0 compound was run by applying the ratio of the peak area of the FAME in the standards to the peak area of the IS against the ratio of the concentration of the FAME to the concentration of the IS. The concentration of FAME in the heptadecanoic acid solution was then determined using the area ratio and the calibration plot.

The composition of the FAs (μM) in the samples was then recalculated and used to determine percentage fatty acid composition.

2.2.5.1 Method validation of GC-FID/GC-MS

Prior to analysing experimental samples various experiments were carried out to validate the chromatographic method including response linearity, detection and quantification limits, robustness, recovery, and precision of the analytical procedure.

For GC-MS analysis, calibration curves with a range of concentrations as previously reported was constructed and used to determine the linearity via the values of correlation, coefficient (r) obtained, and the sensitivity of the detector via the values of slope obtained from linear regression equations for the analyte.

The precision of the method was checked through the repeatability and reproducibility experiment. This was done for both GC-MS and GC-FID experiments. The repeatability of the method was calculated by using the measured data of a single day, and the reproducibility of the method was calculated by using the measured data of three successive days. Coefficient of variation were calculated to assess the repeatability and reproducibility of the method.

2.2.5.2 GC/FID method validation for fatty acid analysis

To develop a simple, robust and reliable extraction and analytical method for FFA, control standard was run four times within the same day (Repeatability), four times for 4 different days (Reproducibility) and coefficient of variation of each fatty acid calculated for the retention times (RT) and peak areas (PA; Table 2.7). For example, the results, running the control standard of C11:0 fatty acid showed very low coefficient of variation in repeatability and reproducibility in retention time (RT) and peak areas (PA) respectively, (Average CV~0.001min RT & ~0.11 PA). This similarity was seen in the rest of all other fatty acids in the control run. Other

measures considered in optimizing the parameters/conditions for the analysis of the free fatty acids, include sample solvent selection, inlet temperature, column temperature and temperature program, stationary phase, inlet type, sample size and injection technique

To optimise for volume of plasma for fatty acid extraction, different volumes of plasma but were spiked with the same concentration of C11 (0.2mg/mL) and then the amount of FA recovered as response into the detector was measured. Plasma volume of 50µL diluted with 450µL of PBS was chosen since it produced the maximum fatty acid recovery when compared with 20 µL, 40 µL and 200 µL diluted with different volume of PBS (table 2.8). Again, the CV (~0.21 PA) for the FA recovered is very low (represented by peak areas) (table 2.8).

Table 2.7: Repeatability and reproducibility of sample (C11:0).

Day	**Retention time(minutes)**	**Peak Areas (PA)**
1	5.047	4384.4
	5.049	3829.5
	5.045	4360.5
	5.04	4596.2
Mean	**5.045**	**4292.65**
CV(1)	**0.0008**	**0.076**
2	5.070	1561.28
	5.068	1883.81
	5.064	2437.98
	5.066	3487.35
Mean	**5.067**	**2342.61**
CV(2)	**0.00051**	**0.096**
3	5.048	1785.77
	5.054	3055.79
	5.056	2251.7
	5.060	2501
Mean	**5.055**	**2398.57**
CV(3)	**0.00098**	**0.22**
4	5.053	2638.6
	5.055	2521.28
	5.054	2631.72
	5.052	2883.18
Mean	5.054	**2668.70**
CV(4)	**0.00026**	**0.057**
CV for 1-4	**0.002**	**0.315**

Table 2.8: Optimization for plasma volume of C11

Volume of plasma	**Retention time**	**Peak Area**
20 µL + 480 µL PBS	-	-
40µL + 460 µL PBS	5.039	5831.74
50 µL + 450 µL PBS	5.039	6413.26
200 µL+ 300 µL PBS	5.044	4227.52
CV	**0.0006**	**0.21**

Determining the percentage recovery of Internal standard spiked into samples is another important measurement to determine the accuracy and reliability of a GC method and is reported as percentage recovery. In determining the GC method for fatty acid analysis, 10µl of 0.2mg/µl of C11:0 was added to 450µL of PBS before extraction and methylation (table 2.9). After extraction and methylation, the FAME was resuspended into 20µl of hexane before injection into the GC apparatus. The concentrations of the FAs in the non-spiked plasma were subtracted from the concentrations in the spiked plasmas and the recovery percentages (R %) were calculated by dividing the calculated concentrations by the expected concentrations.

Table 2.9: Percentage recovery of GC method

Sample	Retention time	Peak Area	Calculated spiked (mg/ml)	Conc. Recovery	% Recovery
Plasma + C11	6.458	4651.61	0.137532	0.687659	68.76586
Plasma alone	-	-	-		
Internal standard	6.448	2266.08	0.2		

2.2.5.3 GC-MS method validation for fatty acid analysis

Standard curve for heptadecanoic acid versus undecanoic acid.

The concentration of the heptadecanoic acid (HA) was determined using their peak area with reference to internal standard, undecanoic acid (UA) (see Figure 2.6) assayed daily in a 0.2M chloroform from stock solutions of each compound (table 2.10).

Table 2.10 Standard curve for heptadecanoic acid versus undecanoic acid

HA(Dil)			UA(Dil)		
Volume	Wt.	Conc. (Wt/Mwt)	Volume	Wt.	Conc.
µl	µg	µmol	µl	µg	µmol
50	0.10	0.000372712	250	2.62	0.014087
100	0.20	0.000745424	250	2.62	0.014087
200	0.40	0.001490849	250	2.62	0.014087
300	0.60	0.002236273	250	2.62	0.014087
250	0.50	0.001863561	0	0.00	0.000000
0	0	0	250	2.62	0.014087

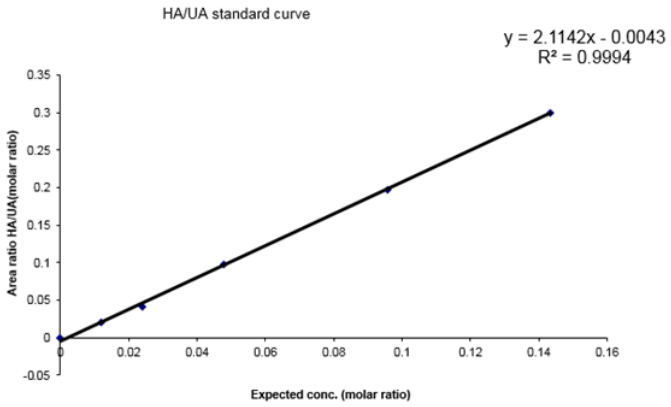

Figure 2.6: Typical standard (calibration) curve used in the determining the concentration of C17:0 using standard fatty acids.
Standard curve constructed using C17:0 against internal standard C11:0

2.3 Immunohistochemistry

Immunohistochemistry is a technique used for detecting the expression of biological markers in formalin-fixed and paraffin-embedded tissues Nguyen et al (2013). Thus, it is an effective method for the detection of a specific protein in tissues. In this thesis, the immunohistochemistry (IHC) technique was employed to evaluate the expression of proteins involved in the peroxisomal and mitochondrial pathway of fatty acid oxidation and lipid

metabolism associated with metabolic changes following low protein or high fat dietary treatment relative to normal diet controls. The first major step in an IHC is tissue preparation which determines the quality of overall imaging results. The preparation step includes fixation, embedding and sectioning. After tissue preparation step, the sections are immunohistochemically stained for imaging analysis (figure 2.7).

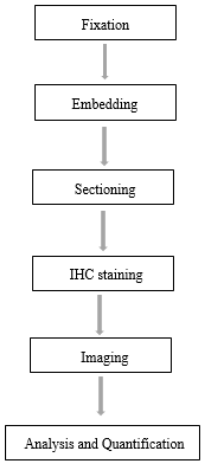

Figure 2.7: Project pathway for IHC technique
The IHC steps consist of fixation, embedding, sectioning, staining, imaging, analyses and quantification.

2.3.1 Fixation

Fixation is a complex series of chemical events for preserving cellular architecture and composition of cells in the tissue to allow them to withstand subsequent processing. The aim of fixation is to harden, preserve, prevent changes such as autolysis and putrefaction of tissue etc. Thavarajah et al (2012). In this thesis, 10% formalin was selected for fixation as it is the most widely used fixative in pathology labs worldwide. It is convenient in handling with high degree of accuracy and extreme adaptability. Thavarajah et al (2012). Routine fixation in histological methods with buffered 4-10% paraformaldehyde is typical but there are a variety of fixatives and fixation methods.

2.3.2 Embedding

Embedding is the orientation of tissue in melted paraffin or agar which when solidified provides a firm medium for keeping intact all parts of the tissue when sections are cut. Paraffin embedding provides a permanent archival block that can be cut at thicknesses ranging from 3 to 10μm. These thinner sections give better microscopic resolution and are useful for various staining applications. Antigen retrieval techniques are usually needed for immunohistochemical stains.

2.3.3 Sectioning

After embedding, paraffin-embedded tissue blocks are chilled on ice before sectioning.

Thin paraffin blocks are normally cut with microtome.

The microtome procedures used are described below:

Paraffin-embedded tissue blocks were chilled on ice before sectioning. The cold wax was to allow thinner sections to be obtained by providing support for harder elements within the tissue specimen. Following this, water bath filled with ultrapure water was prepared. To begin the procedure, the blade was placed in the holder to ensure it is secure and the clearance angle was set. The clearance angle is to prevent contact between the knife facet and the face of the block. Then the paraffin block was inserted and orientated so that the blade will cut straight across the block. The block is carefully approached with the blade and a few thin sections are cut to ensure the positioning is correct. Any adjustment is made if necessary. The block is then trimmed to expose the tissue surface to a level where a representative section can be cut. Trimming is normally done at a thickness of 10-30 μm. Sections at a thickness of about 5 μm were cut.

Using tweezers, the ribbons of sections were taken and drop in water to float them on the surface in the water bath so they flatten out. Again, the tweezers were used to separate the sections. Finally, the sections were collected out of the water bath and put in wells filled with phosphate buffered saline.

2.3.4 Immunohistochemistry staining

During immunohistochemistry staining, a careful work up and inclusion of positive and negative controls is undertaken to ensure the final label is specific and sensitive are required. If this is not done the result is in question as merely an artefact of processing and staining. Work up requires titration of the antibody concentration and a sensitive positive control. Antigen retrieval may be required for most aldehyde fixed tissues and is essential to reveal antigens in the tissue. Polyclonal and monoclonal antibodies are mostly used and they have the ability to label target proteins. To detect a specific protein (antigen) from the formalin-fixed paraffin-embedded tissue, the tissue is incubated with a primary antibody that specifically binds to the target protein (antigen). After primary antibody incubation, any unbound antibody is washed off with a buffer (e.g. using a tris buffered saline with tween i.e. TBS buffer). The tissue is incubated again but this time with a secondary antibody that recognises and binds specifically to the primary antibody (Figure 2.8). The secondary antibody used in this thesis was biotinylated and through conjugation with the vector elite avidin-biotin peroxidase complex (ABC), the peroxidase was developed by NOVA red chromogen to produce colour or light, permitting it to be detected, imaged and quantified. Through these processes, therefore, the IHC technique allows the detection and quantification of target proteins from among a formalin-fixed paraffin embedded tissue.

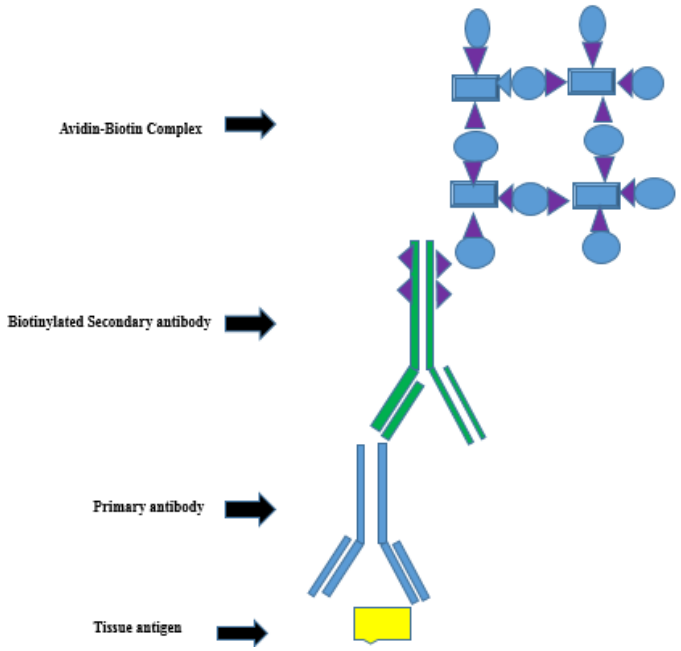

Figure 2.8: The primary and secondary antibody complex in immunohistochemistry

Regardless of the great utility of IHC, there are some limitations. IHC is less sensitive quantitatively than immunoassays such as Western blotting or ELISA, however, it enables the observation of processes in the context of intact tissue. This makes it especially useful for assessing the progression and treatment of diseases such as fatty liver. Generally, the information gained from IHC combined with microscopy literally provides a "big picture" that can help make sense of data obtained using other methods. IHC-P refers to the staining of tissues that have been fixed and then embedded in paraffin before being sectioned.

The steps used in this thesis for the immunohistochemistry studies are detailed below:

2.3.5 Preparation of liver samples

Following SPF high fat or Nottingham low protein feeding of mice as described previously in 2.1.3, part of the liver tissue was fixed in a 10% formalin solution. A 2 ml of formalin in microfuge tube was used for each ~100 mg of liver tissue. The tissue was fixed for a minimum 48 hours at room temperature before transferring to new labelled-tubes and stored in fridge for

long term storage. To minimize variability of the study, all fixed tissues were kept at this standard condition.

Prior to tissue embedding in paraffin wax, excess fixative was removed by washing 3 times in PBS (Thermo-Fisher, UK). Liver sections were cut on a microtome to a thickness of 3μm (Leica Biosystems, UK) and then mounted on microscope slides. Before proceeding with the staining protocol, the slides were deparaffinised and rehydrated. Complete removal of paraffin was performed to avoid poor staining of the section. Briefly, deparaffinization was performed as follows:

After placing the slides in a rack, washes were performed according to steps 1-7 respectively,

1. Xylene: 3 x 3 minutes
2. 100% ethanol: 3 minutes
3. 100% ethanol: 3 minutes
5. 70 % ethanol: 3 minutes
6. 50 % ethanol: 3 minutes
7. dH20 to rinse.

All slides were kept in water until ready to continue with the next step since drying out could cause non-specific antibody binding and therefore high background staining.

2.3.6 Immunohistochemical staining

Following dewaxing and rehydration steps, endogenous peroxidase blocking was performed before antigen retrieval. In this thesis, all IHC stainings were performed by Katherine Walker and the Veterinary histopathology lab team. Briefly the following steps were used during immunohistochemical staining:

1. Endogenous peroxidase blocking was performed by exposing slides to 3% hydrogen peroxide in methanol for 15 minutes.
2. Slides were washed for 10 minutes in distilled H_20 and 2x 5minutes in TBS.

3. Antigen retrieval was performed using proteinase kinase (PK) for 10 minutes. PK was diluted at 40µl per 2ml TBS (0.02mg/ml). This antigen retrieval method serves to break the methylene bridges and expose the antigenic sites in order to allow the antibodies to bind.

4. Slides were washed 2x 5minutes in TBS

5. Slides were exposed to 10% normal blocking serum in TBS for 20mins at room temperature.

6. Primary antibody was diluted in TBS was applied to slides and incubated for 18-22 hours at 4°C. For all experiments, primary antibody dilution was 1:100 following titration experiments conducted to select optimised concentration.

7. Slides were washed 2x 5minutes in TBS

8. Biotinylated secondary antibody diluted in TBS was applied to slides incubated for 2 hours at 4°C. While 1:250 dilutions were used for the secondary antibodies, the primary antibody dilutions varied as shown in table 2.11

9. Slides were washed 2x 5minutes in TBS

10. Slides were exposed to conjugate ABC for 30minutes.

11. Slides were washed 2x 5minutes in TBS

12. To visualise protein with chromogen, NOVA RED chromogen was applied for 10 min at room temperature.

13. Slides were washed 2x 5minutes in TBS and then washed in dH20

14. Slides were counterstained with haematoxylin.

15. Dehydrated in ethanol, cleared in xylene and mounted on a slide with DPX.

Table 2.11**:** Primary antibody dilutions for immunohistochemistry

Description	**Catalase**	**PEX-14**	**Goat Anti-Rabbit IgG H&L (HRP)**
Species used to raise antibody	Rabbit	Rabbit	Goat
Target antigen species	Mouse, rat, human	Human, mouse, rat	Rabbit
Antigen target	Catalase	PEX-14	IgG
Antibody isotype	IgG	IgG	IgG
Clonality	Polyclonal	Polyclonal	Polyclonal
Antibody code from supplier and source	Abcam (Ab16731)	Abcam(ab10999)	Abcam (6721)
Dilution	1:100	1:100	1:250

2.3.7 Control check

A negative antibody control was set up by omitting the primary antibody and replacing with TBS. A positive tissue control was also set up to ensure that the antibody was performing as expected.

2.3.8 Microscopy and image analyses

Section images were acquired using a DMR Leica microscope equipped with a High-End DP 72 Olympus digital camera (using ×60 lenses) and projected onto a computer monitor. The immunoreactivity was detected and the relative quantification of immunostaining was performed by ImageJ software, NIH, USA). Arbitrary numbers obtained from ImageJ entered into Prism vs 8 (GraphPad, UK) were analysed using student t-test with Mann Whitney comparison test between two groups with $P<0.05$ considered to be significant.

2.4 Polymerase chain reaction

Polymerase chain reaction (PCR) is a molecular biology technique used to make many copies of a section of a gene (or DNA), which allows for the detection and/or identification of gene sequences. PCR was developed by Kary Mullis in 1983, Mullis et al (1987). PCR can be performed using DNA from a variety of biological samples including tissues (e.g. from liver, skin, etc.), fluids (e.g. blood, saliva), and hair.

PCR employs two main reagents – primers (these are short single strand DNA fragments (usually between 20-30 nucleotides long) known as oligonucleotides that are a complementary sequence to the target DNA (region) and a DNA polymerase.

The DNA polymerase is an important enzyme in the PCR technique as this enzyme links complimentary deoxynucleotides (adenine, thymine, guanine, and cytosine i.e. A, T, G, C) to an existing DNA template or complementary DNA (cDNA) (i.e. a short DNA strand), Garibyan & Avashia (2013). The template DNA or cDNA), DNA polymerase, deoxynucleotides, and primers, together with an appropriate buffer and magnesium source, are put in a thermal cycler and this allows repeated cycles of DNA amplification to occur via the following steps: denaturation, hybridisation/annealing, and elongation, Garibyan and Avashia (2013). The thermal cycler can be programmed to heat up at a high temperature of 90-95°C, to allow the double stranded DNA to split into two single stranded DNAs (denaturation). The temperature can then be reduced to the primer specific temperature (usually between 50-60°C) for the primers to bind to the complementary sequence of the single stranded DNA (annealing). After primer annealing, the temperature is then increased (to usually 72°C) and this allows the DNA polymerase enzyme to join the deoxynucleotides to the primer, thereby extending the DNA, Garibyan and Avashia (2013). These steps can be repeated to double the amount of amplified DNA molecules.

2.4.1 Real time quantitative PCR

Real time quantitative PCR (RTqPCR) is used to monitor the amplification of a targeted DNA molecule during the PCR in real-time. It can be used to detect and quantify target DNA in real time. It is reported to be more sensitive than microarrays in detecting small changes in expression but requires more input ribonucleic acid (RNA) and is less adaptable to high-throughput studies, Wang et al (2006).

Using RNA extracts, the process involves the conversion of the RNA to complementary DNA (cDNA) - this process is known as reverse transcription. This step is followed by the use of fluorescent reporters and a PCR reaction to amplify and detect specific genes. Normally, two types of fluorescent reporters are commonly used; these are SYBR green and Taqman probes. In this thesis, SYBR green fluorescence reporter was used for multiple genes studies as SYBR® Green was more economical choice than any other.

The light source in the RT-qPCR instrument emits fluorescent signal in the presence of fluorescent molecules (eg SYBR green dye) in the PCR reaction mixture. As the amplification continues, the fluorescence accumulated is detected by the instrument after every cycle and this is translated into a RT-qPCR graph. (Figure 2.9). RTqPCR requires the sequence of the specific target gene of interest to be known at hand (in order to design the PCR primers). Therefore, this technique can only be used for studying known genes. Similar to traditional PCR, RTqPCR uses *Taq* polymerase, buffer, dNTPs, and primers to amplify small amounts of DNA (or cDNA). It only differs from the conventional PCR with the addition of a fluorescent signal in each RT-qPCR reaction, which is monitored by a special, computerized thermocycler, Thornton& Basu (2011)

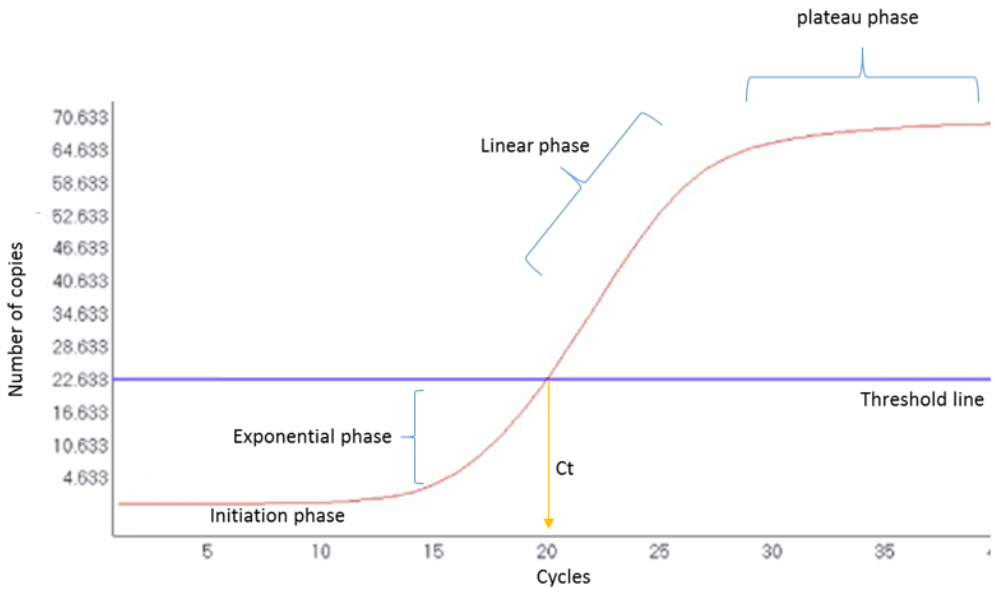

Figure 2.9: A typical real-time PCR amplification curve.
Real-time PCR amplification curves are divided into phases: the exponential phase where the reagents are in abundance and PCR product doubles in every cycle, the linear phase where the reagents begin to run out and the PCR reaction slows down, and the plateau phase where the reactions are depleted and stops. Real-time PCR amplification results focus on the exponential phase since this phase provides the most accurate data for quantitation. Within the exponential phase two values are calculated: (a) the threshold line which is the level at which a reaction reaches a fluorescent intensity above background, and (b) threshold cycle (Ct) which is the PCR cycle number at which the fluorescent signal of the reaction crosses the threshold. This Ct value is used in quantitation. It is used to calculate the initial DNA copy number, because the Ct value is inversely related to the starting amount.

Generally, RT-qPCR can be combined with reverse transcription, after which quantification of the cDNA may be performed with RT-qPCR. In this thesis, RNA was extracted from mice livers and reverse transcribed into cDNA. The genes of interest investigated here included the fatty acid binding protein 1 (*FABP1),* fatty acid binding protein (*FABP3),* fatty acid desaturase *(FADS2),* fatty acid desaturase 1 (*FADS1*), stearoyl-CoA desaturase *(SCD1),* elongation of very long chain fatty acids protein 6 *(ELOVL 6),* propionyl-CoA carboxylase *(PCCA),* branch chain keto acid dehydrogenase alpha *(BCKHDα),* 2-hydroxyacyl-CoA lyase 1*(HACL1),* carnitine palmitoyltransferase 1b muscle *(CPT1B),* malonyl-CoA decarboxylase *(MLYCD),* catalase *(CAT),* carnitine palmitoyltransferase 2 *(CPT2),* tumour necrosis factor *(TNF-α),*

thioredoxin 1*(TRX1)*, glutathione reductase that are associated with fatty acids transport, metabolism, oxidative stress and inflammation.

Notwithstanding the numerous merits associated with PCR, in practice the technique can fail for various reasons. Since qPCR is highly sensitive technique, it is prone to contamination from extraneous DNA, resulting in the amplification of spurious DNA products. It is therefore necessary to address contamination with extraneous DNA adopting a laboratory procedure that separate pre-PCR mixtures from any potential source of DNA contaminants. Such laboratory measures may include spatial separation of PCR set-up areas from areas used for purification or analysis of PCR products, as well as thorough cleaning of the working bench between reaction set-ups. Robust primer design techniques are very essential in improving the yield of PCR products and avoiding the formation of spurious PCR products. Apart from these, other critical issues defining the reliability of real time quantitative PCR data are the choice of housekeeping (reference) genes and the sample preparation methods. The ideal housekeeping gene selected must exhibit stable expression levels but because not all currently available housekeeping genes may fulfil this prerequisite, there is the need to test and verify for constant expression of the chosen reference to obtain a reliable data. Alternatively, two or more reference genes may be used in the experimental setup for data analysis as done in this thesis.

2.4.1.1 Study primers and design

In this thesis a total of eight metabolic genes of interest, four inflammatory genes and two reference genes were selected and studied. The metabolic genes of interest selected were *FABP1*, *FABP3*, *FADS2*, *FADS1*, *SCD1*, *ELOVL 6*, *PCCA*, *BCKHD* α, *HACL*1, the inflammatory genes was *TNF*- α and antioxidant genes included *TRX1*, *GSR*. The two selected reference genes were phosphoglycerate kinase 1 (*PGK1*) and TATA-box binding protein (*TBP*)

which have been validated in previous studies and reported to be most stable pair reference gene for the liver tissue as stability expression was determined by geNorm and NormFinder algorithm, Lucas et al. (2011).

The nucleotide sequence of each of the targeted genes specific for *Mus musculus* (mouse) was retrieved from GenBank (https://www.ncbi.nlm.nih.gov/genbank/) and a blast search conducted for verification. The coding sequence of the matching contigs for each gene of interest was used in designing the primers using Primer3Plus (http://www.bioinformatics.nl/cgi-bin/primer3plus/primer3plus.cgi/), Sgamma et al (2016). To select the ideal primer pair, different factors were taken in consideration and set as parameters e.g. annealing temperature (60-67°C), GC content (40-60%), an optimum primer length of 20-24 base pairs and a maximum product size of 233 base pairs (see Table 2.12).

Primer secondary structures of each amplicon were examined via Beacon Designer Free Edition software (www.premierbiosoft.com/qOligo/Oligo.jsp?PID=1). Primer dimers and non-specific amplifications were further checked post-PCR, if any, by analysing the melting curve data.

Table 2.12: Target primers and their annealing temperatures

Gene Name	Gene Symbol	Accession Number	Forward Primer	Reverse Primer	Amplicon Length
fatty acid binding protein 1, liver	*FABP1*	NM_017399.4	acttctccggcaagtaccaa	ttccctttctggatgaggtc	214
fatty acid binding protein 3, liver	*FABP3*	NM_010174.1	ctttgtcggtacctggaagc	cagagcgctggtcatgtagt	222
fatty acid desaturase 2	*FADS3*	NM_019699.1	attcgggagaagatgctacg	aagaacttgcccacgaagtc	233
stearoyl-Coenzyme A desaturase 1	*SCD1*	NM_009127.4	ttccctcctgcaagctctac	cagagcgctggtcatgtagt	156
fatty acid desaturase 1	*FADS1*	NM_146094.2	ccagctttgaacccaccaa	Catgaggcccatcgctcta	130
ELOVL family member 6, elongation of long chain fatty acids	*ELOVL 6*	NM_130450.2	Cagggaggaagggctatggcag	cgaacagggaggaggcgaaca	81
phytanoyl-coA hydroxylase	*PCCA*	NM_010726.2	Acccactcaggcacaagcaaga	Tttctctgccatctcgacaacttcc	162
2-hydroxyacyl-CoA lyase 1	*HACL-1*	NM_019975.3	agaactgccttcctcgccacagg	caccttccacacagatgacccgct	135
TATA binding protein	*TBP*	NM_013684.3	Ggtatctgctggcggtttggct	aaggtggaaggctgttgttctggtc	199
branched chain ketoacid dehydrogenase E1, alpha polypeptide	*BCKDH α*	NM_007533.5	tggatgctgccccctgtgct	Gccctggtcccttcccaccc	194
cluster of differentiation 36	*CD36*	NM_001159558.1	Gatgacgtggcaaagaacag	Tcctcggggtcctgagttat	151
carnitine palmitoyltransferase 1b, muscle	*CPT1B*	NM_009948.2	Ggtcccataagaaacaagacctcc	cagaaagtacctcagccaggaaag	195
malonyl-CoA decarboxylase	*MLYCD*	NM_001364328.1	gttctcctccggcttcct	Gtttttcacagggtgcacag	179
carnitine palmitoyltransferase 2	*CPT2*	NM_009949.2	gct ttc caa ccc gat ctc ct	tgt gag cgg aag atc cca ac	217
Catalase	CAT	NM_009804.2	Agcgaccagatgaagcagtg	Tccgctctctgtcaaagtgtg	181
phosphoglycerate kinase 1	*PGK1*	NM_008828	tacctgctggctggatggaagacc	cacagcctcggcatatttct	65
tumor necrosis factor	*TNF- α*	NM_013693.3	Tgacccctttactctgaccct	Ggaccctgagccataatcccc	93
thioredoxin 1	*TRX 1*	NM_011660.3	Cctccccgcaacagccaaaa	Agcagagaagtccaccacgaca	106
glutathione reductase	*GSR*	NM_010344.4	cgactgcctttaccccgatg	Gcccccattttcaccgctac	166

List of primers designed for the study

2.4.1.2 RNA isolation

In this thesis, two methods of RNA isolation were employed: total RNA extraction using RNA extraction using RNeasy® Mini Kit (Qiagen, UK) and TRIzol™ Reagent (Thermo scientific, UK).

Liver RNA extraction with RNeasy® Mini Kit

Total RNA was extracted from the liver of a low protein diet experimental mice using the RNeasy Lipid Tissue Mini Kit (QIAGEN, UK) according to the manufacturer's instructions. Briefly, thirty-five milligram of the frozen liver tissue samples were dissected out on ice for total RNA extraction using RNeasy® Mini Kit (Qiagen, UK). Each 35 mg tissue was homogenised using 600 µL buffer RLT (lysis buffer) and the supernatant was carefully removed. 600 µL of 70% ethanol was added to the lysate and thoroughly mixed by pipetting. 650 µL from each sample, including any precipitate, was transferred into an RNA mini spin column placed in a 2 ml collection tube and centrifuged for 15 s at 8,000 *g*, with the flow through subsequently discarded. Then 700 µL of Buffer RW1 (washing buffer) was added to the RNeasy spin column and centrifuged for 15 s at 10,000 *g,* with the flow through subsequently discarded. The samples were then gently washed by adding 500 µl of buffer RPE (mild washing buffer) to the RNeasy spin column and centrifuging for 15 s at 8,000 *g*, and the flow through discarded. Again, the samples were gently washed twice by adding 500 µL of Buffer RPE to the RNeasy spin column and centrifuging for 2 min at 8,000 *g*. The RNeasy spin column was then changed and centrifuged for 1 min at 8,000 *g* in order to dry the membrane. Finally, the RNeasy spin column was placed in a new 2 ml collection tube and 35 µL of RNase-free water was added directly to the spin column membrane and centrifuged for 1 min at 10,000 *g*. In order to obtain a high RNA yield (> 30 µg), the final step was repeated. The sample was then transferred into an Eppendorf tube and kept on ice. RNA was quantified using the

Nanodrop ND-1000 spectrophotometer, with A260/A280 absorbance ratios of ≥ 1.9 accepted for use.

Liver RNA extraction with TRIzol™ Reagent

Total RNA was extracted from the liver of SPF mice using the TRIzol™ Reagent (Thermo Scientific, UK) according to the manufacturer's instructions. The details of the extraction are as follows: A 5 ml of TRIzol reagent was pipetted into a sterile 50ml falcon tubes on ice. This was immediately homogenised using the IKA Ultra-Turrax homogeniser for 30 seconds. Following homogenisation, the samples were incubated for 5 mins at room temperature to allow nucleoprotein complexes to completely disassociate). It was then centrifuged for 10 mins at 12 000 x g in 4^{o}C. This was to ensure an optional removal of any insoluble material such as protein, fat, polysaccharides, extracellular material etc) leaving RNA in the supernatant. The supernatants were transferred into a fresh, cold tube. 1 ml of 1-bromo-3-chloropropane **(**BCP) was added to the 5 ml of TRIzol and capped before vortexing for 15 seconds. It was incubated at room temperature for 5 mins and centrifuged at 12 000 x g for 10 mins at 4^{o}C. The aqueous phase (upper layer) containing the RNA was transferred into a fresh tube. To precipitate the RNA, 1 ml of isopropanol was added to the aqueous phase. This was vortexed for 10 seconds and incubated at room temperature for 10 minutes before centrifuging at 12 000 x g for 8 mins at 4^{o}C. The supernatant was discarded carefully without disturbing the pellet. The precipitated RNA forms a gel-like or white pellet on the side and bottom of the tube. Further, a 2ml of 75% ethanol was added to wash the RNA pellet, centrifuged at 7500 x g for 5 mins to remove the ethanol. The RNA pellet was air dried. Finally, the RNA pellet was dissolved in 50 uL of nuclease-free water and stored at -80^{o}C for long term storage. RNA isolation with Trizol reagent was further treated with DNAse digestion kit. The TURBO DNA-free™ DNase treatment kit (Ambion Inc, USA) was used to remove genomic DNA contamination following the manufacturer’s guidelines. The concentration and quality of the RNA sample was then

verified by spectrometry using A260/280 ratios, with a Nanodrop Lite Spectrophotometer (Thermo Scientific, UK). This was achieved by placing 1 µL of the RNA sample on the Nanodrop Lite Spectrophotometer (detail RNA concentration found in Appendix, table 1). To ensure optimal amount of RNA is extracted from the liver, RNA quantified with A260/A280 absorbance ratios of ≥1.9 was accepted for use.

2.4.1.3 cDNA synthesis

All cDNA were synthesised using 2.0 µg of the cleaned total RNA from each liver sample using nanoScript2 cDNA synthesis kit (Primerdesign, UK) following the manufacturer's instructions. In brief, a reaction mix was prepared comprising: 2.0 µg RNA template, 1.0 µL RT primer and nuclease-free water adjusted to give a total volume of 10 µL. The reaction mix was then incubated in a heated water bath at 65°C for 5 minutes and immediately transferred onto ice to cool. A 10 µL reaction mix consisting: 5 µL nanoScript2 4x buffer, 1 µL nanoScript2 reverse transcriptase, 1 µL of dNTP mix 10mM and 3.0 µL of nuclease-free water was added to each of the samples on ice and vortexed. The samples were initially incubated at 25 µL for 5 minutes and then at 42 µL for 20 minutes and finally heat inactivated for 10 min at 75°C. The cDNA samples were then stored at -20°C until ready to use. Reverse transcriptase negative (RT-) controls were also prepared to check for genomic DNA contamination during real-time PCR (RTqPCR).

2.4.1.4 Quantitative real-time PCR

The RT-qPCR analysis was carried out using Stratagene (Thermo Scientific, UK) or Quant studio 7 Real-Time PCR system (Thermo Scientific, UK). RTqPCR reactions for tissue samples were prepared using Precision Mastermix (Primer Design, UK) containing SYBR Green, with a final concentration of 300 nM each of forward and reverse primers and 1 µL cDNA in a 20 µL reaction volume. Each sample was analysed in triplicate, using clear 96-well

plates (Axygen). For comparative studies between plates, a calibrator sample was included to control for inter-assay variation. Absence of contaminating genomic DNA was confirmed by analysis of RT-ve samples alongside a positive control. Triplicate reactions containing water in place of cDNA (‘no template controls') were also included for each assay. Thermal cycling and fluorescence detection were performed using a DNA Engine thermal cycler and Chromo4 Real-Time Detector (BioRad, UK) with Opticon Monitor v3.1 software. Thermal cycling conditions were 95 °C for 5 min enzyme activation, then 40 cycles of 95 °C for 15 s followed by 60 °C for 1 min with a final extension step of 10 min at 72 °C. A melting curve was run to check the specificity of the amplified products. For each primer pair, efficiency (*E*) was determined across a range of standard dilutions (using a minimum 5 log range) and calculated according to the formula $E = 101/\text{slope}$. An efficiency of 2 would represent 100% efficiency, i.e., a doubling of fluorescent signal with each cycle of the PCR. All primer pairs used in this study showed efficiency greater than 90% ($E > 1.9$).

2.4.1.5 Relative quantification and statistical analysis

Analysis of exported threshold cycle (Ct) values was performed in Microsoft Excel 2007. Ct values were converted to relative expression values using the dCt method and reference gene stability was determined using the VBA applets for geNorm (Vandesompele et al 2002) and NormFinder, Andersen et al, 2004). The data was then normalised to two genes: *PGK1* and *TBP* which are stable in hepatic tissue. Normalisation factors derived from the geNorm output were then used to normalise the expression of each individual gene for comparison between treatment groups. The data from the varied diet studies were entered into Prism vs 8 (GraphPad, UK) and analysed using a Students t-test with Man-Whitney test to compare two treatments.

2.5 16S ribosomal RNA Gene Sequencing

Next-generation sequencing (NGS) is a rapid, accurate, and inexpensive technique of profiling complex microbial communities. Generally, there are two common methods of sequencing the microbiome:16S rRNA sequencing and shotgun metagenomics. In this thesis, the 16S RRNA sequencing technique was employed in the microbial characterization of faecal samples obtained from SPF mice in response to high fat diet. The method is most commonly used to profile microbiota and it is based on sequencing of the gene encoding the small subunit of ribosomal RNA (16S). 16S rRNA gene sequencing has revolutionized the microbiome field by enabling researchers to determine the taxonomic composition of a given sample cheaply and easily, Rosen & Palm (2017). Insofar as function correlates with taxonomy, 16S rRNA gene sequencing can reveal the role of particular microbes, as certain effects on the host can vary predictably across taxonomic groups, Langille et al (2013).

The metagenomics sequencing workflow involves DNA extraction, library preparation, amplicon sequencing, and microbial bioinformatics analysis. The steps applied in this thesis are described briefly as follow:

Faecal DNA extraction

Fresh faecal samples were collected from the animals in each group (n = 10 per group). Total genomic DNA was extracted using the MP Biomedicals DNA isolation kit (Fisher Scientific, UK) following their instruction manual for rapid isolation of genomic DNA from human and animal stool samples using the FastPrep system. Briefly, about 50mg faecal sample was weighed into a 2ml lysing matrix E tube, and 825 µL sodium phosphate buffer and 275 µL of PLS solution were added and vortexed. The mixture was centrifuged for 5 minutes at 14,000 x g. After decanting the supernatant, 978 µL sodium phosphate buffer and 122 µL MT buffer were added and vortexed briefly. This was followed by homogenization in FastPrep 24

instrument at 6.0m/s for 40 second. The homogenized samples were then centrifuged at 14,000 x g for 5 minutes before the supernatant was transferred to a clean 2.0mL centrifuge tube. 250 µL of PPS solution was added, mixed by shaking, and incubated for 10 minutes at 4 degrees Celsius before centrifuging for 2 minutes at 14,000 x g. Whilst samples were being centrifuged, 1ml of binding matrix solution was added to a clean 15ml conical tube. The supernatant from the centrifuged samples was added to the binding matrix solution in the conical tube and placed on a shaker for 5 minutes. This was followed by centrifugation for 2 minutes at 14,000 x g. Samples were decanted. The binding mixture pellet (BMP) was gently resuspended with 1ml Wash Buffer #1. The BMP was transferred to a SPIN filter tube and centrifuged for 1 minute at 14,000 x g. 500 µL of prepared Wash Buffer #2 was added to the spin filter tube and gently resuspended the pellet using the force of the liquid from the pipette tip. The samples were centrifuged for 2 minutes at 14,000 x g and the flow-through discarded. The centrifugation was repeated for 2 minutes to extract residual ethanol from the binding matrix and to dry the samples. Finally, the spin filter tube is transferred to a clean 1.9ml catch tube and 60µL TES elution solution was added, vortexed and centrifuged to elute the DNA in the catch tube ready to use.

The concentration and integrity of bacterial DNA were assessed using a Cubit (Thermo Scientific, appendix: table 1) and agarose gel electrophoresis, respectively. The 16S rRNA gene amplicon sequencing was performed on the Illumina MiSeq platform using universal primers 341F, 5′-CCTAYGGGRBGCASCAG-3′; and 806R, 5′-GGACTACNNGGGTATCTAAT-3′ targeting the V3-V4 hypervariable regions. The MiSeq instrument utilizes a double-sided, single-lane flow cell and reagent cartridge supplied in kit form. Sequencing is performed by recording the synthesis of DNA strands in clusters of sample templates attached to the flow cell. Each newly attached base liberates a fluorescent dye that is excited by diode lasers (530 & 660 nm) and imaged using two digital cameras. Sequential interrogation of bases allows for

the flexible adjustment of read length during a run. Up to 96 samples may be sequenced in a single run with DNA libraries prepared with indexed or bar-coded adapters.

Microbial Bioinformatic analyses

Raw data were merged and filtered to get clean data. The effective data was used to do operational taxonomic unit (OTU) cluster and species annotation for the respective sequence of each OTU. The relative species, evenness and abundance distribution were analyzed with alpha diversity and beta diversity. Downstream statistical analysis to explain the community construction differences between samples or among groups were performed via principal coordinate analyses (PCoA). Statistic methods such as T-test, MetaStat, LEfSe, Anosim and MRPP were employed to test the significance of community composition and structure differences between groups.

2.6 General statistical analyses

All except microbial sequencing data were analysed using Prism vs 8 (GraphPad, UK). Data were assessed initially for normality using Kolmogorov-Smirnov test which determines if the test is insignificant (>0.05) to confirm normal distribution or if the test is significant (<0.05), to be non-normal. We confirmed the data for fatty acids, gene expression and immunohistochemical data were non-normal and therefore analysed using suitable non-parametric statistical tool, Mann Whitney U-test. Statistic methods such as MetaStat, LEfSe, Anosim and MRPP were employed in the microbial gene sequencing data analyses to test the distribution and significance of community composition and structure difference between groups. Data were presented as mean ± SEM. Statistical differences were considered significant at $p < 0.05$. A typical box-and-whisker plot is illustrated below in figure 2.10:

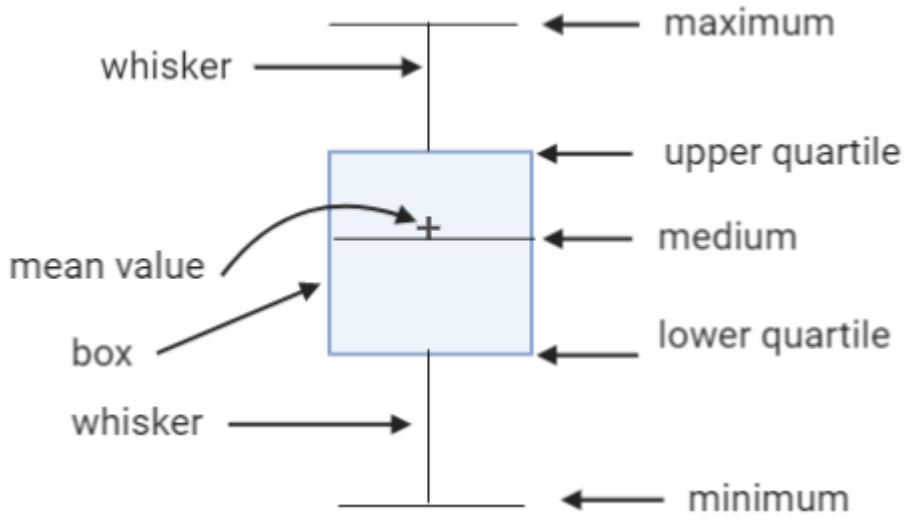

Figure 2.10: Box-and-whisker plot

Chapter 3

3.0 Study of the effects of high fat diet on the metabolism of fatty acids of mice exposed to normal husbandry or a specific germ-free environment

Abstract

Previous evidence suggests that HFD induces obesity-related metabolic diseases such as NAFLD through altered specific fatty acid metabolism. One critical fatty acid group is OCFA which recent studies suggest are inversely associated with NAFLD. The hypothesis was that high fat diet induces changes to specific fatty acids particularly OCFAs leading to the development of NAFLD.

Through feeding of C57B/6J mice with high fat diet in conventional or specific pathogen free environments, we comprehensively investigated possible contributions of these fatty acids from the diet, on fatty acid metabolic pathways. The investigations were done through a combination of fatty acid analysis by GC-MS, gene expression analyses by qPCR and immunohistochemical analyses of specific proteins. Circulating and liver OCFA including C15:0, C17:0 were decreased in HFD-fed mice in all dietary fat conditions studied and was associated with lower expression of *HACL1*. Overall, we show that impairment of OCFA metabolism after HFD was independent of growth environment. However, in contrast to normal husbandry, mice maintained at SPF conditions showed no change in even chain saturated fatty acids, an increase in MUFA and lower PUFA after a HFD which could be attributed to lower FADS2 expression.

3.1 Introduction

Obesity, NAFLD and related comorbidities are multifactorial condition resulting from the interaction between the environment, genetic and life-style factors, Annalisa et al (2014). Diet is an important lifestyle factor involved in the genesis, prevention and control of NAFLD, diabetes, obesity and other metabolic diseases, and can influence the gut microbiota, Lazar et al (2019). Many popular dietary patterns exist including Mediterranean, gluten-free, vegan, Western (high fat) and omnivore diets. Among these dietary patterns, high fat diet has been studied extensively and been associated with several metabolic phenotypes, Waqar et al (2010), Moreno-Fernández et al (2018), Julibert et al (2019).

Evidence from previous studies has associated a low-grade, chronic inflammatory state to obesity and its related metabolic conditions, including type 2 diabetes, metabolic syndrome, and NAFLD. It is well known that inflammatory mediators such as C-reactive protein, IL6, fibrinogen and plasminogen activator inhibitor-1 are synthesized in the liver and increased in NAFLD patients, Tarantino et al (2016). Moreover, it is reported that TNF-α, IL6 are increased, and are considered to be the major inflammatory mediators found in NAFLD, whereas IL-10 and adiponectin are decreased, Asrih et al (2013). Thioredoxin-interacting protein (TXNIP) is involved in regulation of inflammation, stress, and apoptosis, Shalev (2014). Despite the role of inflammatory cytokines mediating several metabolic diseases, the influence of dietary fat on inflammation is less understood.

Oxidative stress is an imbalance between the production and the elimination of ROS as well as decreased production/availability of antioxidants, Klandorf & Van Dyke (2012). ROS and oxidative stress are known to induce cell death through necrotic and/or apoptotic mechanisms, resulting in cellular and tissue injury. Oxidative stress is thought to play a critical role in initiation and progression of various liver diseases including NASH. The oxidative stress

triggers hepatic damage by inducing irreversible alteration of lipids, proteins and DNA as well as modulating pathways that control normal biological functions, Li et al (2015). The role of several antioxidants including catalase, GSR, Trx in obesity and its associated metabolic diseases have been studied, Amirkhizi et al (2010), Kumar et al (2013). However, this chapter goes further to investigate the effect of dietary fat on these antioxidants at the molecular level in the liver.

High intake of fat has been shown to be associated with increased lipotoxicity and hypertriglyceridemia, Jacobs et al (2004), Schrauwen (2007), Badin et al (2013). Moreover, there is a paucity of data regarding the association between plasma odd-chain fatty acids in subjects with obesity, type 2 diabetes and NAFLD. However, the influence of dietary fat on OCFA metabolism has not been studied.

It is thought that environmental condition where an organism is raised and fed can influence their metabolic outcome. For instance, feeding mice with HFD at normal husbandry environment caused them to gain weight whereas, those raised in a germ-free (GF) environment on same diet remained lean although their daily amount of food consumption was dramatically increased. Again, a study showed that mice consuming a HFD that had a high composition of both fat and sucrose was associated with a greater lipogenic effect on a normal husbandry fed mice compared to mice fed at GF environment, Annalisa et al (2014).

In this chapter 3, we assessed the impact of dietary fat on lipid metabolism in mice fed at different environment by performing comprehensive serum and liver fatty acid analyses using the state-of-the-art GC-MS. This was achieved by feeding male C57BL/6J mice with high fat diets based on lard at both conventional and specific pathogen free (SPF).

3.1.1 Aims

This study was aimed at investigating the effect of dietary fat on lipid metabolism in mice fed at normal husbandry or specific pathogen free environment. These experiments were set up to test the hypothesis that high fat diet intake would reduce serum and liver OCFA content and this is influenced by feeding at normal husbandry or SPF environment. The following were the specific objectives carried out:

1. Serum and liver FA analyses of all dietary fat models were performed by GC-MS
2. Hepatic transcript expression related to specific fatty acid changes in the liver/serum of dietary fat in SPF mice were characterized using qPCR
3. Basic liver histological technique, H&E staining was used to investigate hepatic lipid accumulation in SPF mice.
4. Peroxisome biogenesis protein expressions in fixed liver tissue were performed using immunohistochemistry technique in SPF mice.

The following figure 3.0 summarizes the experimental design of the study.

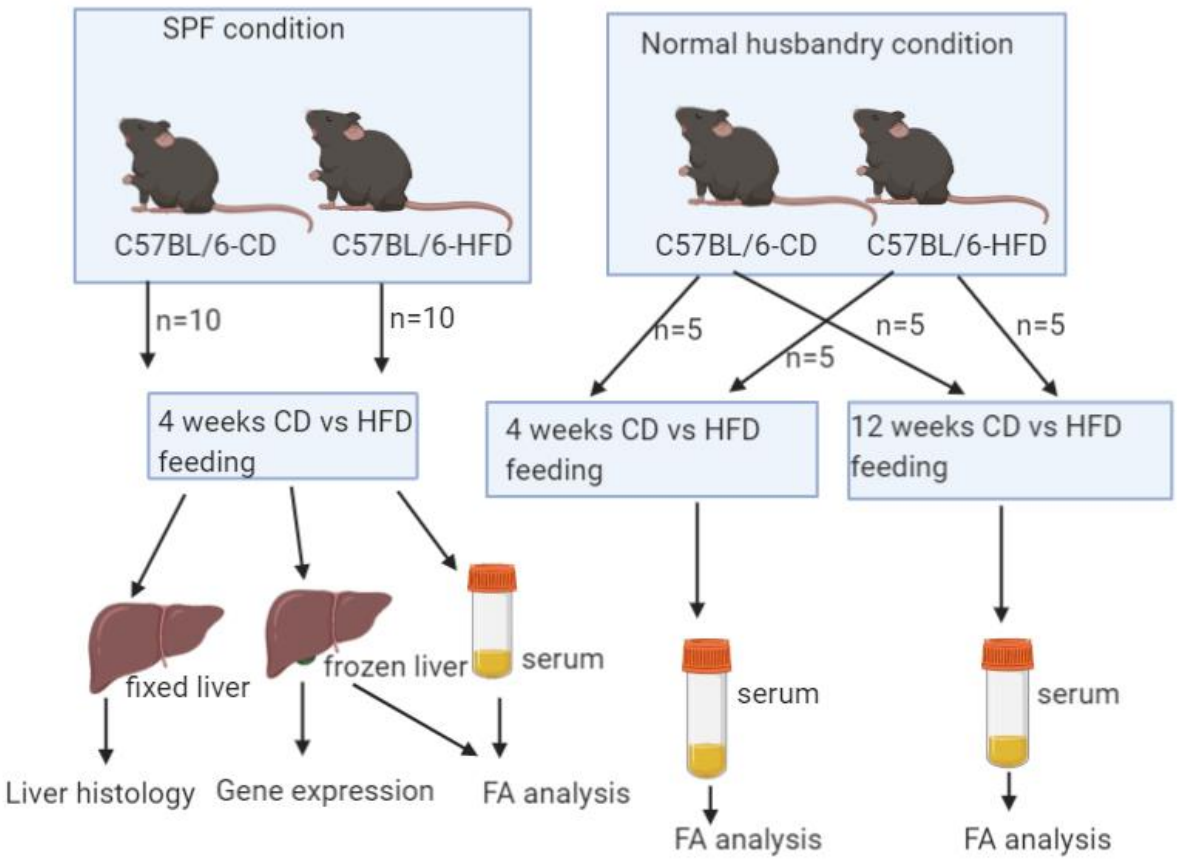

Figure 3.0: Experimental design of the study.

Male C57BL/6 mice fed CD, control diet or HFD, high fat dietary challenge at SPF condition or normal husbandry condition for 4 or 12 weeks (n=5 or 10 animals per group).

3.2 Method

3.2.1 High fat diet and sample collection

For a detailed description of the animal housing and HFD treatment procedures see Chapter 2. In brief, four groups of C57Bl/6 male mice were used to assess the influence of dietary fat on lipid metabolism in mice fed at either normal husbandry or SPF condition; two groups were kept on a chow diet (n = 5-10/group) and two groups on a high-fat diet (n = 5-10/group), from each subset there were both conventional or specific pathogen free (SPF) groups. The animals in the high fat diet (HFD) treated group received a 60% fat, 20% carbohydrate and 20% protein per kcal% while the animals in the control (CD)-treated group received a 10% fat, 70% carbohydrate and 20% protein per kcal%. All high fat diet studies were carried out in Nanjing- China SPF facility, China. All animals were given ad libitum of water and food prior to experimental treatment. After either 4- or 12-week period of feeding, the animals were killed via a cervical dislocation of the neck and blood samples were collected via heart puncture. The blood samples were allowed to clot on ice before centrifugation at 10,000 x g, 4 °C for 10 minutes to collect serum. Isolated serum was aliquoted, snap frozen and stored at -80 °C. Some of the liver samples were dissected out on ice, snap-frozen and stored at -80°C and others were fixed in 10% formalin. In this project, GC-MS-based analyses were carried out on serum and liver tissues. RT-qPCR analyses was performed on other snap frozen liver tissues, then the fixed liver tissues were used for the immunohistochemistry analyses.

3.2.2 GC-MS analyses

3.2.2.1 Serum and liver extract preparation and GC-MS experiments

The serum and liver sample preparation procedure has been described in Chapter 2, sections 2.2.1 and 2.2.2

3.2.2.2 Fatty acid methyl esters (FAMEs) derivatization

Fatty acids were derivatized using 200 μL toluene (Thermo-Fisher, UK), 1.5 mL methanol and 0.3 mL of 6.3% HCl in methanol at 35°C for 10 minutes for both serum (50 μL) and liver (50mg) samples, in PTFE-sealed glass vials. This was followed by derivatization to FA methyl esters (FAMEs) before subsequent extraction with 1 mL of hexane and 1 mL of water, then evaporated under nitrogen and resuspended in 70 μL of hexane in case of serum samples or in 150 μL for liver samples prior to analyses by gas chromatography (GC)

3.2.2.3 Gas chromatographic and mass spectrometry analyses.

Serum and liver fatty acid analyses were done using Agilent GC7890 system linked to a MSD5975 with electron impact ionization (70 eV). For details and column information have been described in Chapter 2, section 2.2.4.2

3.2.2.4 Fatty acid identification, data mining and normalization

All GC-MS spectral analyses were done using chemstation analyses software, FA were identified by matching mass spectra of samples with mass spectral library (eg NIST library) and/or reference standard (37 FAME mix). In addition, identified FA were based on GC retention times.

The internal standard (C11:0) was used to normalise mass spectral data for statistical analyses.

3.2.3 Real time qPCR

The Quant studio 7 RT-qPCR instrument was used to quantify the changes in mRNA levels of all genes studied in this high fat diet study (see Table 2.10). Primer information including selected genes, methods used in designing and verifying them have been as previously described (Chapter 2, section 2.4.1.2). The animals were sacrificed after 4 or 12-weeks of

feeding and the liver tissues removed and snap-frozen and then stored at -80°C until analysis (as previously described in Chapter 2, section 2.1.2). The RNA extraction procedure, the reverse transcription of RNA to complementary DNA (cDNA), and the RT-qPCR processes have been described in Chapter 2, section 2.2.1.3.

3.2.4 Histology & Immunohistochemistry

Basic staining technique, H&E was used to stain for lipid deposition in fixed liver tissue. Immunohistochemistry (IHC) technique was applied to evaluate the effects of high fat diet intake on catalase (1:100; Abcam (Ab16731)) and PEX-14 (1:100; Abcam (ab10999)) protein expression in the fixed liver tissues (as previously described in Chapter 2, section 2.3.5). Incubation of primary antibodies prior to conjugation with secondary antibody, goat anti-rabbit IgG H&L (HRP) (1:250; Abcam (6721)). In each HFD and control groups, samples from five animals selected for immunohistochemical analyses. Images of slides were captured with brightfield microscopy (as previously described in Chapter 2, section 2.3.4.1 and 2.3.4.3).

3.3 Results

3.3.1 Short-term effects of high fat and normal chow diets on fatty acid composition in serum mice fed in a conventional environment

Total serum fatty acid concentration

When male mice were fed with a high fat or a normal chow diets (control) for four weeks, no statistically significant differences were apparent when the total serum lipid concentration when compared between the 2 diets (figure 3.1). The absolute serum fatty acid concentrations and relative proportional measures were similar (table 3.1a & 3.1b in appendix).

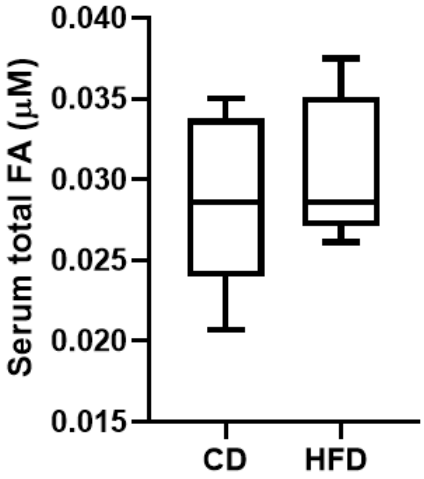

Figure 3.1: Effect of high fat diet on total lipid concentration in mouse serum Total fatty acids was measured in the serum of mice. Values are given as means ± SEM for n=5.

Table 3.1a: Fatty acid composition of short term HFD feeding in conventional mice

Group of FA	**% of total serum FA**	**CD Median (min-max)**	**HFD Median (min-max)**	***p-value***
ECFA	C14:0	0.78 (0.70-1.40)	0.35 (0.32-0.46)	0.0079
	C16:0	26.13(24.23-28.13)	28.26(27.45-35.48)	0.0952
	C18:0	6.62 (4.70-8.08)	14.33(12.12-18.10)	0.0079
	Total ECFA	32.51(31.62-36.93)	42.51(43.09-53.97)	0.0079
OCFA	C15:0	0.12 (0.09-0.15)	0.08 (0.06-0.11)	0.0159
	C17:0	0.29 (0.24-0.32)	0.16 (0.12-0.20)	0.0079
	Total OCFA	0.42(0.34-0.44)	0.25(0.20-0.28)	0.0079
MUFA	C16:1	1.99 (1.74-2.26)	7.85 (5.16-10.75)	0.0079
	C18:1	30.36(28.54-35.04)	17.63(15.84-19.83)	0.0079
	Total MUFA	32.38(30.53-36.99)	24.79(22.80-27.84)	0.0079
PUFA	C18:2n6	26.03(24.49-28.05)	25.80(19.92-28.03)	0.5476
	C18:3n3	2.57 (1.73-9.81)	2.41(1.80-2.72)	0.5476
	C20:4n6	1.82 (1.70-2.33)	1.72 (1.02-2.32)	0.5476
	Total PUFA	32.07(30.08-36.16)	29.92(22.97-32.90)	0.1508
Activity ratio	C16:1/C16:0	0.07 (0.06-0.09)	0.24(0.15-0.39)	0.0079
	C18:1/C18:0	5.08(3.76-6.28)	1.31(0.97-1.44)	0.0079
	C20:4n6/C18:2n6	0.07 (0.06-0.09)	0.07 (0.05-0.09)	0.6905

$p<0.05$, Control vs HFD, n=5, min-minimum, max-maximum

Even-chain saturated fatty acids

Among the even-chain saturated fatty acids, C18:0 after high fat diet was significantly higher compared to control ($p<0.001$, figure 3.2). The even-chain saturated fatty acids C14:0 in the serum was significantly lower level in HFD group compared to control ($p<0.05$, figure 3.2). There was no difference in serum content of C16:0 between the two diets. Moreover, total even-chain saturated fatty acids (C14:0, C16:0 & C18:0 combined) was significantly higher in HFD compared to CD fed groups (table 3.1).

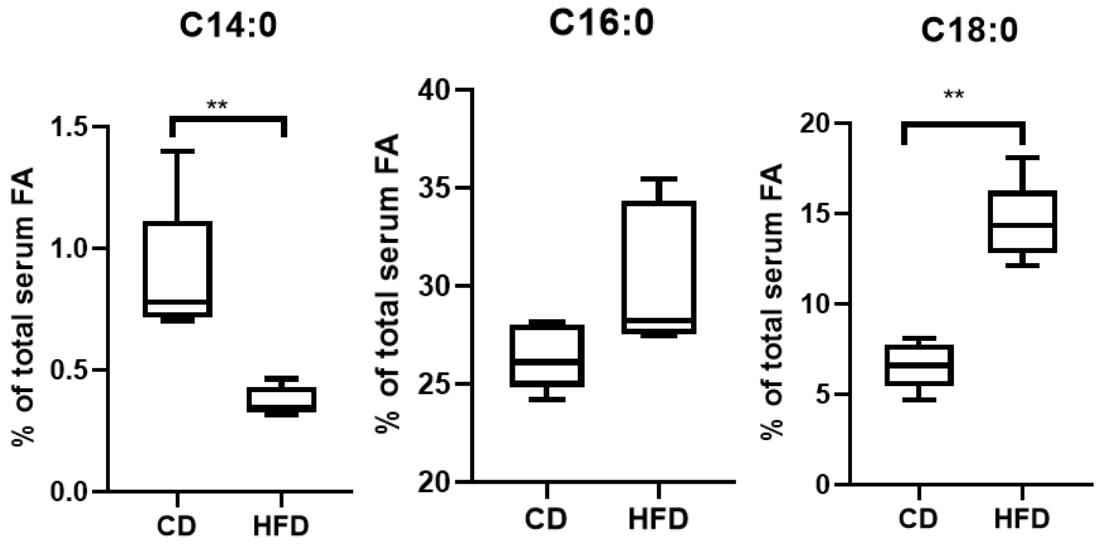

Figure 3.2: Effect of high fat diet on even-chain saturated fatty acid proportion in mouse serum
Fatty acids were measured in the serum of mice by GC-MS. Values are given as means ± SEM for n=5. **p<0.001 HFD vs CD

Odd-chain saturated fatty acids

In order to assess the effect of HFD on odd-chain saturated fatty acids (OCFAs), we analysed serum from mice after 4 weeks of feeding. Total serum OCFA showed a significant difference between the 2 diets ($p<0.001$, table 3.1). Both the C15:0 and C17:0 fatty acids were significantly lower after the HFD ($p<0.05$, figure 3.3).

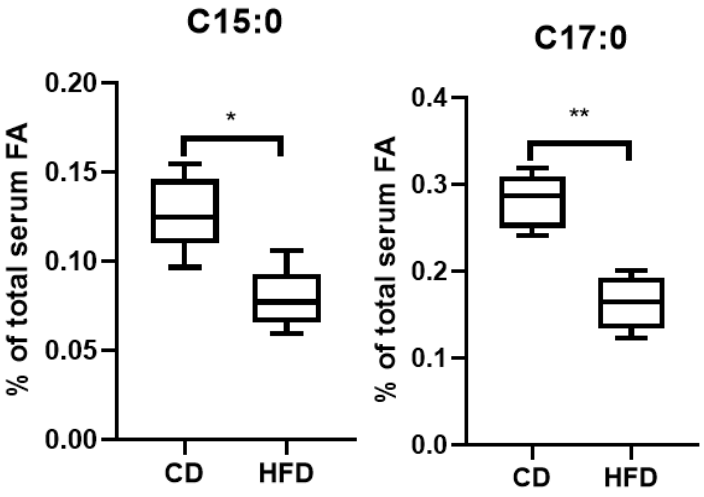

Figure 3.3: Effect of high fat diet on odd-chain saturated fatty acid proportion in mouse serum
Fatty acids were measured in the serum of mice by GC-MS. Values are given as means ± SEM for n=5. *p<0.05, **p<0.001 HFD vs CD

Mono-unsaturated fatty acids

The total MUFAs (C16:1 and C18:1 combined) were significantly lower in mice fed the HFD relative to those on normal chow diet (p<0.001, table 3.1). Both the C16:1 and C18:1 fatty acid changed in opposite directions in response to the diets (table 3.1). Among the MUFAs, there was significantly higher level in serum content of C16:1 between the HFD and control diet (p<0.001). On the contrary, short-term high fat feeding resulted in significantly lower content of serum 18:1 fatty acid in HFD compared to control (p<0.05, figure 3.4).

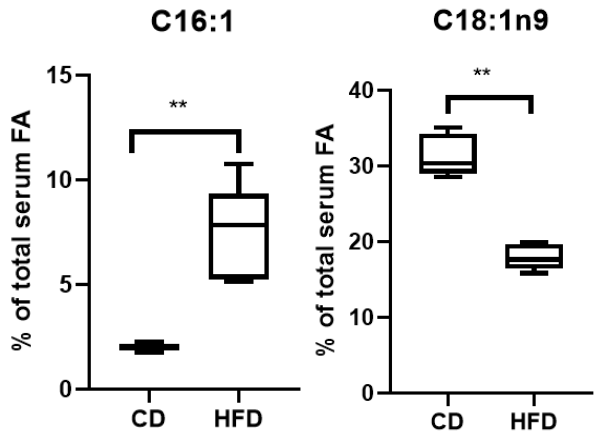

Figure 3.4: Effect of high fat diet on mono-unsaturated fatty acid proportion in mouse serum
Fatty acids were measured in the serum of mice by GC-MS. Values are given as means ± SEM for n=5. **p<0.001 HFD vs CD

Polyunsaturated fatty acids

The total PUFAs (C18:2, C18:3 and C20:4 combined) did not show a significant difference between high fat diet and normal chow diet groups (table 3.1). Moreover, these fatty acids individually were not significantly different following 4 weeks of high fat intake (figure 3.5).

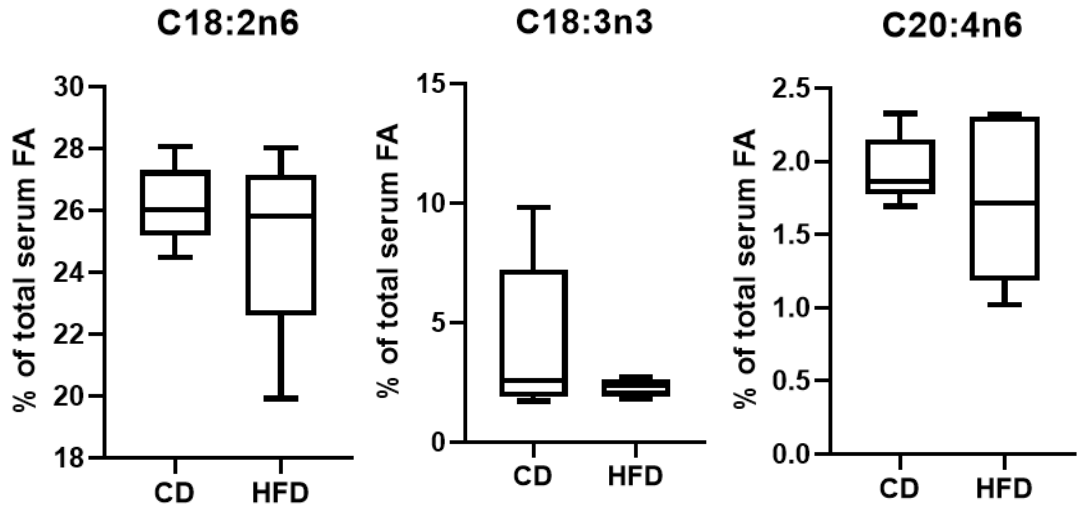

Figure 3.5: Effect of high fat diet on polyunsaturated fatty acid proportion in mouse serum
Fatty acids were measured in the serum of mice by GC-MS. Values are given as means ± SEM for n=5.

Indices of desaturation enzyme activity.

The 16:1n−7/16:0 ratio was significantly higher in the serum tissue of mice fed HFD compared to control ($p<0.001$). Interestingly, the 18:1*n*−9/18:0 ratio, however, was significantly lower in the serum after the HFD ($p<0.001$, **Table 3.1**) and the total MUFA to SFA ratio was significantly lower indicating decreased SCD1 activity. In the serum, the 20:4*n*−6/18:2*n*−6 ratios were not significant in response to short-term high-fat feeding.

3.3.2 Long-term effects of high fat and normal chow diets on fatty acid composition in serum of mice fed in a conventional environment

Total serum fatty acid concentration

Here, we have fed C57B/6 male mice with a high fat or a normal chow diets (control) for twelve weeks. We observed a higher but not statistically significant increase in total serum lipid concentration in HFD compared control diet (figure 3.6). The absolute serum fatty acid concentrations and relative proportional measures were similar (table 3.2a & 3.2b in appendix)

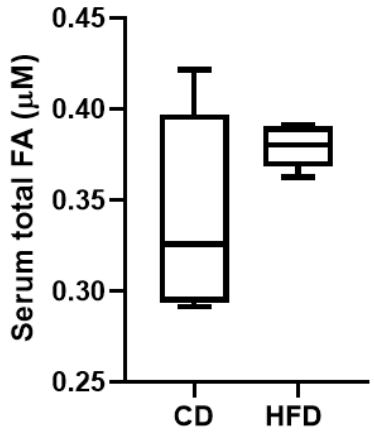

Figure 3.6: Effect of 12-week high fat intake on total lipid concentration in mouse serum Total fatty acids was measured in the serum of mice. Values are given as means ± SEM for n=5.

Table 3.2a: Fatty acid composition of long term HFD feeding in conventional mice

Group of FA	**% of total serum FA**	**CD Median (min-max)**	**HFD Median (min-max)**	***p-value***
ECFA	C14:0	0.87 (0.66-1.33)	0.34 (0.32-0.43)	0.0079
	C16:0	25.50(23.28-27.30)	25.47(24.20-26.67)	0.9999
	C18:0	6.92 (5.91-9.12)	12.01(10.74-14.72)	0.0079
	Total ECFA	34.22(30.11-37.10)	37.34(36.76-41.81)	0.0159
OCFA	C15:0	0.18 (0.16-0.20)	0.11 (0.06-0.12)	0.0079
	C17:0	0.21 (0.20-0.32)	0.20 (0.18-0.23)	0.2222
	Total OCFA	0.40 (0.38-0.49)	0.29 (0.26-0.35)	0.0079
MUFA	C16:1	1.98 (1.29-2.48)	6.47 (5.09-9.74)	0.0079
	C18:1	30.82(29.56-33.03)	16.33(16.08-18.13)	0.0079
	Total MUFA	32.88(31.53-34.92)	23.96(21.45-26.01)	0.0079
PUFA	C18:2n6	25.05(23.13-26.73)	26.59(21.66-26.79)	0.6905
	C18:3n3	0.22 (0.17-0.32)	0.20(0.19-0.22)	0.4206
	C20:4n6	7.34 (5.16-10.50)	14.14 (9.79-14.46)	0.0159
	Total PUFA	33.86(29.61-35.18)	38.35(33.29-41.45)	0.0556
Activity ratio	C16:1/C16:0	0.08(0.06-0.11)	0.24(0.20-0.40)	0.0079
	C18:1/C18:0	4.31(3.38-5.59)	1.34(1.23-1.53)	0.0079
	C20:4n6/C18:2n6	0.29 (0.21-0.43)	0.54(0.42-0.65)	0.0317

$p<0.05$, Control vs HFD, n=5

Even-chain saturated fatty acids

Similar to short-term HFD experiment, for the even-chain saturated fatty acid, the serum concentration of C18:0 after the HFD was significantly higher compared to control ($p<0.001$, figure 3.7). However, the even-chain saturated fatty acids serum concentration of C14:0 was lower in HFD fed mice compared to control ($p<0.001$). Again, the proportion of C16:0 in the serum was insignificant between the 2 diets. Analyses of total even-chain saturated fatty acids (C14:0, C16:0 and C18:0 combined) showed a significant increase in HFD mice relative to CD groups ($p<0.001$, table 3.2).

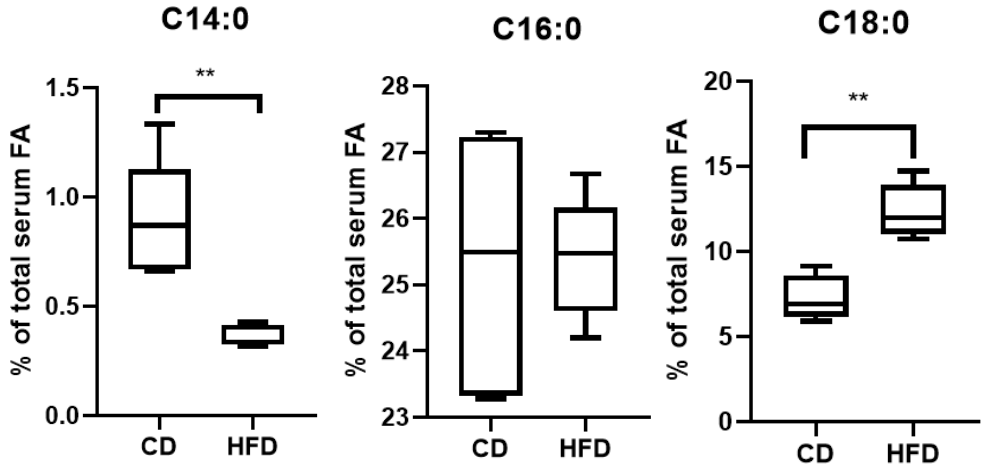

Figure 3.7: Effect of long-term high fat diet on even-chain saturated fatty acid proportion in mouse serum
Fatty acids were measured in the serum of mice by GC-MS. Values are given as means ± SEM for n=5. **p<0.001 HFD vs CD

Odd-chain saturated fatty acids

Here total serum odd-chain saturated fatty acids (C15:0 & C17:0) showed a significant decrease in mice fed HFD compared to those on normal chow diet ($p<0.001$, table 3.2). Whilst odd-chain saturated fatty acid C15:0 was significantly lower in response to the high diet ($p<0.001$, figure 3.8), and the C17:0 fatty acid proportion was not different between the 2 diets.

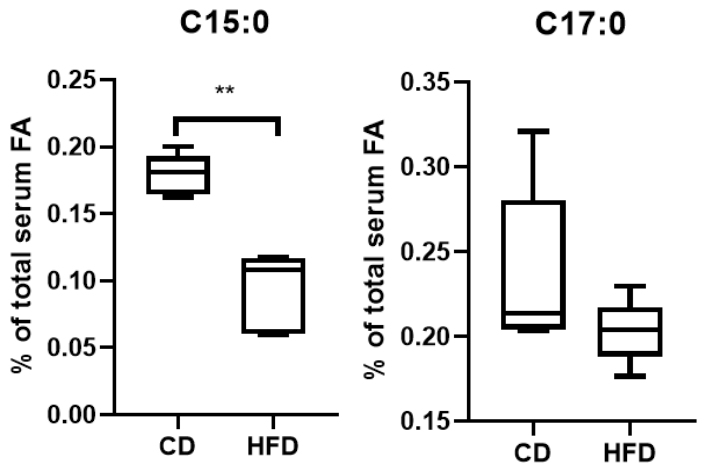

Figure 3.8: Effect of long-term high fat diet on odd-chain saturated fatty acid proportion in mouse serum
Fatty acids were measured in the serum of mice by GC-MS. Values are given as means ± SEM for n=5. **p<0.001 HFD vs CD

Mono-unsaturated fatty acids

Here, we observed similar trend as short term HFD intake. Thus, the total MUFAs (C16:1 and C18:1 combined) decreased significantly in mice fed the high fat diet for 12 weeks relative to those on normal chow diet ($p<0.001$, table 3.2). Also, both the C16:1 and C18:1 fatty acid changed in opposite directions in response to the diets (table 3.2). There was a significant higher in serum content of C16:1 in HFD fed mice compared to those on control diet ($p<0.001$, figure 3.9). However, long-term high fat feeding resulted in significantly lower content of serum 18:1 fatty acid in HFD compared to control ($p<0.001$, figure 3.9).

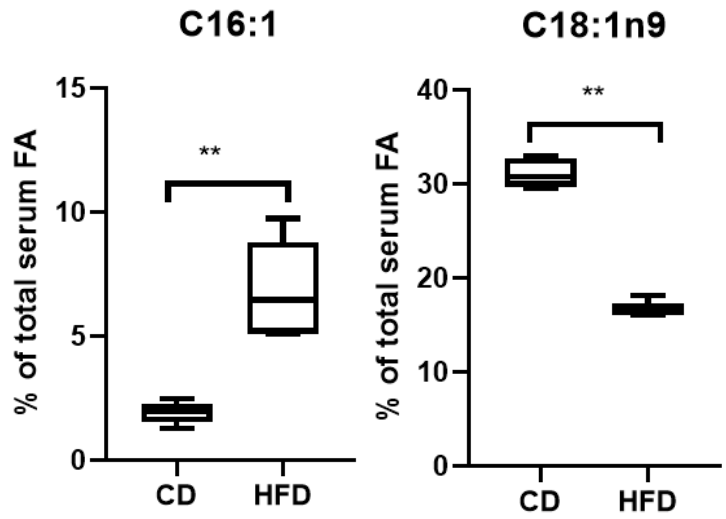

Figure 3.9: Effect of long-term high fat diet on monounsaturated fatty acid proportion in mouse serum
Fatty acids were measured in the serum of mice by GC-MS. Values are given as means ± SEM for n=5. **p<0.001 HFD vs CD

Polyunsaturated fatty acids

The proportion of total PUFAs (C18:2, C18:3 and C20:4 combined) was significantly higher in HFD compared to CD groups (table 3.2). When the PUFAs were analysed individually, both C18:2 & C18:3 were not statistically different following 12 weeks of high fat intake (figure 3.10). In contrast, arachidonic acid (20:4n–6) was higher in response to the high fat diet which resulted in significant differences between the 2 diets ($p<0.05$, figure 3.10).

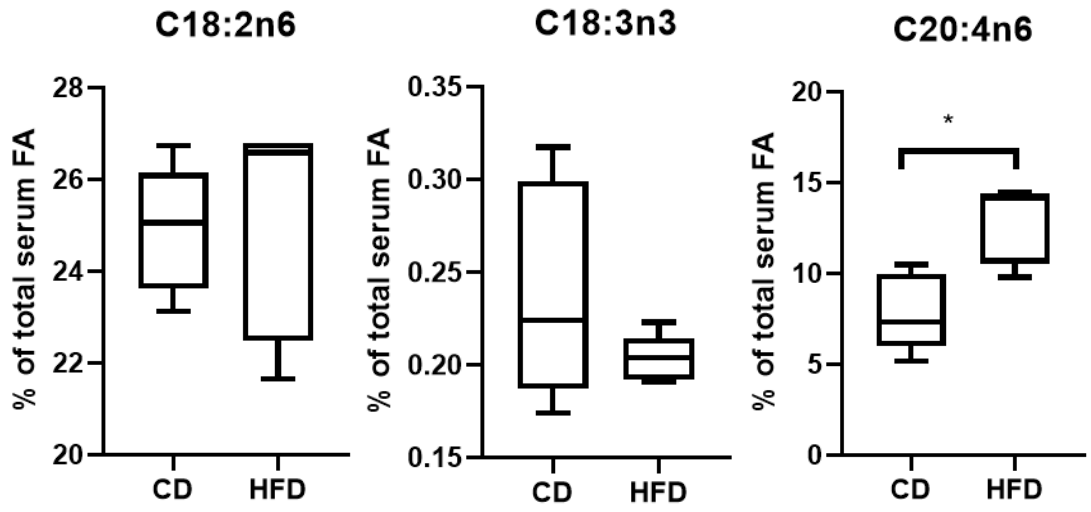

Figure 3.10: Effect of high fat diet on serum polyunsaturated fatty acid in mouse
Fatty acids were measured in the serum of mice by GC-MS. Values are given as means ± SEM for n=5. $p<0.05$, HFD vs CD

Indices of desturation enzyme activity.

Again, similar to observation of short term HFD feeding the 16:1n−7/16:0 ratio was significantly higher in the serum tissue of mice fed HFD compared to control ($p<0.001$). However, the 18:1*n*−9/18:0 ratio was significantly lower in the serum of HFD versus CD ($p<0.001$, table 3.2) indicating decreased SCD1 activity. Additionally, we found an increase in 20:4*n*−6/18:2*n*−6 ratios in response to long-term high-fat feeding.

3.3.3 Effect of high fat intake on serum and liver fatty acids in mice raised in SPF environment

3.3.3.1 Growth rate of specific pathogen free mice fed high fat diet

Mice raised in specific pathogen free (SPF) facility adapted to a defined normal rodent diet (chow) were switched to a lard-based high-fat diet (chapter 2, table 2.3). During the first 4 weeks of high fat diet (HFD) feeding, SPF mice significantly gained body weight (chapter 2, figure 3a). Starting from baseline (week 0) to week 4, both HFD and control diet (CD) mice significantly increased body weight over time. A significant increase in body weight between HFD-fed mice and CD mice was first evident at week 1 ($p<0.0001$). Increases in body weight

of HFD mice remained significantly greater than CD mice from week 2 onward ($p<0.001$ between HFD mice and CD mice at week 2; all others $p<0.05$), figure 3a

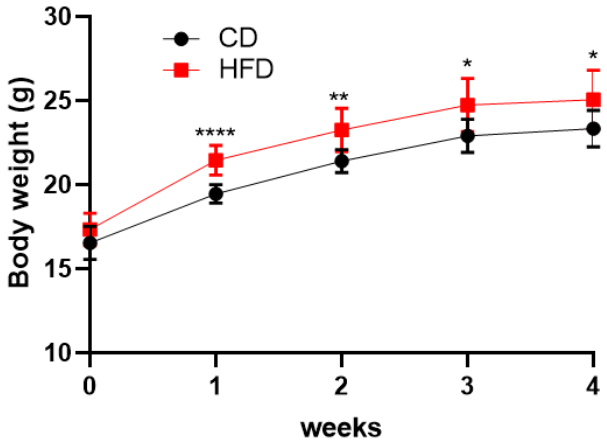

Figure 3a: Dietary fat from lard increases body weight in SPF mice.

Body weight gain during the first 2 weeks of experimental feeding. ****$p < 0.0001$ and **$p < 0.001$ for HFD relative to CD; $p < 0.05$ to the end of the feeding trial (3 & 4 weeks). SPF CD: n = 10; SPF HFD: n = 10.

3.3.3.2 High fat diet intake did not affect total serum and liver lipid concentrations in in SPF mice.

Male C57B/6 mice were fed a high fat diet in SPF environment for 4 weeks. GC-MS analyses of both serum and liver samples from these mice showed no significant difference in fatty acid concentration between HFD and CD (figure 3.11). The absolute fatty acid concentrations and relative proportions of serum and liver obtained from mice after 4 weeks of HFD feeding at SPF condition are shown in table 3.3 & 3.4 respectively. Both absolute FA concentrations and proportional measures showed a similar pattern of FA changes although the effect was more clearly observed in relative proportions (table 3.3a & 3.4b in appendix).

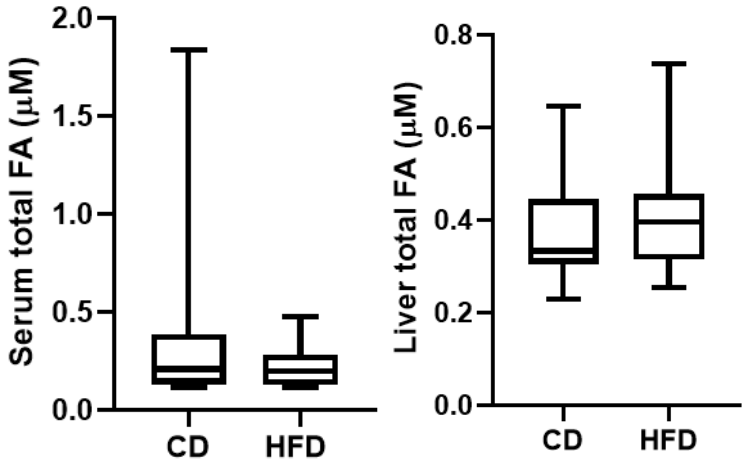

Figure 3.11: Effect of high fat intake on total lipid concentration in the serum and liver in SPF mice

Fatty acids were measured in the serum of mice by GC-MS. Values are given as means ± SEM for n=10.

Table 3.3a: Fatty acid composition of serum in HFD-fed SPF mice

Group of FA	**% of total serum FA**	**CD**	**HFD**	***p-value***
		Median (min-max)	**Median (min-max)**	
ECFA	C14:0	1.14 (0.93-1.34)	1.01 (0.58-1.33)	0.1128
	C16:0	26.59(21.74-30.72)	28.12(23.84-31.44)	0.3562
	C18:0	8.59 (6.75-9.89)	9.93(7.60-11.45)	0.0789
	Total ECFA	36.30(32.68-41.29)	38.69(33.19-43.54)	0.1333
OCFA	C15:0	0.11 (0.08-0.13)	0.04 (0.03-0.06)	0.0001
	C17:0	0.23 (0.22-0.39)	0.25 (0.21-0.28)	0.8254
	Total OCFA	0.34 (0.33-0.48)	0.29(0.24-0.34)	0.0002
MUFA	C16:1	2.75 (1.70-3.96)	2.36 (1.75-2.89)	0.2428
	C18:1	22.06(19.27-23.55)	29.39(24.72-33.05)	0.0001
	Total MUFA	23.98(22.53-26.43)	32.00(26.61-35.05)	0.0001
PUFA	C18:2n6	34.33(28.92-37.01)	24.49(21.50-26.76)	0.0001
	C18:3n3	0.28 (0.21-0.76)	0.16(0.06-0.36)	0.0101
	C20:4n6	5.79 (4.07-11.52)	7.61 (1.69-15.51)	0.4967
	Total PUFA	40.73(37.77-43.94)	31.69(26.34-40.31)	0.0001
Activity ratio	C16:1/C16:0	0.10 (0.08-0.14)	0.08(0.06-0.11)	0.0508
	C18:1/C18:0	2.32 (2.21-3.41)	2.82(2.38-4.34)	0.0760
	C20:4n6/C18:2n6	0.16 (0.11-0.39)	0.31(0.07-0.72)	0.1276

$p<0.05$, Control vs HFD, n=10

Table 3.4a: Fatty acid composition of liver in HFD-fed SPF mice

Group of FA	**% of total liver FA**	**CD**	**HFD**	***p-value***
		Median (min-max)	**Median (min-max)**	
ECFA	C14:0	0.47 (0.36-1.05)	0.53 (0.46-0.74)	0.1431
	C16:0	29.52(24.51-37.06)	27.32(22.36-33.58)	0.2176
	C18:0	11.27 (7.94-16.18)	9.87(7.33-13.23)	0.3150
	Total ECFA	41.36(33.54-53.70)	37.95(30.28-45.28)	0.2176
OCFA	C15:0	0.22 (0.20-0.25)	0.15 (0.13-0.18)	0.0001
	C17:0	0.43 (0.37-0.59)	0.35 (0.32-0.38)	0.0001
	Total OCFA	0.66 (0.58-0.83)	0.49(0.47-0.53)	0.0001
MUFA	C16:1	1.43 (0.79-2.36)	1.13 (0.85-1.90)	0.2176
	C18:1	19.80(17.06-26.43)	26.73(22.44-32.27)	0.0021
	Total MUFA	21.22(17.85-28.79)	27.87(23.52-33.83)	0.0039
PUFA	C18:2n6	28.94(25.88-37.53)	24.96(21.24-28.37)	0.0021
	C18:3n3	0.26 (0.20-0.61)	0.54(0.35-0.74)	0.0005
	C20:4n6	7.56 (4.44-11.95)	8.08 (6.12-10.60)	0.7959
	Total PUFA	37.35(35.85-43.94)	33.47(30.71-35.40)	0.0001
Activity ratio	C16:1/C16:0	0.05 (0.02-0.09)	0.04(0.03-0.07)	0.6842
	C18:1/C18:0	1.72(1.08-3.32)	2.71(1.84-4.40)	0.0185
	C20:4n6/C18:2n6	0.26 (0.14-0.44)	0.32 (0.22-0.48)	0.3930

$p<0.05$, Control vs HFD, n=10

3.3.3.3 SPF mice fed high fat diet showed no differences in serum and liver concentration of even-chain saturated fatty acids

After analysing the content of total even-chain fatty acids (C14:0, C16:0 &C18:0 combined), we observed no significant changes between HFD and CD fed groups either in serum or liver tissues (table 3.3 & 3.4). There was no significant difference between HFD versus CD groups in individual ECFAs concentration (i.e C14:0, C16:0 or C18:0) in both serum and liver (figure 3.12).

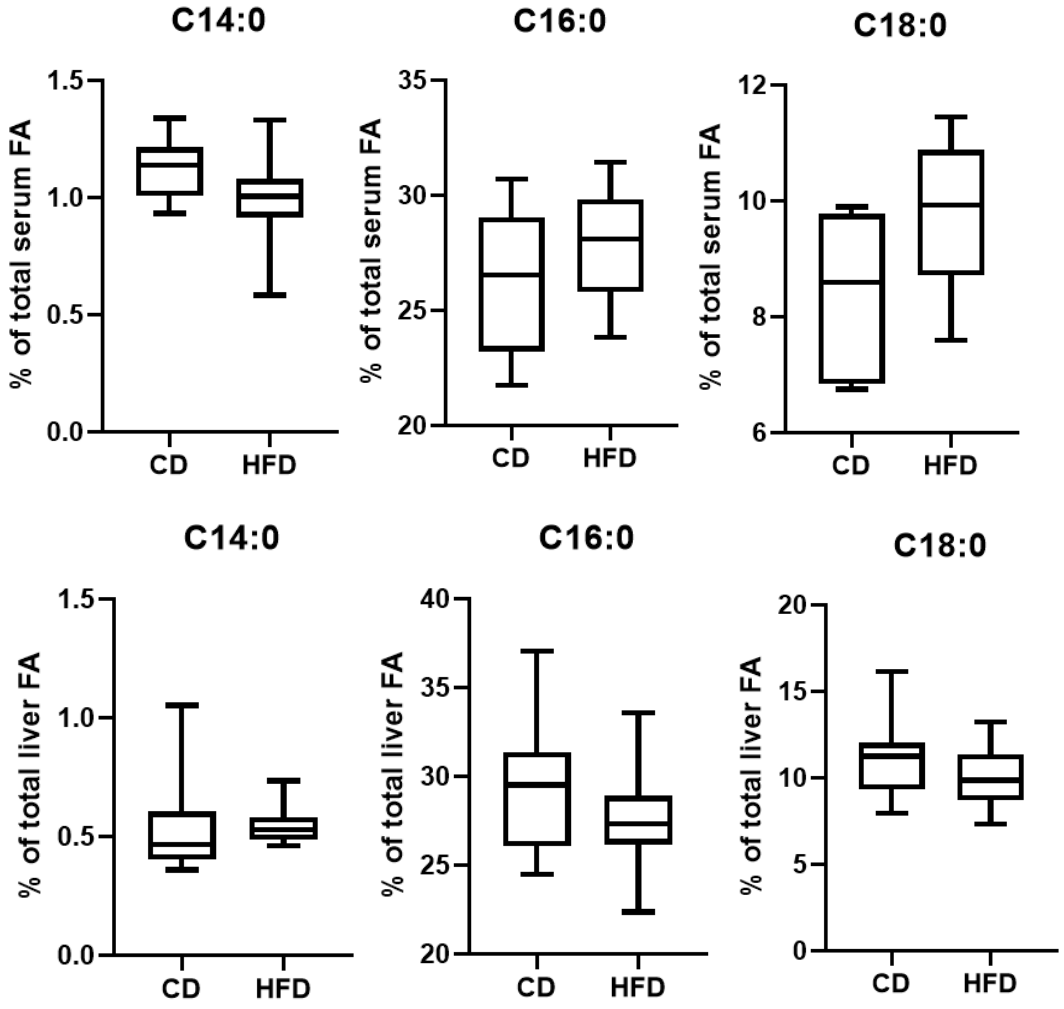

Figure 3.12: Effect of high fat intake on even-chain saturated FA proportion in the plasma and liver in SPF mice
Fatty acids were measured in the serum of mice by GC-MS. Values are given as means ± SEM for n=10.

3.3.3.4 Effect of high fat intake on odd-chain saturated FA concentration in the serum and liver in SPF mice

Analysis of serum fatty acid profiles revealed HFD fed mice displayed lower levels of odd-chain saturated fatty acids (C15:0 & C17:0 combined) when compared to CD mice (table 3.3, $p< 0.0001$). Similarly, in the liver samples, we observed that HFD fed mice showed lower level of total OCFA relative to CD fed mice (table 3.4, $p<0.0001$). Analysis of specific odd-chain fatty acids revealed HFD fed mice displayed significantly lower proportion of serum pentadecanoic acid (figure 3.13, $p<0.0001$) but no significant difference in serum heptadecanoic acids when compared to CD fed mice. In the liver, HFD mice displayed a lower content of both C15:0 ($p<0.05$) and C17:0 ($p<0.05$) levels compared to CD fed group (figure 3.13).

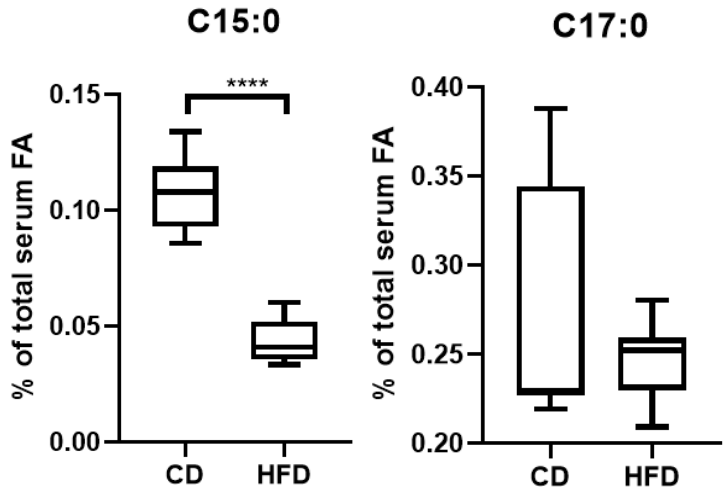

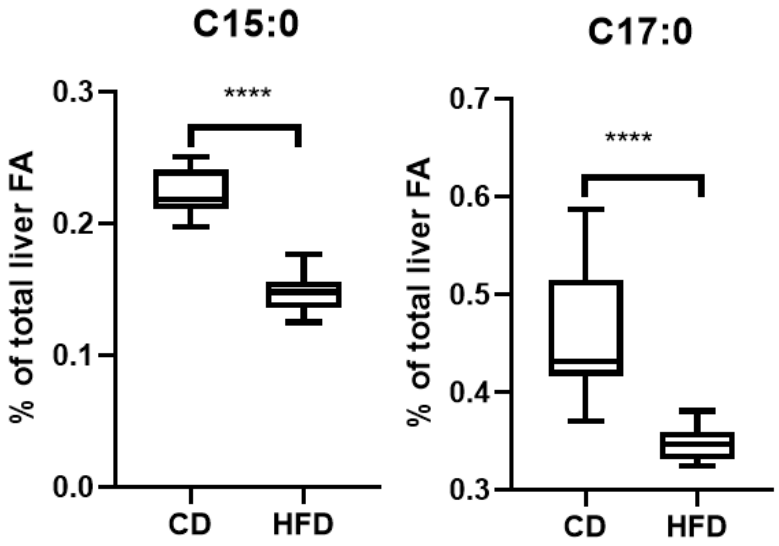

Figure 3.13: Effect of high fat intake on odd-chain saturated FA proportion in the serum and liver in SPF mice

Fatty acids were measured in the serum of mice by GC-MS. Values are given as means ± SEM for n=10. ****p<0.0001 HFD vs CD)

3.3.3.5 Effect of high fat intake on monounsaturated FA concentration in the serum and liver in SPF mice

Here, analyses of total MUFAs (C16:1 & C18:1combined) of HFD fed mice showed elevated levels of total MUFA compared to CD group both in serum (table 3.3; p<0.001) and liver (table 3.4: p<0.0001). Moreover, analyses of individual MUFAs showed higher proportion of C18:1n9 in HFD compared to CD in either serum or liver tissues, however, C16:1 showed no difference between HFD and CD in serum and liver samples (figure 3.14).

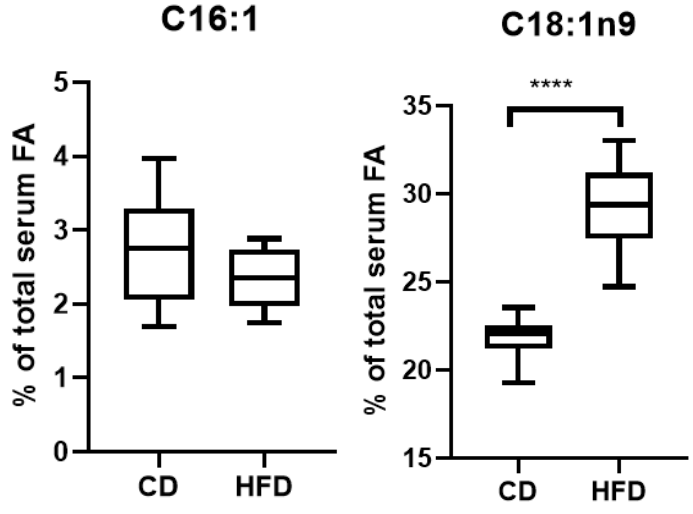

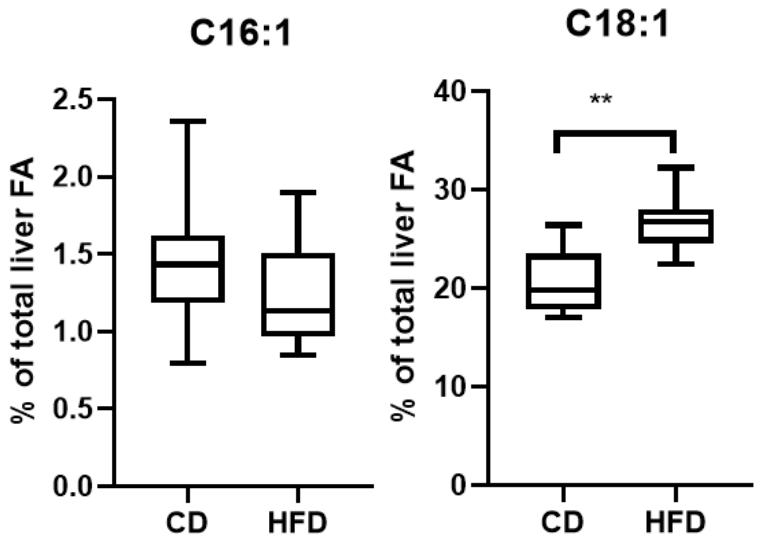

Figure 3.14: Effect of high fat intake on monounsaturated FA proportion in the serum and liver in SPF mice

Fatty acids were measured in the serum of mice by GC-MS. Values are given as means ± SEM for n=10. **p<0.001, ****p<0.0001 HFD vs CD.

3.3.3.6 Polyunsaturated fatty acid concentrations were reduced in HFD fed SPF mice

When total PUFAs were analysed in serum, we observed a significantly lower proportion in SPF-mice fed HFD compared to CD (table 3.3: p<0.0001). Moreover, there was a significantly lower proportion of total PUFA in the liver of HFD fed mice relative to the control group (table 3.4: p<0001). There was no significant differences between the two diets in C20:4n-6 in either serum or liver. However, the percentage of serum C18:3n3 (p<0.05) or C18:2n6 (p<0.001) were lower in HFD compared to CD fed mice (figure 3.15). In the liver the proportion of C18:3n3 (p<0.0001) was higher in HFD, however, C18:2n6 (p<0.001) was lower relative to CD (figure 3.15).

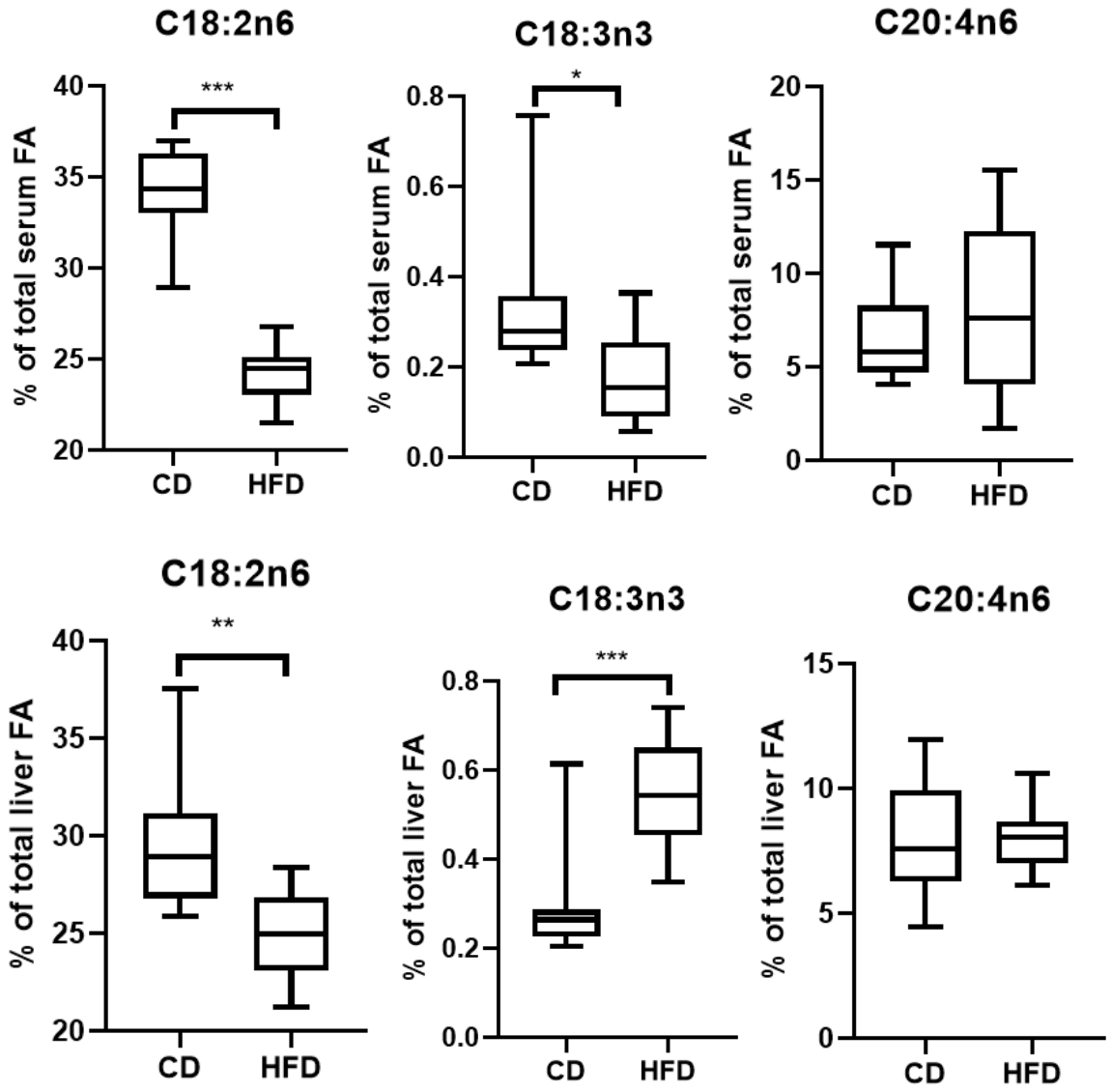

Figure 3.15: Effect of high fat intake on polyunsaturated FA proportion in the serum and liver in SPF mice

Total fatty acids was measured in the serum and liver of mice. Values are given as means ± SEM for n=10. **p<0.001 HFD vs CD; ***p<0.0001 HFD vs CD)

Indices of desturation enzyme activity.

Here, we assessed alternative markers for enzyme activities and observed no significant difference between HFD and CD with regards to serum 16:1n−7/16:0 and C20:4/C18:2 ratios. However, the 18:1*n*−9/18:0 ratio was significantly higher in the serum of HFD versus CD ($p<0.05$, table 3.3). There was no difference in liver 16:1n−7/16:0, 18:1*n*−9/18:0 and 20:4*n*−6/18:2*n*−6 ratios, between the two diets (table 3.4) under SPF conditions.

3.3.3.7 Effect of a high fat diet on expression of genes involved in fatty acid uptake in SPF condition

Here we have investigated the effect of HFD on two fatty acid transporters (*CD 36* and *FABP3*) after four weeks of feeding under specific pathogen free condition. Gene expression analyses of these fatty acid transporters did not differ between mice fed 60% HFD and those that consumed chow diet (CD) containing 10% fat (Figure 3.16).

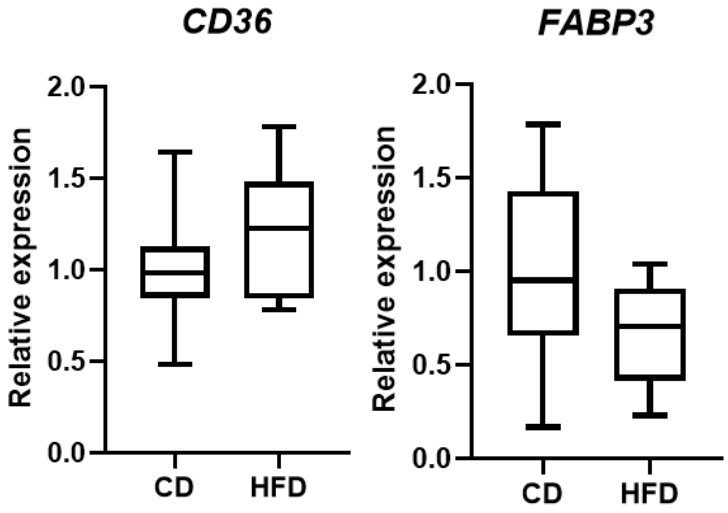

Figure 3.16: Effect of HFD on *CD36* and *FABP3* mRNA expressions.

Mean relative transcript expression of genes involved in hepatic fatty acid uptake in mouse liver. Values are given as means ± S.E.M for n=10; Abbreviations: *CD36*: cluster of differentiation; *FABP3*: fatty acid binding protein 3.

3.3.3.8 Effect of high fat diet on fatty acid genes related to specific fatty acid metabolism

To understand the mechanisms underlying fatty acid changes observed in the plasma and liver of mice fed under SPF condition, we performed gene expression analyses on 7 genes involved in specific fatty acid synthesis. They include stearoyl co-A desaturase 1 (*SCD1*), fatty acid desaturase 2 (*FADS2*), ELOVL family member 6, elongation of long chain fatty acids (*ELOVL 6*), 2-hydroxyacyl-CoA lyase 1(*HACL1*), branched chain ketoacid dehydrogenase E1, alpha polypeptide (*BCKDHA*) and phytanoyl-coA hydroxylase (*PCCA*). The mRNA levels of steroyl co-A desaturase 1 (*SCD1*; $p<0.001$), fatty acid desaturase 2 (*FADS2;* $p<0.001$), ELOVL family member 6, elongation of long chain fatty acids (*ELOVL6*; $p<0.0001$), and 2-hydroxyacyl-CoA lyase 1 (*HACL-1*, $p<0.05$) were significantly lower expressed among mice fed high fat diet compared to mice on chow diet (figure 3.17). However, there was no significant difference in expression of branched chain ketoacid dehydrogenase E1, alpha polypeptide (*BCKDHA*) and phytanoyl-coA hydroxylase (*PCCA*) observed mice fed high fat diet and control diet. (Figure 3.17)

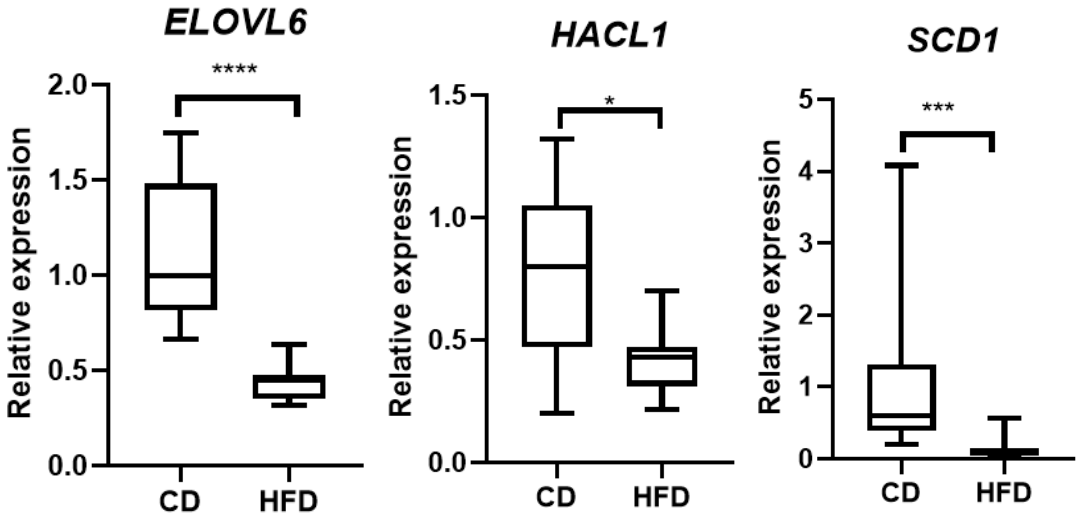

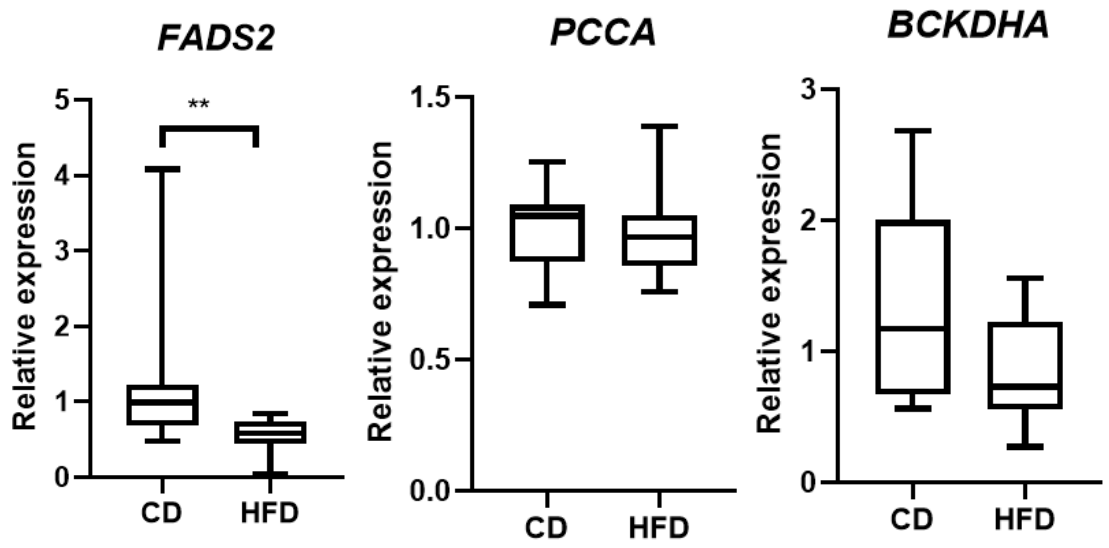

Figure 3.17: Effect of a 4-week HFD feeding on *ELOVL6, HACL1, SCD1, FADS2, PCCA* and *BCKDHA* mRNA expressions in SPF mice.
Mean relative transcript expression of genes related to specific fatty acid changes in mouse liver. Values are given as means ± S.E.M for n=10; *p<0.05, ****p<0.0001 CD vs HFD.

3.3.3.9 High fat diet did not alter the expression of genes involved in inflammation or anti-oxidant genes

Fatty acids particularly n-6 PUFA are known to be pro-inflammatory and pro-oxidant. Here, we analysed specific genes involved in inflammation or anti-oxidant activities. TNF-α gene expression, involved in inflammation, was statistically insignificant between high fat diet (HFD) group and control diet (CD) group (figure 3.19). Moreover, glutathione reductase (*GSR*), and thioredoxin 1 (*TRX1*) genes which are antioxidants were not altered in HFD fed mice (figure 3.18).

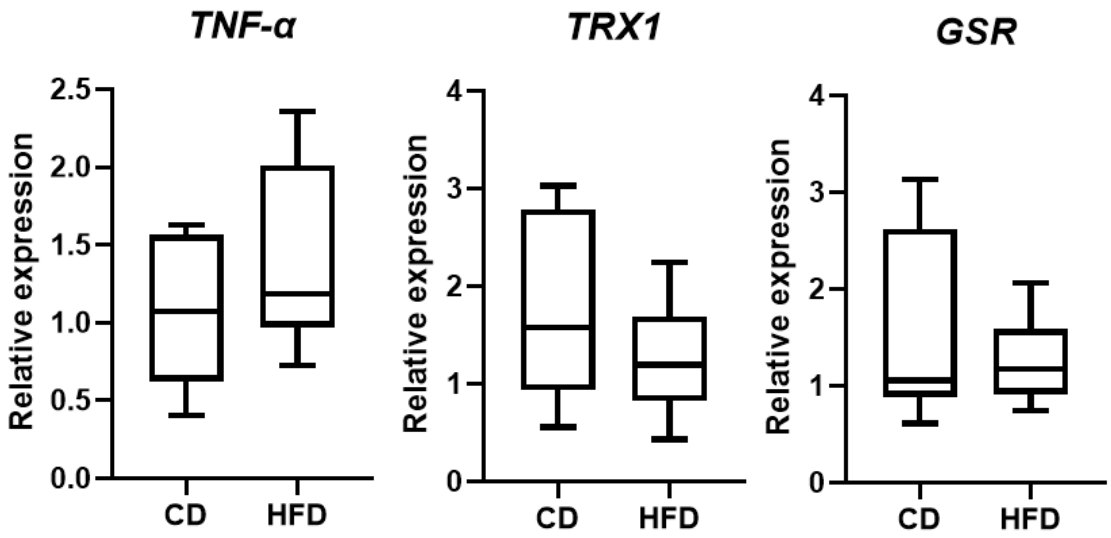

Figure 3.18: Effect of HFD on pro-inflammatory and anti-oxidant mRNA expression in SPF mice.
Mean relative transcript expression of genes involved pro-inflammatory and antioxidant activities in mouse liver. Values are given as means ± S.E.M for n=10

3.3.3.10 Induction of steatosis in SPF mice through high fat diet

Mice were maintained on either 60% high fat diet or control diet containing 10% of fat in a specific pathogen free environment for four weeks. Following this, part of the liver was fixed in 10% formalin for histological analyses. The liver H&E staining of control mice showed normal architecture without any evidence of steatosis. In contrast, the HFD feeding induced histological steatosis in the liver (figure 3.19).

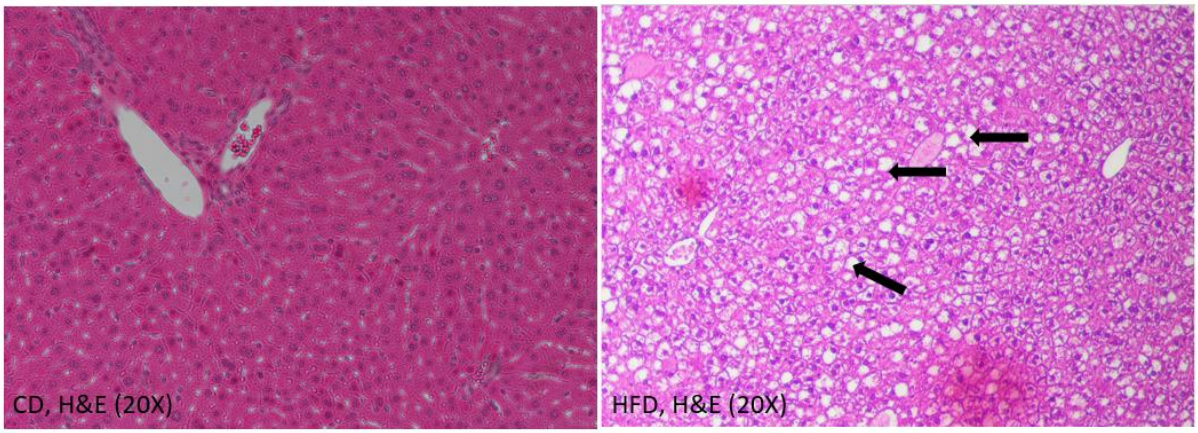

Figure 3.19: Hepatic steatosis in the livers of SPF mice on high fat diet and appears as vacuolation in H&E stain.

Representative chow diet group (CD) mouse and representative high fat diet (HFD) mouse liver. Representative liver sections stained with haematoxylin and eosin (original magnification 20×). Arrows indicate large lipid droplets in HFD liver sections. Each image is a representative section from one mouse out of five different mice per dietary group.

3.3.3.11 High fat diet induces peroxisomal biogenesis protein expression in liver tissues

To test whether a high fat diet can induce the expression of peroxisomal biogenesis protein, an experimental design was employed by feeding mice with a 60% high fat diet (HFD) and compared to a control diet (CD) containing 10% of fat. Peroxisomal biogenesis protein, peroxin 14 (PEX14) which is thought to be superior for detection of true abundance and distribution of peroxisomes compared to others including catalase were analysed using immunohistochemistry following a 4-week high fat diet intake Grant et al (2013). In response to the HFD, PEX-14 expression was increased in HFD compared to CD (figure 3.20 B & C).

A.

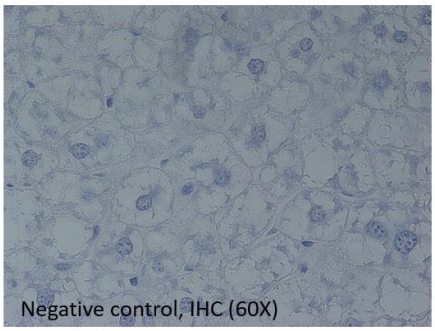

B.

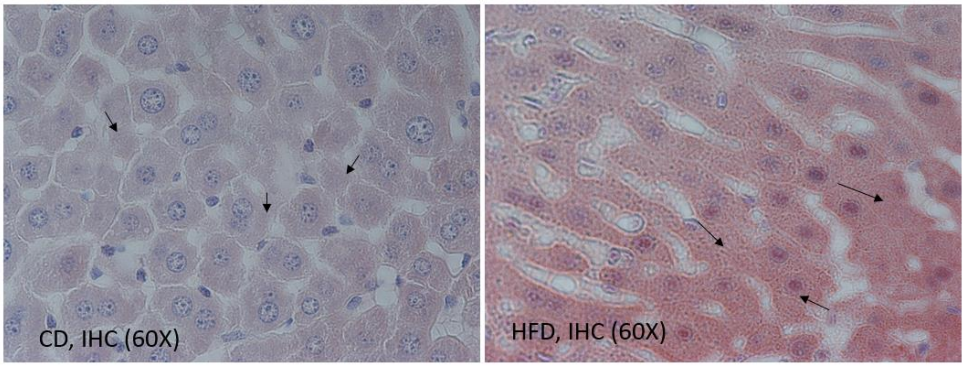

C.

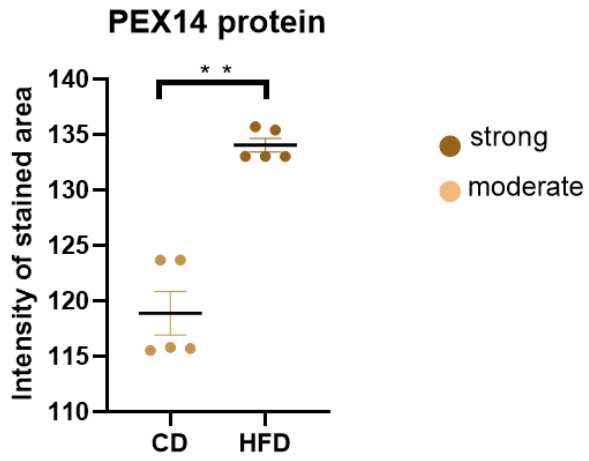

Figure 3.20: Immunostaining of PEX 14 in liver from 4-week CD and HFD mice at SPF condition

Immunohistochemistry was performed on mice obtained from CD and HFD using anti-PEX14 antibody. Arrors head indicate PEX 14 staining in the liver cells. Negative control slide is unstained set-up by omitting primary antibody. Nuclei were counterstained with haematoxylin. (original magnification 60×). A: Negative control: B: A representative section from one mouse liver out of five different mice per group; C. IHC analyses of PEX14 stained intensity in arbitrary units (**p<0.001 HFD vs CD).

Furthermore, we analysed another protein, catalase, an important antioxidant defence enzyme. Here, after 4 weeks of high fat feeding in SPF mice and immunostaining of the liver, the HFD group showed higher expression of catalase protein than CD group as shown in (figure 3.21 A &B).

A.

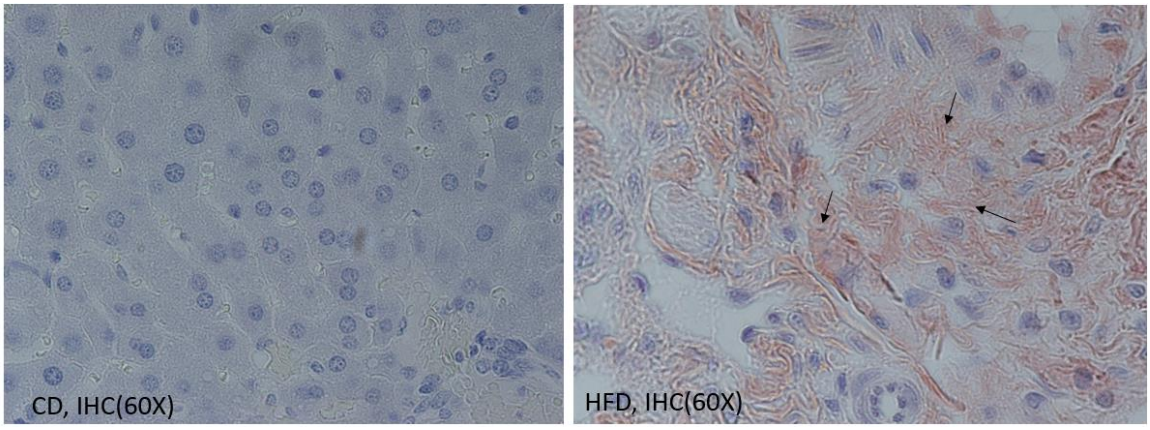

B.

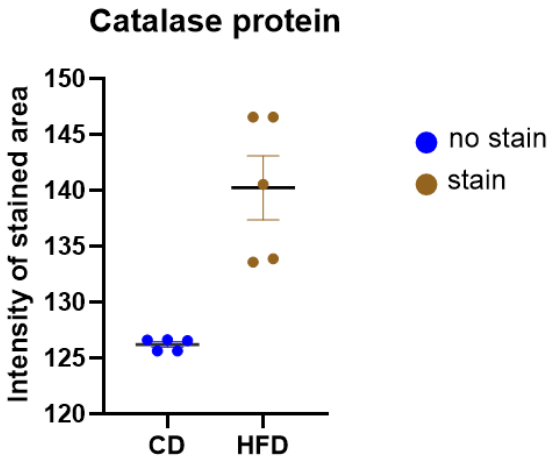

Figure 3.21: Immunostaining of catalase in liver from 4-week CD and HFD mice at SPF condition.

Immunohistochemistry was performed on mice liver obtained from CD and HFD using anti-catalase antibody. Arrows head indicate PEX-14 staining in liver cells. Negative control slide is unstained set-up by omitting primary antibody. Nuclei were counterstained with haematoxylin. (original magnification 60×) A representative section from one mouse liver out of five different mice per group; B: IHC analyses of catalase stained intensity in arbitrary units.

3.4 Discussion

3.4.1 Principal findings

Gowth environment such as normal husbandry, germ free (GF) and specific pathogen free (SPF) conditions have particularly been employed in biomedical research to better understand the molecular mechanisms underlying diet–host interactions, Kübeck et al (2016); Dobson et al (2019). It is well known that the HFD diet modifies liver and serum FA distribution, Tranchida et al (2012). However, the effect of high fat feeding on plasma and liver FA distribution under SPF condition have not been investigated. Here, we provide some novel insights into the biochemical and metabolic mechanism of action of 4-week HFD-fed mice under SPF condition. We also provide a comprehensive fatty acid profile of mice that have been fed with high fat diet in a conventional environment for either 4 or 12 weeks respectively. For this purpose, a GC-MS, Rt-qPCR and immunohistochemistry approaches were employed to analyse the serum, and liver samples of mice that have undergone dietary challenge. Our data indicate changes in plasma and liver FA composition after 4 weeks of HFD feeding in SPF mice that are different from normal husbandary animals receiving the same diet, apart from OCFA. Indeed, the serum and liver FA profile in HFD-fed SPF mice were characterized by a decrease proportion of OCFA notably C15:0 and C17:0, respectively as well as by a higher proportion of MUFA compared to CD fed mice under same condition. Moreover, we showed similar changes in fatty acid profile in HFD-fed under normal husbandry condition for 4 and 12 weeks respectively, except an observation of a decrease proportion in serum palmitoleic acid (C16:1) in HFD-fed SPF mice relative to CD. Although high fat diet induced-obesity and metabolic dysfunction is well established in the literature Buettner et al (2007), this study suffer from carbohydrate confounding limitation. Therefore, in the present study it is possible that the lipid metabolic changes observed in HFD fed mice relative to CD fed mice were in part influenced by imbalance of carbohydrate contents between the HFD and control diet.

3.4.2 Body weight and total lipid concentration in SPF mice

A four-week HFD regimen was used in the current study to examine the effect of the HFD lipid metabolism and how changes in lipid metabolism are influenced by gut microbiota. Obesity-prone mice (C57Bl/6) have a thrifty phenotype marked by a consistent, increased storage of fat into adipose tissue and decreased oxidation in skeletal muscle, Even et al (2017); Nicholson et al (2010). Under SPF condition, HFD-fed mice significantly gained body weight gain compared to CD fed mice as previously been reported in HFD-fed SPF mice, Kübeck et al (2016). We reported no significant changes in liver or serum total lipid concentrations in our current study. Previous studies showed that total serum FFA level was not different between control diet and HFD, Björntorp et al (1969), conflicting with the elevated FFA levels previously reported in the serum of obese human subject. Furthermore, another study reported no changes in plasma total free fatty acid but decreased in plasma total triglyceride (TG) and increased liver total TG after 3 weeks of HFD fed mice relative to CD fed mice, Liu et al (2015). Our study adds to existing data that suggest that obesity and its associated pathologies are not always linked with elevated serum FFA and other lipid subclasses, Liu et al (2015).

3.4.3 Effect of HFD on ECFA and MUFA in SPF mice

Changes in saturated fatty acids and MUFAs are associated with non-alcoholic fatty liver disease or diabetes in humans. In the current study, 4 weeks of HFD feeding significantly increased both serum MUFA (29%) and liver MUFA (26%) content compared to control. However, there were no significant change in ECFA in both serum and liver of HFD-fed SPF mice relative to control. Of the two MUFAs, oleic acid, largely accounted for the increased percentage of MUFA in the serum and liver C18:1 (92.6% and 95.4%, respectively) of HFD fed mice. Palmitoleic acid (C16:1) in the serum and liver of HFD fed mice was 7.4% and 4.4%, respectively. A previous study reported an increased composition of oleic acid and decreased

stearic acid in both liver and serum samples of cats fed HFD compared to control, Fujiwara et al (2015). The increased proportion of 18:1(n-9) in the HFD group after 4 weeks, reflects the dietary proportion of this FA, as well as an increased in Δ9D indexes [also known as stearoyl-CoA desaturase (SCD)], activity as indicated by the significantly increased ratio of [18:1(n-9)/18:0] used as a surrogate measure of this activity. In the present study, we found one of the SCD1 indices, SCD18 (18:1/18:0), in the serum and liver samples to be increased in the HFD fed SPF group. However, SCD16 (16:1/16:0) in the serum and liver was not significant in HFD fed SPF mice. SCD1 is predominantly expressed in the liver and plays an important role in the conversion of saturated fatty acids (C16:0 and C18:0) derived from dietary fatty acids or from *de novo* lipogenesis into MUFA (C16:1 and C18:1). Previous studies have reported that liver *SCD1* mRNA expression is positively correlated with SCD1 desaturase indices in the liver and the plasma FA, Sjögren et al (2008); Liu et al (2015). Previous studies have reported SCD1 indices to correlate positively with NAFLD, Kotronen et al (2009).

3.4.4 Effect of HFD on PUFA in SPF mice

Long-chain polyunsaturated fatty acids (LC-PUFA) form an integral component of all cell membranes and play critical role for normal cellular function, Burdge et al (2002). Here, we observed a significant decreased in total PUFA composition of liver or serum in mice fed high fat diet under SPF condition. Interestingly, serum C18:3n3 was decreased in the plasma but increased in the liver of HFD-fed SPF mice compared to control. The observation of decreased total PUFA in the liver and serum was not surprising since the fat source in HFD diets was lower in total PUFA (33.3%). The decreased serum C18:3n3 is likely as a result of the low amount of this fatty acid component of the HFD diet. However, in terms of the increased liver levels of this C18:3n3, since there was a decreased dietary supply in the HFD diets, increased availability of this FA would be achieved by mobilisation of C18:3n6 from adipose tissue to the liver, and/or down-regulation of C20:4n6 which would require decreased activity of

enzymes and transport proteins involved in this pathway Burdge et al (2002). However, in our study we observed no changes in the proportion of C20:4n6 in the liver or serum of HFD fed mice. Interestingly our HFD SPF model showed lower levels of liver C18:3n6 and no changes in C20:4n6, indicating anti-inflammatory effect. n-6 FAs, formed by FADS2 activity, are known to be pro-inflammatory.

3.4.5 Effect of HFD on OCFA in SPF mice

Many studies have shown an inverse association between circulating odd chain fatty acids (OC-FAs); pentadecanoic acid (C15:0) and heptadecanoic acid (C17:0), with metabolic disease risk, Forouhi et al (2014); Jenkins et al (2017). Here, we investigated the effect of high fat diet on circulating and liver levels of C15:0 and C17:0 under SPF condition. To do this, we performed analyses on liver and serum of mice fed a high fat diet or control diet. We observed that, the serum C15:0 levels decreased (63.3%) as expected compared to control. There was a lower level of serum C17:0 (7.4%) in HFD-fed SPF mice although this was not statistically significant. Combination of these FAs resulted in significant decreased in total OCFA in the HFD-fed SPF mice relative to control. Similar trends were observed in the liver where there was a significant reduction in C15:0 (31.8%) and C17:0 (22.2%) in mice fed high fat diet compared to control. To our knowledge, no other study has directly measured parameters of these odd chain fatty acids in high fat-fed mice. These findings of a decrease in content of serum and liver OCFA support the suggestion of an increased NAFLD risk in subjects on Westernized (high fat) diet, Yoo et al (2017); Jensen et al (2018). Several studies have documented that OCFA can originate from ruminant fat and milk, Mika et al (2016) and other studies have also suggested these FAs can be synthesized *de novo* in mammals, Pfeuffer & Jaudszus (2011); Jenkins et al (2017). In our studies, the fact that both CD and HFD components did not contain these OCFA-rich diets mean the observation of the decrease in OCFA in HFD-fed SPF may be related to alteration of *de novo* synthesis of these FAs.

3.4.6 Effect of high fat diet on fatty acid profile under normal husbandry conditions

Here, to understand how feeding mice under normal husbandry condition changes specific fatty acid profile in the blood particularly OCFAs, we fed groups of mice with high fat diet or chow with similar dietary compositions as used for the SPF experiment in a normal husbandry environment for either 4 weeks or 12 weeks. Analyses of the serum fatty acid profile of these mice showed a similar change in fatty acid profile between 4 weeks and 12 weeks HFD-fed normal husbandry mice. In either 4 weeks or 12 weeks HFD-fed mice, we observed an increased serum levels of ECFA, C16:1/C16:0 ratio whilst OCFA, MUFA and C18:1/C18:0 levels in the serum were decreased. The observation of decreased serum levels of OCFA suggests that there was no evidence that the SPF environment has an impact on circulating levels of OCFAs in the mice. However, the increased levels of MUFA and its enzymatic activity suggest that MUFA can be influenced by SPF condition in the mice.

3.4.7 Effect of HFD on the expression of *CD 36*, and *FABP3* in SPF mice

CD36 is a multiligand class B scavenger receptor with high affinity for lipids and lipid-containing ligands and it is known for its lipid uptake function in liver, macrophages, skeletal muscle, and the heart, Garbacz et al (2016). Liver-specific knockout of CD36 in mice decreases hepatic lipid levels in both genetic and diet-induced steatosis, Ipsen et al (2018). Fatty acid-binding proteins (FABPs) are a group of molecules that coordinate lipid responses in cells and are strongly associated with metabolic and inflammatory pathways, Furuhashi & Hotamisligil (2008).

In this study, we report that a 4-week high fat diet at SPF condition had no significant changes of the mRNA expression *CD36* and *FABP3* in the mice liver. This is contrary to previous findings where mice fed a high fat diet for 6 weeks developed hepatic steatosis alongside increased mRNA and protein expression of *CD36*, Koonen et al (2007); Wilson et al (2015). It

can be explained that the high but insignificant expression of these fatty acid transporters could be as a result of the short duration (4 weeks) of feeding compared to what has been reported in other studies. Metabolic response to high fat diet is reported to be time dependent, Tranchida et al (2012).

3.4.8 Effect of HFD on specific fatty acid gene expression in SPF mice

The mechanism by which obesity and hepatic steatosis are induced by a high fat diet requires analyses of gene expression to track changes at the molecular level in the liver in response to increased fat consumption. Following observation of consistent OCFA profile changes in the serum and liver, we selected some specific genes (*ELOVL 6, SCD1, HACL1, FADS2* and *PCCA*) related to unsaturated and odd-chain fatty acid synthesis to assess their expression in the liver of mice fed under SPF environment. ELOVL family member 6 (Elovl6) is a microsomal enzyme involved in the elongation of saturated and monounsaturated FAs with 12, 14, and 16 carbons, Matsuzaka et al (2002). Loss of Elovl6 function was reported to reduce stearate (C18:0) and oleate (C18:1n-9) levels and increase palmitate (C16:0) and palmitoleate (C16:1n-7) levels, Matsuzaka et al (2007). In this study, loss of *ELOVL6* mRNA expression was observed despite no change in ECFA.

The enzyme stearoyl-CoA desaturase 1 (SCD1), is predominantly expressed in the liver, and converts nutrient or *de novo* lipogenesis-derived saturated fatty acids (16:0 and 18:0) to monounsaturated fatty acids (16:1n-7 and 18:1n-9) and thereby prevents their lipotoxic effects, Silbernagel et al (2012). In our current study we reported a decreased in *SCD1* mRNA expression and increased C18:1 in HFD-SPF fed mice. In the down-regulation of hepatic *SCD1* expression, increased in MUFA may be because the MUFA did not get further desaturated to C18:2 by FADS2 which was also lower in our HFD-SPF mice. Branched fatty acids (e.g., phytanic acid) undergo α-oxidation via phytanoyl-CoA hydroxylase (PHYH) and 2-

hydroxyacyl-CoA lyase (HACL1), both located in peroxisomes. PHYH introduces a 2-hydroxy group into phytanoyl-CoA, whereas HACL1 catalyses the cleavage between the first and the second carbon atoms, yielding formyl-CoA and pristanal, Jenkins et al (2017). Delta-5 (D5D, FADS1) and delta-6 desaturases (D6D, FADS2) are key enzymes involved in the metabolism of n-3 and n-6 PUFAs, which enable alpha-linolenic acid (ALA) and linoleic acid (LA) to produce long-chain polyunsaturated fatty acids (LC-PUFAs), Tosi et al (2014). In the SPF HFD study, we observed a systemic decrease in C18:2 and C18:3, which was reflected by a significant decrease in *FADS2* mRNA expression. PCCA is the key enzyme in the catabolic pathway of odd chain fatty acids, isoleucine, threonine, methionine and valine. It has been shown that PCCA -/- mice exhibit fatal extreme ketoacidosis as well as fatty liver, Miyazaki et al (2001).

Branched-chain α-ketoacid (BCKA) dehydrogenase complex (BCKDC) plays a role in regulating branched-chain amino acid (BCAA) metabolism at the level of BCKA catabolism. Evidence suggest metabolism of branch-chain amino acids in adipose tissue results in odd-chain fatty acid synthesis, Crown et al (2015).

In this study, we report that HFD significantly reduced *SCD1* mRNA in the liver compared to mice on chow under SPF condition. This was contrary to increase SCD1 enzyme activity and C18:1 content observed in the liver and serum of SPF mice. This difference is partly due to the fact that only 50% of transcript changes were converted to protein level, and also activity can be further regulated post-transcriptionally. Interestingly, we saw significantly decreased expression of *FADS2, ELOVL6* and *HACL1* following high fat intake for 4 weeks. The repression of *HACL1* mRNA expression in the liver was not surprising since this gene has been linked odd-chain fatty acid metabolism. It is possible that impairment of *HACL1* resulted in lower OCFA levels in the liver of HFD-fed SPF mice. As *ELOVL6* is thought to be involved in multiple fatty acid synthesis, the lower expression of this gene in the liver of mice fed high

fat diet may contribute to a lower proportion of PUFA. In the current study, lower content of PUFA in the dietary fat compared to control diet may account for the lower serum and liver levels in the HFD mice compared to CD mice. Moreover, lower level of systemic PUFA may result in down-regulation of *ELOVL6* since they have been implicated in PUFA metabolism, Sun et al (2013). The decreased expression of *SCD1* mRNA, *ELOVL6* mRNA and *FADS2* mRNA may be accounted for by several factors as expression of these genes are further regulated by several transcriptional factors including ChREBP and SREBP-1c which require peroxisome proliferator-activated receptor co-activator-1α (*PGC-1α*). These transcription factors can in turn be regulated by diet and hormones (eg insulin), Mauvoisin & Mounier (2011); Bae et al (2016). Interestingly, another PUFA metabolic gene *PCCA* which is involved in OCFA metabolism was not significantly different between mice fed high fat diet and the control. To the best of our knowledge no study has reported on *PCCA* mRNA levels in response to high fat dietary intake. Again, we did not observe a significant change in the expression of *BCKDHA* in the liver of mice fed high fat diet relative to control group. A previous study demonstrated that hepatic *BCKDC* kinase was down-regulated resulting in activation of hepatic BCKDC in rats fed HFD for 12 weeks, which implies that events associated with HFD feeding may promote BCKA catabolism, Kadota et al (2013). The differences in experimental design may account for the reason why we did not observe a significant change in *BCKDHA* mRNA expression, besides they measured activity of the enzymes as opposed to our expression analyses.

3.4.9 Effect of HFD on the expression of *TNF-α*, *GSR* and *TRX1* in SPF mice

TNF- α is a proinflammatory cytokine which is produced by macrophages/monocytes during acute inflammation. It is responsible for a diverse range of signalling events within cells, leading to necrosis or apoptosis, Idriss & Naismith (2000). TNF-α mediates hepatic inflammation, oxidative stress, and apoptosis or necrosis of liver cells, Seo et al (2013). Glutathione reductase (EC 1.8.1.7) catalyses the reduction of glutathione disulfide (GSSG) to the sulfhydryl form glutathione (GSH), and it is a critical molecule in resisting oxidative stress and maintaining the reducing environment of the cell, Deponte et al (2013). Thioredoxin 1, an antioxidant, is involved in providing reducing equivalents to thioredoxin peroxidases and ribonucleotide reductase, the regulation of transcription factor activity, and plays an important role in the regulation of enzyme activity, Lustgarten et al (2011). The expression of glutathione (GSR) and thioredoxin (TRX) antioxidant system can further be regulated by nuclear factor E2-related factor 2 (Nrf2) hence playing an important role in maintaining the redox homeostasis of the cell, Tonelli et al (2018).

In this study, we evaluated the effect of high fat diet on the expression of *TNF*- α, *GSR* and *TRX1* following a 4-week high fat feeding regimen. Here, following an exposure to increased lipotoxicity as a result of HFD intake, we thought this would correlate with increased in oxidative stress in mitochondria, however, whilst there was a general trend of increase expression of *TNF*-α and decrease *GSR* mRNA and *TRX1* mRNA expression in the liver of HFD-fed SPF mice relative to control fed mice, these were statistically insignificant. This reflects the moderate effect of our 4-week high fat intake on the liver of mice fed under SPF condition. It is well known that elevated dietary fat intake results in reduction of antioxidant activity and expression, Ibrahim et al (1997); Qin et al (2014).

3.4.10 High fat diet feeding under SPF condition results in hepatic steatosis in mice

It is well known that high fat feeding causes accumulation of lipid in the liver, Luo et al (2015); Meli et al (2013); Longato et al (2013).

In this study, we performed H&E analyses to confirm whether lipid accumulated in the liver of mice fed high fat diet for 4 weeks under SPF conditions. There was increased accumulation of lipid in the liver of high fat fed mice compared to the control. This observation was similar to that reported previously for mice fed under conventional condition.

3.4.11 Effect of high fat diet on peroxisome content in SPF mice

Peroxisomes are involved in the catabolism of very long chain fatty acids (>C20:0 FA), branched chain fatty acids which are then mainly provided for further degradation in mitochondria, Reddy & Hashimoto (2001); Schrader et al (2013); Sassa T, Kihara (2014). It is suggested that hepatic steatosis is a metabolic manifestation of a loss or dysfunction of the organelles involved in lipid catabolism which include peroxisomes and mitochondria, van Zutphen et al (2016). Markers for identifying peroxisome in tissues include peroxin 14 (PEX-14), catalase and ATP Binding Cassette Subfamily D Member 3 (ABCD3). Among these PEX-14 has been reported to be an optimal marker for identification and localization of peroxisomes in different cell types, tissues, and species, Grant et al (2013).

In this study, we evaluated the content of peroxisome in the liver of SPF mice following a 4-week high fat diet regimen. This was done by immunohistochemical analyses of two key peroxisomal markers-PEX-14 and catalase. We observed an increased in PEX 14 as well as peroxisomal catalase in the liver of mice fed HFD diet compared to control. To our knowledge no study has reported changes in catalase and PEX 14 content in mice fed high fat diet using brightfield microscopy. With other microscopic analyses our study is supported by previous findings where electron microscopy analyses of hepatic peroxisomes of rats fed a high-fat diet

were more abundant than in the case of normal rats Ishii et al (1980). Moreover, in a clinical study, peroxisomal proliferation in liver cells appeared early in the cirrhotic process, De Craemer et al (1993). Combining evidence from our study and previous studies, we hypothesize that peroxisomal content may increase in response to initial metabolic stress. It is not known whether they disappear as the diseases progress. More studies are needed to define peroxisomal changes in diet associated liver diseases.

3.5 Conclusion

To understand how dietary fat affect specific fatty acids (eg OCFAs), we performed analyses of fatty acid profile of serum and liver obtained from mice fed under normal husbandry or SPF environment. Overall, serum OCFA profile of HFD-fed SPF mice resembled that of the HFD-fed conventional mice. Constrasting effects were seen for oleic acid (C18:1) that was decreased in serum of HFD-fed conventional mice but increased in HFD-fed SPF mice. Nonetheless, high fat diet at 4 weeks irrespective of SPF environment or not resulted in decrease levels of serum OCFA, particularly C15:0. To further understand the mechanisms underlying fatty acids changes by a high fat diet, we performed several analyses of metabolic gene expression, and saw loss of *HACL1*, *SCD1* and *ELOVL6* after HFD in SPF mice. Histological analyses confirmed deposition of lipid droplet in fixed liver tissues as well as proliferation of perioxisomes as indicated by catalase and PEX-14 proteins in fixed liver tissues. The changes in OCFA, *HACL1*, catalase and PEX-14 proteins in our HFD animal models is important to explain the inverse association between OCFA and NAFLD in humans. It is important to note that extrapolating findings from animal studies into humans remains a challenge and therefore we suggest further validation experiment in other animal models such as Sprague-Dawley rats in order to translate the findings into humans.

Chapter 4

4.0 Effect of high fat diet on gut microbiota in SPF mice

Abstract

In a strictly controlled specific pathogen free environment study, a high fat diet influence on the gut microbiota was studied. After a 4-weeks of being on normal rodent diet (chow), mice were assigned to either the control-diet (10% fat, 70% carbohydrate and 20% protein per kcal%, n = 10) or a high-fat diet (60% fat, 20% carbohydrate and 20% protein per kcal%, n =10) for 4 weeks. Faecal samples were collected after 4 weeks of feeding. The faecal microbiota of mice were characterized by 16S rRNA gene sequencing. Here we show that the phyla Firmicutes and Proteobacteria increased whereas Verrucomicrobia, Actinobacteria, Saccharibacteria, Spirochaetes were decreased in the gut microbiota of HFD mice compared to control. Moreover, a remarkable reduction of bacteria especially *Akkermansia*, *Lactobacillus*, *Bifidobacterium* in HFD mice were observed relative to the control. Increased abundance of propionate-producing gut microbiota such as of Lachnospiraceae and Clostridiales in HFD mice were observed. Finally, we report that the gut microbiota profile of HFD-fed mice under SPF condition was not different from HFD-fed mice under normal husbandry environment reported in the literature.

4.1 Introduction

The human gut contains a large number of microorganisms, collectively referred to as the microbiota. It is known that a healthy human harbours more than 10^{14} microbial cells and is dominated by anaerobic bacteria including up to about 1,000 species. These bacterial genes outweigh the host genome by a factor of 150 times. The majority of these microbiota in the human body reside in the colon, Canny & McCormick (2008). This microbial community performs significant physiological functions, including metabolic regulation of glucose and lipid metabolism, Prakash et al (2011). It is reported that whilst intestinal microbiota plays an important role in maintaining human health, metabolic disorders including diabetes can intend lead to intestinal microflora imbalance, which will further aggravate metabolic disorders, thus forming a vicious cycle, Liu & Lou (2020).

There exists an extensive inter-individual diversity in microbiota composition, Rosen & Palm (2017). The diverse nature of this ecosystem is shaped by events in early life; however, this can change over time through interactions between its constituents as well as dietary and health factors affecting the host such as medications, disease state as well as host genetics, Weinstock (2012). It is generally thought that more than 90% of the gastrointestinal microbiota belong to phyla Firmicutes (gram positive) and Bacteroidetes (gram negative), Allin et al (2015), however, there are minority phyla such as Verrucomicrobia (gram negative), Actinobacteria (gram positive) and Proteobacteria (gram negative), Jasirwan et al (2019). Changes in the composition of gut microbiota as well as components and metabolites derived from intestinal microbiota are thought to play a key role in modulating the pathological process of NAFLD.Such components include lipopolysaccharides, peptidoglycan, and extracellular vesicles, and metabolites ranging from SCFAs, indole and its derivatives, trimethylamine, secondary bile acids, to carotenoids and phenolic compounds, Ji et al (2019). SCFAs are volatile fatty acids (acetate, propionate, and butyrate) produced via fermentation of soluble

dietary fibers and nondigestible carbohydrates by gut microbes, den Besten et al (2013). Bacteriodales and Clostridiales (specifically Lachnospiraceae) are the primary producers of propionate within the gut microbiome, Tian et al (2019). Moreover, at the phylum level, butyrate is generally produced by Firmicutes, while acetate and propionate are predominant products of Bacteroidetes, Jasirwan et al (2019. It is reported that long chain OCFA may be synthesized via propionic acid produced by the gut microbiota, Pfeuffer & Jaudszus (2016). Whether changes in propionate-derived gut microbiota affect long OCFA (particularly, C15:0 & C17:0) leading NAFLD have not been studied.

With recent development of next generation sequencing (NGS) technologies, a great number of novel microbiota have been identified by employing metagenomic or single cell sequencing and bioinformatic strategies including 16S rRNA gene sequencing, molecular operational taxonomic unit (mOTU) analysis or metagenomic linkage group (MLG) analysis, Rajilic-Stojanovic & de Vos (2014).

Previous study showed that a high fat diet intake in mice changed the microbiota unfavourably, resulting in increased Firmicutes and decreased Bacteriodetes, He et al (2018). Moreover, a high fat diet reduced the abundance of Lactobacillus intestinalis and high abundance of Clostridiales, Bacteroidales, and Enterobacteriales, Lecomte et al (2015). A mice study showed different type of lipids influence the microbiota distinctively. While lard-fed mice harboured increased numbers of *Bacteroides sp*. and *Bilophila* sp. and reduced levels of *Desulfovibrio* sp, those fed with fish oil had increased lactic acid bacteria (*Lactobacillus sp*. and *Streptococcus* sp.), Verrucomicrobia (*A. muciniphila*), and Actinobacteria (*Bifidobacterium sp.* and *Adlercreutzia* sp.) and mice fed with a diet rich in milk fat or supplemented with taurocholic acid (a biliary acid) showed increased levels of *Bilophila wadsworthia*, Devkota et al (2013). Furthermore, the possible detrimental effect on hepatic lipid metabolism of high fat diets are

thought be mediated via the microbiota, which can cause inflammation and oxidative stress, Marciano & Vajro (2017); Clemente et al (2018).

Although few studies have explored the influence of high fat diet on the composition of the microbiota, little is known about those related to propionate-derived gut microbiota producers. Moreover, almost all previous studies on the effect of high fat diet on the gut microbiota have utilized normal husbandry mice. Therefore, in this thesis we investigated in our strictly controlled diet study (chapter 4) the influence of dietary fat on the gut microbiota of mice fed at SPF condition.

4.1.1 Aim

This study was aimed at characterising the faecal gut microbiota from mice fed a high fat diet in SPF conditions and compared with control diet fed mice under the same conditions using 16S rRNA sequencing technology. The experiment tested the hypothesis that high fat diet changes to OCFA is mediated by altered propionate-derived gut microbiota.

4.1.1.2 Objective

The faecal gut microbiota of the high fat diet model were characterized by 16S rRNA sequencing platform

4.2 Method

4.2.1 High fat diet and sample collection

For a detailed description of the animal housing and HFD treatment procedures see Chapter 2. In brief, two groups of C57Bl/6 male mice were used to assess the influence of high fat diet on gut microbiota in SPF mice for 4 weeks; the control group was fed chow diet (10% fat, 70% carbohydrate and 20% protein per kcal%, n = 10) and treatment group was fed a high-fat diet (60% fat, 20% carbohydrate and 20% protein per kcal%, n =10). All animals were raised and

fed under specific pathogen free (SPF) facility. In this study, following faecal DNA extraction, samples were sent to Novogene Company Ltd, Cambridge, UK for microbial sequencing and bioinformatics analyses.

Faecal samples collected from the animals were processed for microbiome sequencing. Mice that were fed either a control (chow) diet or high fat diet were analyzed, totaling 20 mice. DNA was extracted from the animals' faeces, and the 16S rRNA gene V3-V4 hypervariable region was sequenced on the lllumina MiSeq platform using universal primers 341F, 5′-CCTAYGGGRBGCASCAG-3′; and 806R, 5′-GGACTACNNGGGTATCTAAT-3′. High-quality paired-end reads were combined with tags with an average read length of 250 base pair using FLASH (Fast Length Adjustment of Short reads, V1.2.7), Magoč & Salzberg (2011). Noisy sequences of raw tags were filtered by QIIME (V1.7) pipeline under specific filtering conditions to obtain high-quality clean tags, Caporaso et al (2010). The tags were compared with the reference database using UCHIME algorithm to detect chimera sequences and deleted. Sequence data analysis were performed by Uparse software (Uparse v7.0.1001) using all the effective tags, Edgar (2013). The representative OTU sequences were taxonomically classified using Mothur software against the SSUrRNA database of SILVA Database, Wang et al (2007). A 97% identity was used for clustering reads into OTUs (operational taxonomic units) discarding reads that failed to match the reference sequences. The OTUs and phylogenetic tree generated were used for diversity analysis. The QIIME 1.7.0 software package was utilized for analysis and comparison of microbial communities from high-throughput sequencing data. Statistical measures can be run in QIIME to compare and contrast microbial communities and measure significant differences between communities, Caparaso et al (2010). To estimate the diversity of the microbial community of the sample, we calculated the within-sample (α) diversity using the unique OTUs (known as the observed species metric) in each dietary group and beta diversity was calculated using the phylogenetic-based UniFrac metric and was

visualized with principal coordinate analysis (PCoA). Linear discrimination analysis coupled with effect size (LEfSe) was performed to identify the bacterial taxa differentially represented between groups at the genus or higher taxonomy levels.

To evaluate the effect of HFD on the gut microbiota after 4-weeks of feeding SPF mice, some specific OTUs were compared between control (C) and HFD (H) groups. The differences between groups with normal distribution were evaluated by MetaStat, LEfSe and Anosim to find distributions of OTUs that were significantly different between HFD and Control.

4.3 Results

4.3.1 Microbial diversity

Alpha-diversity analysis indicated no significant difference in the richness of molecular species between HFD and control fed mice. Moreover, when considering most dominant species by taking into account evenness via calculation of Shannon effective counts, mice on HFD showed no difference in counts of species from those fed control diet (figure 4.1).

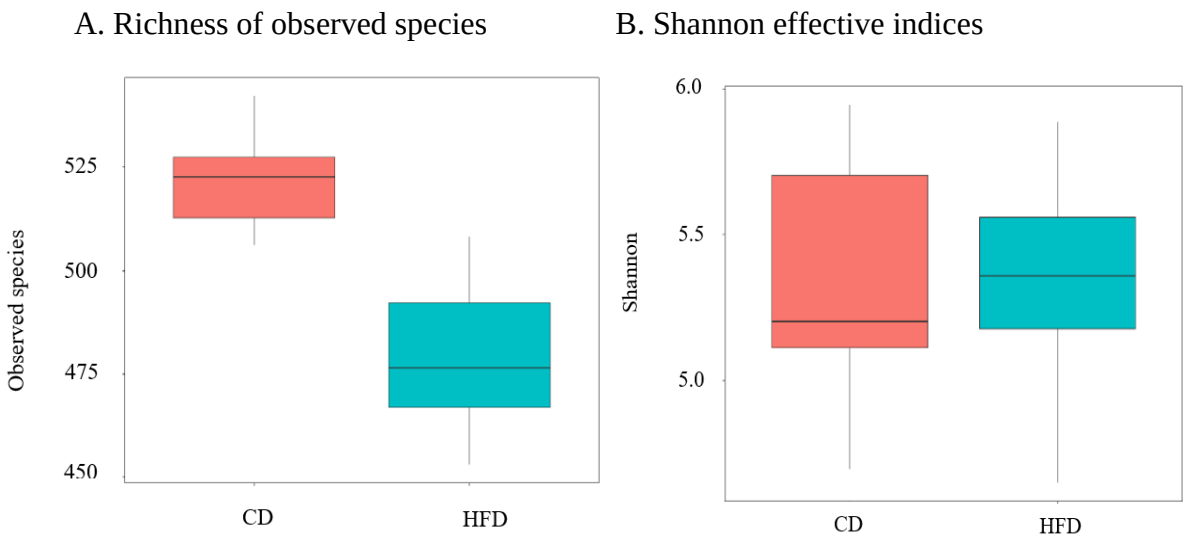

Figure 4.1: Alpha diversity analyses of SPF mice fed a high fat diet.

Mice were fed either control diet, CD; High fat diet, HFD. Values are given as means ±S.E.M for n=10

4.3.2 *Beta* diversity analyses

4.3.2.1 Principal coordinate analyses

Weighted Unifrac and Unweighted Unifrac, and Non-metric multi-dimensional scaling analysis (NMDS) based principal coordinates analysis (PCoA) revealed HFD group to display a distinct microbiota community that clustered separately from the control group (figure 4.2 A-C).

A.

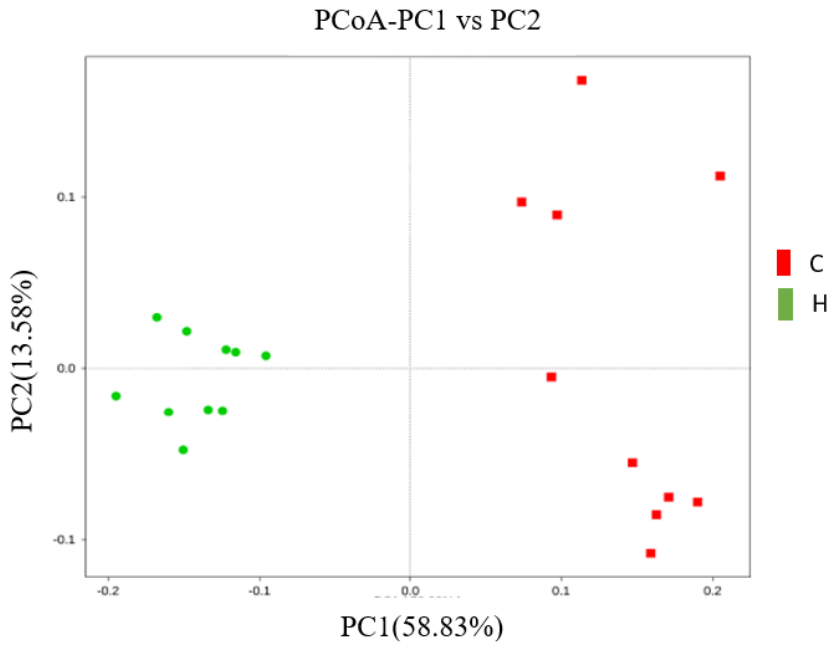

Figure 4.2A: Weighted Unifrac *Beta* analysis showing principal co-ordinates analysis PC1 Vs. PC2.

HFD group clustered distinctly different from the control group, n=10. (C: Control diet; H: High fat diet.).

B.

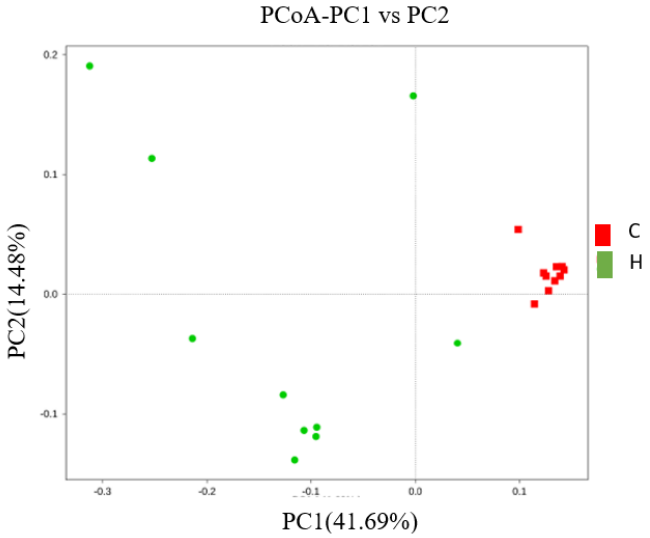

Figure 4.2B: Unweighted Unifrac *Beta* analysis showing principal co-ordinates analysis PC1 Vs. PC2.

HFD group clustered distinctly different from the control group, n=10. (C: Control diet; H: High fat diet).

C.

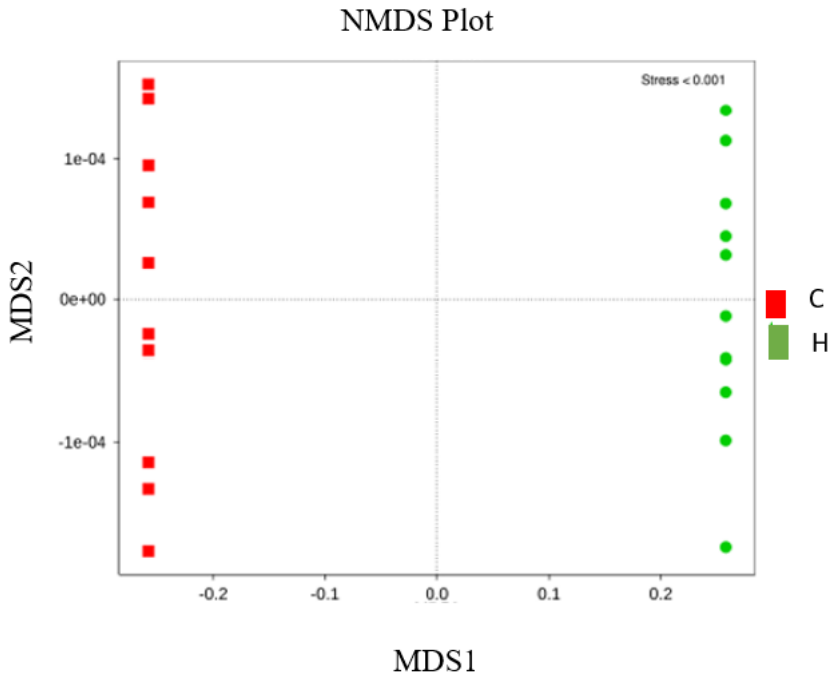

Figure 4.2C: NMDS based *Beta* analysis showing principal co-ordinates analysis PC1 Vs. PC2.

HFD group clustered distinctly different from the control group, n=10. (C: Control diet; H: High fat diet.).

4.3.3 Taxonomy summary of phyla

Metastats analyses at the phylum level shows that HFD were associated with a decrease in the relative sequence abundance of phyla Verrucomicrobia, Actinobacteria, Saccharibacteria, Spirochaetes and an increase in Proteobacteria (Figure 4.3 A-E, $p<0.01$)

A. Verrucomicrobia

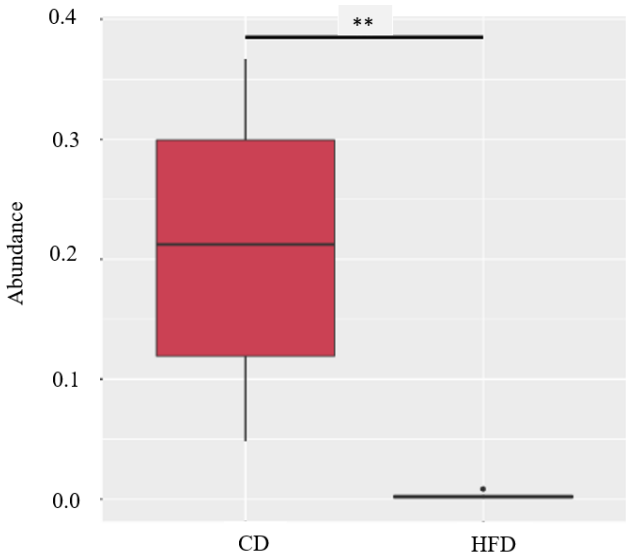

B. Proteobacteria

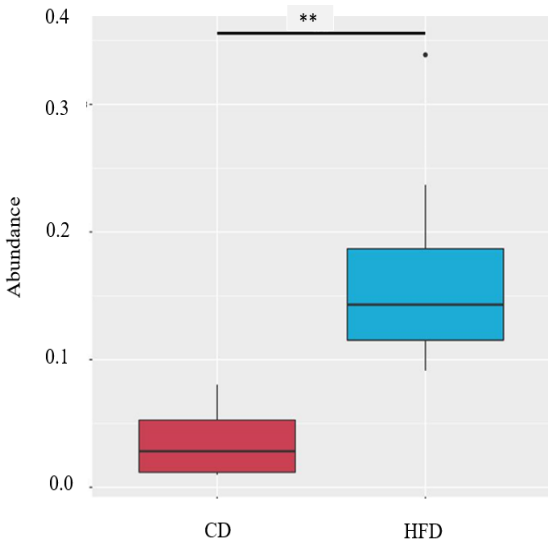

C. Actinobacteria

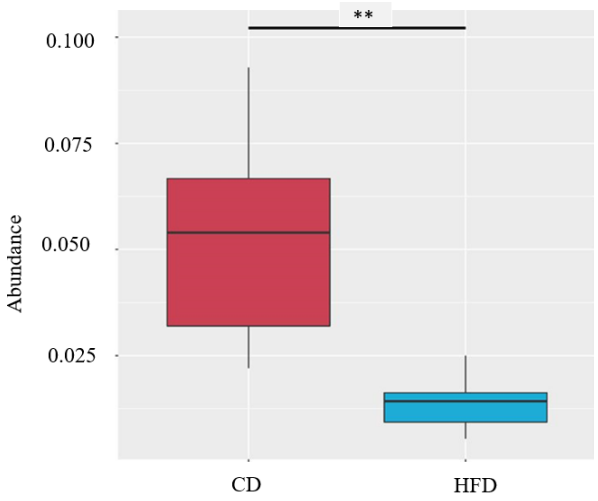

D. Saccharibacteria

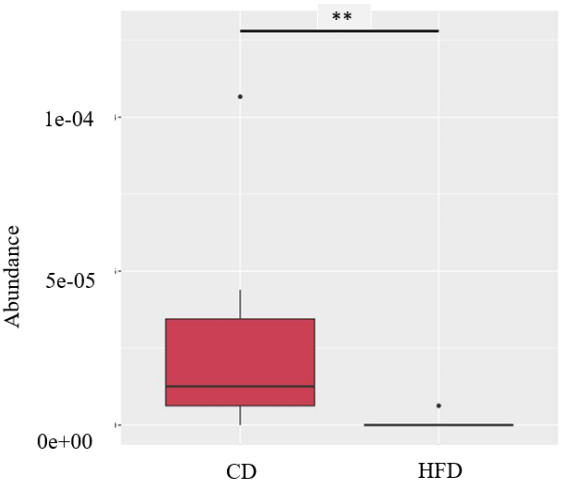

E. Spirochaetes

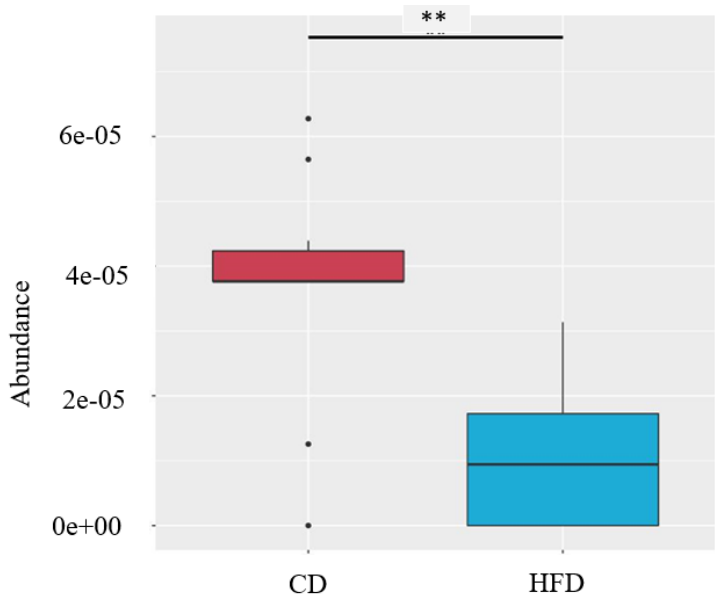

Figure 4.3: Box plots showing relative sequence abundance of taxonomic groups that were significantly different between mice fed CD or HFD fed mice.

Horizontal line represents the two groups with significant variation. " ∗ " represents significant variation (q value < 0.05) while " ∗ ∗ " represents highly significant difference (q value < 0.01, n=10).

4.3.4 Bacterial microbiota composition

Here we investigated the specific changes of microbiota in mice fed a high fat diet and those on the control diet, we assessed the relative abundance of taxa after 4 weeks. At the phylum level, the Verrucomicrobia was depleted in the HFD group after 4 weeks of feeding. However, Proteobacteria and Firmicutes phyla increased in HFD fed group within the same period feeding (figure 4.4 A). At the genus level, we observed 35 bacterial taxa that displayed different abundance between HFD and control group in the taxonomic abundance heatmap (figure 4.4 B). Compared with the control group, 10 bacterial taxa were enriched in the HFD group, while 25 bacterial taxa were depleted in the HFD group. The HFD-enriched bacterial taxa included *Clostridium, Eubacterium, Faecalibaculum, Erysipelatoclostridium, Desulfovibrio, Odoribacter, Alistipes, Romboustsia, Mucispirillum*, and unidentified members of

Lachnospiraceae. Bacterial taxa that were depleted in the HFD group included *Roseburia*, *Lactobacillus*, *Akkermansia*, *Bifidobacterium* etc, which were significantly more abundant in CD (Figure 4.4B).

A.

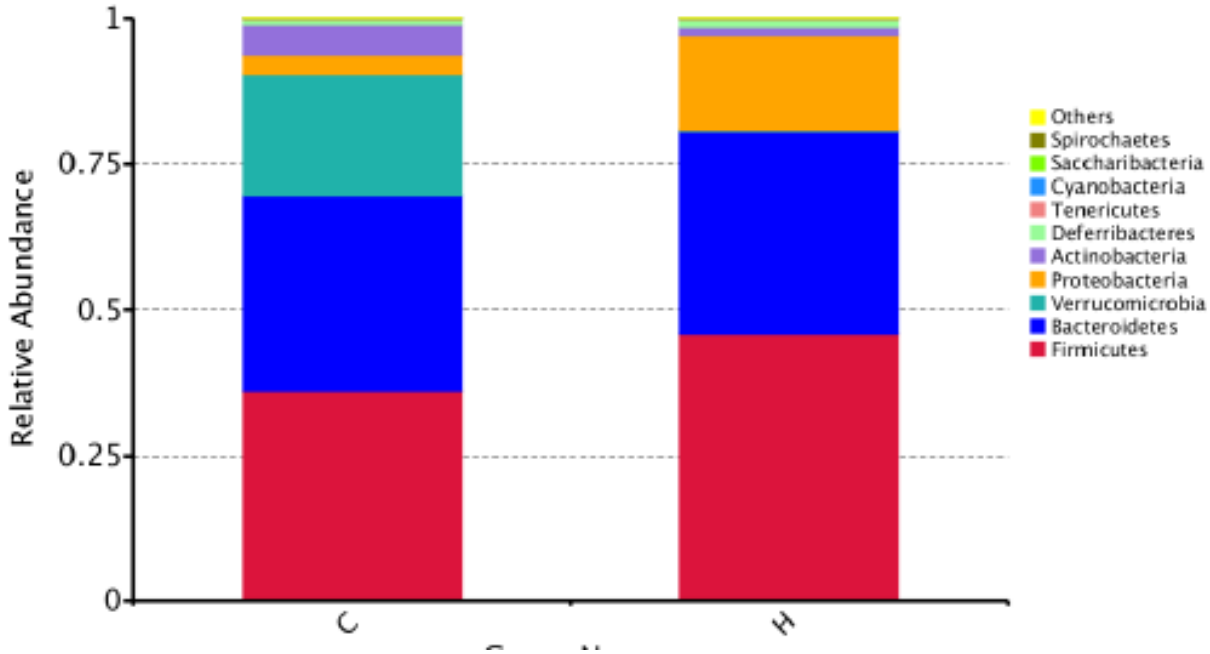

Figure 4.4A: Dietary fat effect on dominant gut bacteria phyla.

The composition of gut microbiota at the phylum level were dominated by Firmicutes, Bacteroidetes and Proteobacteria in HFD treated group (H) whilst Firmicutes, Bacteroidetes and Verrucomicrobia dominated the control group (C), n=10

B.

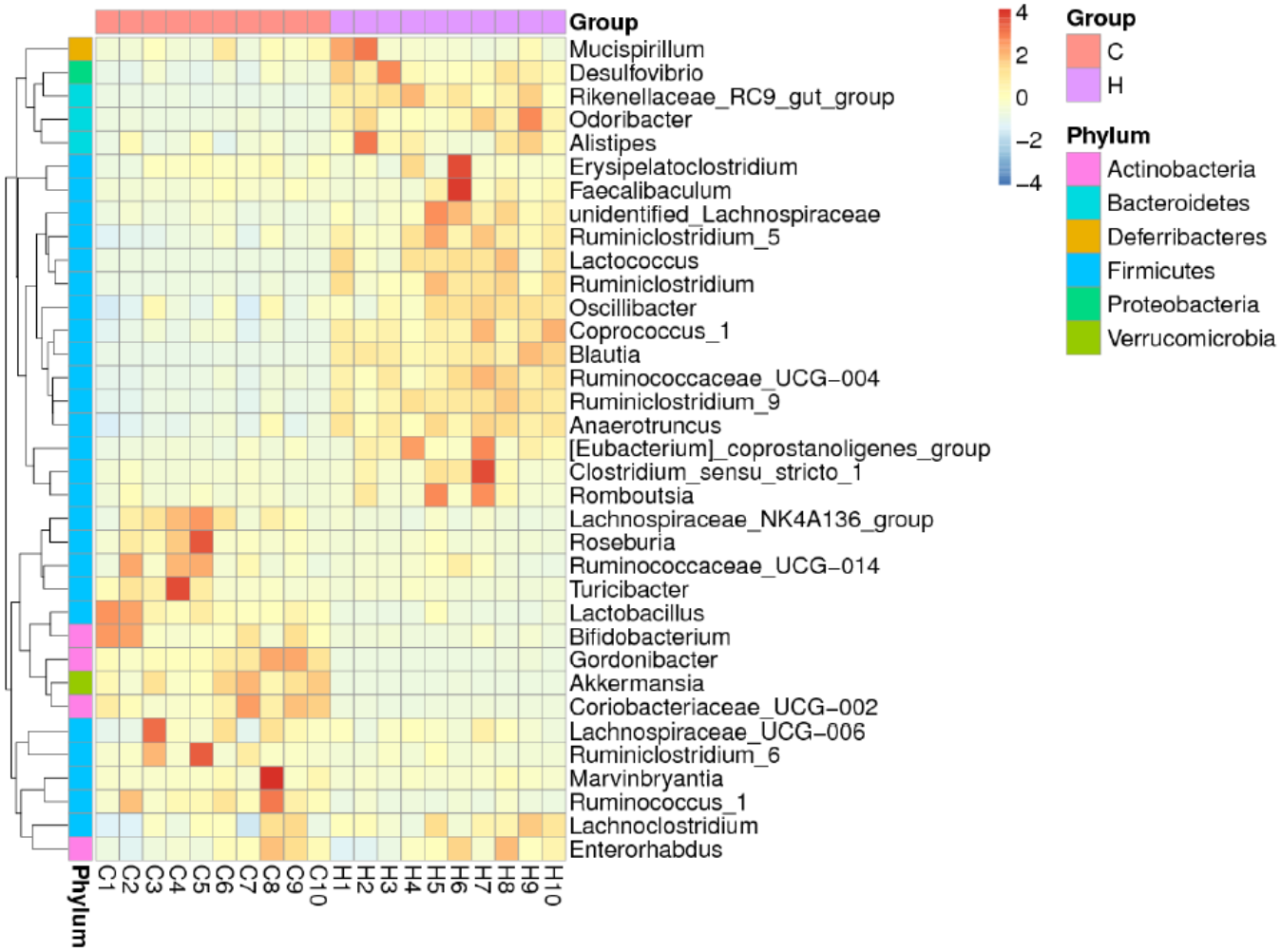

Figure 4.4B: Dietary fat effect on gut bacteria at the generic level.

The heatmap shows 35 differentially abundant genera between HFD and control treatment. Each column represents a sample from HFD or control treatment. (C: Controls (C1, C2, C3…); H: High fat diet (H1, H2, H3….), n=10).

4.3.5 LEfSe (linear discriminant analysis (LDA) Effect Size) analysis detects biomarkers

To identify bacterial taxa that significantly differentiated between control and HFD groups, a metagenomic biomarker discovery approach (LEfSe) was used. The results from the LDA score and cladogram showed that in the genus/species level of *Eubacterium*, *Odoribacter*, *Lactococcus*, *Lactococcus lactis*, *Desulfovibrio* and *Blautia* were significantly enriched in the HFD group, while sequences from *Lactobacillus reuteri*, *Lactobacillus murinus*, unclassified

member of Coriobacteriaceae, Lachnospiraceae, *Akkermansia spp*. were more abundant in control group (Figure 4.5A & B).

At the family level, HFD was associated with an increase in the relative sequence abundance of Desulfovibrionaceae, Lachnospiraceae, Rikenellaceae, Streptococcaceae, Ruminococcaceae, Porphyromonadaceae. On the contrary, mice on control diets after 4 weeks were characterized by abundance of family Verrucomicrobiaceae, Lactobacillaceae, and unclassified Bactriodales S24_4 group (Figure 4.5A & B).

At the order level, HFD group after 4 weeks of feeding was enriched with Clostridiales and Desulfovibrionales whilst the control group was enriched with order Coriobacteriales, Lactobacillales and verrucomicrobiales (Figure 4.5A & B).

A.

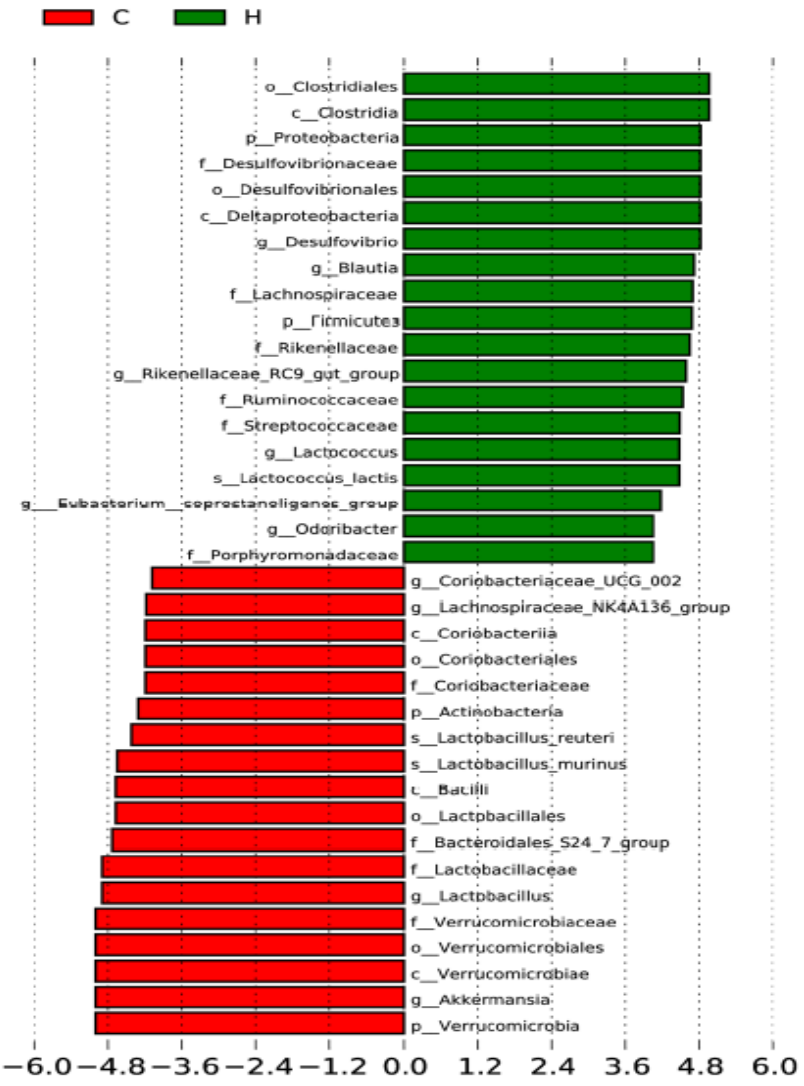

Figure 4.5A: LDA score showing enrichment of bacteria at different taxonomic levels

HFD fed mice were enriched in *Lactococcus*, *Lactococcus lactis*, *Desulfovibrio*, *Blautia*, Desulfovibrionaceae, Lachnospiraceae, Rikenellaceae, Clostridiales and Desulfovibrionales, whilst control group was enriched by *Lactobacillus reuteri*, *Lactobacillus murinus*, unclassified member of Coriobacteriaceae, Lachnospiraceae, *Akkermansia spp*., Verrucomicrobiaceae, Lactobacillaceae, unclassified Bactriodales S24_4 group, Coriobacteriales, Lactobacillales and verrucomicrobiales.

B.

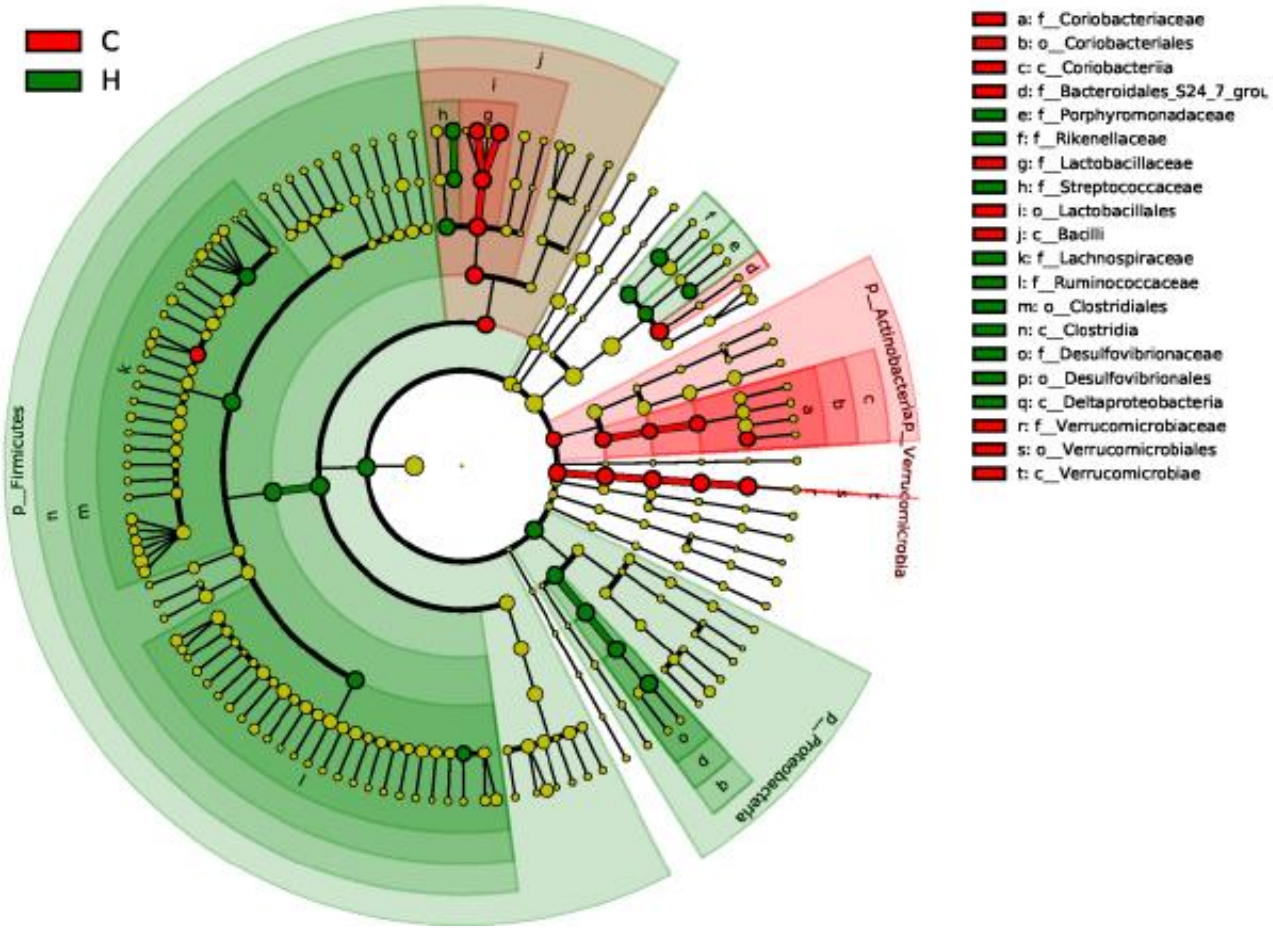

Figure: 4.5B: Cladogram score showing enrichment of bacteria at different taxonomic levels

HFD fed mice were enriched in Streptococaceae, Porphyromonadaceae, Desulfovibrionaceae, Lachnospiraceae, Rikenellaceae, Clostridia, Clostridiales and Desulfovibrionales, Deltaprotebacteria, whilst control group was enriched by Lactobacillaceae, Lactobacilliales, Bacilli, Coriobacteriaceae, Coriobacteria, Verrucomicrobiaceae, Vericomicrobiae and verrucomicrobiales.

4.4 Discussion

The current study measured the changes in gut microbiome following consumption of a high-fat or control diet in SPF mice. Alterations of the gut microbiome has been linked to the pathogenesis of fatty liver disease and associated metabolic diseases, Campo et al (2019). Although the effect of a high fat diet on gut microbiota has been studied extensively, most of these studies have been investigated using normal husbandry C57BL/6 mice model and other animal models. Here, we have performed a comprehensive gut microbiota profiling of faecal samples obtained from mice fed a high fat diet for 4-weeks under SPF condition. Herein, we conducted 16S rRNA gene sequencing to characterize the bacterial of faecal samples obtained from mice fed a high fat diet for 4-weeks under SPF condition. In our current study, there was no difference between HFD fed mice and control in terms of alpha diversity which indicates species richness or Shannon effective counts (figure 4.1). In a previous study where mice were fed high fat diet based on lard (LHFD) or palm oil (PHFD) under SPF, alpha-diversity analysis showed no difference in the richness of molecular species, however, when Shannon effective counts were calculated, mice on both HFD were characterized by higher counts of species compared to control, Kübeck et al (2016). As our high fat diet was also based on lard and fed for 4 weeks, the increased diversity not observed in the current study may be due to age of the mice. Whilst our mice were put on high fat diet when they were 4 weeks old, the previous study mice were 12-weeks old when they were put on high fat diet and fed for 4 weeks, Kübeck et al (2016). Many factors have been reported to influence the diversity of gut microbiota including age, antibiotic treatment and diet, Cho et al (2012); Enqi et al (2019). It has been reported that lower bacterial diversity is observed in people with inflammatory bowel disease, psoriatic arthritis, type 1 diabetes, atopic eczema, coeliac disease, obesity, type 2 diabetes, and arterial stiffness, relative to healthy controls, Valdes et al (2018). This trend of a lower microbial

diversity was observed in our study though not statistically significant, and it is possible that the insignificant difference may be due to the low sample size of our study.

Beta diversity analyses showed that the composition of gut microbiota in the HFD group at 4 weeks was distinctly different from that of the control group. The gut microbial community of the HFD group was characterized by compositional changes in phylum level, including striking depletion of Verrucomicrobia phylum. Moreover, gut microbial community of HFD decreased in abundance of Actinobacteria, Saccharibacteria, Spirochaetes phyla and an increased abundance of Firmicutes, Proteobacteria phyla when compared to control, Tomas et al (2016); He et al (2018). This finding is in line with a previous study that compared control diet group and HFD group after 12 weeks of feeding and reported a higher proportion of sequences assigned to Firmicutes and Proteobacteria and lower proportion of sequences assigned to Bacteroidetes and Verrucomicrobia in HFD group compared to control. This implies that the microbial profile of HFD under SPF conditions is similar to that of conventional environment at least at the phylum level, He et al (2018). Moreover, mice fed a HFD for 4 weeks had a decreased abundance of *Akkermansia spp* belonging to the Verrucomicrobia phylum. *Akkermansia spp*, has been reported to maintain gut barrier function and suggested as biomarker for a healthy gut, since members of *Akkermansia* have been associated with intestinal health and improvement of the metabolic condition in obesity-related disorders including NAFLD and type 2 diabetes subjects, Everard et al (2013). Moreover, Everard et al reported that daily administration of A. muciniphila could counteract the deleterious metabolic features induced by a HFD in mice, Everard et al (2013). Apart from *Akkermansia*, other beneficial bacteria at the genus level such as *Roseburia*, *Lactobacillus*, *Bifidobacterium* were reduced in HFD-fed SPF mice compared to control group. It is not surprising that mice on control diet showed increased abundance of *Bifidobacterium* relative to HFD mice since this diet had high amount of carbohydrate (70% by weight) compared to the high fat diet (20% by

weight). *Bifidobacteria* are known to grow on carbohydrates, Duncan et al (2007). It has also been reported that the administering probiotics containing *Bifidobacteria* to NAFLD patients reduced levels of TNF-α, C-reactive protein, transaminase enzymes, endotoxins, and NASH scores, which are risk factors for NAFLD progression, Tojo et al (2014). More importantly, in our current study, an increased abundance of propionate-producing gut bacteria taxa of Lachnospiraceae and Clostridiales were observed in HFD fed mice compared to control. This suggests that changes in these bacteria taxa may affect propionate levels which in turn may mediate changes in OCFA metabolism observed in high fat diet studies reported in Chapter 3, hence contributing to the development of NAFLD. Other HFD-enriched bacterial taxa related to NAFLD and reported in current study include, *Eubacterium*, *Desulfovibrio* and *Blautia.* Consistent with previous findings, high fat diet has been associated with increased abundance of *Clostridium, Eubacterium, Desulfovibrio* and *Blautia,* Xiao et al (2017); He et al (2018); Rohr et al (2019). Moreover, a study in population of NAFLD patients showed an increased in Proteobacteria, Enterobacteriaceae, Lachnospiraceae, Escherichia, and Bacteroidete, Jasirwan et al (2019). Furthermore, at genus levels *Oscillobacter* was lower in NAFLD whereas *Ruminococcus*, *Blautia,* and *Dorea* were increased in NASH, Grabherr et al (2019).

4.5 Conclusion

We investigated the impact of a HFD on gut microbiota after 4 weeks of feeding SPF mice to identify propionate-derived gut microbiota related to diet-associated NAFLD via possible changes to OCFA. First, we observed that changes in gut microbiota following HFD fed under specific pathogen free environment is not different from those reported for conventional mice. Significant differences were seen in commensal bacteria at the phylum level with loss or reduction of phyla Verrucomicrobia, Actinobacteria, Saccharibacteria, Spirochaetes and increased abundance of Firmicutes and Proteobacteria. Within the genus level beneficial

bacteria such as *Akkermansia*, *Lactobacillus*, *Bifidobacterium* were reduced in HFD-fed SPF mice, whilst *Clostridium, Eubacterium, Desulfovibrio* and *Blautia* were enriched in HFD-fed SPF mice. The loss or decrease abundance of these beneficial microbes observed in our HFD mice models have also reported in previous human NAFLD study Grabherr et al (2019). Moreover, these shift in bacterial composition by high fat diet particularly propionate-producing bacteria may underly the changes in OCFA associated with NAFLD.

Chapter 5

5.0 Effect of a low protein diet on fatty acid metabolism in serum and liver of mice at normal husbandry condition

Abstract

Protein malnutrition has been associated with increased risk of metabolic diseases including NAFLD. Manipulation of the dietary macronutrient composition, such as changing dietary protein content, has the potential to affect lipid metabolism and storage in the liver. In observational studies, serum OCFA is inversely associated with several metabolic diseases including type 2 diabetes and NAFLD. Here we hypothesized that lower OCFA content may underpin the mechanism of protein malnutrition-associated NAFLD.

To study this, male C57BL/6 mice were fed either a low protein diet (LPD), a LPD ssupplemented with methyl donors (MD-LPD) or normal protein diet (NPD) (9% or 18% by body weight, respectively) for 7 weeks prior to culling to collect tissues. In parallel, another set of male C57BL/6 mice were fed MD-NPD, MD-LPD or LPD for eight weeks prior to culling to collect tissues. Serum and liver fatty acid analyses was performed by GC-FID/MS, peroxisomal proteins were characterized using IHC and brightfield microscopy, and hepatic FA metabolic transcripts analyses by RT-qPCR. In this study, we showed that carbohydrate-rich (Aston) LPD reduced serum OCFA, increased CD36 mRNA expression. Whilst serum and liver OCFA was not altered in the relatively reduced carbohydrate-rich (Nottingham) LPD, hepatic lipid accumulation was observed suggesting fat deposition may occur prior to systemic fatty acid profile changes.

5.1 Introduction

Emerging evidence shows that a low protein diet increases the risk of cardiometabolic diseases including type 2 diabetes and NAFLD, Watkins et al (2016). A study in mice shows that feeding of a low protein diet (LPD) resulted in a significant reduction in glucose tolerance as well as elevated adiposity, Watkins & Sinclair (2014). Whether the impaired glycaemic response to a low protein diet is as a result of changes to circulatory odd-chain fatty acids remains to be determined.

Proteins serve as important metabolic fuel source. Excess proteins cannot be stored and must be converted into glucose or triglycerides. The liver plays an important role in the regulation of the metabolism of amino acids and proteins. In endogenous protein metabolism, the liver is essential for the formation of plasma proteins (eg albumin, clotting factors), amino acid interconversion (synthesis of all non-essential amino acids), deamination of amino acids to produce energy and urea synthesis (for ammonia excretion), Charlton (1996). However, this is not enough and therefore additional amino acids should be supplied in diet particularly because humans cannot synthesize all of the 20 amino acids used to build proteins. Disordered protein and amino acid metabolism is a common feature of patients with liver disease especially those as results of protein-calorie malnutrition (PCM). PCM is defined as a wasting condition resulting from a diet deficient in both calories and protein, Charlton (1996).

Methionine is an amino acid required for protein synthesis. Methionine adenosylated product, *S*-adenosylmethionine is an important substrate for methylation in epigenetic and epigenomic pathways, Robinson et al (2016). It has been reported that methyl donor deficiency induces liver steatosis and predisposes to metabolic syndrome, de Conti & Pogribny (2017). Methyl donor supplementation reverted the high fat sucrose (HFS)-diet-induced hepatic TG accumulation in rats after 8 weeks of feeding Cordero et al (2013).

NAFLD is linked with increased liver lipid production through *de novo* lipogenesis (DNL). The DNL pathway from protein energy sources involves synthesis of fatty acid using acetyl-coenzyme A (CoA) as a carbon source, which is generated from metabolic reactions such as the deamination of amino acids. The pathway is initiated by carboxylation of acetyl-CoA to malonyl-CoA by acetyl-CoA carboxylase (ACC). Malonyl-CoA is then transferred to a complex multifunctional enzyme, fatty acid synthase (FAS). Multiple steps of activation of acetyl-CoA to malonyl-CoA, transferring to FAS and addition to the lengthening carbon chain to produce palmitate. Fatty-acyl chains are then incorporated into different classes of lipid species, including triglyceride and phospholipids, Charidemou et al (2019). An isocaloric low protein high carbohydrate diet (6% protein, 16.3 kJ/g) reduced liver weight and increased the lipid content compared to control (17% protein, 16.3 kJ/g) in the livers of rats fed for 2 weeks. This was attributed to the reduction in protein intake since the smaller supply of the amino acids in the diet impaired hepatic protein synthesis such as lipoprotein generation. It is thought that impairment in lipoprotein synthesis has the potential to limit the transport of FA to peripheral tissues, Menezes et al (2013).

Apart from *de novo* synthesis of fatty acids, the gut also contributes to the fatty acid pool. Dietary fat in the form of di- and triglycerides is hydrolysed into monoglyceride and free fatty acids by pancreatic lipase in the small intestine. As monoglycerides and fatty acids are liberated via the action of lipase, they retain their association with bile acids and complex with other lipids to form mixed micelles. Long chain fatty acids are absorbed by the epithelial cells of the small intestinal villi called enterocytes, re-esterified and finally incorporated into chylomicrons as triglyceride. Chylomicrons are formed in the endoplasmic reticulum of enterocytes and undergo exocytosis before entering the lymphatic system, Stahl et al (1999).

In this study, we have employed both GC/FID and GC/MS-based metabolomics approaches in order to explore the effects of two LPD models of different carbohydrate content and

composition on systemic fatty acid profile in mice. We used qPCR technique to explore the mechanisms underlying systemic fatty acid changes in the liver of the Aston LPD study. Following comparative differences in fatty acid profiles between the two LPD models, we used immunohistological approach to study changes in peroxisomal biogenesis markers in the Nottingham LPD model.

5.1.1 Aims

This study was aimed at evaluating the effect of dietary protein treatments on systemic metabolism of lipid using metabolomics, transcriptomics and immunohistochemistry approaches. The experiment tests the hypothesis that a low protein diet affects odd chain fatty acid metabolism leading to pathogenesis of obesity-associated metabolic diseases including non-alcoholic fatty liver disease.

Specific objectives of the study were:

1. Serum and liver FA analyses of mice fed NPD, LPD and MD-LPD in a dietary protein model where protein energy loss is compensated for by increasing only carbohydrate were performed using GC-FID (Aston LPD study).
2. Hepatic transcript expression related to specific fatty acid changes and pathways were analysed by qPCR in mice fed NPD, LPD or MD-LPD (Aston LPD study).
3. Serum and liver FA analyses of mice fed MD-NPD, LPD and MD-LPD in a dietary protein model where loss of protein is compensated by nutritional composition balance were analysed using GC-MS (Nottingham LPD study).
4. Basic liver histological technique, H&E staining was used to investigate hepatic lipid accumulation of mice fed MD-NPD, LPD and MD-LPD (Nottingham LPD study).
5. Peroxisome biogenesis protein expressions in fixed liver tissue were performed using immunohistochemistry technique following 8 weeks of feeding regimen and compared between MD-NPD, LPD and MD-LPD groups (Nottingham LPD study).

The following figure 5.0 shows the details of the experimental design employed in this study

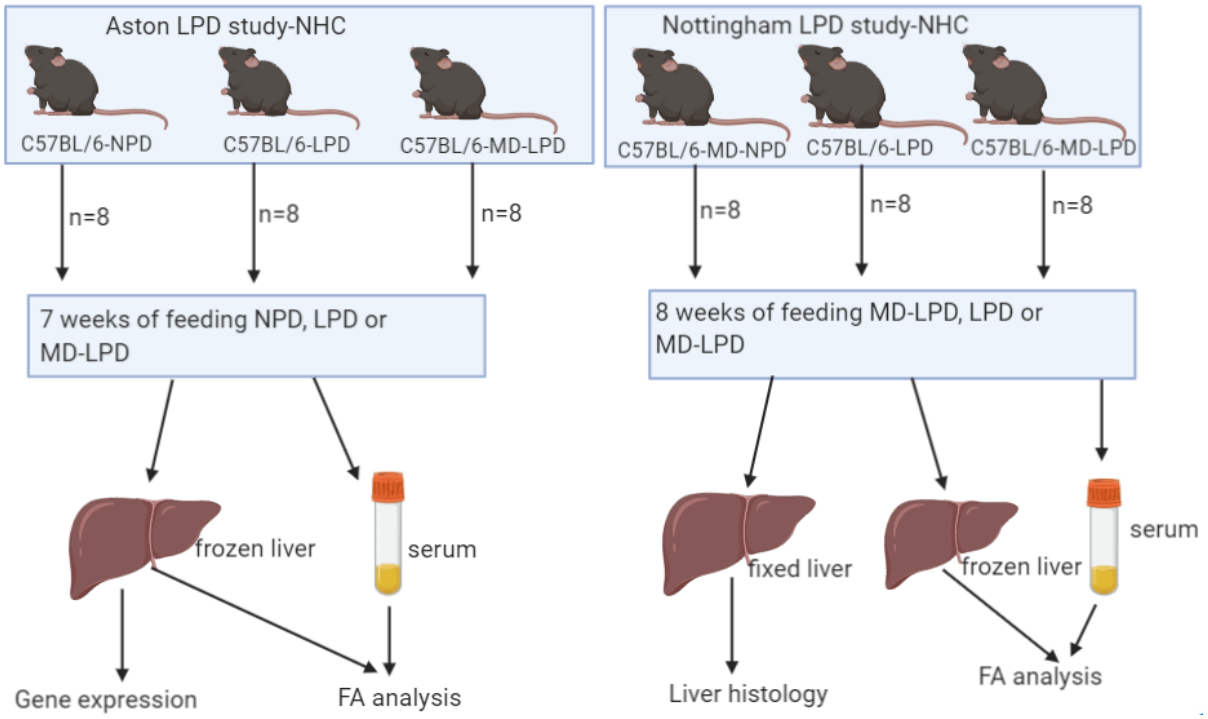

Figure 5.0: Experimental design of the Aston and Nottingham LPD studies.

Male C57BL/6 mice were fed NPD, LPD or MD-LPD for 7 weeks (Aston LPD study) whilst in the Nottingham LPD study, male C57BL/6 mice were fed MD-NPD, LPD or MD-LPD for 8 weeks (n=8 mice per group).NPD-Normal protein diet, LPD-Low protein diet, MD-LPD-Low protein diet with methyl donor supplements, MD-NPD-Normal protein diet with methyl donor supplements, NHC-Normal husbandry condition.

5.2 Method

5.2.1 Low protein diet and sample collection

For a detailed description of the animal housing and dietary treatment procedures see Chapter 2. In brief, male mice (8 per group) were assigned to three treatment groups i.e. NPD, LPD and MD-LPD treated groups (Aston LPD study). The animals in the normal protein diet treated control group received a 18% casein protein while the animals in the LPD-treated group received a 9% casein protein and MD-LPD treated group receiving 9% casein protein with methyl donors consisting of 5 g/kg diet choline chloride, 15 g/kg diet betaine, 7.5 g/kg diet

methionine, 15 mg/kg diet folic acid, 1.5 mg/kg diet vitamin B12. The three diets were isocaloric and given *ad libitum* for 7 weeks. Another male mice (8 per group) were treated with different dietary low protein composition i.e. MD-NPD, LPD and MD-LPD (Nottingham LPD study) for 8 weeks. In both studies, after the period of feeding, the animals were killed via a cervical dislocation of the neck and blood samples were collected via heart puncture and allowed to clot before centrifuging to collect the serum. Liver samples were dissected out on ice, snap-frozen and stored at -80°C or fixed in 10% formalin. In this project, both GC-FID and mass spectrometry-based analyses were carried out on serum and liver tissues. RT-qPCR analyses was performed on other snap frozen liver tissues and then the fixed liver tissues were used for the immunohistochemistry analyses.

5.2.2 GC-FID &GC-MS experiments

5.2.2.1 Serum and liver extract preparation and GC-FID/MS experiments

The serum and liver sample preparations were performed as described in Chapter 2, sections 2.2.1 and 2.2

5.2.2.2 Preparation of fatty acid methyl esters (FAMEs)

Fatty acids were methylated using 200 μL toluene (Thermo-Fisher, UK), 1.5 mL methanol and 0.3 mL of 6.3% HCl in methanol at 35°C for 10 minutes (for liver (50 μLsamples) or 100 °C for 1 hour (for serum 50 μL samples), in PTFE-sealed glass vials. Specifically, the serum derivatization of Aston LPD study was long and harsh (100 °C for 1 hour). All other samples from both models were derivatised at shorter conditions (35°C for 10 minutes). In either serum or liver tissues, the FA methyl esters (FAMEs) were subsequently extracted with 1 mL of hexane and 1 mL of water, evaporated under nitrogen and resuspended in 20 μl of hexane in case of serum samples or in 150 μL hexane for liver samples prior to analyses by gas chromatography (GC).

5.2.2.3 Gas chromatographic and mass spectrometry analyses.

The Aston LPD serum sample analyses were done using GC-FID. The serum of Nottingham-LPD were analysed by GC-MS. Liver samples of both models were analysed using GC-MS. For full details of analyses and column information have been described in Chapter 2, section 2.2.4.1.

Liver FA analyses was done using Agilent GC7890 system linked to a MSD5975 with electron impact ionisation (70 eV). For details and column information have been described in Chapter 2, section 2.2.4.2.

5.2.2.4 Fatty acid identification, data mining and normalization

For GC-FID analyses, retention times of each chromatographic peak were compared with retention times of reference standard sample run in the same method along with the sample analyses. The reference standard used in this experiment is 37 FAME standard mix. Other properties used in accurate identification of sample is shape matching.

In the case of GC-MS analyses, identification of fatty acids were based on matching mass spectra of samples with mass spectral library (eg NIST library) and/or reference standard (37 FAME mix). In addition, identified FA were based on GC retention times.

Peak areas were normalized by dividing each peak area value by the area of the internal standard (undecanoic acid) for a given sample.

5.2.3 Real time quantitative PCR

After 7 weeks on the low protein diet feeding regimen, the real-time quantitative PCR (RT-qPCR) technique was used to quantify the changes in mRNA levels of several metabolic and inflammatory genes (see Table 2.10). The primers for these genes were selected, designed and verified as previously described (Chapter 2, section 2.4.1.2). The animals were sacrificed after

the 7-weeks of feeding and the liver tissues removed and snap-frozen and then stored at -80°C until analysis (as previously described in Chapter 2, section 2.1.2s). The RNA extraction procedure, the reverse transcription of RNA to complementary DNA (cDNA), and the RT-qPCR processes have been described in Chapter 2, section 2.2.1.3.

5.2.4 Immunohistochemistry

The immunohistochemistry technique was employed to examine the effects of low protein diet intake on catalase (1:100; Abcam (ab16731)), PEX-14 (1:100; Abcam (ab10999)) protein expression in the fixed liver tissues (as previously described in Chapter 2, section 2.3.5). The primary antibodies were incubated with secondary antibody, goat anti-rabbit IgG H&L (horseradish peroxidase (HRP)) (1:250; Abcam (6721)). The animals were sacrificed after the end of low protein diet experiment and the livers removed and fixed in 10% of formalin and then stored at -4°C until analysis There were five animals assigned of each dietary group selected for immunohistochemistry analyses. Images of slides were captured with brightfield microscopy (as previously described in Chapter 2, section 2.3.4.1 and 2.3.4.3).

5.3 Results

Metabolic response to protein loss compensated by only carbohydrate (The Aston low protein diet study).

To understand the metabolic response to a low protein diet where protein loss has been replaced by carbohydrate, we fed mice with either NPD, LPD or MD-LPD for 7 weeks and assessed their growth rate, serum and liver fatty acid profiles, as well as mechanism underlying lipid metabolism and oxidative stress.

5.3.1 Growth rate of low protein diet fed mice (Aston LPD study)

To study the effect of protein restriction on body weight for 7 weeks, eight-week-old C57BL/6 males were housed singly and fed three different diets either control normal protein diet (NPD; n = 8) isocaloric low protein diet (LPD; n = 8) or MD-LPD; n=8) *ad libitum* for at least 7 weeks (Table 2.1). Overall, the weights of the animals receiving NPD (controls) or LPD were statistically lower from MD-LPD fed mice ($p < 0.05$; n=8 mice) from week 5 to the day they were sacrificed (week 7). (Figure 5a). There were no difference between LPD and MD-LPD groups.

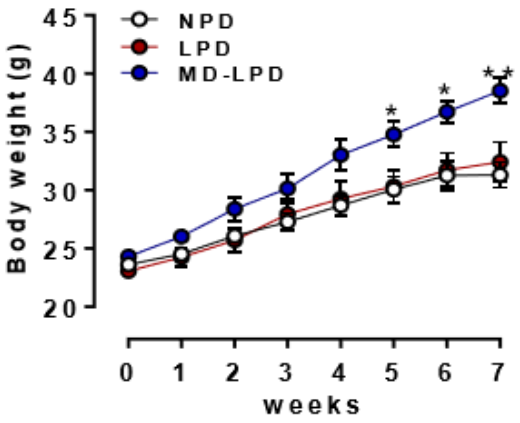

Figure 5a: Body weight changes with time (Aston LPD sudy).

Data represent mean ± SEM. Male mice with normal-protein diet (LPD; 18% casein protein; n=8), male mice with low-protein diet (LPD; 9% casein protein; n=8), male mice with LPD supplemented with methyl donors (MD-LPD; 9% casein protein with methyl donors (5 g/kg diet choline chloride, 15 g/kg diet betaine, 7.5 g/kg diet methionine, 15 mg/kg diet folic acid, 1.5 mg/kg diet vitamin B12; n=8). *p<0.05; **p<0.001.

5.3.2 Effect of low protein diet on serum and liver fatty acids

Here we present serum and liver fatty acid profiles of fatty acids in NPD, LPD and MD-LPD group after 7 weeks of feeding (table 5.1 & 5.2).

Table 5.1: Fatty acid composition of serum in mice fed with low protein diet (Aston LPD study)

Group of FA	% of total serum FA	NPD	LPD	MD-LPD
		Median (min-max)	Median (min-max)	Median (min-max)
ECFA	C10:0	5.86 (4.28-8.89)	2.28(1.20-6.00)**	6.85 (5.26-8.47)##
	C12:0	3.02 (1.89-6.79)	1.89(1.22-3.08)*	7.42(3.97-10.22)###
	C14:0	5.23 (4.12-6.43)	2.00(1.49-2.65)***	5.79 (4.28-6.29)###
	C16:0	22.43(21.53-26.45)	16.39(14.29-35.34)*	16.39(16.74-29.40)
	C18:0	13.77 (9.85-17.03)	16.47(15.27-19.16)**	15.70(10.21-17.25)
	C22:0	0.80 (0.30-1.03)	0.42 (0.34-1.62)	0.42 (0.34-1.62)##
	C24:0	0.70 (0.56-2.29)	4.34 (2.41-5.84)***	0.72 (0.27-1.75)###
	Total ECFA	53.59 (49.29-57.50)	43.89(43.57-65.21)	56.23(52.76-.21)##
OCFA	C15:0	1.39 (1.27-3.44)	1.07 (0.81-3.07)*	2.06 (1.06-2.61)
	C17:0	5.81 (3.88-8.22)	2.87 (1.66-4.93)**	8.56 (6.09-9.69)##
	Total OCFA	7.08 (5.21-10.56)	4.14 (3.04-6.03)*	9.94 (8.24-11.54)###
MUFA	C16:1	1.39 (1.04-2.91)	0.80 (0.68-1.45)*	1.20 (0.89-1.63)#
	C18:1	13.95(12.49-15.81)	15.45(10.66-19.12)	12.18(9.62-12.89)#
	Total MUFA	15.40(13.81-18.24)	16.34(12.12-19.90)	13.56(10.68-14.10)#
PUFA	C18:2n6	18.96(15.93-22.04)	18.65(11.96-19.62)	11.70(5.27-14.71)##
	C20:4n6	2.94 (1.28-3.93)	15.71(3.55-17.57)**	7.28 (2.08-9.36)#
	C22:2	1.55 (0.89-3.38)	0.60 (0.39-2.44)*	0.59 (0.49-1.51)
	Total PUFA	23.32(20.07-26.44)	35.16(17.96-36.42)	20.00(7.87-25.30)##
Activity ratio	C16:1/C16:0	0.06 (0.05-0.13)	0.05 (0.04-0.07)	0.06 (0.04-0.10)
	C18:1/C18:0	1.07 (0.91-1.27)	0.93 (0.70-1.01)	0.77 (0.66-1.02)
	C20:4n6/C18:2 n6	0.17 (0.06-0.21)	0.85 (0.30-0.99)***	0.62 (0.39-0.67)

*p<0.05 LPD vs NPD, #p<0.05 MD-LPD vs LPD

Table 5.2: Fatty acid composition of liver in mice fed low protein diet (Aston LPD study)

Group of FA	% of total liver FA	NPD Median (min-max)	LPD Median (min-max)	MD-LPD Median (min-max)
ECFA	C14:0	0.64 (0.42-0.80)	0.93 (0.48-0.80)*	1.24 (0.92-1.07)#
	C16:0	29.30(24.18-39.72)	26.81(20.59-31.85)	26.57(23.32-34.36)
	C18:0	12.27 (6.93-19.95)	7.15(6.04-10.32)*	6.92 (5.47-8.46)
	Total ECFA	41.82(33.02-56.42)	35.77(27.89-43.07)*	34.81(31.46-41.77)
OCFA	C15:0	0.15 (0.09-0.20)	0.12 (0.11-0.21)	0.12 (0.10-0.18)
	C17:0	0.12 (0.11-0.21)	0.12 (0.10-0.18)	0.16 (0.13-0.19)
	Total OCFA	0.43(0.23-0.60)	0.30(0.26-0.49)	0.28(0.26-0.34)
MUFA	C16:1	2.33 (0.79-5.47)	3.61 (1.73-4.13)	4.00 (3.03-5.79)
	C18:1	22.44(14.35-38.34)	32.11(24.37-38.14)	37.61(34.03-39.75)
	Total MUFA	24.47(15.66-43.81)	35.56(26.66-42.11)	42.17(37.15-45.03)
PUFA	C18:2n6	20.91(12.79-27.36)	21.08(19.54-29.34)	17.79(14.10-21.38)#
	C18:3n3	0.50 (0.28-0.90)	0.55(0.26-1.51)	0.36 (0.28-0.53)
	C20:4n6	0.55 (0.26-1.51)	0.36 (0.28-0.53)	0.36 (0.28-0.53)#
	Total PUFA	29.22(17.45-35.52)	28.04(24.08-40.86)	22.07(18.55-26.98)
Activity ratio	C16:1/C16:0	0.07(0.03-0.18)	0.13(0.07-0.15)	0.14(0.12-0.23)
	C18:1/C18:0	1.86(0.72-5.53)	4.78(2.36-5.82)*	5.61(4.02-7.17)
	C20:4n6/C18:2n6	0.36(0.23-0.65)	0.27(0.21-0.38)*	0.25(0.19-0.30)

*p<0.05 LPD vs NPD; #p<0.05 MD-LPD vs LPD

5.3.2.1 Effect of reduced protein intake on total fatty acid concentrations in liver and serum

To investigate the effect of low protein diet on total fatty acid concentration of mice after 7 weeks of feeding, we analysed serum and liver samples using absolute concentration of the fatty acids. There were significant differences between dietary groups in serum total fatty acid concentrations in mice (figure 5.1). Thus, analysis of serum total fatty acids in the male mice revealed a significant increase in level of total FA in LPD mice compared to NPD ($p<0.0001$). The increased in serum FA concentration may result from FA released into circulation from adipose tissue hydrolysis. However, MD-LPD males displayed a significantly lower total serum FA concentration when compared to LPD-fed male mice ($p<0.05$). This suggests that methyl donor attenuated the metabolic effect of LPD and improved FA profile. Interestingly, there was no significant difference between groups in liver total lipid concentration in mice at the end of 7 weeks of dietary feeding (figure 5.1).

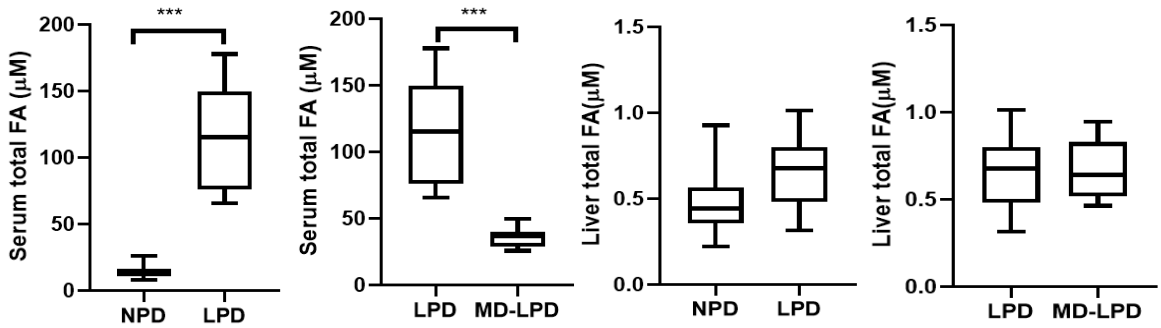

Figure 5.1: Effect of diet on total fatty acid concentration in serum and liver (Aston LPD study)

Total fatty acids were measured in the serum and liver of mice. Values are given as means ± SEM for n=8. ***p<0.0001 LPD vs NPD, MD-LPD vs LPD

5.3.2.2 Effect of reduced protein intake on mouse serum and liver even-chain saturated fatty acid

To assess the effect of low protein diet on even-chain saturated fatty acid, we analysed serum and liver samples from the mice after 7 weeks of feeding. The percentage of even-chain SFAs in serum were not significantly different in LPD mice when compared to NPD group, however, the MD-LPD group showed significantly higher even-chain SFAs compared to the LPD group ($p<0.001$, table 5.1). In contrast, the liver proportion of even-chain SFAs to all other fatty acids was significantly reduced in LPD relative to NPD ($p<0.05$, table 5.2). The addition of MD-LPD had no effect on liver even-chain SFA proportion when compared to the LPD fed group (table 5.2). A total of seven specific ECFAs were detected in the serum sample analyses: capric acid (C10:0), lauric acid (C12:0), myristic acid (C14:0), palmitic acid (C16:0), stearic acid (C18:0), behenic acid (C22:0), and lignoceric acid (C24:0) with C16:0 and C18:0 being the most abundant (table 5.3). On the other hand, in the liver sample analyses, a total of the three dominant specific even-chain FAs were detected: C14:0, C16:0, C18:0 (table 5.2). LPD was associated with decreased concentrations of serum C10:0, C14:0 and C16:0 ($p<0.05$) and increase concentrations of serum C18:0 ($p<0.05$) and C24:0 ($p<0.001$), compared to NPD (figure 5.2). However, MD-LPD showed increase proportion of serum C10:0 ($p<0.001$), C12:0 ($p<0.05$) and C14:0 ($p<0.001$) but decrease C24:0 ($p<0.0001$) compared to LPD (figure 5.2). In contrast, hepatic C18:0 ($p<0.001$) concentration was significantly lower in the LPD fed mice compared to NPD group (figure 5.2). However, there was no significant difference in liver C14:0 and C16:0 concentration between NPD and mice fed the LPD. Similar to serum MD-LPD levels of C14:0 ($p<0.001$), there was an increase concentration of hepatic C14:0 ($p<0.05$) when compared to LPD fed mice.

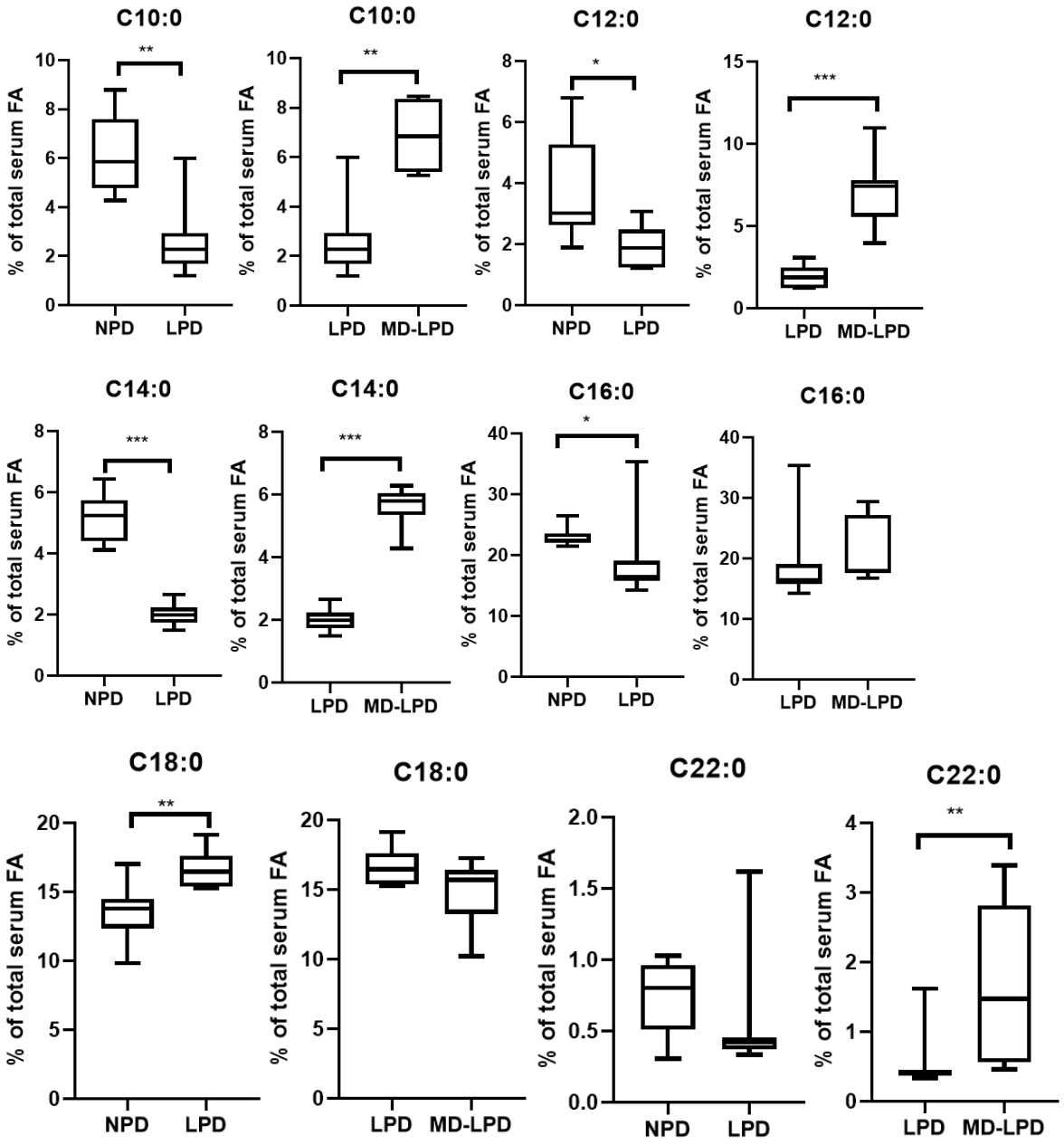
C10:0
**
% of total serum FA
NPD
LPD
C10:0
**
% of total serum FA
LPD
MD-LPD
C12:0
*
% of total serum FA
NPD
LPD
C12:0
***
% of total serum FA
LPD
MD-LPD
C14:0
***
% of total serum FA
NPD
LPD
C14:0
***
% of total serum FA
LPD
MD-LPD
C16:0
*
% of total serum FA
NPD
LPD
C16:0
% of total serum FA
LPD
MD-LPD
C18:0
**
% of total serum FA
NPD
LPD
C18:0
% of total serum FA
LPD
MD-LPD
C22:0
% of total serum FA
NPD
LPD
C22:0
**
% of total serum FA
LPD
MD-LPD

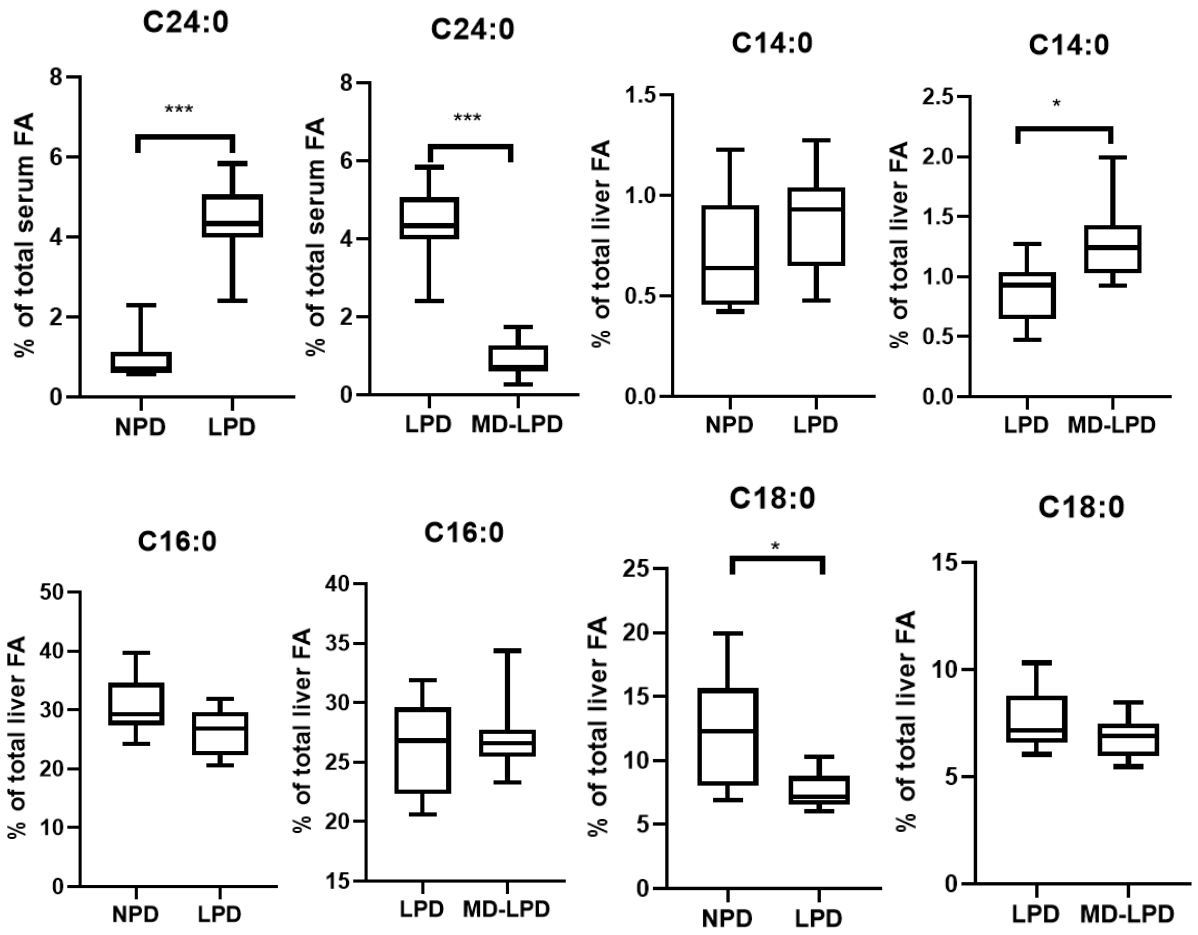

Figure 5.2: Effect of low protein intake on even-chain saturated FA in the serum and liver (Aston LPD study)
Specific ECFAs were measured in the serum and liver of mice. Values are given as means ± SEM for n=8. *p<0.05, **p<0.001, ***p<0.0001 LPD vs NPD; *p<0.05, **p<0.001, ***p<0.0001 MD-LPD vs LPD

5.3.2.3 Serum and liver odd-chain saturated fatty acids (OCFAs) in a low protein fed mice.

To investigate OCFA changes following a 7 week of low protein diet intake, we performed analysis of serum and liver samples obtained from the mice. There were significant intergroup differences in the serum total OCFA proportions (table 5.1), however, no significant differences were observed between dietary groups in liver total OCFA proportion (table 5.1). Serum proportion of odd-chain SFAs were significantly lower in LPD fed group compared to NPD group ($p<0.05$), whereas serum total OCFAs were significantly higher in MD-LPD

relative to LPD fed group (table 5.1, p<0.0001). Two specific OCFAs were detected in both serum and liver sample analyses: pentadecanoic acid (C15:0) and heptadecanoic acid (C17:0) (tables 5.2 & 5.2). The proportion of serum C17:0 or C15:0 was significantly lower in LPD animals compared to NPD (p<0.05). However, the proportion of serum C17:0 in MD-LPD mice was significantly higher when compared to those fed with LPD (figure 5.3, p<0.001). There were no effects of MD-LPD upon serum C15:0 content versus LPD. There were no significant effects of dietary protein intake on liver C15:0 or C17:0 levels between dietary groups (data not shown).

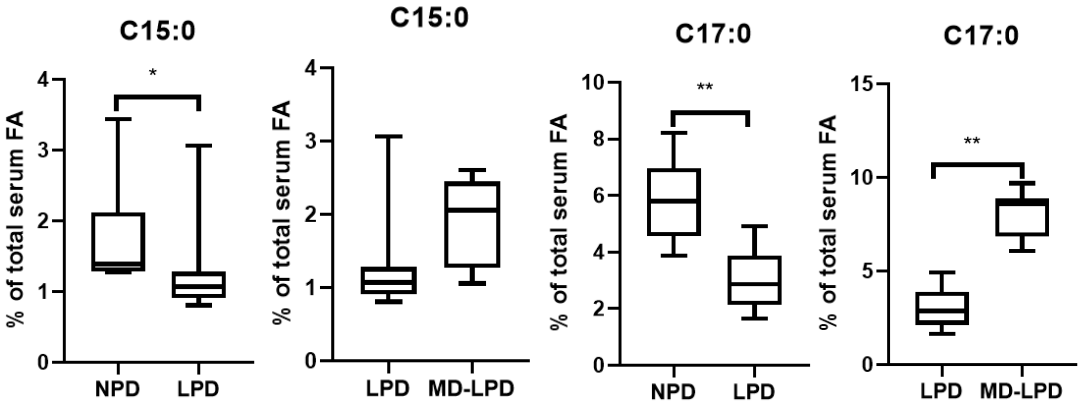

Figure 5.3: Effect of low protein intake on odd-chain saturated FA in the serum (Aston LPD study)
Specific OCFAs was measured in the serum and liver of mice. Values are given as means ± SEM for n=8. *p<0.05 LPD vs NPD; **p<0.001 MD-LPD vs LPD

5.3.2.4 Effect of low protein diet on mouse serum and liver monounsaturated fatty acid (MUFA) concentrations

In order to assess the impact of low protein diet on MUFA, serum and liver samples were analysed. The proportion of MUFA in serum and liver between NPD, LPD and MD-LPD is shown in table 5.1 & 5.2. In our dietary model for seven weeks, the sum of MUFA in either plasma or liver was not statistically significant between dietary groups. Serum content of palmitoleic acid (C16:1 FA) was significantly reduced in LPD fed mice than NPD group (p<0.05), however, they were reversed when LPD was compared with MD-LPD in the serum

(figure 5.4, $p<0.05$). On the contrary, whilst serum proportion of oleic acid (C18:1 FA) was significantly lower in MD-LPD relative to LPD ($p<0.05$), there was no change when LPD was compared with NPD (Figure 5.4). Interestingly, individual MUFA such as palmitoleic acid (C16:1) and oleic acid (C18:1) in the liver of animals fed either NPD, LPD or MD-LPD did not differ between groups (figure 5.4).

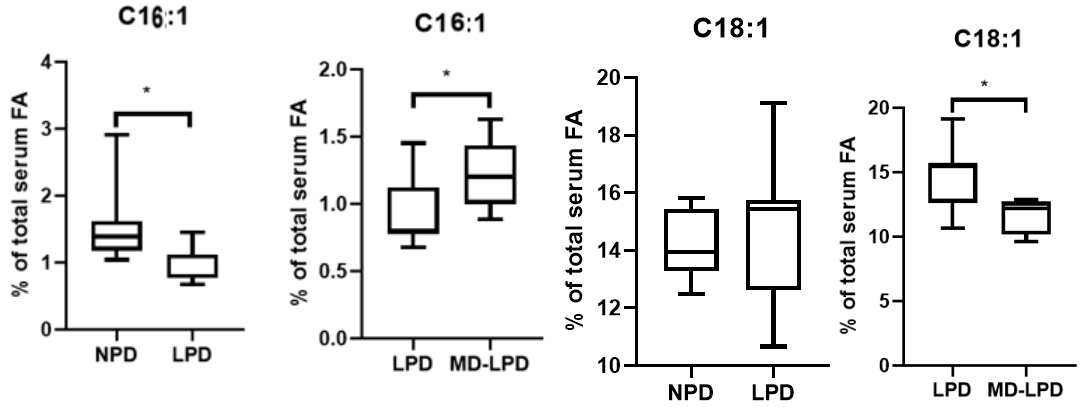

Figure 5.4: Effect of low protein intake on monounsaturated FA content in the serum and liver (Aston LPD study)
Specific MUFAs were measured in the serum and liver of mice. Values are given as means ± SEM for n=8. *p<0.05 LPD vs NPD; *p<0.05 MD-LPD vs LPD)

5.3.2.5 Effect of reduced protein intake on mice serum and liver PUFA

To assess whether a low protein feeding alters PUFA distribution in the blood and liver after 7 weeks of feeding mice with NPD, LPD and MD-LPD diets, we analysed PUFA of LPD fed mice and compared it with the control (NPD) group. Also, serum and liver content of PUFA of MD-LPD fed mice were compared with LPD fed mice. Here, we observed that serum n-6 PUFA content was significantly lower in MD-LPD than LPD ($p<0.001$). There was no significant difference in serum n-6 PUFA between LPD and NPD (Table 3.1). Similar to serum n-6 PUFA concentration, there were significantly lower levels of total n-6 PUFA in MD-LPD fed mice compared to LPD ($p<0.05$), however, no observable change were recorded in liver n-6 PUFA between LPD and NPD (table 5.2). With the method used for serum fatty acid analyses, a total of three specific n-6 PUFAs were detected from the dietary protein study

subjects: linoleic acid (C18:2), arachidonic acid (C20:4) and *cis*-13,16-docosadienoic acid (C22:2). In the liver fatty acid analyses too, two specific n-6 PUFAs were detected including linoleic acid (C18:2n6) and arachidonic acid, and an n-3 PUFA, linolenic acid (C18:3n3). In both serum and liver n-6 PUFA analyses, C18:2n6 & C20:4n6 were the most abundant (Table 5.1 &5.2). The serum proportion of C20:4n6 FA were significantly higher in LPD compared to NPD ($p<0.001$), however, this was lowered when MD-LPD was compared with LPD. (Figure 5.5). Conversely, serum C22:2 were significantly lower in LPD group compared to NPD ($p<0.05$), whilst no significant difference was obtained between MD-LPD and LPD (Figure 5.5). In terms of serum content of C18:2n6, analyses of intergroup differences showed that there were significantly lower levels in MD-LPD compared to LPD ($p<0.05$), although no significant difference was seen when LPD fed mice were compared with NPD. (Figure 5.5). Surprisingly, in the liver neither C18:2n6, C18:3n3 nor C20:4n6 were significantly affected by LPD when subjected to multiple comparison analyses. Although, we could observe a trend for increased concentration of C18:2n6 and C18:3n3 in LPD fed mice compared to NPD, these were statistically insignificant (data not shown).

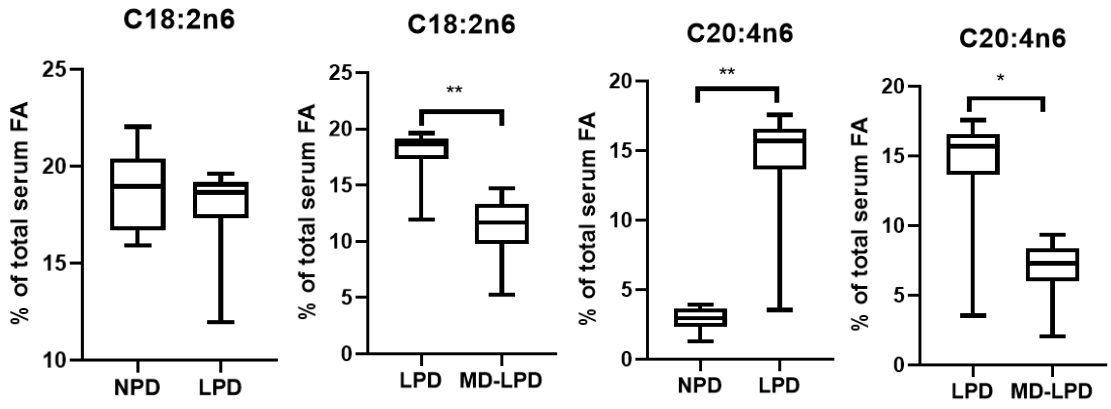

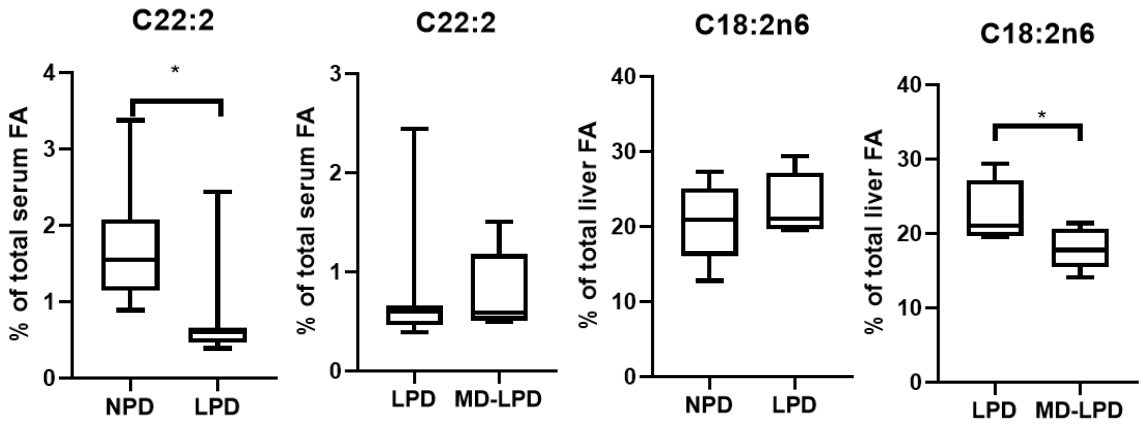

Figure 5.5: Effect of low protein intake on polyunsaturated FA content in the serum and liver (Aston LPD sudy)
Specific PUFAs were measured in the serum and liver of mice. Values are given as means ± SEM for n=8. *p<0.05, **p<0.001 LPD vs NPD; *p<0.05 MD-LPD vs LPD

5.3.2.6 Indices of desturation enzyme activity

The surrogate markers of enzyme activities of serum and liver of mice on NPD, LPD and MD-LPD are shown in table 5.1 & 5.2. The C18:1/C18:0 ratio was not significant in serum FAs between dietary groups after the seven weeks of feeding. However, the serum C20:4/C18:2 ratios were significantly higher in LPD fed group compared to NPD fed mice ($p<0.0001$) although no significant difference was found between LPD versus MD-LPD groups. The C16:1/C16:0 ratio was not significantly different in the liver tissue fatty acids between NPD, LPD or MD-LPD, however, the C18:1/C18:0 ratios were significantly lower in liver fatty acids of LPD compared to NPD which indicates reduced SCD1 activity. Interestingly, in the liver fatty acids the C20:4n6/C18:2n6 ratios were significantly lower in LPD groups relative to NPD in response to dietary protein feeding ($p<0.05$). No significant changes of C20:4/18:2 ratios were observed in liver fatty acids between LPD and MD-LPD.

5.3.3 Effect of a low protein diet on expression of genes involved in fatty acid uptake.

To understand the mechanisms underlying a low protein diet associated NAFLD, we performed gene expression analyses on two key genes involved in hepatic fatty acid transport (cluster of

differentiation (*CD 36*) and fatty acid binding protein (FABP)) using liver tissues obtained from mice following 7 weeks of a low protein dietary challenge using RT-PCR.

After the 7-week feeding regimen, the mice in the 9% LPD group showed a significant upregulation of *CD 36* expression in the liver compared to NPD group ($p<0.001$). There were no changes in *CD 36* expression between LPD versus MD-LPD groups. Moreover, when we assessed the expression of two fatty acid binding genes-*FABP1* and *FABP3* we observed no significant difference between NPD and LPD as well as LPD versus MD-LPD (Figure 5.6).

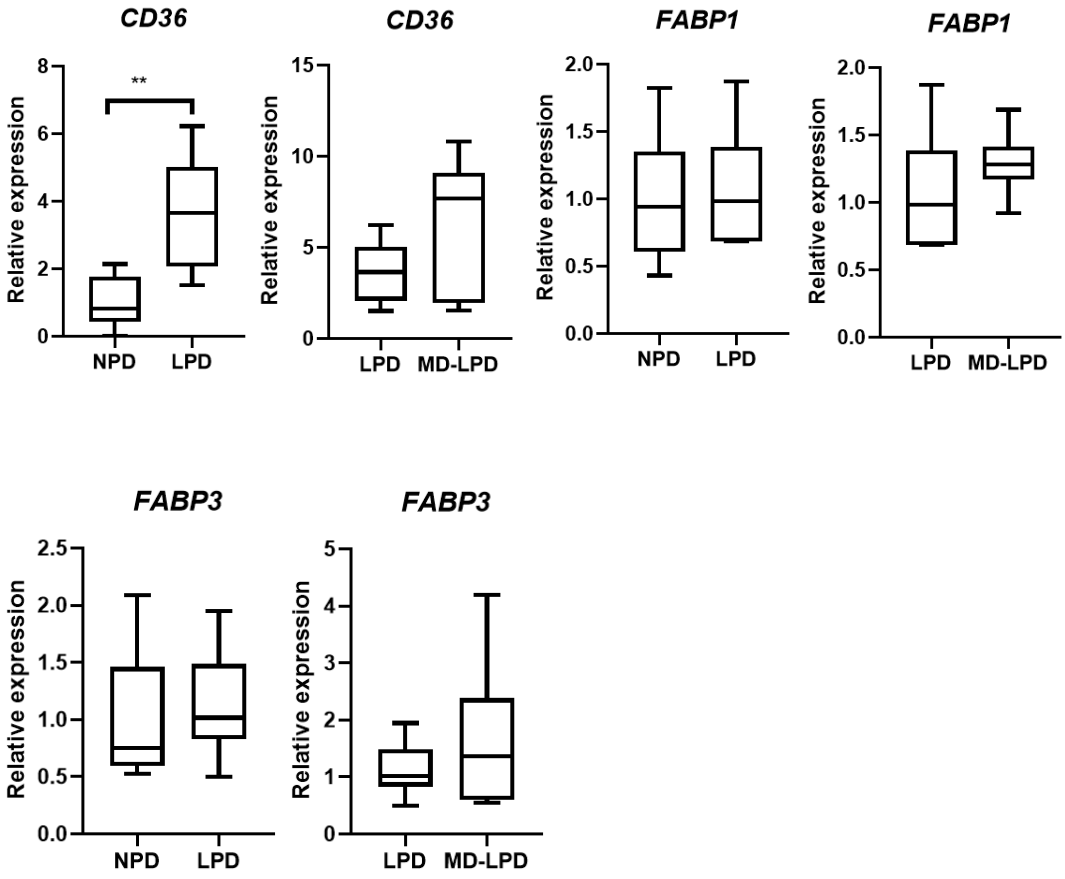

Figure 5.6: Effect of LPD on *CD36, FABP1* and *FABP3* mRNA expressions (Aston LPD study).

Mean relative transcript expression of genes involved in hepatic fatty acid uptake in mouse. Values are given as means ± S.E.M for n=8; **p<0.001 LPD vs NPD. Abbreviations: *CD36* (cluster of differentiation; *FABP1*: fatty acid binding protein 1; *FABP3*: fatty acid binding protein 3.

5.3.4 Identification of specific fatty acid gene expression synthesis changes during a low protein intake in mice

Following changes in composition of fatty acid profiles observed in the liver and serum of mice fed with low protein diet in the presence and absence of methyl donor, we performed gene expression analyses on specific genes related to metabolism of saturated fatty acid (SFA), MUFA, OCFA and PUFA. The selected genes include stearoyl-CoA desaturase *(SCD1),* fatty acid desaturase 1 *(FADS1*), fatty acid desaturase 2 *(FADS2),* 2-hydroxyacyl-CoA lyase 1*(HACL1)*. There were no significant changes in the mRNA expressions of *SCD1*, *FADS1* and *FADS2* after 7 weeks of low protein in mice compared with control (NPD). Furthermore, *FADS1* expression was significantly increased in MD-LPD group compared to LPD ($p<0.001$). However, no significant changes were observed between MD-LPD and LPD relative to *SCD1* and *FADS2* expression. Finally, *HACL-1*, a gene which is thought to play a role in odd-chain fatty acid metabolism was not altered in the liver in the LPD fed group compared to NPD (Figure 5.7).

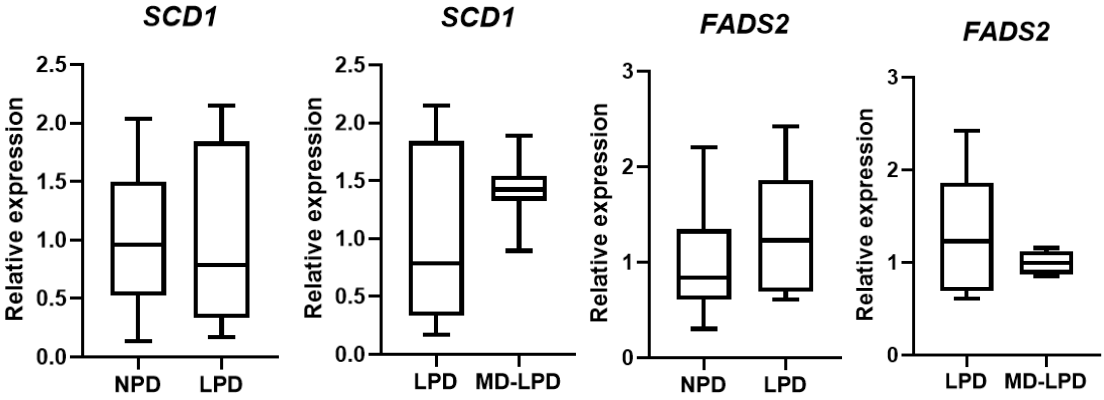

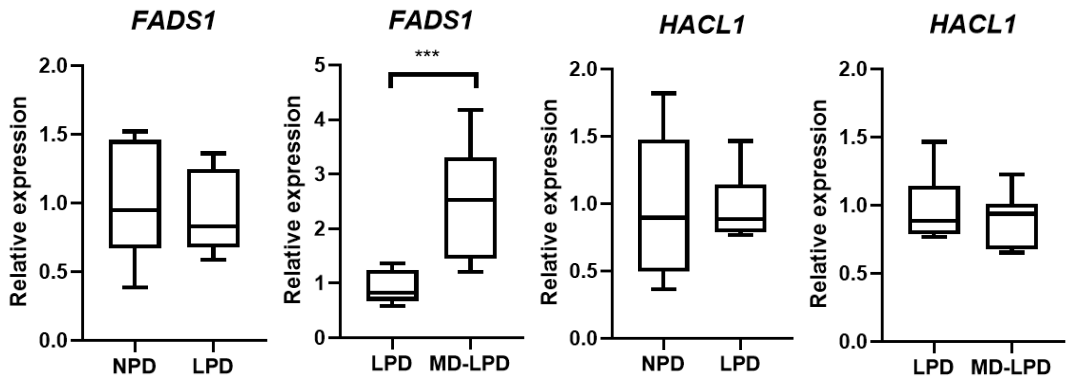

Figure 5.7: Effect of diet on mouse liver *SCD1, FADS1, FADS2* and *HACL-1* mRNA expression (Aston LPD study).
Mean relative transcript expression of genes related specific fatty acid changes in mouse. Values are given as means ± S.E.M for n=8; ***p<0.0001 LPD vs MD-LPD. Abbreviations: scd1: stearoyl-CoA desaturase; *FADS1*: fatty acid desaturase 1; *FADS2*: fatty acid desaturase 2; *HACL-1*: 2-hydroxyacyl-CoA lyase 1

5.3.5 Low protein intake does not alter the expression of mitochondrial, peroxisomal redox and inflammatory genes and genes related to lipid metabolism

In exploring the relationship between liver tissue and a low protein diet associated NAFLD, we tested the effect of a low protein diet on mitochondrial, peroxisomal, inflammatory and other gene expression in liver tissue. At the end of the low protein experiment mRNA analysis carnitine palmitoyltransferase 1b, muscle (*CPT1*), carnitine palmitoyltransferase 2(*CPT2*), malonyl-CoA decarboxylase (*MLYCD*), catalase (*CAT*), branched chain ketoacid dehydrogenase E1, alpha polypeptide (*BCKDHA*) and tumor necrosis factor (*TNF-* α). We did not observe any significant differences between NPD and LPD (Figure 5.8). Similarly, these genes were insignificant between LPD and MD-LPD except genes encoding *CAT* and *TRX1* that were increased in MD-LPD relative to LPD ($p<0.05$).

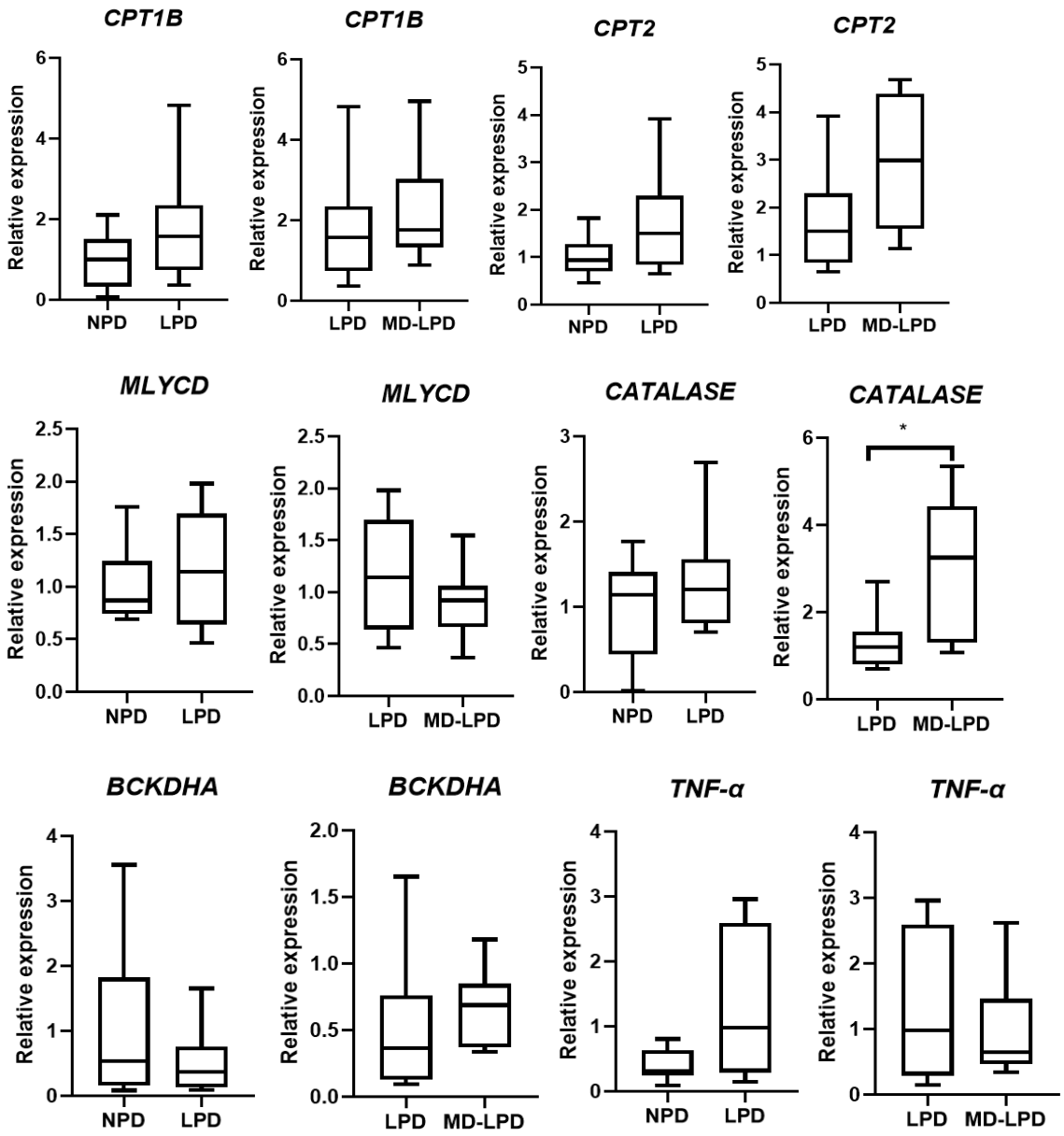
CPT1B
Relative expression
NPD
LPD
CPT1B
Relative expression
LPD
MD-LPD
CPT2
Relative expression
NPD
LPD
CPT2
Relative expression
LPD
MD-LPD
MLYCD
Relative expression
NPD
LPD
MLYCD
Relative expression
LPD
MD-LPD
CATALASE
Relative expression
NPD
LPD
CATALASE
*
Relative expression
LPD
MD-LPD
BCKDHA
Relative expression
NPD
LPD
BCKDHA
Relative expression
LPD
MD-LPD
TNF-α
Relative expression
NPD
LPD
TNF-α
Relative expression
LPD
MD-LPD

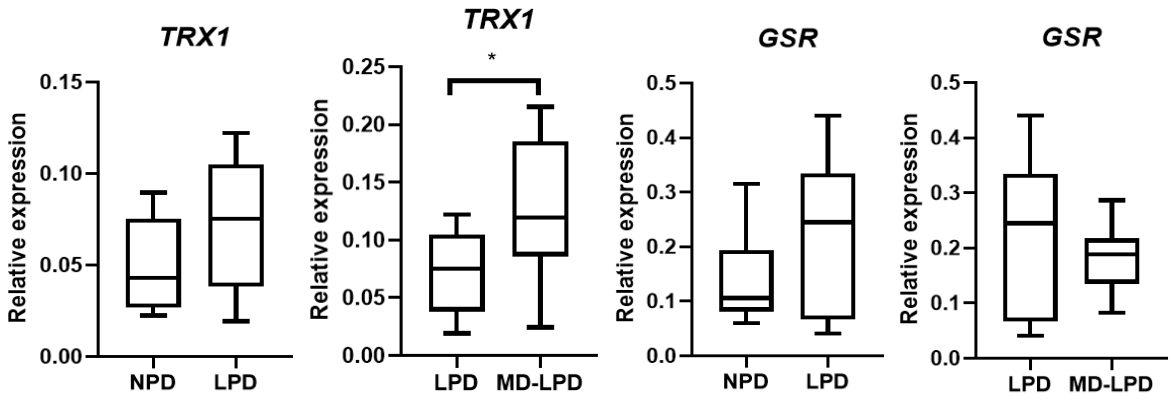

Figure 5.8: Effect of diet on mouse liver *CPT1B, CPT2, FADS1, MLYCD, CATALASE, BCKDHA, TNF-α, TRX1* and *GSR* mRNA expression (Aston LPD study).
Mean relative transcript expression of genes involved in hepatic mitochondrial, peroxisomal and inflammatory genes and genes related to lipid metabolism in mouse. Values are given as means ± S.E.M for n=8, *p<0.05 MD-LPD vs LPD

5.3.6 Low protein diet in which protein loss is adjusted across all dietary components (The Nottingham low protein diet study).

In order to further understand whether LPD-mediated metabolic phenotype was not solely by replacement of protein loss with extra carbohydrate, we designed a low protein dietary study where protein loss is compensated for by nutritional balance of all dietary components. Here, mice were fed with MD-NPD, MD-LPD and LPD for 8 weeks and we measured their body weight, blood insulin, serum and liver fatty acids as well as liver peroxisomal biogenesis markers.

5.3.6.1 Growth rate and glucose response to low protein diet fed mice

To evaluate the effect of protein restriction on body weight for 8 weeks, eight-week-old C57BL/6 males were housed singly and fed three different diets either control normal protein diet with methyl donor component (MD-NPD; n = 8), low protein with methyl donors(MD-LPD; n = 8) without methyl donors (LPD; n=8) *ad libitum* for 8 weeks (Table 2.1). There were no changes in body weight between MD-NPD and MD-LPD as well as between MD-LPD versus LPD from the start (0 week) until week 8 where the MD-LPD fed group gained significant weight compared to either LPD or NPD (figure 5b). Following weight

measurement, we performed glucose tolerance test to assess the mice metabolic response to glucose after 2 hours of glucose bolus administration. Here, no observable glucose intolerance was observed between MD-NPD and MD-LPD, neither was there any changes between MD-LPD and LPD (chapter 2, figure 2.3).

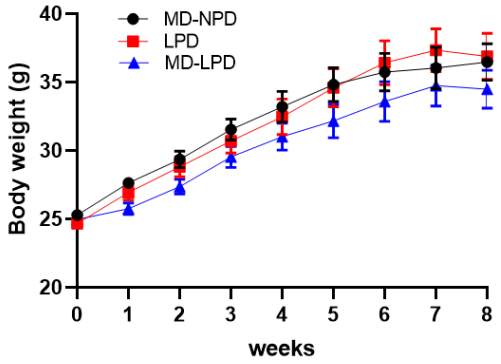

Figure 5b: Body weight changes with time (Nottingham LPD study).

Data represent mean ± SEM. Male mice with MD-NPD; 18% casein protein, LPD; 9% casein protein; n=8 and male mice fed with MD-LPD, n=8. There were no significant changes in weight between between MD-NPD vs MD-LPD or LPD vs MD-LPD from beginning (week 0) to the end of feeding (week 8)

5.3.6.2 Effect of low protein diet on serum fatty acids (Nottingham LPD study)

Here serum fatty acid profiles of fatty acids in MD-NPD, MD-LPD and LPD group following 8 weeks of feeding is presented in table 5.3.

Table 5.3: Fatty acid composition of serum in mice fed with low protein diet (Nottingham LPD study)

Group of FA	% of total serum FA	MD-NPD Median (min-max)	MD-LPD Median (min-max)	LPD Median (min-max)
ECFA	C14:0	2.01 (1.57-3.14)	1.85 (1.40-2.25)	1.74 (1.16-2.74)
	C16:0	30.93(28.10-33.68)	29.85(28.85-30.93)	30.02(27.46-33.17)
	C18:0	11.74 (9.75-25.79)	10.04(8.76-12.22)*	11.01 (9.86-15.55)
	Total ECFA	44.00(40.96-61.85)	42.18(40.14-43.65)	43.33(41.06-46.83)
OCFA	C15:0	0.26 (0.08-0.26)	0.08 (0.07-0.09)	0.13 (0.08-0.15)
	C17:0	0.18 (0.11-0.86)	0.16 (0.11-0.21)	0.20 (0.15-0.26)
	Total OCFA	0.32(0.21-1.12)	0.24(0.20-0.38)	0.34(0.24-0.40)
MUFA	C16:1	6.26 (3.17-8.83)	6.21 (3.26-7.39)	5.17 (2.29-6.91)
	C18:1	23.82(13.62-25.85)	24.67(22.88-26.37)	23.10(20.19-25.43)#
	Total MUFA	29.47(16.79-34.68)	31.02(26.92-33.69)	28.13(22.47-32.02)
PUFA	C18:2n6	23.67(19.78-29.56)	26.08(24.24-28.46)	26.88(24.06-29.98)
	C18:3n3	0.24 (0.19-0.26)	0.23(0.04-0.34)	0.27 (0.14-0.31)
	C20:4n6	0.53 (0.22-0.87)	0.59 (0.49-1.51)	0.69 (0.40-0.88)
	Total PUFA	24.57(20.24-30.32)	26.81(25.10-29.69)	27.94(25.08-30.84)
Activity ratio	C16:1/C16:0	0.20(0.09-0.29)	0.21(0.11-0.26)	0.17(0.07-0.25)
	C18:1/C18:0	2.05(0.53-2.65)	2.34(1.94-3.01)	2.12(1.30-2.34)#
	C20:4n6/C18:2n6	0.01(0.01-0.02)	0.01(0.01-0.02)	0.01(0.01-0.02)

*p<0.05, MD-NPD vs MD-LPD; #P<0.05, MD-LPD vs LPD

5.3.6.3 Effect of dietary protein intake on serum and liver total fatty acid concentrations in MD-NPD, MD-LPD and LPD fed mice

Similar to the Aston LPD study, we investigated the effect of dietary protein intake on total fatty acid concentration of mice after 8 weeks of feeding. As stated earlier, this new protein study differs from the Aston LPD study by the fact that protein loss is compensated for by all other dietary components not only carbohydrate as in the Aston low protein study. Here we observed no difference between MD-NPD vs MD-LPD or MD-LPD vs LPD in both serum and liver total fatty acid concentrations in mice (figure 5.9).

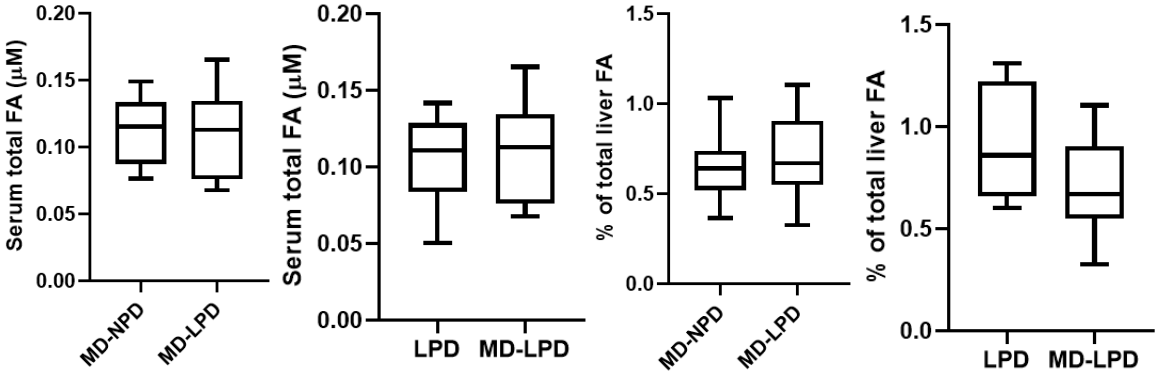

Figure 5.9: Effect of diet on total fatty acid concentration in serum and liver (Nottingham LPD study)
Total fatty acids were measured in the serum and liver of mice. Values are given as means ± SEM for n=8.

5.3.6.4 Effect of dietary protein on serum and liver ECFA, MUFA, PUFA and OCFA content in MD-NPD, MD-LPD and LPD fed mice

Here, we fed mice on normal protein with and low protein with or without methyl donor for 8 weeks and assess their effect on ECFA, OCFA, MUFA and PUFA in both serum and liver samples from these mice:

(a) ECFA

After 8 weeks of feeding, we observed that the sum of ECFAs in both serum and liver were not different between MD-NPD and MD-LPD or between MD-LPD and LPD (table 5.3). Moreover, analyses of individual ECFA showed a lower content of C18:0 in MD-LPD

compared to MD-NPD (data not shown). When MD-LPD was compared with LPD to assess the effect of methyl donor composition in the diet, the proportion of C18:0 in the serum was not different between these groups. Serum C14:0 and C16:0 contents were not different between groups. Similarly, proportion of C14:0, C16:0 and C18:0 in the liver was not different between groups (liver data not shown).

(b) OCFA

Here, when OCFA content in the serum and liver was analysed there was no observable changes between MD-NPD and MD-LPD. Similarly, no changes were observed when MD-LPD was compared to LPD (table 5.3). However, although insignificant, the trend of lower OCFA (including Specifically C15:0 and C17:0) in MD-LPD relative to MD-NPD were observed in both the serum and liver samples analysed (liver data not shown).

(c) MUFA

We analysed MUFA content in both serum and liver and observed no significant changes between groups (table 5.3 & 5.4). Individual MUFAs such as C16:1 and C18:1 proportion did not change in serum and liver when MD-NPD was compared to MD-LPD. The proportion of C18:1 was higher in the serum of MD-LPD compared LPD (figure 5.10).

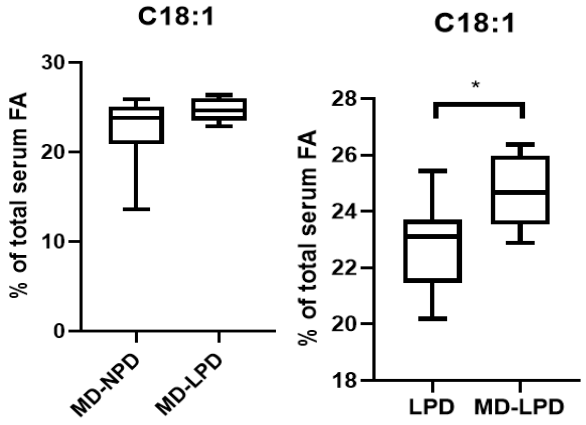

Figure 5.10 Effect of dietary protein intake on MUFA in the serum and liver (Nottingham LPD study)
Specific MUFAs was measured in the serum and liver of mice. Values are given as means ± SEM for n=8. *p<0.05 LPD vs MD-LPD

(d) PUFA

Here, when serum and liver content of PUFA were assessed, there was no difference between dietary groups (table 5.3). Similarly, individual PUFA C18:2n6, C18:3n3 and C20:4n6 levels in both serum and plasma were not different between MD-NPD and MD-LPD. In terms of methyl donor effect, we observed a higher proportion of C20:4n6 in MD-LPD compared to LPD in the liver after 8 weeks of feeding (figure 5.11).

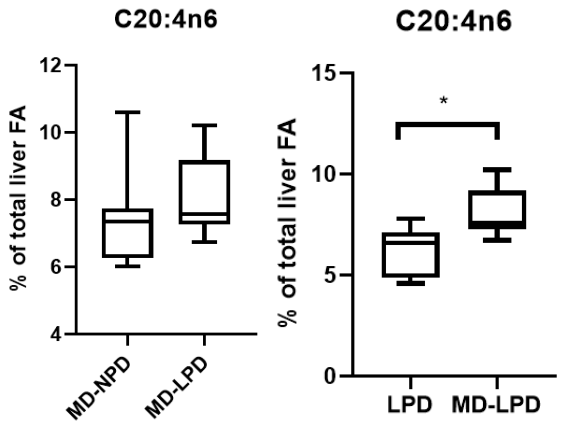

Figure 5.11 Effect of dietary protein intake on PUFA in the serum and liver (Nottingham LPD study)

Specific PUFAs was measured in the serum and liver of mice. Values are given as means ± SEM for n=8. *p<0.05 LPD vs MD-LPD

5.3.6.5 Low protein diet results in hepatic steatosis in mice (Nottingham LPD study)

After 8-week feeding regimen, we performed H&E staining to confirm the presence of lipid droplets in mice fed a low protein diet study where protein loss is compensated for by all dietary components and assessed whether this is improved in the presence of methyl donor supplementation. Brightfield microscopy imaging analyses revealed extensive hepatic steatosis developed in the livers of 9% LPD mice, however, accumulation of lipid droplets disappeared in MD-LPD mice (Figure 5.12). The data clearly indicate that mice in the 9% LPD group may have developed hepatic steatosis.

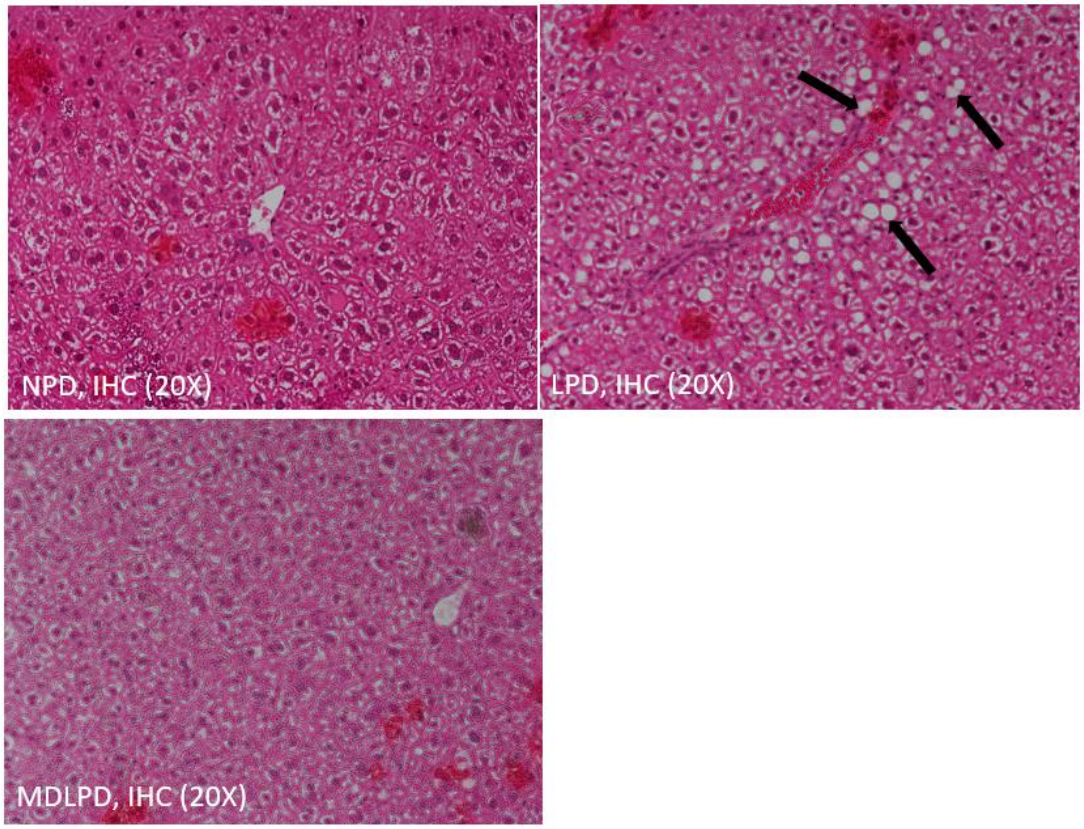

Figure 5.12: Low protein diet consumption leads to hepatic steatosis (Nottingham LPD study).

Representative normal protein diet group (MD-NPD) mouse, low protein diet group (LPD) mouse and representative MD-LPD mouse liver. Representative liver sections stained with haematoxylin and eosin (original magnification 20×). Arrows indicate large lipid droplets in LPD. Each image is a representative section from one mouse out of five different mice per dietary groups.

5.3.6.6 Immunohistochemistry staining shows increased PEX-14 staining in low protein fed mice (Nottingham LPD study).

To investigate peroxisome biogenesis and localization, IHC was performed on fixed liver tissues isolated from MD-NPD, MD-LPD and LPD mice using anti-PEX 14 and anti-catalase antibodies. Male mice liver sections obtained from LPD fed group were stained more strongly for PEX-14 than MD-LPD group, MD-NPD staining intensity was not different MD-LPD (figures 5.13).

A.

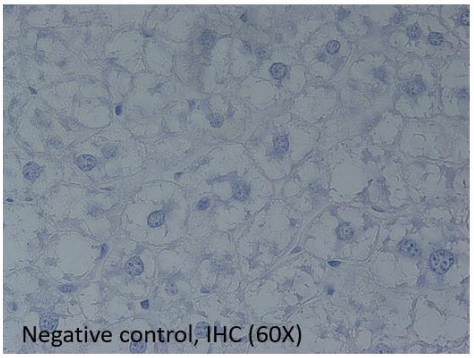
Negative control, IHC (60X)

B.

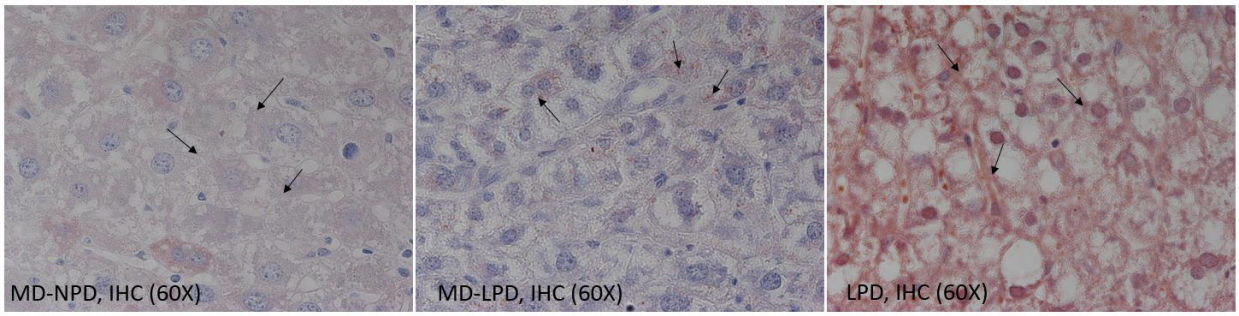
MD-NPD, IHC (60X)
MD-LPD, IHC (60X)
LPD, IHC (60X)

C.

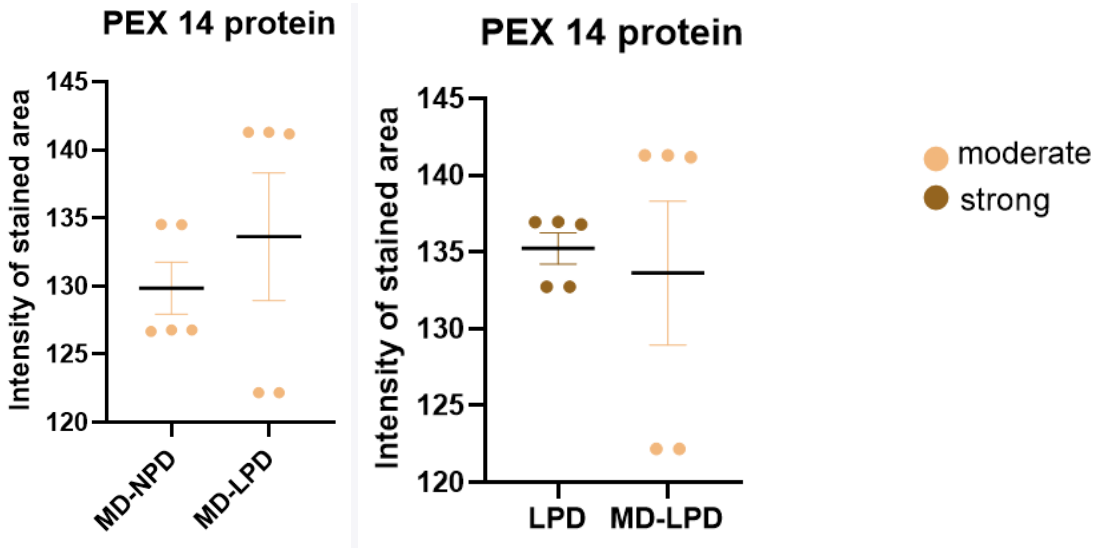

Figure 5.13: Immunostaining for PEX 14 in mouse liver from 8-week MD-NPD, MD-LPD and LPD mice (Nottingham LPD study)

IHC was performed on mouse liver obtained from MD-NPD, MD-LPD and LPD using anti-PEX 14 antibody. Arrows head indicate PEX 14 staining in liver cells. Negative control slide is unstained set-up by omitting primary antibody. Nuclei were counterstained with haematoxylin (original magnification 60×). A: Negative control; B. A representative section from one mouse liver out of five different mice per group; C: IHC analyses of PEX 14 intensity in arbitrary units.

Moreover, we observed no catalase expression in liver after NPD whereas LPD and MD-LPD both expressed catalase although the later was less immunostaining was less with methyl donor supplementation (figure 5.14).

A.

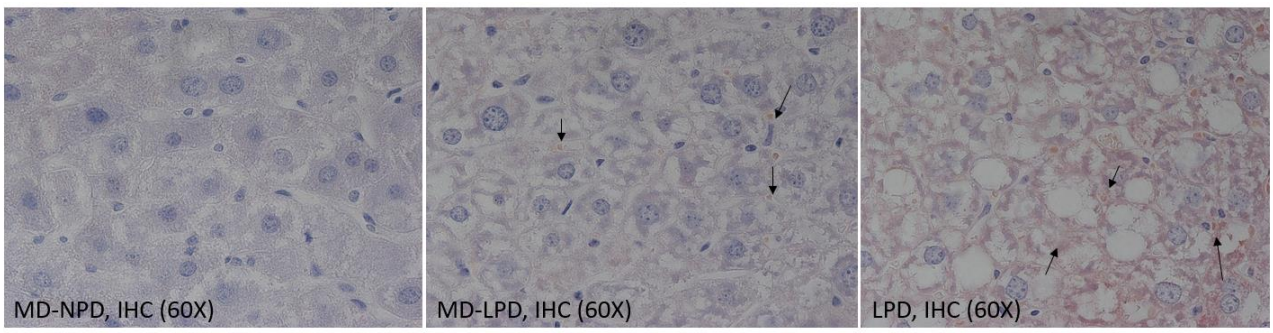

B.

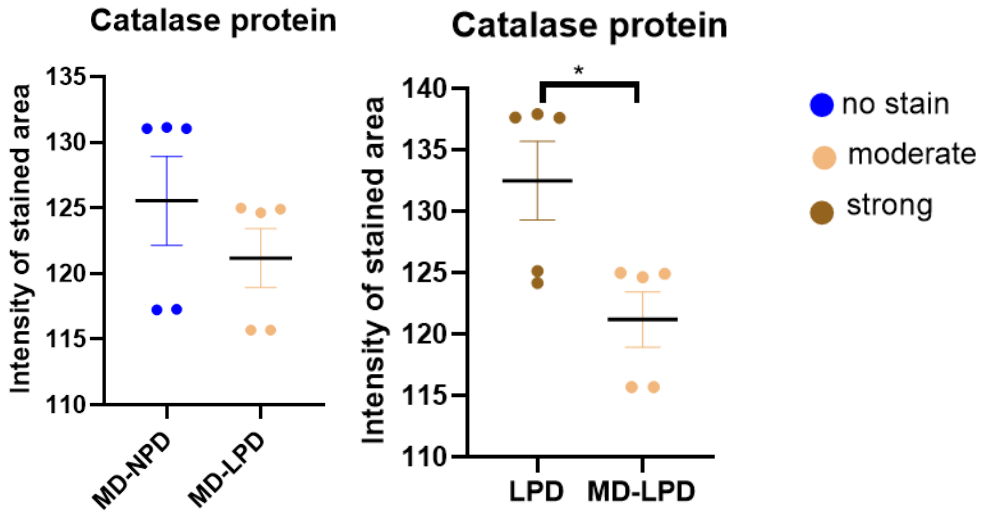

Figure 5.14: Immunostaining of catalase from 8-week MD-NPD, MD-LPD and LPD mice (Nottingham LPD study).

Immunohistochemistry was performed on mice liver obtained from NPD, LPD and MD-LPD using catalase antibody. Arrows head indicate catalase staining in liver cells. Negative control slide is unstained set-up by omitting primary antibody. Nuclei were counterstained with haematoxylin (blue colour). (original magnification 60×) A: A representative section from one mouse liver out of five different mice per group; B: IHC analyses of catalase stained intensity in arbitrary units (*P <0.05; LPD vs MD-LPD).

5.4 Discussion

5.4.1 Principal findings and low protein feeding

The present chapter describes the effects of two different low protein diets on the circulating and liver fatty acid levels in mice. In the first protein (Aston LPD) study, protein deficit was replaced with carbohydrate, therefore metabolic effect of this diet may largely be influenced by the increased carbohydrate rather than decreasing protein. Then a second protein (Nottingham LPD) study where protein loss was compensated for by nutrient balanced achieved from adjusting all dietary components. We hypothesized that if no effect of Nottingham LPD on lipid profile is observed then, the replacement of carbohydrate in Aston LPD would be driving lipid metabolism changes. Measurements were done on serum and liver samples from both models. In addition, this chapter examined the mechanisms underlying a low protein diet induced changes to fatty acid profile in mice using Aston LPD study. Using the Nottingham LPD model, we assessed the impact of a low protein diet on hepatic lipid accumulation as well as its effect on specific protein expressions involved in peroxisome biogenesis using immunohistochemistry approach. The study from the Aston LPD model shows that a low protein diet reduces the levels of total serum OCFA (and C17:0). Methyl donor supplementation in most cases suppressed the effect of this low protein diet on systemic metabolism of lipid. CD 36 gene was upregulated in the liver after a low protein diet intake. On the contrary, in the Nottingham LPD model, no changes in fatty acid profile including OCFA were observed in both serum and liver samples obtained from mice after 8 weeks on respective diets. Interestingly in Nottingham LPD, we observed lipid accumulation in the liver as well as enhanced protein expression of catalase and PEX-14, a marker of peroxisome biogenesis in the liver tissues. It can therefore be inferred that lipid accumulation in the liver may occur prior to systemic lipid changes.

5.4.1.1 Effect of a low protein diet on fatty acid composition (Aston LPD study)

There appears to be some support for the hypothesis that altered fatty acid homeostasis in the liver and serum are the main factors underlying NAFLD symptoms Cortez-Pinto et al (2006); Yoo et al. 2017; Perdomo et al (2019). The amount of hepatic lipids can be manipulated by the macronutrient composition of the diet by modulating liver fatty acid uptake, lipogenesis, fatty acid oxidation and triglyceride secretion Postic& Girard (2008).

A low protein diet intake can alter liver fat, Kwon et al (2012); Zutphen et al (2016). Despite evidence of low protein diet associated with fat accumulation in the liver, to the best of our knowledge no study has reported their effect on fatty acid profile may have implications in the pathogenesis of NAFLD. In this thesis, we have used a lipidomic approach to study the amounts and types of lipids that accumulate within the serum and liver in a low protein diet-associated NAFLD and provided some novel and interesting insights into the pathophysiology of the condition.

Here, the effects of a low protein diet on these fatty acid compositions in plasma and liver have been characterised in C57Bl/6 male mice.

5.4.1.2 LPD increases serum total fatty acid concentration but not in the liver

Previous studies have reported an increase in total lipid content in patients with NAFLD and NASH. This was explained to be driven by increased in triglyceride content, Puri et al (2007). Moreover, another study reported no significant differences between liver and plasma total lipid concentrations following a 20-day 9% low protein diet intake in female non-pregnant rats. In this thesis, using the Aston LPD model, we observed increase level of total lipid in the serum, however there was no significant difference between a low protein diet and normal protein diet groups in C57B/6 male mice fed a low protein diet for 7 weeks. It is possible that the increased serum concentration of total lipid we observe in our studies may be because of the long duration of feeding. However, this remains to be determined. Rietman reported that short term

increasing dietary protein in healthy subjects improved lipid metabolism, however, a high protein intake was related to a fatty liver, Rietman (2015). We also observed a decrease in serum total lipid when a low protein diet was supplemented with methyl donors. Methyl groups are important for many cellular functions including DNA methylation, phosphatidylcholine synthesis, and protein synthesis. The methyl group can directly be delivered by dietary methyl donors, including methionine, folate, betaine, and choline, Obeid (2013). The present study is in agreement with previous study that reported that dietary supplementation with methyl donors reduces fatty liver and modifies the fatty acid synthase DNA methylation profile in rats fed an obesogenic diet, Cordero et al (2013). ECFA palmitate (C16:0) and stearate (C18:0) are known to be substantially accumulated in NAFLD, Ogawa et al (2018); Nault et al (2013).

5.4.1.3 LPD intake produces differential effects on levels of even-chain saturated fatty acids

Even-chain saturated fatty acids have been studied widely and have shown to play a significant role on human health, Zheng et al (2017). In this thesis, using the Aston LPD model, we have shown a comprehensive report on serum and liver ECFA contents in mice fed a low protein diet. A low protein diet was associated with selective changes in the ECFA proportions in liver and serum. In particular, serum FA levels from animals fed a low protein diet were altered in identified specific ECFAs than FA profile in the liver. Importantly, we determined serum concentrations of the major specific ECFA in the serum and the liver- palmitic acid (C16:0) and stearic acid (C18:0) which play a significant role in the pathogenesis of NAFLD. We showed that 7 weeks of a low protein diet intake results in decrease concentration of capric acid (C10:0), myristc acid (C14:0), palmitic acid (C16:0). However, proportion of serum stearic acid (C18:0) and lignoceric acid (C24:0) were increased. These dietary protein effects were mostly reversed by methyl donors supplementation of the low protein diet. Interestingly, despite the markedly effects in circulation, we observed no significant difference in specific ECFA between dietary groups in the liver. One possible explanation for the different patterns

of a low protein diet-associated changes in lipid composition is selective incorporation of individual ECFA species into different hepatic lipid pools destined either for incorporation into tissue or mobilisation from the liver.

5.4.1.4 Serum OCFA in LPD fed mice

Odd chain saturated fatty acids have increasingly become important target in recent studies because of its consistent inverse association with metabolic diseases. For instance, both C15:0 and C17:0 have been negatively correlated with NAFLD and other metabolic diseases, Pfeuffer & Jaudszus (2016); Mika et al (2016); Yoo et al (2017); Jenkins et al (2017). In this thesis, using Aston LPD model, we determined serum and liver contents of C15:0 and C17:0. Moreover, we showed that dietary low protein intake decreased serum OCFA, however, the levels were improved when a low protein diet was supplemented with methyl donors. Although, a similar trend was observed in the livers, these were statistically insignificant. To best of our knowledge, we have for the first time determined a reduced OCFA profile in response to a low protein diet challenge in mice. This study further our understanding that a decrease in the contents of OCFA observed may be associated with increased NAFLD risk in subjects consuming a low protein diet. Due to the fact that the mice consumed a diet lacking C15:0 and C17:0 in both control and treatment groups suggests that these FAs can also be synthesized *de novo* via alpha oxidation pathway in mammals as proposed by previous studies, Crown et al (2015); Jenkins et al (2015).

5.4.1.5 Effect of LPD on MUFA levels

MUFAs are largely known to be associated with reduced risk of NAFLD, Kani et al (2014). In order to understand how a low protein diet affect MUFA, using Aston LPD model, we analysed serum and liver content of MUFA following seven weeks of feeding. We reported no significant effect of reduced protein intake on total MUFA between NPD and LPD in either liver or plasma tissues. In humans, studies by Bozzetto et al (2012), Ryan et al (2013), and Properzi et al (2018) showed reductions of intrahepatic tryglyceride (IHTG) when a high-MUFA Mediterranean diet was consumed. These studies are contrary to our current finding in mice study where no effect of dietary protein on MUFA was found. The difference may be in part due to physiological difference or different dietary design. However, in terms specific FA, we revealed that specific MUFA (C16:1) was decreased in the serum of mice fed a LPD compared to NPD. Specific MUFA C16:1 proportion was raised whilst C18:1 content was reduced by methyl donor supplementation of LPD suggesting methyl donor intake has a differing effect on individual MUFA. Further studies on the role of methyl donour on MUFA metabolism particularly, oleic acid would be beneficial since oleic acid is known to be protective against cardiometabolic diseases, Perdomo et al (2015).

5.4.1.6 Effect of LPD on PUFAs

Polyunsaturated fatty acids (PUFA), linoleic acid (LA, 18:2 n-6) is a short chain precursor that is converted into biologically active long chain (LC) PUFA such as arachidonic acid (20:4n-6), Jeyapal et al (2018). These LA fatty acids can only be sourced from diet, hence termed essential fatty acids, Russo (2009). Few clinical evidence available suggest that linoleic acid is associated with reduced IHTG. For instance, Bjermo et al (2012) demonstrated that a high intake of n-6 PUFA (10–15 % total energy from linoleic acid) in abdominally-obese men and women for 10 weeks reduced IHTG compared with a higher intake of SFA, in the context of

an isoenergetic diet. Moreover, in a double-blind follow-up study, Rosqvist et al (2014) observed that a similarly high intake of n-6 PUFA (10–15 % total energy) during hyperenergetic conditions for 7 weeks did not lead to accumulation of IHTAG, which was in contrast to the group consuming SFA.

In the present study, using the Aston LPD model, we observed no significant effect in total PUFA between LPD and NPD in analyses of serum and liver tissues obtained from the experimental mice. However, our finding is in line with previous animal study where a 9% low protein diet administered to non-pregnant female rats for 20 days had no effect on plasma and liver fatty acids, Burdge et al (2002). Supplementing LPD with methyl donors reduced the concentrations of PUFA compared LPD group. This suggests methyl donors may have the potential to reverse the deleterious effect of "bad" fats whilst increasing the levels of "good" fats.

Interestingly, analyses of individual n-6 PUFAs showed a significant increase in serum concentration of arachidonic acid (C20:4n6). Higher levels of arachidonic acid have been associated with pathogenesis of NAFLD, Juárez-Hernández et al (2015).

5.4.2.1 LPD induced CD36/FAT but no changes in FABP expressions in Aston LPD study

CD36 is a member of the class B scavenger receptor family with the ability to bind long-chain fatty acids, phospholipids, and collagen, Febbraio et al (2002). CD36 is less expressed in normal hepatocytes however evidence shows that its expression is increased with lipid-rich diets, hepatic steatosis, and NAFLD, Wilson et al (2015). Moreover, increased liver CD36 expression can cause increase in fatty acid uptake as well as triglyceride accumulation, in many mouse strains including C57BL/6, CD36 has been identified as the gene most correlated with fatty liver, Wilson et al (2015). Fatty acid binding proteins (FABPs) also play active role in long chain fatty acid (LCFA) uptake and metabolism in the liver, Atshaves

et al (2010). FABP1 knockdown in the liver was associated with a decrease in liver weight and hepatic triglyceride accumulation, Mukai et al (2017).

In this study, while a low protein diet does not significantly alter FABP1 and FABP3 expressions in the examined liver tissues, LPD treatment significantly elevated the expression of *CD36* in mice liver (Figure 3.8). This finding may support the role of this CD36 in the pathogenesis of non-alcoholic fatty liver disease. Previous findings have reported a role for *CD36* in hepatic fatty acid uptake and hepatic steatosis in rodents, Sheedfar et al (2014). To the best of our knowledge, we have for the first time demonstrated the involvement of a low protein diet in liver fat accumulation via altered *CD36* expression. Again, in our current studies we found no significant difference in expression in the *FABP1* and *FABP3*, however, there seemed to be a trend of increased expression of either *FABP1* and *FABP3* following a low protein fed in mice. A study showed that a high-carbohydrate diet increases *FABP1* content in the liver, Wang et al (2015).

5.4.2.2 LPD and specific fatty acid gene expression in Aston LPD model

Here, some specific genes involved in fatty acid metabolism were studied following changes in levels of fatty acids in the liver. The enzyme stearoyl-CoA desaturase-1 (*SCD1*) is predominantly expressed in the liver and catalyzes the synthesis of monounsaturated long-chain FAs from saturated fatty acyl-CoAs, Peter et al (2010). In this study, using the Aston LPD model, we observed no significant changes in hepatic *SCD1* expression in response to the 7-week low protein diet. Our finding is contrary to previous study where a 4% low protein reduced scd1 mRNA expression in liver of wild-type mice after 27 weeks of feeding regime, Laeger et al (2016). This discrepancy may reflect the short period of feeding (7 weeks) and slightly higher proportion of protein (9%w/w) used in our study. Endogenous synthesis of long chain polyunsaturated fatty acids (LCPUFAs) and the degree of unsaturation of the biological

membranes are largely dependent on the actions of fatty acid desaturases Fads1(Δ5-desaturase), Fads2 (Δ6-/Δ8-/Δ4-desaturase) and elongation of very long-chain fatty acids proteins (Elovls). FADS1 is the only mammalian Δ-5 fatty acid desaturase enzyme capable of producing the important polyunsaturated fatty acids (PUFAs) arachidonic acid (AA) and eicosapentaenoic acid (EPA) from substrates dihomo-γ-linolenic acid (DGLA) and eicosatetraenoic acid (ETA), respectively, Tanaka et al (2019). In this study, gene expression of both fads1 and fads2 were not altered after 7-weeks of low protein intake. This may reflect the observation of PUFA profiles in the liver and serum. Interestingly, supplementing low protein diet with methyl donors increased the expression *FADS1*. Previous studies have linked increased delta-5-desaturase (D5D) activity (*FADS1*) to be associated with a lower risk metabolic disease including NAFLD. Some studies have demonstrated a role of Hacl-1 in the biogenesis of odd chain saturated fatty acids (C15:0 and C17:0), Shibata et al (2012); Jenkins et al (2017); Kitamura et al (2017). This study therefore tested the effect of low protein diet on the expression of this gene in mice liver to understand if *HACL1* may be involved in reduction of liver OCFA observed. However, we did not observe any significant difference in expression between dietary groups. Knockout Hacl1 was associated with significantly lower levels of plasma and liver C17:0 concentrations, Jenkins et al (2017).

5.4.3 Effect of LPD on lipid oxidation and inflammatory genes using the Aston LPD model

There were no significant changes in gene expression encoding enzymes involved in mitochondrial fatty acid transport (*CPT1* and *CPT2*) in the livers of mice with a low protein diet. Our finding is in contrast to previous study that reported that a decreased level of hepatic *CPT1A* mRNA and *CPT2* mRNA, and development of fatty liver in growing rats fed low protein diets, Kuwahata et al (2011). The difference observation from the current study may be attributed to the different experimental study design. Levels of cpt1a protein change during development and in response to nutritional status, Kuwahata et al (2011.

In the same time, another important gene, malonyl CoA decarboxylase (*MLYCD*) that promotes oxidation in the peroxisome was not altered in liver tissue of mice with protein restriction in our study. *MLYCD* overexpression is thought to decrease circulating free fatty acid (FFA) and liver triglyceride content, An et al (2004). So far studies on impact of diet on mlycd expression in the liver are rare and would require further study. Analyses of gene expression of hepatic *BCKDHA* in mice with protein restriction showed no significant difference compared to control mice in our current study. Branched-chain α-keto acid dehydrogenase (BCKDH) complex catalyses the irreversible oxidative decarboxylation of branched-chain α-keto acids, Webb et al (2019). A previous study in pigs show that a 14% crude protein diet increased hepatic metabolism of branched-chain amino acid, aromatic amino acid and gene expressions of *BCKDHA* than a 20% crude protein diet, Li et al (2015). *BCKDHA* complex gene was shown to decrease in expression of NASH as well as decreased in expression of BCKDH complex inhibiting kinase, BCKDK gene Lake et al (2015). Moreover, when catalase expression in the liver was assessed in mice with protein malnutrition, there was no changes from those on normal diet. Catalase has been reported to play a role in lipid dysfunction, Heit et al (2017). Catalase deficiency in mice has been reported to increase the likelihood of fatty liver, Heit et al (2017). The fact that arachidonic acid concentration in the serum was increased in LPD fed mice, we measured *TNF*- α mRNA to assess inflammation in the liver of these mice. We observed no changes in expression of *TNF*- α. Our finding is in line with previous study where liver mRNA expression of *TNF*-α did not show significant changes of rats placed on low-protein (protein-energy density of 0.012 MJ/60 ml) compared to controls receiving normal energy and protein energy density of 0.047 MJ/60 ml, Raina et al (2014). *TNF*-α trimer initiates inflammatory and immunoregulatory responses by binding to two distinct cell surface receptors of 55 kDa, (*TNFR-I*) and 75 kDa (*TNFR-II*) Tartaglia & Goeddel (1992). However, in Raina et al findings they observed an increase in *TNF*-α, *TNFR-I*, and *TNFR-II* protein expressions in

the liver of these rats placed on LP compared with control. These means that nutritional manipulations alter the differential expression of protein and mRNA of *TNF*-α and its receptors in organs and muscle, Raina et al (2014). Furthermore, there were no changes in expression of *TRX1* mRNA and *GSR* mRNA expression in LPD fed mice relative to NPD, however, supplementation of LPD with methyl donor increased *TRX1* mRNA and *GSR* mRNA expression suggesting methyl donor protection against LPD-induced oxidative stress.

5.4.4 No effect of low protein diet on systemic fatty acid profile and GTT in the Nottingham LPD study

Having observed changes in fatty acid profile in the liver and serum following the Aston LPD study, we set up the Nottingham LPD study to evaluate the real contribution of decreasing dietary protein. The experimental set up and conditions were similar to the Aston's LPD study. However, in this study loss of protein in MD-LPD or LPD were balanced by adjusting the nutrient composition of all nutrients including fibre, fat, minerals etc. In evaluating the effect of this model on serum and liver FA concentrations we observed no significant difference between MD-NPD and MD-LPD as well as no methyl donor effect on this model demonstrated by no changes in MD-LPD compared to LPD group. Analyses of total ECFA (except specifically C18:0), MUFA, PUFA and OCFA showed no changes in proportion between MD-NPD and MD-LPD in both serum and liver samples. These were not surprised as measurement of growth rate and glucose tolerance of these mice showed no effect. As we observed potential effect of methyl donor supplementation on poor diet in the Aston LPD study, in this dietary protein (Nottingham LPD) study we observed that methyl donor rich diet increased the proportion of serum C18:1 and liver C20:4n6. This suggests that methyl donor has potential to ameliorate the metabolic effect of protein malnutrition.

5.4.5 LPD induces hepatic steatosis confirmed by H&E analyses using the Nottingham LPD

Having observed a clear difference in lipid profile between Aston LPD and Nottingham LPD and further observed no significant metabolic effect of Nottingham LPD, we explored further the effect of Nottingham LPD on hepatic lipid accumulation. Our current study shows that this dietary protein restriction induces a fatty liver in mice. Similar findings have been reported in other animal studies. A study in young male rhesus monkeys for 9 weeks showed livers of the protein-deficient animals to be grossly fatty, Kumar et al (1972). Another study found that protein restriction (8% by body weight) induced hepatic steatosis (fatty liver) after examining liver sections with H&E and oil red O staining in a 4-week fed rats, Kang et al (2011). Our study together with others strongly support the hypothesis that a low protein diet is a key driver of NAFLD. Clinically, severe malnutrition in young children have been associated with signs of hepatic dysfunction such as steatosis, van Zutphen et al (2016).

5.4.6 LPD and peroxisomal biogenesis and localization in the Nottingham LPD study

Peroxisomes and mitochondria dysfunction are implicated in various disorders affecting the liver including non-alcoholic fatty liver disease, Begriche et al (2013). Peroxisomes are important for bile acid synthesis, β-oxidation of very long chain fatty acids (VLCFA), α-oxidation of methyl-branched phytanic acid and the biosynthesis of ether phospholipid (plasmalogen), Argyriou et al (2016); van Zutphen et al (2016). Peroxisome biogenesis involves the different processes required to assemble and maintain functional peroxisomes and this include matrix protein import, synthesis of new organelles, and fission of existing organelles, Argyriou et al (2016). Catalase is considered to be an important antioxidant enzyme in peroxisome and used as a marker of peroxisome function, Antonenkov et al (2010). Aside catalase and ABCD3 being frequently used as markers for the localization of peroxisomes in morphological experiments, recent study has identified peroxisome biogenesis protein PEX14

as optimal biomarker for identification and localization of peroxisomes in tissues and species, Grant et al (2013). The role of peroxisome biogenesis PEX14 and catalase in metabolic phenotype is not well defined. In this thesis, we observed increased IHC staining of peroxisomal membrane protein PEX14 in the liver of mice with protein restriction. Moreover, catalase expressions were detected in LPD and MD-LPD but no expression in MD-NPD in mice livers. This observation of higher catalase staining in MD-LPD group in this Nottingham LPD study is in line with our earlier observation of higher mRNA expression of *CATALASE* in MD-LPD mice of the Aston LPD study (figure 5.8). This means methyl donor may play a role in catalase regulation in the liver. Our finding is in contrast with previous observation where there was decreased immunofluorescence staining of peroxisomal membrane protein PEX14 and catalase after 4 weeks of LPD in rats, van Zutphen et al (2016). This difference is possibly likely to be due to differences in dietary design.

5.5 Conclusion

The current study shows that a low protein diet (Aston LPD study) where protein loss has been replaced with only carbohydrate, decreases the levels of OCFAs in the serum and the liver, with this effect being reversed in most cases with the supplementation of methyl donors. However, a low protein diet (Nottingham LPD study) with protein loss replaced by adjusting all nutrients composition to achieve a balance showed no effect on OCFA in the serum and the liver. Additionally, evaluation of liver histology revealed increased lipid accumulation in the liver after a low protein diet treatment despite no changes in systemic lipid profile. This means liver lipid accumulation may occur before any systemic metabolic changes. In the Nottingham LPD, evaluation of the protein markers showed increased expression of catalase and PEX-14 in the liver. Given that peroxisomes and catalase overexpression sometimes is associated with fatty liver Marcolin et al (2011), the increased of these two protein targets by a low protein diet indicates that the long-term effects of this diet could potentially impair liver function. In the

Aston LPD, gene expression study revealed an upregulation of *CD 36* gene which is known to be involved in fatty acid uptake into the cell. With ethical challenges involved in clinical studies to evaluate the impact of low protein diet on OCFA metabolism and understand whether dietary effect of LPD is due to protein deficiency rather than carbohydrate quality or quantity, this animal model study provides an important insight to explain the mechanism underlying the lower OCFA concentration in NAFLD patients. This is particularly important since proportion of OCFA in the mice after dietary regimen was less than 1% similar to what has been reported in few epidemiological case-control studies of metabolic disorders including NAFLD, Mika et al (2016); Jenkins et al (2017). Further investigations of these molecular changes may help in translating these findings in humans.

Chapter 6

6.0 General Discussion and Future work

6.1 General discussion

Non-alcoholic fatty liver disease (NAFLD) remains the most frequently occurring chronic liver disease globally, Younossi et al (2016). In general, abnormalities in *de novo* lipogenesis of fatty acids in hepatocytes, the retention of lipids due to impaired hepatocyte apolipoprotein secretion, impaired oxidative pathway, dyslipidemia, insulin resistance as well as changes in environmental factors (including diet and gut microbiota) have been implicated in the pathophysiology of NAFLD, Kneeman et al (2012); Hartmann & Schnabl (2018). Impairment of mitochondria and peroxisome biogenesis and functions affect lipid metabolism and storage in the liver, Nassir & Ibdah (2014); Gusdon et al (2014); van Zutphen et al (2016). In addition, several studies have suggested that changes in the gut microbiota diversity and functions contribute to NAFLD pathology, Everard et al (2013); Zhu et al (2015); Houghton et al (2016). Moreover, poor diet may cause NAFLD possibly influencing the gut microbiota and hepatic metabolism of lipid, Velázquez et al (2019). Indeed, observations from dietary studies indicate that dietary patterns including high fat diets and low protein diets have become major risk factors for pathogenesis of NAFLD, Kumar et al (1972); van Zutphen et al (2016); Jensen et al (2018). Therefore, this thesis explored the effect of varying dietary fat or dietary protein availability on lipid metabolism with particular interest on OCFA whose changes via peroxisomal biogenesis and/or the gut microbiota is thought to mediate the pathogenesis of NAFLD. Combining all evidence from dietary fat and dietary protein, table 6.1 highlights the similarities and differences in response to poor quality diet.

Table 6.1: Differences and similarities between poor diets and metabolic outcomes.

Diet	**High fat**	**High fat**	**High fat**	**Aston LPD**	**Nottingham LPD**
Condition	SPF	Normal husbandry	Normal husbandry	Normal husbandry	Normal husbandry
Feeding duration (weeks)	4	4	12	7	8
Dietary composition	60% fat, 20% carbohydrate and 20% protein per kcal%	60% fat, 20% carbohydrate and 20% protein per kcal%	60% fat, 20% carbohydrate and 20% protein per kcal%	10% fat, 81% carbohydrate and 9% protein per kcal%	22.5% fat, 68.5 carbohydrate and 9% protein per kcal%
Tissues analysed	Serum and liver	Serum	Serum	Serum and liver	Serum
Even-chain SFA	No effect in serum or liver	Increased in serum	Increased in serum	No effect in serum/liver	No effect
MUFA	Increased in serum and liver	Decreased in serum	Decreased in serum	No effect in serum/liver	No effect
OCFA	Decreased in serum and liver	Decreased in serum	Decreased in serum	Decreased in serum but no effect in liver	No effect
PUFA	Decreased in serum and liver	No effect in serum	Increased in serum	No effect in serum/liver	No effect
Fatty acid transport and synthesis pathway	Decrease in hepatic expression of *HACL1*, *ELOVL 6*, *SCD1*, *FADS2* but no change in *CD 36*, *FABP3*, *FADS1*, *BCKDHA*	-	-	Upregulation of hepatic *CD 36* gene but no change in *HACL1*, *FABP3*, *SCD1*, *FADS2*, *BCKDHA*	-
Peroxisome biogenesis (PEX14 expression)	Higher	-	-	-	Higher
Redox and inflammation	No change in expression of *GSR*, *TRX*, *TNF-α* Increased catalase immunostain	-	-	No change in expression of *GSR*, *TRX*, *TNF-* α	- Increased catalase immunostain
Confirmation of fatty liver	Yes	-	-	-	Yes

As summarized above in table 6.1, in this thesis, 4-week old C57BL/6 male mice were HFD for four weeks at SPF facility. Furthermore, other mice were fed HFD for 4-or-12 weeks in a conventional animal house. Following dietary feeding, serum and liver samples were analysed

for fatty acid profiles. In Chapter 3 of this thesis, we found that in both short- and long-term high fat feeding in a normal husbandry environment, total (even-chain) SFA in the serum was increased due to an accumulation of C18:0 only whilst serum total OCFA and total MUFA were decreased. However, whilst there was no change in total PUFA in HFD fed mice relative to CD in short term fat feeding, serum total PUFA proportion increased in the long term. In the same vein, mice fed HFD in an SPF environment showed decreased serum total OCFA (and specifically OCFA C15:0), total PUFA (and specifically PUFA C18:3n3) and increased total MUFA (specifically C18:1n9) but no change in total (even-chain) SFA. Similarly, in the liver of HFD-fed SPF mice showed a decrease in total OCFA (and specific OCFA C15:0 & C17:0), total PUFA (and specific PUFA C18:3n3) and increased total MUFA (specifically C16:1) with no effect on total SFA. From the findings reported in this chapter, it can be concluded that OCFA was consistently decreased in response to all HFD. In clinical epidemiology study an inverse association between OCFA and NAFLD risk has been reported. Unlike OCFA, some findings of other classes of fatty acids such as MUFA and PUFA changes in mice were not consistent with studies in human.

Given that changes in fatty acid composition were observed in the serum and liver of HFD-fed SPF mice relative to control, we sought to understand if these changes were related to changes in lipogenic pathways in the liver. We observed no significant changes to genes encoding *CD 36*, *FABP3*, *PCCA* and *BCKDHA* in HFD-fed SPF mice compared to control. However, gene expression of *ELOVL6, SCD1* and *FADS2* were down-regulated in HFD mice compared to control after 4 weeks of feeding. *HACL-1* pathway which is thought to be involved in OCFA metabolism was also down-regulated which suggest that it may mediate the lower OCFA concentrations in NAFLD.

Some studies have shown that a high dietary PUFA resulted in down-regulation of genes involved in lipogenesis pathway (particularly, acetyl coenzyme A carboxylase (*ACC*), fatty

acid synthase (*FAS*) and stearoyl CoA desaturase (*SCD1*)), Sampath & Ntambi (2005); Salter & Tarling (2007); Jump (2008). However, in our current study, we reported either no changes or low levels of PUFA in either the serum or liver of HFD-fed SPF mice and this could account for the observation of no changes in many of the lipogenic pathways. It is also possible these PUFAs have been taken up by the cells to regulate transcription factors such as SREBP that control lipid metabolism. Moreover, the observation of down-regulation of expression of gene for *ELOVL 6* partially reaffirms the direction of the lipogenic mechanism in the high fat fed mice. It is reported that dietary polyunsaturated fatty acids can cause a profound suppression of *ELOVL6* expression and this may play important role in *de novo* synthesis of long-chain saturated and monounsaturated fatty acids in conjunction with *FAS* and *SCD1,* Matsuzaka et al (2002); Matsuzaka et al (2009).

Again, in chapter 3, another significant finding was the observation of increased expression of catalase and PEX14 proteins (markers of peroxisome localization) in HFD-SPF fed mice compared to control. The alpha oxidation pathway involving *HACL1* is known to occur in the peroxisome, therefore changes in structure or biogenesis of this organelle may affect the regulation of OCFA. However, the fact that *HACL1* mRNA decreased whilst peroxisome markers (PEX14 and catalase protein) increased suggest that metabolic enzyme regulation may not be associated with peroxisome biogenesis.

Having observed the changes in OCFA in response to HFD, in chapter 4, we sought to investigate whether the effect of HFD on OCFA was related to changes in gut microbiota involved in propionate synthesis which is a precursor for long chain OCFA biosynthesis. Here, we reported an increased abundance of propionate-producing gut bacteria taxa of Lachnospiraceae and Clostridiales in HFD fed mice compared to control suggesting that changes in these bacteria taxa may affect propionate levels which in turn may be the underlying factor resulting in the OCFA alterations observed in the HFD studies reported in Chapter 3,

thereby contributing to the development of NAFLD. In previous clinical study, at the genus levels abundance of *Ruminococcus*, *Blautia*, and *Dorea* were increased in NASH patients, Grabherr et al (2019). In our current study, *Blautia* was also elevated in abundance in HFD-fed SPF mice.

Following our investigations on the impact of dietary fat on OCFA and other lipid metabolism, we set to understand how dietary protein too influence these same parameters in mice. In order to achieve this, in chapter 5, two low protein diet models that differed in carbohydrate content and composition were studied to understand the role of dietary protein in lipid metabolism. The purpose of the second low protein diet study (Nottingham LPD) was to address the high carbohydrate confounder in the first dietary protein study (Aston LPD). The findings in Chapter 5 show that feeding C57BL/6 male mice with carbohydrate-rich LPD (Aston LPD) for 7 weeks resulted in significant decreased serum total OCFA (and specific OCFA C17:0), no changes in serum total even-chain SFA (but decreased in specific SFA C10:0, C14:0, C16:0), no changes in serum total MUFA (but decreased in specific MUFA C16:1) and no effect on serum total PUFA (but increased in specific PUFA C20:4 and decreased PUFA C22:2) compared to NPD fed mice. On the otherhand feeding C57BL/6 male mice with relatively reduced carbohydrate-based LPD for 8 weeks resulted in no effect in serum and liver OCFA, MUFA, ECFA (except decreased C18:0) and PUFA. The fact that OCFA was reduced in carbohydrate rich-LPD diet reinforce the potential impact of suboptimal nutrition in OCFA metabolism. It is interesting to note that when the carbohydrate confounder was controlled for in the Nottingham LPD study, we observed no effect of dietary protein on OCFA. However, this Nottingham LPD showed hepatic lipid accumulation despite no effect on fatty acid profile suggesting protein malnutrition play a role in the development of NAFLD and that metabolic changes and fat storage occur before systemic lipid alteration.

Also, in chapter 5, the effect of methyl donors on systemic lipid changes were also tested using both the Aston LPD and Nottingham LPD models. In the Aston LPD model where LPD increased or decreased a specific FA, methyl donor supplementation of the low protein (MD-LPD) reversed that. For instance, decreased C10:0, C14:0 etc in LPD group were increased in MD-LPD group whereas increased C24:0, C18:1, C20:4 etc by LPD were decreased in MD-LPD group. These alteration patterns in the serum were also observed in the liver except that most of these were statistically insignificant. Methyl donor improved antioxidant gene expression in the liver of Aston LPD model.

Following the Nottingham LPD, despite methyl donor generally showing mild effect on systemic lipid profile, we observed few changes in specific FAs such as increase in liver C18:1 and serum C18:0 in MD-LPD. Combining the evidence from the two LPD models demonstrates the potential role of methyl donors in lipid metabolism and oxidative stress.

In trying to understand the mechanism underlying changes in fatty levels in response to LPD, in chapter 5 there was increased hepatic expression of gene encoding *CD36* enzyme in LPD mice relative to NPD and down-regulated in MD-LPD mice compared to LPD in the Aston LPD model. However, we observed no changes in *HACL1* expression in the Aston LPD model as reported in the HFD-SPF model which shows that any contribution to changes in systemic OCFA may differ according to diet and this warrants further studies. Finally, similar to our HFD-SPF model, LPD mice showed higher catalase and PEX14 was reported.

Despite significant revelation of the major influence of suboptimal nutrition on OCFA and also the fact that changes to this class of fatty acids may be in part as results of altered specific gut microbiota and changes in peroxisomal biogenesis thereby resulting in NAFLD. This study suffers from some limitations. Although experimental HFD and to lesser extent LPD C57BL/6 are well-established and validated animal model for evaluating the development of metabolic diseases including NAFLD, Jump et al (2018), there are limitations in extrapolating findings

from experimental animal models and to humans. For instance, there were contrary observation of changes in certain subclasses of lipids such as PUFA, MUFA which are different from those reported in human studies. Again, in our HFD model studies, there was carbohydrate confounder which was not controlled for and this may contribute to the changes in lipid metabolism including OCFA or gut microbiota. This makes it difficult to attribute the molecular changes in HFD in chapters 3 and 4 to dietary fat alone. Moreover, other limitations of the study include small sample sizes, short and non-uniform durations within either HFD models or LPD models. Therefore, we suggest future studies should take these into consideration to allow fair comparison between models.

In summary this thesis helps to improve understanding of why people consuming suboptimal diets may have an increased risk for NAFLD disease and suggests that improving diet, targeting lipid accumulation, peroxisomal biogenesis and gut microbiota may slow down NAFLD progression.

6.2 Future work

The findings in this thesis indicate that high dietary fat or low dietary protein have an effect on liver fat accumulation and impair lipid metabolism. The current studies werer mainly focused on short term dietary effects; future research on dietary fat/protein should focus on more long-term consequences of fat/protein intake in relation to lipid metabolism and address the molecular mechanisms. We would suggest, a strictly controlled dietary study should be performed for at least 3 months. This time-frame is necessary to control for possible confounding factors such as age, duration of feeding etc, which might affect the results from long-term observational studies.

Insulin resistance is one of the hallmarks of NAFLD, Utzschneider & Kahn (2006) and should be measured in future study. In this thesis, we focused on measuring total fatty acids, future

studies can explore on the effect of dietary fat/protein on specific lipid sub-classes including triglyceride, phospholipid, oxysterol esters etc. One possible mechanism underlying the low protein diet associated with hepatic lipid accumulation was up-regulation of *CD 36* enzyme in mice as reported in this thesis. This would benefit from in-vitro mechanistic validation in future dietary protein study.

Moreover, in this thesis, we reported decreased concentration of OCFA in four dietary challenge studies as well as down-regulation of *HACL1*(gene related to OCFA metabolism) in high fat diet fed mice. We suggest carrying out a dietary intervention study using major dietary source of OCFA such as dietary fibre, Weitkunat et al (2017)) would be useful to understand if these fatty acid profiles will change. Future molecular studies exploring transcriptional factors eg ChREBP, SREBP1 and Nrf2 response to dietary fat/protein challenged would provide further explanation to our current findings.

"Metagenomic" analyses (16S rRNA sequencing) was not performed for the protein study for lack of time and funding. As we discovered novel microbiota biomarkers relating to NAFLD in our high fat diet study. It would also be good in a future study to perform a comprehensive microbiota analyses to understand the effect of dietary protein on the gut microbiota to identify more NAFLD related microbiota changes. Additionally, a study to transplant beneficial bacterial lost due to poor quality of diet (high dietary fat or low dietary protein) can be considered to assess their effect on metabolic health.

7.0 References

Abedi E, Sahari MA. Long-chain polyunsaturated fatty acid sources and evaluation of their nutritional and functional properties. Food science & nutrition. 2014 Sep;2(5):443-63.

Adamska A, Rutkowska J. Odd-and branched-chain fatty acids in milk fat--characteristic and health properties. Postepy higieny medycyny doswiadczalnej (Online). 2014 Aug; 68:998-1007.

Alcock J, Maley CC, Aktipis CA. Is eating behavior manipulated by the gastrointestinal microbiota? Evolutionary pressures and potential mechanisms. Bioessays. 2014 Oct;36(10):940-9.

Alexandratos N. The Mediterranean diet in a world context. Public health nutrition. 2006 Feb;9(1a):111-7.

Allin KH, Nielsen T, Pedersen O. Mechanisms in endocrinology: gut microbiota in patients with type 2 diabetes mellitus. European journal of endocrinology. 2015 Apr 1;172(4): R167-77.

Amirkhizi F, Siassi F, Minaie S, Djalali M, Rahimi A, Chamari M. Is obesity associated with increased plasma lipid peroxidation and oxidative stress in women? Arya Atherosclerosis. 2010 Dec 8;2(4).

An J, Muoio DM, Shiota M, Fujimoto Y, Cline GW, Shulman GI, Koves TR, Stevens R, Millington D, Newgard CB. Hepatic expression of malonyl-CoA decarboxylase reverses muscle, liver and whole-animal insulin resistance. Nature medicine. 2004 Mar;10(3):268.

Ander BP, Dupasquier CM, Prociuk MA, Pierce GN. Polyunsaturated fatty acids and their effects on cardiovascular disease. Experimental & Clinical Cardiology. 2003;8(4):164.

Annalisa N, Alessio T, Claudette TD, Erald V, Antonino DL, Nicola DD. Gut microbioma population: an indicator really sensible to any change in age, diet, metabolic syndrome, and life-style. Mediators of inflammation. 2014;2014.

Anstee QM, Targher G, Day CP. Progression of NAFLD to diabetes mellitus, cardiovascular disease or cirrhosis. Nature reviews Gastroenterology & hepatology. 2013 Jun;10(6):330.

Antonenkov VD, Grunau S, Ohlmeier S, Hiltunen JK. Peroxisomes are oxidative organelles. Antioxidants & redox signaling. 2010 Aug 15;13(4):525-37.

Ara N, Nakkanong K, Lv W, Yang J, Hu Z, Zhang M. Antioxidant enzymatic activities and gene expression associated with heat tolerance in the stems and roots of two cucurbit species ("Cucurbita maxima" and "Cucurbita moschata") and their interspecific inbred line "Maxchata". International journal of molecular sciences. 2013 Dec;14(12):24008-28.

Araújo AR, Rosso N, Bedogni G, Tiribelli C, Bellentani S. Global epidemiology of non-alcoholic fatty liver disease/non-alcoholic steatohepatitis: What we need in the future. Liver International. 2018 Feb; 38:47-51.

Araya J, Rodrigo R, Videla LA, Thielemann L, Orellana M, Pettinelli P, Poniachik J. Increase in long-chain polyunsaturated fatty acid n− 6/n− 3 ratio in relation to hepatic steatosis in patients with non-alcoholic fatty liver disease. Clinical science. 2004 Jun 1;106(6):635-43.

Araya J, Rodrigo R, Videla LA, Thielemann L, Orellana M, Pettinelli P, Poniachik J. Increase in long-chain polyunsaturated fatty acid n− 6/n− 3 ratio in relation to hepatic steatosis in patients with non-alcoholic fatty liver disease. Clinical science. 2004 Jun 1;106(6):635-43.

Argyriou C, D'Agostino MD, Braverman N. Peroxisome biogenesis disorders. Translational science of rare diseases. 2016;1(2):111.

Aristizabal J, González-Zapata L, Estrada-Restrepo A, Monsalve-Alvarez J, Restrepo-Mesa S, Gaitán D. Concentrations of plasma free palmitoleic and dihomo-gamma linoleic fatty acids are higher in children with abdominal obesity. Nutrients. 2018 Jan;10(1):31.

Arner P. The adipocyte in insulin resistance: key molecules and the impact of the thiazolidinediones. Trends in Endocrinology & Metabolism. 2003 Apr 1;14(3):137-45.

Asrih M, Jornayvaz FR. Inflammation as a potential link between nonalcoholic fatty liver disease and insulin resistance. The Journal of endocrinology. 2013 Sep;218(3): R25-36.

Atkinson LL, Kelly SE, Russell JC, Bar-Tana J, Lopaschuk GD. MEDICA 16 inhibits hepatic acetyl-CoA carboxylase and reduces plasma triacylglycerol levels in insulin-resistant JCR: LA-cp rats. Diabetes. 2002 May 1;51(5):1548-55.

Atshaves BP, Martin GG, Hostetler HA, McIntosh AL, Kier AB, Schroeder F. Liver fatty acid-binding protein and obesity. The Journal of nutritional biochemistry. 2010 Nov 1;21(11):1015-32.

Azad MB, Konya T, Maughan H, Guttman DS, Field CJ, Chari RS, Sears MR, Becker AB, Scott JA, Kozyrskyj AL. Gut microbiota of healthy Canadian infants: profiles by mode of delivery and infant diet at 4 months. Cmaj. 2013 Mar 19;185(5):385-94.

B. Krachler, M. Norberg, J.W. Eriksson, G. Hallmans, I. Johansson, B. Vessby *et al.* Fatty acid profile of the erythrocyte membrane preceding development of type 2 diabetes mellitus Nutr Metab Cardiovasc Dis, 18 (2008), pp. 503-510

Bäckhed F, Ding H, Wang T, Hooper LV, Koh GY, Nagy A, Semenkovich CF, Gordon JI. The gut microbiota as an environmental factor that regulates fat storage. Proceedings of the National Academy of Sciences. 2004 Nov 2;101(44):15718-23.

Badin PM, Vila IK, Louche K, Mairal A, Marques MA, Bourlier V, Tavernier G, Langin D, Moro C. High-fat diet-mediated lipotoxicity and insulin resistance is related to impaired lipase expression in mouse skeletal muscle. Endocrinology. 2013 Apr 1;154(4):1444-53.

Bae JS, Oh AR, Lee HJ, Ahn YH, Cha JY. Hepatic Elovl6 gene expression is regulated by the synergistic action of ChREBP and SREBP-1c. Biochemical and biophysical research communications. 2016 Sep 23;478(3):1060-6.

Baothman OA, Zamzami MA, Taher I, Abubaker J, Abu-Farha M. The role of gut microbiota in the development of obesity and diabetes. Lipids in health and disease. 2016 Dec 1;15(1):108.

Barrows BR, Parks EJ. Contributions of different fatty acid sources to very low-density lipoprotein-triacylglycerol in the fasted and fed states. The Journal of Clinical Endocrinology & Metabolism. 2006 Apr 1;91(4):1446-52.

Barrows BR, Timlin MT, Parks EJ. Spillover of dietary fatty acids and use of serum nonesterified fatty acids for the synthesis of VLDL-triacylglycerol under two different feeding regimens. Diabetes. 2005 Sep 1;54(9):2668-73.

Bastard JP, Maachi M, van Nhieu JT, Jardel C, Bruckert E, Grimaldi A, Robert JJ, Capeau J, Hainque B. Adipose tissue IL-6 content correlates with resistance to insulin activation of glucose uptake both in vivo and in vitro. The Journal of Clinical Endocrinology & Metabolism. 2002 May 1;87(5):2084-9.

Beenakkers AT, Van der Horst DJ, Van Marrewijk WJ. Role of lipids in energy metabolism. InEnergy metabolism in insects 1981 (pp. 53-100). Springer, Boston, MA.

Begriche K, Massart J, Robin MA, Bonnet F, Fromenty B. Mitochondrial adaptations and dysfunctions in nonalcoholic fatty liver disease. Hepatology. 2013 Oct;58(4):1497-507.

Begriche, K., Igoudjil, A., Pessayre, D., & Fromenty, B. (2006). Mitochondrial dysfunction in NASH: causes, consequences and possible means to prevent it. Mitochondrion, 6(1), 1-28.

Bjermo H, Iggman D, Kullberg J, Dahlman I, Johansson L, Persson L, Berglund J, Pulkki K, Basu S, Uusitupa M, Rudling M. Effects of n-6 PUFAs compared with SFAs on liver fat, lipoproteins, and inflammation in abdominal obesity: a randomized controlled trial. The American journal of clinical nutrition. 2012 May 1;95(5):1003-12.

Bjørndal B, Berge C, Ramsvik MS, Svardal A, Bohov P, Skorve J, Berge RK. A fish protein hydrolysate alters fatty acid composition in liver and adipose tissue and increases plasma carnitine levels in a mouse model of chronic inflammation. Lipids in health and disease. 2013 Dec;12(1):143.

Björntorp P, Bergman H, Varnauskas E. Plasma free fatty acid turnover rate in obesity. Acta medica Scandinavica. 1969 Jan 12;185(1-6):351-6.

Boden, G. Obesity, Insulin Resistance and Free Fatty Acids. Curr. Opin. Endocrinol. Diabetes Obes. 2011, 18, 139–143.

Boraschi D, Italiani P, Weil S, Martin MU. The family of the interleukin-1 receptors. Immunological reviews. 2018 Jan;281(1):197-232.

Boyd SD, Liu Y, Wang C, Martin V, Dunn-Walters DK. Human lymphocyte repertoires in ageing. Current opinion in immunology. 2013 Aug 1;25(4):511-5.

Bozzetto L, Prinster A, Annuzzi G, Costagliola L, Mangione A, Vitelli A, Mazzarella R, Longobardo M, Mancini M, Vigorito C, Riccardi G. Liver fat is reduced by an isoenergetic MUFA diet in a controlled randomized study in type 2 diabetic patients. Diabetes care. 2012 Jul 1;35(7):1429-35.

Bozzetto L, Prinster A, Annuzzi G, Costagliola L, Mangione A, Vitelli A, Mazzarella R, Longobardo M, Mancini M, Vigorito C, Riccardi G. Liver fat is reduced by an isoenergetic

MUFA diet in a controlled randomized study in type 2 diabetic patients. Diabetes care. 2012 Jul 1;35(7):1429-35.

Braunersreuther V, Viviani GL, Mach F, Montecucco F. Role of cytokines and chemokines in non-alcoholic fatty liver disease. World journal of gastroenterology: WJG. 2012 Feb 28;18(8):727.

Brenna JT, Plourde M, Stark KD, Jones PJ, Lin YH. Best practices for the design, laboratory analysis, and reporting of trials involving fatty acids. The American journal of clinical nutrition. 2018 Jun 21;108(2):211-27.

Brown AJ, Goldsworthy SM, Barnes AA, Eilert MM, Tcheang L, Daniels D, Muir AI, Wigglesworth MJ, Kinghorn I, Fraser NJ, Pike NB. The Orphan G protein-coupled receptors GPR41 and GPR43 are activated by propionate and other short chain carboxylic acids. Journal of Biological Chemistry. 2003 Mar 28;278(13):11312-9.

Bruschi FV, Tardelli M, Claudel T, Trauner M. PNPLA3 expression and its impact on the liver: current perspectives. Hepatic medicine: evidence and research. 2017; 9:55.

Buchman AL, Dubin MD, Moukarzel AA, Jenden DJ, Roch M, Rice KM, Gornbein J, Ament ME. Choline deficiency: a cause of hepatic steatosis during parenteral nutrition that can be reversed with intravenous choline supplementation. Hepatology. 1995 Nov;22(5):1399-403.

Buettner R, Parhofer KG, Woenckhaus M, Wrede CE, Kunz-Schughart LA, Scholmerich J, Bollheimer LC. Defining high-fat-diet rat models: metabolic and molecular effects of different fat types. Journal of molecular endocrinology. 2006 Jun 1;36(3):485-501.

Buettner R, Schölmerich J, Bollheimer LC. High-fat diets: modeling the metabolic disorders of human obesity in rodents. Obesity. 2007 Apr;15(4):798-808.

Bukong TN, Saha B, Szabo G. HCV, Alcohol, and the Liver. In Hepatitis C Virus II 2016 (pp. 137-163). Springer, Tokyo.

Burdge GC, Dunn RL, Wootton SA, Jackson AA. Effect of reduced dietary protein intake on hepatic and plasma essential fatty acid concentrations in the adult female rat: effect of pregnancy and consequences for accumulation of arachidonic and docosahexaenoic acids in fetal liver and brain. British Journal of Nutrition. 2002 Oct;88(4):379-87.

Cai D, Yuan M, Frantz DF, Melendez PA, Hansen L, Lee J, Shoelson SE. Local and systemic insulin resistance resulting from hepatic activation of IKK-β and NF-κB. Nature medicine. 2005 Feb;11(2):183.

Calder PC, Bosco N, Bourdet-Sicard R, Capuron L, Delzenne N, Dore J, Franceschi C, Lehtinen MJ, Recker T, Salvioli S, Visioli F. Health relevance of the modification of low-grade inflammation in ageing (inflammageing) and the role of nutrition. Ageing research reviews. 2017 Nov 1; 40:95-119.

Calder PC. n− 3 polyunsaturated fatty acids, inflammation, and inflammatory diseases. The American journal of clinical nutrition. 2006 Jun 1;83(6):1505S-19S.

Campo L, Eiseler S, Apfel T, Pyrsopoulos N. Fatty Liver Disease and Gut Microbiota: A Comprehensive Update. Journal of clinical and translational hepatology. 2019 Mar 28;7(1):56.

Cani PD, Delzenne NM. The role of the gut microbiota in energy metabolism and metabolic disease. Current pharmaceutical design. 2009 May 1;15(13):1546-58.

Cani, P. D., Neyrinck, A. M., Fava, F., Knauf, C., Burcelin, R. G., Tuohy, K. M., . . . Delzenne, N. M. (2007). Selective increases of bifidobacteria in gut microflora improve high-fat-diet-induced diabetes in mice through a mechanism associated with endotoxaemia. Diabetologia, 50(11), 2374-2383.

Canny GO, McCormick BA. Bacteria in the intestine, helpful residents or enemies from within? Infection and immunity. 2008 Aug 1;76(8):3360-73.

Caporaso JG, Kuczynski J, Stombaugh J, Bittinger K, Bushman FD, Costello EK, Fierer N, Pena AG, Goodrich JK, Gordon JI, Huttley GA. QIIME allows analysis of high-throughput community sequencing data. Nature methods. 2010 May;7(5):335.

Capurso, C.; Capurso, A. From excess adiposity to insulin resistance: The role of free fatty acids. Vasc. Pharmacol. 2012, 57, 91–97.

Carta G, Murru E, Banni S, Manca C. Palmitic acid: Physiological role, metabolism and nutritional implications. Frontiers in physiology. 2017 Nov 8; 8:902.

Charidemou E, Ashmore T, Li X, McNally BD, West JA, Liggi S, Harvey M, Orford E, Griffin JL. High protein feeding induces de novo lipogenesis in healthy humans: a randomised 3-way crossover study. JCI Insight. 2019 May 30.

Charlton MR. Protein metabolism and liver disease. Bailliere's clinical endocrinology and metabolism. 1996 Oct 1;10(4):617-35.

Chen D, Yang Z, Chen X, Huang Y, Yin B, Guo F, Zhao H, Huang J, Wu Y, Gu R. Effect of Lactobacillus rhamnosus hsryfm 1301 on the gut microbiota and lipid metabolism in rats fed a high-fat diet. J Microbiol Biotechnol. 2015 May 1;25(5):687-95.

Cho I, Yamanishi S, Cox L, Methé BA, Zavadil J, Li K, Gao Z, Mahana D, Raju K, Teitler I, Li H. Antibiotics in early life alter the murine colonic microbiome and adiposity. Nature. 2012 Aug;488(7413):621.

Choi SH, Ginsberg HN. Increased very low-density lipoprotein (VLDL) secretion, hepatic steatosis, and insulin resistance. Trends in Endocrinology & Metabolism. 2011 Sep 1;22(9):353-63.

Clemente JC, Manasson J, Scher JU. The role of the gut microbiome in systemic inflammatory disease. Bmj. 2018 Jan 8;360: j5145.

Compare D, Coccoli P, Rocco A, Nardone OM, De Maria S, Cartenì M, Nardone G. Gut–liver axis: the impact of gut microbiota on non-alcoholic fatty liver disease. Nutrition, Metabolism and Cardiovascular Diseases. 2012 Jun 1;22(6):471-6.

Contemporary Topics in Analytical and Clinical Chemistry, Vol 3, Plenum, New York (1978), pp. 217-251

Cordero P, Gómez-Úriz AM, Campion J, Milagro FI, Martinez JA. Dietary supplementation with methyl donors reduces fatty liver and modifies the fatty acid synthase DNA methylation profile in rats fed an obesogenic diet. Genes & nutrition. 2013 Jan;8(1):105.

Cordero P, Gómez-Úriz AM, Campion J, Milagro FI, Martinez JA. Dietary supplementation with methyl donors reduces fatty liver and modifies the fatty acid synthase DNA methylation profile in rats fed an obesogenic diet. Genes & nutrition. 2013 Jan;8(1):105.

Cortez-Pinto H, Jesus L, Barros H, Lopes C, Moura MC, Camilo ME. How different is the dietary pattern in non-alcoholic steatohepatitis patients? Clinical Nutrition. 2006 Oct 1;25(5):816-23.

Crown SB, Marze N, Antoniewicz MR. Catabolism of branched chain amino acids contributes significantly to synthesis of odd-chain and even-chain fatty acids in 3T3-L1 adipocytes. PLoS One. 2015 Dec 28;10(12): e0145850.

Crown SB, Marze N, Antoniewicz MR. Catabolism of branched chain amino acids contributes significantly to synthesis of odd-chain and even-chain fatty acids in 3T3-L1 adipocytes. PLoS One. 2015 Dec 28;10(12): e0145850.

Dandona P, Weinstock R, Thusu K, Abdel-Rahman E, Aljada A, Wadden T. Tumor necrosis factor-α in sera of obese patients: fall with weight loss. The Journal of Clinical Endocrinology & Metabolism. 1998 Aug 1;83(8):2907-10.

De Carvalho CC, Caramujo MJ. The various roles of fatty acids. Molecules. 2018 Oct;23(10):2583.

de Conti A, Pogribny IP. Epigenetics of Dietary Methyl-Group Donor Deficiency and Liver Cancer. Handbook of Nutrition, Diet, and Epigenetics. 2017:1-6.

De Craemer D, Pauwels M, Roels F. Peroxisomes in cirrhosis of the human liver: a cytochemical, ultrastructural and quantitative study. Hepatology. 1993 Mar;17(3):404-10.

de Fraia Pinto L, Compri CM, Fornari JV, Bartchewsky W, Cintra DE, Trevisan M, de Oliveira Carvalho P, Ribeiro ML, Velloso LA, Saad MJ, Pedrazzoli Jr J. The immunosuppressant drug, thalidomide, improves hepatic alterations induced by a high-fat diet in mice. Liver International. 2010 Apr;30(4):603-10.

de La Serre CB, Ellis CL, Lee J, Hartman AL, Rutledge JC, Raybould HE. Propensity to high-fat diet-induced obesity in rats is associated with changes in the gut microbiota and gut inflammation. American Journal of Physiology-Gastrointestinal and Liver Physiology. 2010 May 27;299(2): G440-8.

De Vadder F, Kovatcheva-Datchary P, Goncalves D, Vinera J, Zitoun C, Duchampt A, Bäckhed F, Mithieux G. Microbiota-generated metabolites promote metabolic benefits via gut-brain neural circuits. Cell. 2014 Jan 16;156(1-2):84-96.

Delgado TC, Pinheiro D, Caldeira M, Castro MM, Geraldes CF, Lopez-Larrubia P, Cerdan S, Jones JG. Sources of hepatic triglyceride accumulation during high-fat feeding in the healthy rat. NMR in Biomedicine: An International Journal Devoted to the Development and Application of Magnetic Resonance In vivo. 2009 Apr;22(3):310-7.

den Besten G, Lange K, Havinga R, van Dijk TH, Gerding A, van Eunen K, Müller M, Groen AK, Hooiveld GJ, Bakker BM, Reijngoud DJ. Gut-derived short-chain fatty acids are vividly assimilated into host carbohydrates and lipids. American Journal of Physiology-Gastrointestinal and Liver Physiology. 2013 Dec 15;305(12):G900-10.

Deponte M. Glutathione catalysis and the reaction mechanisms of glutathione-dependent enzymes. Biochimica et Biophysica Acta (BBA)-General Subjects. 2013 May 1;1830(5):3217-66.

Devkota S, Wang Y, Musch MW, Leone V, Fehlner-Peach H, Nadimpalli A, et al. Dietary-fat-induced taurocholic acid promotes pathobiont expansion and colitis in Il10-/- mice. *Nature.* (2013) 487:104–8. doi: 10.1038/nature11225

Dinarello CA. Immunological and inflammatory functions of the interleukin-1 family. Annual review of immunology. 2009 Apr 23; 27:519-50.

Dingess KA, Valentine CJ, Ollberding NJ, Davidson BS, Woo JG, Summer S, Peng YM, Guerrero ML, Ruiz-Palacios GM, Ran-Ressler RR, McMahon RJ. Branched-chain fatty acid composition of human milk and the impact of maternal diet: The Global Exploration of Human Milk (GEHM) Study. The American journal of clinical nutrition. 2016 Nov 30;105(1):177-84.

Dobson GP, Letson HL, Biros E, Morris J. Specific pathogen-free (SPF) animal status as a variable in biomedical research: Have we come full circle? EBioMedicine. 2019 Mar; 41:42.

Doege H, Baillie RA, Ortegon AM, Tsang B, Wu Q, Punreddy S, Hirsch D, Watson N, Gimeno RE, Stahl A. Targeted deletion of FATP5 reveals multiple functions in liver metabolism: alterations in hepatic lipid homeostasis. Gastroenterology. 2006 Apr 1;130(4):1245-58.

Dominguez-Bello MG, Costello EK, Contreras M, Magris M, Hidalgo G, Fierer N, Knight R. Delivery mode shapes the acquisition and structure of the initial microbiota across multiple body habitats in newborns. Proceedings of the National Academy of Sciences. 2010 Jun 29;107(26):11971-5.

Donnelly KL, Smith CI, Schwarzenberg SJ, Jessurun J, Boldt MD, Parks EJ. Sources of fatty acids stored in liver and secreted via lipoproteins in patients with nonalcoholic fatty liver disease. The Journal of clinical investigation. 2005 May 2;115(5):1343-51.

Duncan SH, Belenguer A, Holtrop G, Johnstone AM, Flint HJ, Lobley GE. Reduced dietary intake of carbohydrates by obese subjects results in decreased concentrations of butyrate and butyrate-producing bacteria in feces. Appl. Environ. Microbiol. 2007 Feb 15;73(4):1073-8.

Duncan SH, Holtrop G, Lobley GE, Calder AG, Stewart CS, Flint HJ. Contribution of acetate to butyrate formation by human faecal bacteria. British Journal of Nutrition. 2004 Jun;91(6):915-23.

Eckburg PB, Bik EM, Bernstein CN, Purdom E, Dethlefsen L, Sargent M, Gill SR, Nelson KE, Relman DA. Diversity of the human intestinal microbial flora. science. 2005 Jun 10;308(5728):1635-8.

Edgar RC. UPARSE: highly accurate OTU sequences from microbial amplicon reads. Nature methods. 2013 Oct;10(10):996.

Eisinger K, Krautbauer S, Hebel T, Schmitz G, Aslanidis C, Liebisch G, Buechler C. Lipidomic analysis of the liver from high-fat diet induced obese mice identifies changes in multiple lipid classes. Experimental and molecular pathology. 2014 Aug 1;97(1):37-43.

El Aidy S, Van den Abbeele P, Van de Wiele T, Louis P, Kleerebezem M. Intestinal colonization: how key microbial players become established in this dynamic process: microbial metabolic activities and the interplay between the host and microbes. Bioessays. 2013 Oct;35(10):913-23.

Engstler AJ, Aumiller T, Degen C, Dürr M, Weiss E, Maier IB, Schattenberg JM, Jin CJ, Sellmann C, Bergheim I. Insulin resistance alters hepatic ethanol metabolism: studies in mice and children with non-alcoholic fatty liver disease. Gut. 2016 Sep 1;65(9):1564-71.

Enqi W, Huanhu Z, Ritu W, Dan X, Han L, Baili W, Gangyi S, Shuchun L. Age-stratified comparative analysis of the differences of gut microbiota associated with blood glucose level. BMC microbiology. 2019 Dec;19(1):111.

Even PC, Virtue S, Morton NM, Fromentin G, Semple RK. are rodent Models Fit for investigation of Human obesity and related diseases? Frontiers in nutrition. 2017 Dec 1; 4:58.

Everard A, Belzer C, Geurts L, Ouwerkerk JP, Druart C, Bindels LB, Guiot Y, Derrien M, Muccioli GG, Delzenne NM, De Vos WM. Cross-talk between Akkermansia muciniphila and intestinal epithelium controls diet-induced obesity. Proceedings of the National Academy of Sciences. 2013 May 28;110(22):9066-71.

Fahy E, Cotter D, Sud M, Subramaniam S. Lipid classification, structures and tools. Biochimica et Biophysica Acta (BBA)-Molecular and Cell Biology of Lipids. 2011 Nov 1;1811(11):637-47.

Faith, J. J., et al. (2013). "The long-term stability of the human gut microbiota." science 341(6141): 1237439.

Falcon A, Doege H, Fluitt A, Tsang B, Watson N, Kay MA, Stahl A. FATP2 is a hepatic fatty acid transporter and peroxisomal very long-chain acyl-CoA synthetase. American Journal of Physiology-Endocrinology and Metabolism. 2010 Jun 8;299(3): E384-93.

Fang J, Holmgren A. Inhibition of thioredoxin and thioredoxin reductase by 4-hydroxy-2-nonenal in vitro and in vivo. Journal of the American Chemical Society. 2006 Feb 15;128(6):1879-85.

Febbraio ML, Guy E, Coburn C, Knapp FF, Beets AL, Abumrad NA, Silverstein RL. The impact of overexpression and deficiency of fatty acid translocase (FAT)/CD36. InCellular Lipid Binding Proteins 2002 (pp. 193-197). Springer, Boston, MA.

Feingold KR, Grunfeld C. Introduction to lipids and lipoproteins. InEndotext [Internet] 2018 Feb 2. MDText. com, Inc.

Ferramosca A, Di Giacomo M, Zara V. Antioxidant dietary approach in treatment of fatty liver: new insights and updates. World journal of gastroenterology. 2017 Jun 21;23(23):4146.

Ferre P, Foufelle F. Hepatic steatosis: a role for de novo lipogenesis and the transcription factor SREBP-1c. Diabetes, obesity and metabolism. 2010 Oct; 12:83-92.

Ferreira AV, Mario ÉG, Porto LC, Andrade SP, Botion LM. High-carbohydrate diet selectively induces tumor necrosis factor-α production in mice liver. Inflammation. 2011 Apr 1;34(2):139-45.

Fievez V, Vlaeminck B, Dhanoa MS, Dewhurst RJ. Use of principal component analysis to investigate the origin of heptadecenoic and conjugated linoleic acids in milk. Journal of Dairy Science. 2003 Dec 1;86(12):4047-53.

Fillmore N, Alrob OA, Lopaschuk GD. Fatty Acid *beta*-Oxidation. AOCS Lipid library, doi. 2011;10.

Folch, J., Lees, M., & Sloane Stanley, G. H. (1957). A simple method for the isolation and purification of total lipides from animal tissues. *J biol Chem*, *226*(1), 497-509.

Forouhi NG, Koulman A, Sharp SJ, Imamura F, Kröger J, Schulze MB, Crowe FL, Huerta JM, Guevara M, Beulens JW, van Woudenbergh GJ. Differences in the prospective association between individual plasma phospholipid saturated fatty acids and incident type 2 diabetes: the EPIC-InterAct case-cohort study. The lancet Diabetes & endocrinology. 2014 Oct 1;2(10):810-8.

François IE, Lescroart O, Veraverbeke WS, Marzorati M, Possemiers S, Evenepoel P, Hamer H, Houben E, Windey K, Welling GW, Delcour JA. Effects of a wheat bran extract containing arabinoxylan oligosaccharides on gastrointestinal health parameters in healthy adult human volunteers: a double-blind, randomised, placebo-controlled, cross-over trial. British Journal of Nutrition. 2012 Dec;108(12):2229-42.

Fretts AM, Imamura F, Marklund M, Micha R, Wu JH, Murphy RA, Chien KL, McKnight B, Tintle N, Forouhi NG, Qureshi WT. Associations of circulating very-long-chain saturated fatty acids and incident type 2 diabetes: a pooled analysis of prospective cohort studies. The American journal of clinical nutrition. 2019 Apr 1;109(4):1216-23.

Frost G, Sleeth ML, Sahuri-Arisoylu M, Lizarbe B, Cerdan S, Brody L, Anastasovska J, Ghourab S, Hankir M, Zhang S, Carling D. The short-chain fatty acid acetate reduces appetite via a central homeostatic mechanism. Nature communications. 2014 Apr 29; 5:3611.

Fujiwara M, Mori N, Sato T, Tazaki H, Ishikawa S, Yamamoto I, Arai T. Changes in fatty acid composition in tissue and serum of obese cats fed a high fat diet. Bmc veterinary research. 2015 Dec;11(1):200.

Furuhashi M, Hotamisligil GS. Fatty acid-binding proteins: role in metabolic diseases and potential as drug targets. Nature reviews Drug discovery. 2008 Jun;7(6):489.

Garbacz WG, Lu P, Miller TM, Poloyac SM, Eyre NS, Mayrhofer G, Xu M, Ren S, Xie W. Hepatic overexpression of CD36 improves glycogen homeostasis and attenuates high-fat diet-induced hepatic steatosis and insulin resistance. Molecular and cellular biology. 2016 Nov 1;36(21):2715-27.

Garg A. High-monounsaturated-fat diets for patients with diabetes mellitus: a meta-analysis. The American Journal of Clinical Nutrition. 1998 Mar 1;67(3):577S-82S.

Garibyan, L., & Avashia, N. (2013). Research techniques made simple: polymerase chain reaction (PCR). *The Journal of investigative dermatology*, *133*(3), e6.

Gibson SA, McFarlan C, Hay S, MacFarlane GT. Significance of microflora in proteolysis in the colon. Appl. Environ. Microbiol. 1989 Mar 1;55(3):679-83.

Goedeke L, Bates J, Vatner DF, Perry RJ, Wang T, Ramirez R, Li L, Ellis MW, Zhang D, Wong KE, Beysen C. Acetyl-CoA Carboxylase Inhibition Reverses NAFLD and Hepatic Insulin Resistance but Promotes Hypertriglyceridemia in Rodents. Hepatology. 2018 Dec 1;68(6):2197-211.

Gong, J.; Campos, H.; McGarvey, S.; Wu, Z.; Goldberg, R.; Baylin, A. Adipose tissue palmitoleic acid and obesity in humans: Does it behave as a lipokine? *Am. J. Clin. Nutr.* 2011, *93*, 186–191.

Gornicka A, Morris-Stiff G, Thapaliya S, Papouchado BG, Berk M, Feldstein AE. Transcriptional profile of genes involved in oxidative stress and antioxidant defense in a dietary murine model of steatohepatitis. Antioxidants & redox signaling. 2011 Jul 15;15(2):437-45.

Grabherr F, Grander C, Effenberger M, Adolph TE, Tilg H. Gut dysfunction and non-alcoholic fatty liver disease. Frontiers in endocrinology. 2019; 10:611.

Grant P, Ahlemeyer B, Karnati S, Berg T, Stelzig I, Nenicu A, Kuchelmeister K, Crane DI, Baumgart-Vogt E. The biogenesis protein PEX14 is an optimal marker for the identification and localization of peroxisomes in different cell types, tissues, and species in morphological studies. Histochemistry and cell biology. 2013 Oct 1;140(4):423-42.

Grant P, Ahlemeyer B, Karnati S, Berg T, Stelzig I, Nenicu A, Kuchelmeister K, Crane DI, Baumgart-Vogt E. The biogenesis protein PEX14 is an optimal marker for the identification and localization of peroxisomes in different cell types, tissues, and species in morphological studies. Histochemistry and cell biology. 2013 Oct 1;140(4):423-42.

Greenblum S, Turnbaugh PJ, Borenstein E. Metagenomic systems biology of the human gut microbiome reveals topological shifts associated with obesity and inflammatory bowel disease. Proceedings of the National Academy of Sciences. 2012 Jan 10;109(2):594-9.

Grundy SM. Factors determining blood cholesterol levels. Encyclopedia of food Sciences and Nutrition. 2003; 2:1237-43.

Gumpen SA, Norum KR. The relative amounts of long-chain acylcarnitines, short-chain acylcarnitines and carnitine in heart, liver and brown adipose tissue from rats fed on rapeseed oil. Biochimica et Biophysica Acta (BBA)-Lipids and Lipid Metabolism. 1973 Jul 19;316(1):48-55.

Guo F, Cavener DR. The GCN2 eIF2α kinase regulates fatty-acid homeostasis in the liver during deprivation of an essential amino acid. Cell metabolism. 2007 Feb 7;5(2):103-14.

Gusdon AM, Song KX, Qu S. Nonalcoholic fatty liver disease: pathogenesis and therapeutics from a mitochondria-centric perspective. Oxidative medicine and cellular longevity. 2014;2014.

Halmos EP, Christophersen CT, Bird AR, Shepherd SJ, Gibson PR, Muir JG. Diets that differ in their FODMAP content alter the colonic luminal microenvironment. Gut. 2015 Jan 1;64(1):93-100.

Hamilton MK, Boudry G, Lemay DG, Raybould HE. Changes in intestinal barrier function and gut microbiota in high-fat diet-fed rats are dynamic and region dependent. American Journal of Physiology-Gastrointestinal and Liver Physiology. 2015 Mar 6;308(10):G840-51.

Hartmann P, Schnabl B. Risk factors for progression of and treatment options for NAFLD in children. Clinical liver disease. 2018 Jan;11(1):11-5.

Haukeland JW, Damås JK, Konopski Z, Løberg EM, Haaland T, Goverud I, Torjesen PA, Birkeland K, Bjøro K, Aukrust P. Systemic inflammation in nonalcoholic fatty liver disease is characterized by elevated levels of CCL2. Journal of hepatology. 2006 Jun 1;44(6):1167-74.

He C, Cheng D, Peng C, Li Y, Zhu Y, Lu N. High-fat diet induces dysbiosis of gastric microbiota prior to gut microbiota in association with metabolic disorders in mice. Frontiers in microbiology. 2018 Apr 9; 9:639.

He XX, Wu XL, Chen RP, Chen C, Liu XG, Wu BJ, Huang ZM. Effectiveness of omega-3 polyunsaturated fatty acids in non-alcoholic fatty liver disease: a meta-analysis of randomized controlled trials. PLoS One. 2016 Oct 6;11(10): e0162368.

Hebbard L, George J. Animal models of nonalcoholic fatty liver disease. Nature reviews Gastroenterology & hepatology. 2011 Jan;8(1):35.

Heit C, Marshall S, Singh S, Yu X, Charkoftaki G, Zhao H, Orlicky DJ, Fritz KS, Thompson DC, Vasiliou V. Catalase deletion promotes prediabetic phenotype in mice. Free Radical Biology and Medicine. 2017 Feb 1; 103:48-56.

Hellerstein MK. De novo lipogenesis in humans: metabolic and regulatory aspects. European journal of clinical nutrition. 1999 Apr 26;53(s1): s53.

Hirosuke O, Noriyasu Y, Junichi N, Isao C. Precursor role of branched-chain amino acids in the biosynthesis of iso and anteiso fatty acids in rat skin. Biochimica et Biophysica Acta (BBA)-Lipids and Lipid Metabolism. 1994 Oct 6;1214(3):279-87.

Hodge AM, English DR, O'Dea K, Sinclair AJ, Makrides M, Gibson RA, Giles GG. Plasma phospholipid and dietary fatty acids as predictors of type 2 diabetes: interpreting the role of linoleic acid. Am J Clin Nutr 2007; 86:189–97.

Hodson L, Rosqvist F, Parry SA. The influence of dietary fatty acids on liver fat content and metabolism. Proceedings of the Nutrition Society. 2020 Feb;79(1):30-41.

Holt H, Wild S, Wood P, Zhang J, Darekar A, Dewbury K, et al. Non-esterified fatty acid concentrations are independently associated with hepatic steatosis in obese subjects. Diabetologia. 2006;49(1):141-8.

Hooper LV, Macpherson AJ. Immune adaptations that maintain homeostasis with the intestinal microbiota. Nature Reviews Immunology. 2010 Mar;10(3):159.

Hooper LV, Xu J, Falk PG, Midtvedt T, Gordon JI. A molecular sensor that allows a gut commensal to control its nutrient foundation in a competitive ecosystem. Proceedings of the National Academy of Sciences. 1999 Aug 17;96(17):9833-8.

Hotamisligil GS, Shargill NS, Spiegelman BM. Adipose expression of tumor necrosis factor-alpha: direct role in obesity-linked insulin resistance. Science. 1993 Jan 1;259(5091):87-91.

Hotamisligil GS. Inflammation, metaflammation and immunometabolic disorders. Nature. 2017 Feb;542(7640):177.

Houghton D, Stewart CJ, Day CP, Trenell M. Gut microbiota and lifestyle interventions in NAFLD. International journal of molecular sciences. 2016 Apr;17(4):447.

How different is the dietary pattern in non-alcoholic steatohepatitis patients? Cortez-Pinto H, Jesus L, Barros H, Lopes C, Moura MC, Camilo ME Clin Nutr. 2006 Oct; 25(5):816-23.

Hsieh FC, Lee CL, Chai CY, Chen WT, Lu YC, Wu CS. Oral administration of Lactobacillus reuteri GMNL-263 improves insulin resistance and ameliorates hepatic steatosis in high fructose-fed rats. Nutrition & metabolism. 2013 Dec;10(1):35.

Huang L, Lin JS, Aris IM, Yang G, Chen WQ, Li LJ. Circulating Saturated Fatty Acids and Incident Type 2 Diabetes: A Systematic Review and Meta-Analysis. Nutrients. 2019 May;11(5):998.

Huang X, Hancock DP, Gosby AK, McMahon AC, Solon SM, Le Couteur DG, Conigrave AD, Raubenheimer D, Simpson SJ. Effects of dietary protein to carbohydrate balance on energy intake, fat storage, and heat production in mice. Obesity. 2013 Jan;21(1):85-92.

Hudgins LC, Hellerstein M, Seidman C, Neese R, Diakun J, Hirsch J. Human fatty acid synthesis is stimulated by a eucaloric low fat, high carbohydrate diet. The Journal of clinical investigation. 1996 May 1;97(9):2081-91.

Hughes RL, Kable ME, Marco M, Keim NL. The Role of the Gut Microbiome in Predicting Response to Diet and the Development of Precision Nutrition Models. Part II: Results. Advances in Nutrition. 2019 Jun 21.

Ibrahim W, Lee US, Yeh CC, Szabo J, Bruckner G, Chow CK. Oxidative stress and antioxidant status in mouse liver: effects of dietary lipid, vitamin E and iron. The Journal of nutrition. 1997 Jul 1;127(7):1401-6.

Idriss HT, Naismith JH. TNFα and the TNF receptor superfamily: Structure-function relationship (s). Microscopy research and technique. 2000 Aug 1;50(3):184-95.

Iggman D, Risérus U. Role of different dietary saturated fatty acids for cardiometabolic risk. Clinical lipidology. 2011 Apr 1;6(2):209-23.

Imajo K, Yoneda M, Kessoku T, Ogawa Y, Maeda S, Sumida Y, Hyogo H, Eguchi Y, Wada K, Nakajima A. Rodent models of nonalcoholic fatty liver disease/nonalcoholic steatohepatitis. International journal of molecular sciences. 2013 Nov;14(11):21833-57.

Ipsen DH, Lykkesfeldt J, Tveden-Nyborg P. Molecular mechanisms of hepatic lipid accumulation in non-alcoholic fatty liver disease. Cellular and molecular life sciences. 2018 Sep 1;75(18):3313-27.

Ishii H, Fukumori N, Horie S, Suga T. Effects of fat content in the diet on hepatic peroxisomes of the rat. Biochimica et Biophysica Acta (BBA)-Lipids and Lipid Metabolism. 1980 Jan 18;617(1):1-1.

Jacobs B, De Angelis-Schierbaum G, Egert S, Assmann G, Kratz M. Individual serum triglyceride responses to high-fat and low-fat diets differ in men with modest and severe hypertriglyceridemia. The Journal of nutrition. 2004 Oct 1;134(6):1400-5.

Jasirwan co, Lesmana Cr, Hasan I, Sulaiman As, Gani Ra. The role of gut microbiota in non-alcoholic fatty liver disease: pathways of mechanisms. Bioscience of Microbiota, Food and Health. 2019:18-032.

Jenkins B, De Schryver E, Van Veldhoven PP, Koulman A. Peroxisomal 2-Hydroxyacyl-CoA Lyase Is Involved in Endogenous Biosynthesis of Heptadecanoic Acid. Molecules. 2017 Oct;22(10):1718.

Jenkins B, West JA, Koulman A. A review of odd-chain fatty acid metabolism and the role of pentadecanoic acid (C15: 0) and heptadecanoic acid (C17: 0) in health and disease. Molecules. 2015 Feb;20(2):2425-44.

Jenkins B, West JA, Koulman A. A review of odd-chain fatty acid metabolism and the role of pentadecanoic acid (C15: 0) and heptadecanoic acid (C17: 0) in health and disease. Molecules. 2015 Feb;20(2):2425-44.

Jenkins BJ, Seyssel K, Chiu S, Pan PH, Lin SY, Stanley E, Ament Z, West JA, Summerhill K, Griffin JL, Vetter W. Odd chain fatty acids; new insights of the relationship between the gut microbiota, dietary intake, biosynthesis and glucose intolerance. Scientific reports. 2017 Mar 23; 7:44845.

Jensen VS, Hvid H, Damgaard J, Nygaard H, Ingvorsen C, Wulff EM, Lykkesfeldt J, Fledelius C. Dietary fat stimulates development of NAFLD more potently than dietary fructose in Sprague–Dawley rats. Diabetology & metabolic syndrome. 2018 Dec;10(1):4.

Jensen VS, Hvid H, Damgaard J, Nygaard H, Ingvorsen C, Wulff EM, Lykkesfeldt J, Fledelius C. Dietary fat stimulates development of NAFLD more potently than dietary fructose in Sprague–Dawley rats. Diabetology & metabolic syndrome. 2018 Dec;10(1):4.

Jeyakumar SM, Vajreswari A. Dietary Management of Nonalcoholic Fatty Liver Disease (NAFLD) by n-3 Polyunsaturated Fatty Acid (PUFA) Supplementation: A Perspective on the Role of n-3 PUFA-Derived Lipid Mediators. InDietary Interventions in Liver Disease 2019 Jan 1 (pp. 373-389). Academic Press.

Jeyapal S, Kona SR, Mullapudi SV, Putcha UK, Gurumurthy P, Ibrahim A. Substitution of linoleic acid with α-linolenic acid or long chain n-3 polyunsaturated fatty acid prevents Western diet induced nonalcoholic steatohepatitis. Scientific reports. 2018 Jul 19;8(1):10953.

Ji Y, Yin Y, Li Z, Zhang W. Gut Microbiota-Derived Components and Metabolites in the Progression of Non-Alcoholic Fatty Liver Disease (NAFLD). Nutrients. 2019 Aug;11(8):1712.

Jin R, Willment A, Patel SS, Sun X, Song M, Mannery YO, Kosters A, McClain CJ, Vos MB. Fructose induced endotoxemia in pediatric nonalcoholic fatty liver disease. International journal of hepatology. 2014;2014.

Jones EY, Stuart DI, Walker NP. Structure of tumour necrosis factor. Nature. 1989 Mar;338(6212):225.

Juárez-Hernández E, Chávez-Tapia NC, Uribe M, Barbero-Becerra VJ. Role of bioactive fatty acids in nonalcoholic fatty liver disease. Nutrition journal. 2015 Dec 1;15(1):72.

Julibert A, del Mar Bibiloni M, Tur JA. Dietary fat intake and Metabolic Syndrome in adults: a systematic review. Nutrition, Metabolism and Cardiovascular Diseases. 2019 May 17.

Jump DB, Lytle KA, Depner CM, Tripathy S. Omega-3 polyunsaturated fatty acids as a treatment strategy for nonalcoholic fatty liver disease. Pharmacology & therapeutics. 2018 Jan 1;181:108-25.

Jump DB. Fatty acid regulation of hepatic lipid metabolism. Current opinion in clinical nutrition and metabolic care. 2011 Mar;14(2):115.

Jump DB. N-3 polyunsaturated fatty acid regulation of hepatic gene transcription. Current opinion in lipidology. 2008 Jun;19(3):242.

Jung TW, Kim HC, El-Aty AA, Jeong JH. Maresin 1 attenuates NAFLD by suppression of endoplasmic reticulum stress via AMPK–SERCA2b pathway. Journal of Biological Chemistry. 2018 Mar 16;293(11):3981-8.

Kadota Y, Toyoda T, Kitaura Y, Adams SH, Shimomura Y. Regulation of hepatic branched-chain α-ketoacid dehydrogenase complex in rats fed a high-fat diet. Obesity research & clinical practice. 2013 Dec 1;7(6): e439-44.

Kamari Y, Shaish A, Vax E, Shemesh S, Kandel-Kfir M, Arbel Y, Olteanu S, Barshack I, Dotan S, Voronov E, Dinarello CA. Lack of interleukin-1α or interleukin-1β inhibits transformation of steatosis to steatohepatitis and liver fibrosis in hypercholesterolemic mice. Journal of hepatology. 2011 Nov 1;55(5):1086-94.

Kang W, Lee MS & Baik M (2011) Dietary protein restriction alters lipid metabolism and insulin sensitivity in rats. Asian-Australasian Journal of Animal Sciences 24, 1274-81.

Kani AH, Alavian SM, Haghighatdoost F, Azadbakht L. Diet macronutrients composition in nonalcoholic Fatty liver disease: a review on the related documents. Hepatitis monthly. 2014 Feb;14(2).

Karlsson FH, Tremaroli V, Nookaew I, Bergström G, Behre CJ, Fagerberg B, Nielsen J, Bäckhed F. Gut metagenome in European women with normal, impaired and diabetic glucose control. Nature. 2013 Jun;498(7452):99.

Kaur N, Chugh V, Gupta AK. Essential fatty acids as functional components of foods-a review. Journal of food science and technology. 2014 Oct 1;51(10):2289-303.

Kern PA, Saghizadeh M, Ong JM, Bosch RJ, Deem R, Simsolo RB. The expression of tumor necrosis factor in human adipose tissue. Regulation by obesity, weight loss, and relationship to lipoprotein lipase. The Journal of clinical investigation. 1995 May 1;95(5):2111-9.

Kilberg MS, Balasubramanian M, Fu L, Shan J. The transcription factor network associated with the amino acid response in mammalian cells. Advances in nutrition. 2012 May 4;3(3):295-306.

Kim KA, Gu W, Lee IA, Joh EH, Kim DH. High fat diet-induced gut microbiota exacerbates inflammation and obesity in mice via the TLR4 signaling pathway. PloS one. 2012 Oct 16;7(10): e47713.

Kishimoto T. IL-6: from its discovery to clinical applications. International immunology. 2010 Apr 21;22(5):347-52.

Kitamura T, Seki N, Kihara A. Phytosphingosine degradation pathway includes fatty acid α-oxidation reactions in the endoplasmic reticulum. Proceedings of the National Academy of Sciences. 2017 Mar 28;114(13): E2616-23.

Klandorf H, Van Dyke K. Oxidative and nitrosative stresses: their role in health and disease in man and birds. chapter; 2012 Apr 25.

Kneeman JM, Misdraji J, Corey KE. Secondary causes of nonalcoholic fatty liver disease. Therapeutic advances in gastroenterology. 2012 May;5(3):199-207.

Koca SS, Bahcecioglu IH, Poyrazoglu OK, Ozercan IH, Sahin K, Ustundag B. The treatment with antibody of TNF-α reduces the inflammation, necrosis and fibrosis in the non-alcoholic steatohepatitis induced by methionine-and choline-deficient diet. Inflammation. 2008 Apr 1;31(2):91-8.

Kohli R, Feldstein AE. NASH animal models: are we there yet? Journal of hepatology. 2011 Oct 1;55(4):941-3.

Koliaki C, Szendroedi J, Kaul K, Jelenik T, Nowotny P, Jankowiak F, Herder C, Carstensen M, Krausch M, Knoefel WT, Schlensak M. Adaptation of hepatic mitochondrial function in humans with non-alcoholic fatty liver is lost in steatohepatitis. Cell metabolism. 2015 May 5;21(5):739-46.

Konrad D, Wueest S. The gut-adipose-liver axis in the metabolic syndrome. Physiology 2014;29(5):304-13.

Koo SH. Nonalcoholic fatty liver disease: molecular mechanisms for the hepatic steatosis. Clinical and molecular hepatology. 2013 Sep;19(3):210.

Koonen DP, Jacobs RL, Febbraio M, Young ME, Soltys CL, Ong H, Vance DE, Dyck JR. Increased hepatic CD36 expression contributes to dyslipidemia associated with diet-induced obesity. diabetes. 2007 Dec 1;56(12):2863-71.

Koren O, Goodrich JK, Cullender TC, Spor A, Laitinen K, Bäckhed HK, Gonzalez A, Werner JJ, Angenent LT, Knight R, Bäckhed F. Host remodeling of the gut microbiome and metabolic changes during pregnancy. Cell. 2012 Aug 3;150(3):470-80.

Kotronen A, Seppänen-Laakso T, Westerbacka J, Kiviluoto T, Arola J, Ruskeepää AL, Orešič M, Yki-Järvinen H. Hepatic stearoyl-CoA desaturase (SCD)-1 activity and diacylglycerol but not ceramide concentrations are increased in the nonalcoholic human fatty liver. Diabetes. 2009 Jan 1;58(1):203-8.

Kratz M, Marcovina S, Nelson JE, Yeh MM, Kowdley KV, Callahan HS, Song X, Di C, Utzschneider KM. Dairy fat intake is associated with glucose tolerance, hepatic and systemic insulin sensitivity, and liver fat but not β-cell function in humans. The American journal of clinical nutrition. 2014 Jun 1;99(6):1385-96.

Kübeck R, Bonet-Ripoll C, Hoffmann C, Walker A, Müller VM, Schüppel VL, Lagkouvardos I, Scholz B, Engel KH, Daniel H, Schmitt-Kopplin P. Dietary fat and gut microbiota

interactions determine diet-induced obesity in mice. Molecular metabolism. 2016 Dec 1;5(12):1162-74.

Kübeck R, Bonet-Ripoll C, Hoffmann C, Walker A, Müller VM, Schüppel VL, Lagkouvardos I, Scholz B, Engel KH, Daniel H, Schmitt-Kopplin P. Dietary fat and gut microbiota interactions determine diet-induced obesity in mice. Molecular metabolism. 2016 Dec 1;5(12):1162-74.

Kübeck R, Bonet-Ripoll C, Hoffmann C, Walker A, Müller VM, Schüppel VL, Lagkouvardos I, Scholz B, Engel KH, Daniel H, Schmitt-Kopplin P. Dietary fat and gut microbiota interactions determine diet-induced obesity in mice. Molecular metabolism. 2016 Dec 1;5(12):1162-74.

Kulinski A, Vance DE & Vance JE (2004) A choline-deficient diet in mice inhibits neither the CDP-choline pathway for phosphatidylcholine synthesis in hepatocytes nor apolipoprotein B secretion. Journal of Biological Chemistry 279, 23916-24.

Kumar A, Sharma A, Duseja A, Das A, Dhiman RK, Chawla YK, Kohli KK, Bhansali A. Patients with nonalcoholic fatty liver disease (NAFLD) have higher oxidative stress in comparison to chronic viral hepatitis. Journal of clinical and experimental hepatology. 2013 Mar 1;3(1):12-8.

Kumar R, Prakash S, Chhabra S, Singla V, Madan K, Gupta SD, Panda SK, Khanal S, Acharya SK. Association of pro-inflammatory cytokines, adipokines & oxidative stress with insulin resistance & non-alcoholic fatty liver disease. The Indian journal of medical research. 2012 Aug;136(2):229.

Kumar V, Deo MG, Ramalingaswami V. Mechanism of Fatty Liver, in Protein Deficiency: An experimental study in the rhesus monkey. Gastroenterology. 1972 Mar 1;62(3):445-51.

Kuwahata M, Kubota H, Amano S, Yokoyama M, Shimamura Y, Ito S, Ogawa A, Kobayashi Y, Miyamoto KI, Kido Y. Dietary medium-chain triglycerides attenuate hepatic lipid deposition in growing rats with protein malnutrition. Journal of nutritional science and vitaminology. 2011;57(2):138-43.

Kwon DH, Kang W, Nam YS, Lee MS, Lee IY, Kim HJ, Rajasekar P, Lee JH, Baik M. Dietary protein restriction induces steatohepatitis and alters leptin/signal transducers and activators of transcription 3 signaling in lactating rats. The Journal of nutritional biochemistry. 2012 Jul 1;23(7):791-9.

Laeger T, Albarado DC, Burke SJ, Trosclair L, Hedgepeth JW, Berthoud HR, Gettys TW, Collier JJ, Münzberg H, Morrison CD. Metabolic responses to dietary protein restriction require an increase in FGF21 that is delayed by the absence of GCN2. Cell reports. 2016 Jul 19;16(3):707-16.

Lake AD, Novak P, Shipkova P, Aranibar N, Robertson DG, Reily MD, Lehman-McKeeman LD, Vaillancourt RR, Cherrington NJ. Branched chain amino acid metabolism profiles in progressive human nonalcoholic fatty liver disease. Amino acids. 2015 Mar 1;47(3):603-15.

Lane-Petter W. The Provision and Use of Pathogen-Free Laboratory Animals 1962.

Lang CH, Dobrescu CO, Bagby GJ. Tumor necrosis factor impairs insulin action on peripheral glucose disposal and hepatic glucose output. Endocrinology. 1992 Jan 1;130(1):43-52.

Lazar V, Ditu LM, Pircalabioru GG, Picu A, Petcu L, Cucu N, Chifiriuc MC. Gut Microbiota, Host Organism, and Diet Trialogue in Diabetes and Obesity. Frontiers in Nutrition. 2019;6.

Lecomte V, Kaakoush NO, Maloney CA, Raipuria M, Huinao KD, Mitchell HM, et al. Changes in gut microbiota in rats fed a high fat diet correlate with obesity-associated metabolic parameters. *PLoS ONE*. (2015) 10: e0126931. doi: 10.1371/journal.pone.0126931

Ley RE, Bäckhed F, Turnbaugh P, Lozupone CA, Knight RD, Gordon JI. Obesity alters gut microbial ecology. Proceedings of the National Academy of Sciences. 2005 Aug 2;102(31):11070-5.

Ley RE, Peterson DA, Gordon JI. Ecological and evolutionary forces shaping microbial diversity in the human intestine. Cell. 2006 Feb 24;124(4):837-48.

Li J, Quan N, Bray TM. Supplementation of N-acetylcysteine normalizes lipopolysaccharide-induced nuclear factor κB activation and proinflammatory cytokine production during early rehabilitation of protein malnourished mice. The Journal of nutrition. 2002 Nov 1;132(11):3286-92.

Li L, Zhang P, Zheng P, Bao Z, Wang Y, Huang FR. Hepatic cumulative net appearance of amino acids and related gene expression response to different protein diets in pigs. Livestock Science. 2015 Dec 1; 182:11-21.

Li S, Tan HY, Wang N, Zhang ZJ, Lao L, Wong CW, Feng Y. The role of oxidative stress and antioxidants in liver diseases. International journal of molecular sciences. 2015 Nov;16(11):26087-124.

Li Z, Jin H, Oh SY, Ji GE. Anti-obese effects of two Lactobacilli and two Bifidobacteria on ICR mice fed on a high fat diet. Biochemical and biophysical research communications. 2016 Nov 11;480(2):222-7.

Lim JS, Mietus-Snyder M, Valente A, Schwarz JM, Lustig RH. The role of fructose in the pathogenesis of NAFLD and the metabolic syndrome. Nature reviews Gastroenterology & hepatology. 2010 May;7(5):251.

Lin J, Yang R, Tarr PT, Wu PH, Handschin C, Li S, Yang W, Pei L, Uldry M, Tontonoz P, Newgard CB. Hyperlipidemic effects of dietary saturated fats mediated through PGC-1β coactivation of SREBP. Cell. 2005 Jan 28;120(2):261-73.

Lindenmeyer CC, McCullough AJ. Which patients with nonalcoholic fatty liver disease should undergo liver biopsy? Cleveland Clinic journal of medicine. 2017 Apr;84(4):273.

Liu TW, Heden TD, Matthew Morris E, Fritsche KL, Vieira-Potter VJ, Thyfault JP. High-Fat Diet Alters Serum Fatty Acid Profiles in Obesity Prone Rats: Implications for InVitro Studies. Lipids. 2015 Oct;50(10):997-1008.

Liu Y, Lou X. Type 2 diabetes mellitus-related environmental factors and the gut microbiota: emerging evidence and challenges. Clinics. 2020;75.

Longato L, Tong M, Wands JR, de la Monte SM. High fat diet induced hepatic steatosis and insulin resistance: Role of dysregulated ceramide metabolism. Hepatology Research. 2012 Apr;42(4):412-27.

Louis P, Flint HJ. Formation of propionate and butyrate by the human colonic microbiota. Environmental microbiology. 2017 Jan;19(1):29-41.

Louis P, Hold GL, Flint HJ. The gut microbiota, bacterial metabolites and colorectal cancer. Nature reviews microbiology. 2014 Oct;12(10):661-72.

Lozupone CA, Stombaugh JI, Gordon JI, Jansson JK, Knight R. Diversity, stability and resilience of the human gut microbiota. Nature. 2012 Sep;489(7415):220.

Luo M, Mengos AE, Stubblefield TM, Mandarino LJ. High fat diet-induced changes in hepatic protein abundance in mice. Journal of Proteomics and Bioinformatics. 2012;5(3):60-6.

Lustgarten M, Muller FL, Van Remmen H. An objective appraisal of the free radical theory of aging. InHandbook of the Biology of Aging 2011 Jan 1 (pp. 177-202). Academic Press.

Luukkonen PK, Sädevirta S, Zhou Y, Kayser B, Ali A, Ahonen L, Lallukka S, Pelloux V, Gaggini M, Jian C, Hakkarainen A. Saturated fat is more metabolically harmful for the human liver than unsaturated fat or simple sugars. Diabetes care. 2018 Aug 1;41(8):1732-9.

Luukkonen PK, Sädevirta S, Zhou Y, Kayser B, Ali A, Ahonen L, Lallukka S, Pelloux V, Gaggini M, Jian C, Hakkarainen A. Saturated fat is more metabolically harmful for the human liver than unsaturated fat or simple sugars. Diabetes care. 2018 Aug 1;41(8):1732-9.

Lyall MJ, Cartier J, Richards JA et al. (2017) Methyl donor deficient diets cause distinct alterations in lipid metabolism but are poorly representative of human NAFLD. Wellcome open research 2, 67-67.

M. G. Langille, J. Zaneveld, J. G. Caporaso, D. McDonald, D. Knights, J. A. Reyes, J. C. Clemente, D. E. Burkepile, R. L. Vega Thurber, R. Knight, R. G. Beiko, C. Huttenhower, Nat. Biotechnol. 2013, 31, 814.

Macfarlane GT, Cummings JH, Allison C. Protein degradation by human intestinal bacteria. Microbiology. 1986 Jun 1;132(6):1647-56.

Madeira MS, Rolo EA, Lopes PA, Ramos DA, Alfaia CM, Pires VM, Martins SV, Pinto RM, Prates JA. Betaine and arginine supplementation of low protein diets improves plasma lipids but does not affect hepatic fatty acid composition and related gene expression profiling in pigs. Journal of the science of food and agriculture. 2018 Jan;98(2):598-608.

Magoč T, Salzberg SL. FLASH: fast length adjustment of short reads to improve genome assemblies. Bioinformatics. 2011 Sep 7;27(21):2957-63.

Mandard S, Müller M, Kersten S. Peroxisome proliferator-activated receptor α target genes. Cellular and Molecular Life Sciences CMLS. 2004 Feb 1;61(4):393-416.

Marchesi JR, Adams DH, Fava F, Hermes GD, Hirschfield GM, Hold G, Quraishi MN, Kinross J, Smidt H, Tuohy KM, Thomas LV. The gut microbiota and host health: a new clinical frontier. Gut. 2016 Feb 1;65(2):330-9.

Marciano F, Vajro P. Oxidative Stress and Gut Microbiota. InGastrointestinal Tissue 2017 Jan 1 (pp. 113-123). Academic Press.

Marcolin É, Forgiarini LF, Tieppo J, Dias AS, Freitas LA, Marroni NP. Methionine-and choline-deficient diet induces hepatic changes characteristic of non-alcoholic steatohepatitis. Arquivos de gastroenterologia. 2011 Mar;48(1):72-9.

Martin GG, Atshaves BP, Landrock KK, Landrock D, Schroeder F, Kier AB. Loss of L-FABP, SCP-2/SCP-x, or both induces hepatic lipid accumulation in female mice. Archives of biochemistry and biophysics. 2015 Aug 15; 580:41-9.

Mashek DG. Hepatic fatty acid trafficking: multiple forks in the road. Advances in nutrition. 2013 Nov 6;4(6):697-710.

Massart-Leën AM, Roets E, Peeters G, Verbeke R. Propionate for fatty acid synthesis by the mammary gland of the lactating goat. Journal of Dairy Science. 1983 Jul 1;66(7):1445-54.

Mato JM, Alonso C, Noureddin M, Lu SC. Biomarkers and subtypes of deranged lipid metabolism in non-alcoholic fatty liver disease. World journal of gastroenterology. 2019 Jun 28;25(24):3009.

Matsukawa A, Fukumoto T, Maeda T, Ohkawara S, Yoshinaga M. Detection and characterization of IL-1 receptor antagonist in tissues from healthy rabbits: IL-1 receptor antagonist is probably involved in health. Cytokine. 1997 May 1;9(5):307-15.

Matsuzaka T, Shimano H, Yahagi N, Kato T, Atsumi A, Yamamoto T, Inoue N, Ishikawa M, Okada S, Ishigaki N, Iwasaki H. Crucial role of a long-chain fatty acid elongase, Elovl6, in obesity-induced insulin resistance. Nature medicine. 2007 Oct;13(10):1193.

Matsuzaka T, Shimano H, Yahagi N, Yoshikawa T, Amemiya-Kudo M, Hasty AH, Okazaki H, Tamura Y, Iizuka Y, Ohashi K, Osuga JI. Cloning and characterization of a mammalian fatty acyl-CoA elongase as a lipogenic enzyme regulated by SREBPs. Journal of lipid research. 2002 Jun 1;43(6):911-20.

Matsuzaka T, Shimano H. Elovl6: a new player in fatty acid metabolism and insulin sensitivity. Journal of molecular medicine. 2009 Apr 1;87(4):379-84.

Mauvoisin D, Mounier C. Hormonal and nutritional regulation of SCD1 gene expression. Biochimie. 2011 Jan 1;93(1):78-86.

Mayneris-Perxachs J, Bolick DT, Leng J et al. (2016) Protein-and zinc-deficient diets modulate the murine microbiome and metabolic phenotype. The American journal of clinical nutrition 104, 1253-62.

McCullough AJ. Pathophysiology of nonalcoholic steatohepatitis. Journal of clinical gastroenterology. 2006 Mar 1;40: S17-29.

Mchiza ZJ, Steyn NP, Hill J, Kruger A, Schönfeldt H, Nel J, Wentzel-Viljoen E. A review of dietary surveys in the adult South African population from 2000 to 2015. Nutrients. 2015 Sep;7(9):8227-50.

McMahan RH, Wang XX, Cheng LL, Krisko T, Smith M, El Kasmi K, Pruzanski M, Adorini L, Golden-Mason L, Levi M, Rosen HR. Bile acid receptor activation modulates hepatic

monocyte activity and improves non-alcoholic fatty liver disease. Journal of Biological Chemistry. 2013 Apr 26;288(17):11761-70.

Meli R, Raso GM, Irace C, Simeoli R, Di Pascale A, Paciello O, Pagano TB, Calignano A, Colonna A, Santamaria R. High fat diet induces liver steatosis and early dysregulation of iron metabolism in rats. PLoS One. 2013 Jun 21;8(6): e66570.

Menezes AL, Pereira MP, Buzelle SL, dos Santos MP, de França SA, Baviera AM, Andrade CM, Garófalo MA, do Carmo Kettelhut I, Chaves VE, Kawashita NH. A low-protein, high-carbohydrate diet increases de novo fatty acid synthesis from glycerol and glycerokinase content in the liver of growing rats. Nutrition research. 2013 Jun 1;33(6):494-502.

Meyer BJ, Mann NJ, Lewis JL, Milligan GC, Sinclair AJ, Howe PR. Dietary intakes and food sources of omega-6 and omega-3 polyunsaturated fatty acids. Lipids. 2003 Apr;38(4):391-8.

Miele L, Valenza V, La Torre G, Montalto M, Cammarota G, Ricci R, Masciana R, Forgione A, Gabrieli ML, Perotti G, Vecchio FM. Increased intestinal permeability and tight junction alterations in nonalcoholic fatty liver disease. Hepatology. 2009 Jun;49(6):1877-87.

Mika A, Stepnowski P, Kaska L, Proczko M, Wisniewski P, Sledzinski M, Sledzinski T. A comprehensive study of serum odd-and branched-chain fatty acids in patients with excess weight. Obesity. 2016 Aug;24(8):1669-76.

Miquilena-Colina ME, Lima-Cabello E, Sánchez-Campos S, García-Mediavilla MV, Fernández-Bermejo M, Lozano-Rodríguez T, Vargas-Castrillón J, Buqué X, Ochoa B, Aspichueta P, González-Gallego J. Hepatic fatty acid translocase CD36 upregulation is associated with insulin resistance, hyperinsulinaemia and increased steatosis in non-alcoholic steatohepatitis and chronic hepatitis C. Gut. 2011 Oct 1;60(10):1394-402.

Mirmiran P, Amirhamidi Z, Ejtahed HS, Bahadoran Z, Azizi F. Relationship between diet and non-alcoholic fatty liver disease: a review article. Iranian journal of public health. 2017 Aug;46(8):1007.

Mitsuyoshi H, Yasui K, Harano Y, Endo M, Tsuji K, Minami M, Itoh Y, Okanoue T, Yoshikawa T. Analysis of hepatic genes involved in the metabolism of fatty acids and iron in nonalcoholic fatty liver disease. Hepatology Research. 2009 Apr;39(4):366-73.

Miyazaki T, Ohura T, Kobayashi M, Shigematsu Y, Yamaguchi S, Suzuki Y, Hata I, Aoki Y, Yang X, Minjares C, Haruta I. Fatal propionic acidemia in mice lacking propionyl-CoA carboxylase and its rescue by postnatal, liver-specific supplementation via a transgene. Journal of Biological Chemistry. 2001 Sep 21;276(38):35995-9.

Moreno-Fernandez ME, Giles DA, Stankiewicz TE, Sheridan R, Karns R, Cappelletti M, Lampe K, Mukherjee R, Sina C, Sallese A, Bridges JP. Peroxisomal β-oxidation regulates whole body metabolism, inflammatory vigor, and pathogenesis of nonalcoholic fatty liver disease. JCI insight. 2018 Mar 22;3(6).

Moreno-Fernández S, Garcés-Rimón M, Vera G, Astier J, Landrier J, Miguel M. High Fat/High Glucose Diet Induces Metabolic Syndrome in an Experimental Rat Model. Nutrients. 2018 Oct;10(10):1502.

Mostaza JM, Vega GL, Snell P, Grundy SM. Abnormal metabolism of free fatty acids in hypertriglyceridaemic men: apparent insulin resistance of adipose tissue. J Intern Med 1998; 243:265–274

Mouzaki M, Comelli EM, Arendt BM, Bonengel J, Fung SK, Fischer SE, McGilvray ID, Allard JP. Intestinal microbiota in patients with nonalcoholic fatty liver disease. Hepatology. 2013 Jul;58(1):120-7.

Mozaffarian D. Saturated fatty acids and type 2 diabetes: more evidence to re-invent dietary guidelines. The lancet Diabetes & endocrinology. 2014 Oct 1;2(10):770-2.

Muir K, Hazim A, He Y, Peyressatre M, Kim DY, Song X, Beretta L. Proteomic and lipidomic signatures of lipid metabolism in NASH-associated hepatocellular carcinoma. Cancer research. 2013 Aug 1;73(15):4722-31.

Mukai T, Egawa M, Takeuchi T, Yamashita H, Kusudo T. Silencing of FABP 1 ameliorates hepatic steatosis, inflammation, and oxidative stress in mice with nonalcoholic fatty liver disease. FEBS open bio. 2017 Jul;7(7):1009-16.

Mullis KB, Erlich HA, Arnheim N, Horn GT, Saiki RK, Scharf SJ, inventors; Cetus Corp, assignee. Process for amplifying, detecting, and/or-cloning nucleic acid sequences. United States patent US 4,683,195. 1987 Jul 28.

Myers-Morales T, Bussell KM, D'Orazio SE. Fecal transplantation does not transfer either susceptibility or resistance to food borne listeriosis in C57BL/6 and BALB/c/By mice. F1000Research. 2013;2.

N.G. Forouhi, A. Koulman, S.J. Sharp, F. Imamura, J. Kröger *et al.* Differences in the prospective association between individual plasma phospholipid saturated fatty acids and incident type 2 diabetes: the EPIC-InterAct case-cohort study Lancet Diabetes Endocrinol (2014), p. 2

Nassir F, Ibdah JA. Role of mitochondria in non-alcoholic fatty liver disease. International journal of molecular sciences. 2014 May;15(5):8713-42.

Nault jc, bioulac–sage pa, zucman–rossi je. Reviews in basic and clinical gastroenterology and hepatology. Gastroenterology. 2013; 144:888-902.

Neish AS. Microbes in gastrointestinal health and disease. Gastroenterology. 2009 Jan 1;136(1):65-80.

Ni Y, Zhao L, Yu H, Ma X, Bao Y, Rajani C, et al. Circulating unsaturated fatty acids delineate the metabolic status of obese individuals. EBioMedicine. 2015;2(10):1513-22.

Nicholson A, Reifsnyder PC, Malcolm RD, Lucas CA, MacGregor GR, Zhang W, Leiter EH. Diet-induced obesity in Two C57BL/6 substrains with intact or mutant nicotinamide nucleotide transhydrogenase (Nnt) gene. Obesity. 2010 Oct;18(10):1902-5.

Nicolaides N, Ray T. Skin lipids. III. Fatty chains in skin lipids. The use ofvernix caseosa to differentiate between endogenous and exogenous components in human skin surface lipid. Journal of the American Oil Chemists' Society. 1965 Aug;42(8):702-7.

Niederreiter L, Tilg H. Cytokines and fatty liver diseases. Liver Research. 2018 Mar 1;2(1):14-20.

Nseir W, Hellou E, Assy N. Role of diet and lifestyle changes in nonalcoholic fatty liver disease. World journal of gastroenterology: WJG. 2014 Jul 28;20(28):9338.

Obeid R. The metabolic burden of methyl donor deficiency with focus on the betaine homocysteine methyltransferase pathway. Nutrients. 2013 Sep;5(9):3481-95.

Ogawa Y, Imajo K, Honda Y, Kessoku T, Tomeno W, Kato S, Fujita K, Yoneda M, Saito S, Saigusa Y, Hyogo H. Palmitate-induced lipotoxicity is crucial for the pathogenesis of nonalcoholic fatty liver disease in cooperation with gut-derived endotoxin. Scientific reports. 2018 Jul 27;8(1):11365.

Oliphant K, Allen-Vercoe E. Macronutrient metabolism by the human gut microbiome: major fermentation by-products and their impact on host health. Microbiome. 2019 Dec;7(1):91.

Oosterveer MH, Van Dijk TH, Tietge UJ, Boer T, Havinga R, Stellaard F, Groen AK, Kuipers F, Reijngoud DJ. High fat feeding induces hepatic fatty acid elongation in mice. PloS one. 2009 Jun 26;4(6): e6066.

Ore A, Akinloye OA. Oxidative stress and antioxidant biomarkers in clinical and experimental models of non-alcoholic fatty liver disease. Medicina. 2019 Feb;55(2):26.

Oya J, Nakagami T, Sasaki S, Jimba S, Murakami K, Kasahara T, Wasada T, Sekiguchi H, Hasegawa M, Endo Y, Iwamoto Y. Intake of n-3 polyunsaturated fatty acids and non-alcoholic fatty liver disease: a cross-sectional study in Japanese men and women. European journal of clinical nutrition. 2010 Oct;64(10):1179.

Pachikian BD, Neyrinck AM, Cani PD, Portois L, Deldicque L, De Backer FC, Bindels LB, Sohet FM, Malaisse WJ, Francaux M, Carpentier YA. Hepatic steatosis in n-3 fatty acid depleted mice: focus on metabolic alterations related to tissue fatty acid composition. BMC physiology. 2008 Dec 1;8(1):21.

Paniagua JA, De La Sacristana AG, Romero I, Vidal-Puig A, Latre JM, Sanchez E, Perez-Martinez P, Lopez-Miranda J, Perez-Jimenez F. Monounsaturated fat–rich diet prevents central body fat distribution and decreases postprandial adiponectin expression induced by a carbohydrate-rich diet in insulin-resistant subjects. Diabetes care. 2007 Jul 1;30(7):1717-23.

Parekh PJ, Balart LA, Johnson DA. The influence of the gut microbiome on obesity, metabolic syndrome and gastrointestinal disease. Clinical and translational gastroenterology. 2015 Jun;6(6): e91.

Park MY, Mun ST. Dietary carnosic acid suppresses hepatic steatosis formation via regulation of hepatic fatty acid metabolism in high-fat diet-fed mice. Nutrition research and practice. 2013 Aug 1;7(4):294-301.

Paschos P, Paletas K. Non-alcoholic fatty liver disease and metabolic syndrome. Hippokratia. 2009 Jan;13(1):9.

Patterson E, Wall R, Fitzgerald GF, Ross RP, Stanton C. Health implications of high dietary omega-6 polyunsaturated fatty acids. Journal of nutrition and metabolism. 2012 Apr 5;2012.

Perdomo CM, Frühbeck G, Escalada J. Impact of nutritional changes on nonalcoholic fatty liver disease. Nutrients. 2019 Mar;11(3):677.

Perdomo L, Beneit N, Otero YF, Escribano Ó, Díaz-Castroverde S, Gómez-Hernández A, Benito M. Protective role of oleic acid against cardiovascular insulin resistance and in the early and late cellular atherosclerotic process. Cardiovascular diabetology. 2015 Dec;14(1):75.

Pérez-Carreras, M., Del Hoyo, P., Martín, M. A., Rubio, J. C., Martín, A., Castellano, G., . . . Solis-Herruzo, J. A. (2003). Defective hepatic mitochondrial respiratory chain in patients with nonalcoholic steatohepatitis. Hepatology, 38(4), 999-1007.

Perumpail BJ, Khan MA, Yoo ER, Cholankeril G, Kim D, Ahmed A. Clinical epidemiology and disease burden of nonalcoholic fatty liver disease. World journal of gastroenterology. 2017 Dec 21;23(47):8263.

Peter A, Cegan A, Wagner S, Elcnerova M, Königsrainer A, Königsrainer I, Häring HU, Schleicher ED, Stefan N. Relationships between hepatic stearoyl-CoA desaturase-1 activity and mRNA expression with liver fat content in humans. American Journal of Physiology-Endocrinology and Metabolism. 2010 Nov 2;300(2): E321-6.

Peterson DW, Hayes JM. Signal-to-noise ratios in mass spectroscopic ion-current-measurement systems. InContemporary topics in analytical and clinical chemistry 1978 (pp. 217-252). Springer, Boston, MA.

Pfeuffer M, Jaudszus A. Pentadecanoic and heptadecanoic acids: multifaceted odd-chain fatty acids. Advances in nutrition. 2016 Jul 11;7(4):730-4.

Pooya, S., S. Blaise, M. Moreno Garcia, et al. (2012). Methyl donor deficiency impairs fatty acid oxidation through PGC-1alpha hypomethylation and decreased ER-alpha, ERR-alpha, and HNF-4alpha in the rat liver. J Hepatol 57, 344-351.

Porstmann T, Santos CR, Griffiths B, Cully M, Wu M, Leevers S, Griffiths JR, Chung YL, Schulze A. SREBP activity is regulated by mTORC1 and contributes to Akt-dependent cell growth. Cell metabolism. 2008 Sep 3;8(3):224-36.

Postic C, Girard J (2008) Contribution of de novo fatty acid synthesis to hepatic steatosis and insulin resistance: lessons from genetically engineered mice. J Clin Invest 118: 829–838.

Prakash S, Rodes L, Coussa-Charley M, Tomaro-Duchesneau C. Gut microbiota: next frontier in understanding human health and development of biotherapeutics. Biologics: targets & therapy. 2011; 5:71.

Prigge JR, Coppo L, Martin SS, Ogata F, Miller CG, Bruschwein MD, Orlicky DJ, Shearn CT, Kundert JA, Lytchier J, Herr AE. Hepatocyte hyperproliferation upon liver-specific co-disruption of thioredoxin-1, thioredoxin reductase-1, and glutathione reductase. Cell reports. 2017 Jun 27;19(13):2771-81.

Properzi C, O'Sullivan TA, Sherriff JL, Ching HL, Jeffrey GP, Buckley RF, Tibballs J, MacQuillan GC, Garas G, Adams LA. Ad Libitum Mediterranean and Low-Fat Diets Both Significantly Reduce Hepatic Steatosis: A Randomized Controlled Trial. Hepatology. 2018 Nov 1;68(5):1741-54.

Puri P, Baillie RA, Wiest MM, Mirshahi F, Choudhury J, Cheung O, Sargeant C, Contos MJ, Sanyal AJ. A lipidomic analysis of nonalcoholic fatty liver disease. Hepatology. 2007 Oct;46(4):1081-90.

Putti R, Migliaccio V, Sica R, Lionetti L. Skeletal muscle mitochondrial bioenergetics and morphology in high fat diet induced obesity and insulin resistance: focus on dietary fat source. Frontiers in physiology. 2016 Jan 20; 6:426.

Qiao XL, Dong Y, Feng XY, Wang HQ, Jiang CM. Mechanism of high-fat diet-induced non-alcoholic fatty liver disease. Journal of biological regulators and homeostatic agents. 2019 Jan;33(1).

Qin H, Zhang X, Ye F, Zhong L. High-fat diet-induced changes in liver thioredoxin and thioredoxin reductase as a novel feature of insulin resistance. FEBS open bio. 2014 Jan 1; 4:928-35.

Qin J, Li R, Raes J, Arumugam M, Burgdorf KS, Manichanh C, Nielsen T, Pons N, Levenez F, Yamada T, Mende DR. A human gut microbial gene catalogue established by metagenomic sequencing. nature. 2010 Mar;464(7285):59.

Raatz SK, Bibus D, Thomas W, Kris-Etherton P. Total fat intake modifies plasma fatty acid composition in humans. The Journal of nutrition. 2001 Feb 1;131(2):231-4.

Raina N, Jeejeebhoy KN. Effect of low-protein diet and protein supplementation on the expressions of TNF-α, TNFR-I, and TNFR-II in organs and muscle of LPS-injected rats. American Journal of Physiology-Endocrinology and Metabolism. 2004 Mar;286(3): E481-7.

Rajilić-Stojanović M, de Vos WM. The first 1000 cultured species of the human gastrointestinal microbiota. FEMS microbiology reviews. 2014 Sep 1;38(5):996-1047.

Ralston, J.C.; Zulyniak, M.A.; Nielsen, D.E.; Clarke, S.; Badawi, A.; El-Sohemy, A.; Ma, D.W.; Mutch, D.M. Ethnic- and sex-specific associations between plasma fatty acids and markers of insulin resistance in healthy young adults. Nutr. Metab. 2013, 10, 42. [CrossRef]

Ran-Ressler RR, Devapatla S, Lawrence P, Brenna JT. Branched chain fatty acids are constituents of the normal healthy newborn gastrointestinal tract. Pediatric research. 2008 Dec;64(6):605.

Ratnayake WN, Sarwar G, Laffey P. Influence of dietary protein and fat on serum lipids and metabolism of essential fatty acids in rats. British Journal of Nutrition. 1997 Sep;78(3):459-67.

Reddy JK, Hashimoto T. Peroxisomal β-oxidation and peroxisome proliferator–activated receptor α: an adaptive metabolic system. Annual review of nutrition. 2001 Jul;21(1):193-230.

Redinger, RN. The pathophysiology of obesity and its clinical manifestations. *Gastroenterol Hepatol* 2007; **3**: 856– 863.

Reichardt N, Duncan SH, Young P, Belenguer A, Leitch CM, Scott KP, Flint HJ, Louis P. Phylogenetic distribution of three pathways for propionate production within the human gut microbiota. The ISME journal. 2014 Jun;8(6):1323.

Rietman A, Sluik D, Feskens EJ, Kok FJ, Mensink M. Associations between dietary factors and markers of NAFLD in a general Dutch adult population. European journal of clinical nutrition. 2018 Jan;72(1):117.

Rietman A. Effect of dietary protein on lipid and glucose metabolism: implications for metabolic health. Wageningen University; 2015.

Robertson KL, Rowland NE. Effect of two types of environmental enrichment for singly housed mice on food intake and weight gain. Lab animal. 2005 Oct;34(9):29-32.

Robinson JL, Harding SV, Brunton JA, Bertolo RF. Dietary methyl donors contribute to whole-body protein turnover and protein synthesis in skeletal muscle and the jejunum in neonatal piglets. The Journal of nutrition. 2016 Aug 31;146(10):2007-12.

Roche HM. Fatty acids and the metabolic syndrome. Proceedings of the Nutrition Society. 2005 Feb;64(1):23-9.

Rohr MW, Narasimhulu CA, Rudeski-Rohr TA, Parthasarathy S. Negative effects of a high-fat diet on intestinal permeability: a review. Advances in Nutrition. 2019 Jul 3.

Rosen CE, Palm NW. Functional Classification of the Gut Microbiota: The Key to Cracking the Microbiota Composition Code: Functional classifications of the gut microbiota reveal previously hidden contributions of indigenous gut bacteria to human health and disease. BioEssays. 2017 Dec;39(12):1700032.

Rosen CE[1], Palm NW[1].Functional Classification of the Gut Microbiota: The Key to Cracking the Microbiota Composition Code: Functional classifications of the gut microbiota reveal previously hidden contributions of indigenous gut bacteria to human health and disease.

Rosqvist F, Iggman D, Kullberg J, Cedernaes J, Johansson HE, Larsson A, Johansson L, Ahlström H, Arner P, Dahlman I, Risérus U. Overfeeding polyunsaturated and saturated fat causes distinct effects on liver and visceral fat accumulation in humans. Diabetes. 2014 Jul 1;63(7):2356-68.

Rosqvist F, Iggman D, Kullberg J, Cedernaes J, Johansson HE, Larsson A, Johansson L, Ahlström H, Arner P, Dahlman I, Risérus U. Overfeeding polyunsaturated and saturated fat causes distinct effects on liver and visceral fat accumulation in humans. Diabetes. 2014 Jul 1;63(7):2356-68.

Ruotolo G, Howard BV. Dyslipidemia of the metabolic syndrome. Current cardiology reports. 2002;4(6):494-500.

Russell DW. The enzymes, regulation, and genetics of bile acid synthesis. Annual review of biochemistry. 2003 Jul;72(1):137-74.

Russell WR, Duncan SH, Scobbie L, Duncan G, Cantlay L, Calder AG, Anderson SE, Flint HJ. Major phenylpropanoid-derived metabolites in the human gut can arise from microbial fermentation of protein. Molecular nutrition & food research. 2013 Mar;57(3):523-35.

Russell, W. R., Gratz, S. W., Duncan, S. H., Holtrop, G., Ince, J., Scobbie, L., . . . Wallace, R. J. (2011). High-protein, reduced-carbohydrate weight-loss diets promote metabolite profiles

likely to be detrimental to colonic health–. The American journal of clinical nutrition, 93(5), 1062-1072.

Russo GL. Dietary n− 6 and n− 3 polyunsaturated fatty acids: from biochemistry to clinical implications in cardiovascular prevention. Biochemical pharmacology. 2009 Mar 15;77(6):937-46.

Rustan AC, Drevon CA. Fatty acids: structures and properties. e LS. 2001 May 30.

Rustan AC, Drevon CA. Fatty Acids: Structures and Properties. London: Encyclopedia of Life Sciences.2005

Ryan MC, Itsiopoulos C, Thodis T, Ward G, Trost N, Hofferberth S, O'Dea K, Desmond PV, Johnson NA, Wilson AM. The Mediterranean diet improves hepatic steatosis and insulin sensitivity in individuals with non-alcoholic fatty liver disease. Journal of hepatology. 2013 Jul 1;59(1):138-43.

Ryan MC, Itsiopoulos C, Thodis T, Ward G, Trost N, Hofferberth S, O'Dea K, Desmond PV, Johnson NA, Wilson AM. The Mediterranean diet improves hepatic steatosis and insulin sensitivity in individuals with non-alcoholic fatty liver disease. Journal of hepatology. 2013 Jul 1;59(1):138-43.

Sacks FM, Campos H. Polyunsaturated fatty acids, inflammation, and cardiovascular disease: time to widen our view of the mechanisms. 2006

Salimon, J., et al. (2017). "An accurate and reliable method for identification and quantification of fatty acids and trans fatty acids in food fats samples using gas chromatography." Arabian Journal of Chemistry **10**: S1875-S1882.

Salt WB. Nonalcoholic fatty liver disease (NAFLD): a comprehensive review. JOURNAL OF INSURANCE MEDICINE-NEW YORK THEN DENVER--. 2004;36(1):27-41.

Salter AM, Tarling EJ. Regulation of gene transcription by fatty acids. Animal. 2007 Oct;1(9):1314-20.

Sampath H, Miyazaki M, Dobrzyn A, Ntambi JM. Stearoyl-CoA desaturase-1 mediates the pro-lipogenic effects of dietary saturated fat. Journal of Biological Chemistry. 2007 Jan 26;282(4):2483-93.

Sampath H, Ntambi JM. Polyunsaturated fatty acid regulation of genes of lipid metabolism. Annu. Rev. Nutr. 2005 Jul 11; 25:317-40.

Sanders FW, Griffin JL. De novo lipogenesis in the liver in health and disease: more than just a shunting yard for glucose. Biological Reviews. 2016 May;91(2):452-68.

Santaren ID, Watkins SM, Liese AD, Wagenknecht LE, Rewers MJ, Haffner SM, Lorenzo C, Hanley AJ. Serum pentadecanoic acid (15: 0), a short-term marker of dairy food intake, is inversely associated with incident type 2 diabetes and its underlying disorders. The American journal of clinical nutrition. 2014 Oct 8;100(6):1532-40.

Sassa T, Kihara A. Metabolism of very long-chain fatty acids: genes and pathophysiology. Biomolecules & therapeutics. 2014 Mar;22(2):83.

Sattar N, Forrest E, Preiss D. Non-alcoholic fatty liver disease. bmj. 2014 Jul 29;349: g4596.

Schloss PD, Handelsman J. Status of the microbial census. Microbiol. Mol. Biol. Rev. 2004 Dec 1;68(4):686-91.

Schrader M, Grille S, Fahimi HD, Islinger M. Peroxisome interactions and cross-talk with other subcellular compartments in animal cells. In Peroxisomes and their Key Role in Cellular Signaling and Metabolism 2013 (pp. 1-22). Springer, Dordrecht.

Schrauwen P. High-fat diet, muscular lipotoxicity and insulin resistance. Proceedings of the Nutrition Society. 2007 Feb;66(1):33-41.

Schwarz J, Tome D, Baars A, Hooiveld GJ, Müller M. Dietary protein affects gene expression and prevents lipid accumulation in the liver in mice. PLoS One. 2012 Oct 23;7(10): e47303.

Schwarz JM, Neese RA, Turner S, Dare D, Hellerstein MK. Short-term alterations in carbohydrate energy intake in humans. Striking effects on hepatic glucose production, de novo lipogenesis, lipolysis, and whole-body fuel selection. The Journal of clinical investigation. 1995 Dec 1;96(6):2735-43.

Schwiertz A, Taras D, Schäfer K, Beijer S, Bos NA, Donus C, Hardt PD. Microbiota and SCFA in lean and overweight healthy subjects. Obesity. 2010 Jan;18(1):190-5.

Schwingshackl L, Hoffmann G. Monounsaturated fatty acids and risk of cardiovascular disease: synopsis of the evidence available from systematic reviews and meta-analyses. Nutrients. 2012 Dec;4(12):1989-2007.

Schwingshackl L, Strasser B, Hoffmann G. Effects of monounsaturated fatty acids on cardiovascular risk factors: a systematic review and meta-analysis. Annals of Nutrition and Metabolism. 2011;59(2-4):176-86.

Scorletti E, Bhatia L, McCormick KG, Clough GF, Nash K, Hodson L, Moyses HE, Calder PC, Byrne CD, Welcome Study Investigators, Sheron N. Effects of purified eicosapentaenoic and docosahexaenoic acids in nonalcoholic fatty liver disease: results from the Welcome* study. Hepatology. 2014 Oct;60(4):1211-21.

Scott KP, Martin JC, Campbell G, Mayer CD, Flint HJ. Whole-genome transcription profiling reveals genes up-regulated by growth on fucose in the human gut bacterium "Roseburia inulinivorans". Journal of bacteriology. 2006 Jun 15;188(12):4340-9.

Seo YY, Cho YK, Bae JC, Seo MH, Park SE, Rhee EJ, Park CY, Oh KW, Park SW, Lee WY. Tumor necrosis factor-α as a predictor for the development of nonalcoholic fatty liver disease: a 4-year follow-up study. Endocrinology and Metabolism. 2013 Mar 1;28(1):41-5.

Sethi JK, Vidal-Puig AJ. Thematic review series: adipocyte biology. Adipose tissue function and plasticity orchestrate nutritional adaptation. Journal of lipid research. 2007 Jun 1;48(6):1253-62.

Sevastianova K, Santos A, Kotronen A, Hakkarainen A, Makkonen J, Silander K, Peltonen M, Romeo S, Lundbom J, Lundbom N, Olkkonen VM. Effect of short-term carbohydrate overfeeding and long-term weight loss on liver fat in overweight humans. The American journal of clinical nutrition. 2012 Oct 1;96(4):727-34.

Shalev A. Minireview: Thioredoxin-interacting protein: regulation and function in the pancreatic β-cell. Molecular endocrinology. 2014 Aug 1;28(8):1211-20.

Sharpton SR, Ajmera V, Loomba R. Emerging role of the gut microbiome in nonalcoholic fatty liver disease: from composition to function. Clinical Gastroenterology and Hepatology. 2019 Jan 1;17(2):296-306.

Sheedfar F, Sung MM, Aparicio-Vergara M, Kloosterhuis NJ, Miquilena-Colina ME, Vargas-Castrillón J, Febbraio M, Jacobs RL, de Bruin A, Vinciguerra M, García-Monzón C. Increased hepatic CD36 expression with age is associated with enhanced susceptibility to nonalcoholic fatty liver disease. Aging (Albany NY). 2014 Apr;6(4):281.

Shefer-Weinberg D, Sasson S, Schwartz B, Argov-Argaman N, Tirosh O. Deleterious effect of n-3 polyunsaturated fatty acids in non-alcoholic steatohepatitis in the fat-1 mouse model. Clinical Nutrition Experimental. 2017 Apr 1; 12:37-49.

Shibata R, Gotoh N, Kubo A, Kanda J, Nagai T, Mizobe H, Yoshinaga K, Kojima K, Watanabe H, Wada S. Comparison of catabolism rate of fatty acids to carbon dioxide in mice. European Journal of Lipid Science and Technology. 2012 Dec;114(12):1340-4.

Shrago E. Dietary and nutritional aspects of fatty acid binding proteins. Chemistry and physics of lipids. 1985 Aug 30;38(1-2):131-5.

Sies H, Berndt C, Jones DP. Oxidative stress. Annual review of biochemistry. 2017 Jun 20; 86:715-48.

Silbernagel G, Kovarova M, Cegan A, Machann J, Schick F, Lehmann R, Häring HU, Stefan N, Schleicher E, Fritsche A, Peter A. High hepatic SCD1 activity is associated with low liver fat content in healthy subjects under a lipogenic diet. The Journal of Clinical Endocrinology & Metabolism. 2012 Dec 1;97(12): E2288-92.

Simioni C, Zauli G, Martelli AM, Vitale M, Sacchetti G, Gonelli A, Neri LM. Oxidative stress: role of physical exercise and antioxidant nutraceuticals in adulthood and aging. Oncotarget. 2018 Mar 30;9(24):17181.

Simões, I. C., Fontes, A., Pinton, P., Zischka, H., & Wieckowski, M. R. (2018). Mitochondria in non-alcoholic fatty liver disease. The international journal of biochemistry & cell biology, 95, 93-99.

Singh RK, Chang HW, Yan D, Lee KM, Ucmak D, Wong K, Abrouk M, Farahnik B, Nakamura M, Zhu TH, Bhutani T. Influence of diet on the gut microbiome and implications for human health. Journal of translational medicine. 2017 Dec;15(1):73.

Sjögren P, Sierra-Johnson J, Gertow K, Rosell M, Vessby B, De Faire U, Hamsten A, Hellenius ML, Fisher RM. Fatty acid desaturases in human adipose tissue: relationships between gene expression, desaturation indexes and insulin resistance. Diabetologia. 2008 Feb 1;51(2):328-35.

Smith JJ, Aitchison JD. Peroxisomes take shape. Nature reviews Molecular cell biology. 2013 Dec;14(12):803-17.

Stahl A, Hirsch DJ, Gimeno RE, Punreddy S, Ge P, Watson N, Patel S, Kotler M, Raimondi A, Tartaglia LA, Lodish HF. Identification of the major intestinal fatty acid transport protein. Molecular cell. 1999 Sep 1;4(3):299-308.

Stefan N, Peter A, Cegan A, Staiger H, Machann J, Schick F, Claussen CD, Fritsche A, Häring HU, Schleicher E. Low hepatic stearoyl-CoA desaturase 1 activity is associated with fatty liver and insulin resistance in obese humans. Diabetologia. 2008 Apr 1;51(4):648-56.

Steliou K, Boosalis MS, Perrine SP, Sangerman J, Faller DV. Butyrate histone deacetylase inhibitors. BioResearch open access. 2012 Aug 1;1(4):192-8.

Sumida Y, Niki E, Naito Y, Yoshikawa T. Involvement of free radicals and oxidative stress in NAFLD/NASH. Free radical research. 2013 Nov 1;47(11):869-80.

Sun H, Jiang T, Wang S, He B, Zhang Y, Piao D, Yu C, Wu N, Han P. The effect of LXRα, ChREBP and Elovl6 in liver and white adipose tissue on medium-and long-chain fatty acid diet-induced insulin resistance. Diabetes research and clinical practice. 2013 Dec 1;102(3):183-92.

Sun Q, Ma J, Campos H, Hu FB. Plasma and erythrocyte biomarkers of dairy fat intake and risk of ischemic heart disease. The American journal of clinical nutrition. 2007 Oct 1;86(4):929-37.

Tack CJ, Stienstra R, Joosten LA, Netea MG. Inflammation links excess fat to insulin resistance: the role of the interleukin-1 family. Immunological reviews. 2012 Sep;249(1):239-52.

Takahashi Y, Fukusato T. Histopathology of nonalcoholic fatty liver disease/nonalcoholic steatohepatitis. World journal of gastroenterology: WJG. 2014 Nov 14;20(42):15539.

Tanaka S, Ishihara N, Suzuki S, Watanabe Y, Nagayama D, Yamaguchi T, Ohira M, Saiki A, Tanaka T, Tatsuno I. Fatty acid desaturase 2 is up-regulated by the treatment with statin through geranylgeranyl pyrophosphate-dependent Rho kinase pathway in HepG2 cells. Scientific reports. 2019 Jul 10;9(1):10009.

Tarantino G, Finelli C. Lipids, Low-Grade Chronic Inflammation and NAFLD: A Ménage À Trois? InHandbook of Lipids in Human Function 2016 Jan 1 (pp. 731-759). AOCS Press.

Tartaglia LA, Goeddel DV. Two TNF receptors. Immunology today. 1992 Jan 1;13(5):151-3.

Thavarajah, R., Mudimbaimannar, V. K., Elizabeth, J., Rao, U. K., & Ranganathan, K. (2012). Chemical and physical basics of routine formaldehyde fixation. Journal of oral and maxillofacial pathology: JOMFP, 16(3), 400.

Thies F, Nebe-von-Caron G, Powell JR, Yaqoob P, Newsholme EA, Calder PC. Dietary supplementation with γ-linolenic acid or fish oil decreases T lymphocyte proliferation in healthy older humans. The Journal of nutrition. 2001 Jul 1;131(7):1918-27.

Thornton, B., & Basu, C. (2011). Real-time PCR (qPCR) primer design using free online software. *Biochemistry and Molecular Biology Education*, *39*(2), 145-154.

Tian X, Hellman J, Prakash A. Elevated gut microbiome-derived propionate levels are associated with reduced sterile lung inflammation and bacterial immunity in mice. Frontiers in microbiology. 2019;10:159.

Tilg H, Moschen AR. Inflammatory mechanisms in the regulation of insulin resistance. Molecular medicine. 2008 Mar 1;14(3-4):222-31.

Titchenell PM, Quinn WJ, Lu M, Chu Q, Lu W, Li C, Chen H, Monks BR, Chen J, Rabinowitz JD, Birnbaum MJ. Direct hepatocyte insulin signaling is required for lipogenesis but is dispensable for the suppression of glucose production. Cell metabolism. 2016 Jun 14;23(6):1154-66.

Tojo R, Suárez A, Clemente MG, de los Reyes-Gavilán CG, Margolles A, Gueimonde M, Ruas-Madiedo P. Intestinal microbiota in health and disease: role of bifidobacteria in gut homeostasis. World journal of gastroenterology: WJG. 2014 Nov 7;20(41):15163.

Tomas J, Mulet C, Saffarian A, Cavin JB, Ducroc R, Regnault B, Tan CK, Duszka K, Burcelin R, Wahli W, Sansonetti PJ. High-fat diet modifies the PPAR-γ pathway leading to disruption of microbial and physiological ecosystem in murine small intestine. Proceedings of the National Academy of Sciences. 2016 Oct 4;113(40): E5934-43.

Tonelli C, Chio II, Tuveson DA. Transcriptional regulation by Nrf2. Antioxidants & redox signaling. 2018 Oct 23;29(17):1727-45.

Tonelli C, Chio II, Tuveson DA. Transcriptional regulation by Nrf2. Antioxidants & redox signaling. 2018 Oct 23;29(17):1727-45.

Tosi F, Sartori F, Guarini P, Olivieri O, Martinelli N. Delta-5 and delta-6 desaturases: crucial enzymes in polyunsaturated fatty acid-related pathways with pleiotropic influences in health and disease. InOxidative Stress and Inflammation in Non-communicable Diseases-Molecular Mechanisms and Perspectives in Therapeutics 2014 (pp. 61-81). Springer, Cham.

Tranchida F, Tchiakpe L, Rakotoniaina Z, Deyris V, Ravion O, Hiol A. Long-term high fructose and saturated fat diet affects plasma fatty acid profile in rats. Journal of Zhejiang University Science B. 2012 Apr 1;13(4):307-17.

Turnbaugh PJ, Hamady M, Yatsunenko T, Cantarel BL, Duncan A, Ley RE, Sogin ML, Jones WJ, Roe BA, Affourtit JP, Egholm M. A core gut microbiome in obese and lean twins. nature. 2009 Jan;457(7228):480.

Turnbaugh PJ, Ley RE, Mahowald MA, Magrini V, Mardis ER, Gordon JI. An obesity-associated gut microbiome with increased capacity for energy harvest. nature. 2006 Dec;444(7122):1027.

Turroni F, Milani C, Duranti S, Lugli GA, Bernasconi S, Margolles A, Di Pierro F, van Sinderen D, Ventura M. The infant gut microbiome as a microbial organ influencing host well-being. Italian Journal of Pediatrics. 2020 Dec;46(1):1-3.

Ueland PM (2011) Choline and betaine in health and disease. Journal of inherited metabolic disease 34, 3-15.

Utzschneider KM, Kahn SE. The role of insulin resistance in nonalcoholic fatty liver disease. The Journal of Clinical Endocrinology & Metabolism. 2006 Dec 1;91(12):4753-61.

Valdes AM, Walter J, Segal E, Spector TD. Role of the gut microbiota in nutrition and health. Bmj. 2018 Jun 13;361: k2179.

Valenzuela R, Ortiz M, Hernández-Rodas MC, Echeverría F, Videla LA. Targeting n-3 Polyunsaturated Fatty Acids in Non-alcoholic Fatty Liver Disease. Current medicinal chemistry. 2019.

Valko M, Leibfritz D, Moncol J, Cronin MT, Mazur M, Telser J. Free radicals and antioxidants in normal physiological functions and human disease. The international journal of biochemistry & cell biology. 2007 Jan 1;39(1):44-84.

van den Berg EH, Flores-Guerrero JL, Gruppen EG, de Borst MH, Wolak-Dinsmore J, Connelly MA, Bakker SJ, Dullaart RP. Non-Alcoholic Fatty Liver Disease and Risk of Incident Type 2 Diabetes: Role of Circulating Branched-Chain Amino Acids. Nutrients. 2019 Mar;11(3):705.

van Zutphen T, Ciapaite J, Bloks VW, Ackereley C, Gerding A, Jurdzinski A, de Moraes RA, Zhang L, Wolters JC, Bischoff R, Wanders RJ. Malnutrition-associated liver steatosis and ATP depletion is caused by peroxisomal and mitochondrial dysfunction. Journal of hepatology. 2016 Dec 1;65(6):1198-208.

Velázquez KT, Enos RT, Bader JE, Sougiannis AT, Carson MS, Chatzistamou I, Carson JA, Nagarkatti PS, Nagarkatti M, Murphy EA. Prolonged high-fat-diet feeding promotes non-alcoholic fatty liver disease and alters gut microbiota in mice. World journal of hepatology. 2019 Aug 27;11(8):619.

Venegas DP, Marjorie K, Landskron G, González MJ, Quera R, Dijkstra G, Harmsen HJ, Faber KN, Hermoso MA. Short chain fatty acids (SCFAs)-mediated gut epithelial and immune regulation and its relevance for inflammatory bowel diseases. Frontiers in immunology. 2019;10.

Vital M, Howe AC, Tiedje JM. Revealing the bacterial butyrate synthesis pathways by analyzing (meta) genomic data. MBio. 2014 May 1;5(2): e00889-14.

Vlaeminck B, Fievez V, Cabrita AR, Fonseca AJ, Dewhurst RJ. Factors affecting odd-and branched-chain fatty acids in milk: A review. Animal feed science and technology. 2006 Dec 15;131(3-4):389-417.

Wagenmakers AJ, Frayn KN, Arner P, Yki-Järvinen H. Fatty acid metabolism in adipose tissue, muscle and liver in health and disease. Essays in biochemistry. 2006 Nov 27; 42:89-103.

Wallenius V, Wallenius K, Ahrén B, Rudling M, Carlsten H, Dickson SL, Ohlsson C, Jansson JO. Interleukin-6-deficient mice develop mature-onset obesity. Nature medicine. 2002 Jan;8(1):75.

Wan M, Leavens KF, Saleh D, Easton RM, Guertin DA, Peterson TR, Kaestner KH, Sabatini DM, Birnbaum MJ. Postprandial hepatic lipid metabolism requires signaling through Akt2

independent of the transcription factors FoxA2, FoxO1, and SREBP1c. Cell metabolism. 2011 Oct 5;14(4):516-27.

Wanders RJ. Metabolic functions of peroxisomes in health and disease. Biochimie. 2014 Mar 1; 98:36-44.

Wang Q, Garrity GM, Tiedje JM, Cole JR. Naive Bayesian classifier for rapid assignment of rRNA sequences into the new bacterial taxonomy. Appl. Environ. Microbiol. 2007 Aug 15;73(16):5261-7.

Waqar AB, Koike T, Yu Y, Inoue T, Aoki T, Liu E, Fan J. High-fat diet without excess calories induces metabolic disorders and enhances atherosclerosis in rabbits. Atherosclerosis. 2010 Nov 1;213(1):148-55.

Watkins AJ, Sinclair KD. Paternal low protein diet affects adult offspring cardiovascular and metabolic function in mice. American Journal of Physiology-Heart and Circulatory Physiology. 2014 Mar 21;306(10):H1444-52.

Webb LA, Sadri H, von Soosten D, Dänicke S, Egert S, Stehle P, Sauerwein H. Changes in tissue abundance and activity of enzymes related to branched-chain amino acid catabolism in dairy cows during early lactation. Journal of dairy science. 2019 Apr 1;102(4):3556-68.

Weinstock GM. Genomic approaches to studying the human microbiota. Nature. 2012 Sep;489(7415):250.

Weitkunat K, Schumann S, Nickel D, Hornemann S, Petzke KJ, Schulze MB, Pfeiffer AF, Klaus S. Odd-chain fatty acids as a biomarker for dietary fiber intake: a novel pathway for endogenous production from propionate. The American journal of clinical nutrition. 2017 Apr 19;105(6):1544-51.

Weitkunat K, Schumann S, Nickel D, Hornemann S, Petzke KJ, Schulze MB, Pfeiffer AF, Klaus S. Odd-chain fatty acids as a biomarker for dietary fiber intake: a novel pathway for endogenous production from propionate. The American journal of clinical nutrition. 2017 Apr 19;105(6):1544-51.

Wieckowska A, Papouchado BG, Li Z, Lopez R, Zein NN, Feldstein AE. Increased hepatic and circulating interleukin-6 levels in human nonalcoholic steatohepatitis. The American journal of gastroenterology. 2008 Jun;103(6):1372.

Wigg AJ, Roberts-Thomson IC, Dymock RB, McCarthy PJ, Grose RH, Cummins AG. The role of small intestinal bacterial overgrowth, intestinal permeability, endotoxaemia, and tumour necrosis factor α in the pathogenesis of non-alcoholic steatohepatitis. Gut. 2001 Feb 1;48(2):206-11.

Wilson CG, Tran JL, Erion DM, Vera NB, Febbraio M, Weiss EJ. Hepatocyte-specific disruption of CD36 attenuates fatty liver and improves insulin sensitivity in HFD-fed mice. Endocrinology. 2015 Dec 9;157(2):570-85.

Wong VW, Adams LA, de Lédinghen V, Wong GL, Sookoian S. Noninvasive biomarkers in NAFLD and NASH—current progress and future promise. Nature Reviews Gastroenterology & Hepatology. 2018 Aug;15(8):461-78.

Wueest S, Lucchini FC, Challa TD, Müller W, Blüher M, Konrad D. Mesenteric fat lipolysis mediates obesity-associated hepatic steatosis and insulin resistance. Diabetes. 2016 Jan 1;65(1):140-8.

Xiao L, Sonne SB, Feng Q, Chen N, Xia Z, Li X, Fang Z, Zhang D, Fjære E, Midtbø LK, Derrien M. High-fat feeding rather than obesity drives taxonomical and functional changes in the gut microbiota in mice. Microbiome. 2017 Dec;5(1):43.

Xu H, Uysal KT, Becherer JD, Arner P, Hotamisligil GS. Altered tumor necrosis factor-α (TNF-α) processing in adipocytes and increased expression of transmembrane TNF-α in obesity. Diabetes. 2002 Jun 1;51(6):1876-83.

Y.S. Lee, Y. Cho, M.J. Shin Dietary very long chain saturated fatty acids and metabolic factors: findings from the Korea National Health and nutrition examination survey 2013

Yamaguchi K, Itoh Y, Yokomizo C, Nishimura T, Niimi T, Fujii H, Okanoue T, Yoshikawa T. Blockade of interleukin-6 signaling enhances hepatic steatosis but improves liver injury in methionine choline-deficient diet-fed mice. Laboratory investigation. 2010 Aug;90(8):1169.

Yang SQ, Lin HZ, Lane MD, Clemens M, Diehl AM. Obesity increases sensitivity to endotoxin liver injury: implications for the pathogenesis of steatohepatitis. Proceedings of the National Academy of Sciences. 1997 Mar 18;94(6):2557-62.

Yang WS, Chen PC, Hsu HC, Su TC, Lin HJ, Chen MF, Lee YT, Chien KL. Differential effects of saturated fatty acids on the risk of metabolic syndrome: A matched case-control and meta-analysis study. Metabolism. 2018 Jun 1; 83:42-9.

Yatsunenko T, Rey FE, Manary MJ, Trehan I, Dominguez-Bello MG, Contreras M, Magris M, Hidalgo G, Baldassano RN, Anokhin AP, Heath AC. Human gut microbiome viewed across age and geography. nature. 2012 Jun;486(7402):222.

Yoo W, Gjuka D, Stevenson HL, Song X, Shen H, Yoo SY, Wang J, Fallon M, Ioannou GN, Harrison SA, Beretta L. Fatty acids in non-alcoholic steatohepatitis: Focus on pentadecanoic acid. PloS one. 2017 Dec 15;12(12): e0189965.

Younossi ZM, Koenig AB, Abdelatif D, Fazel Y, Henry L, Wymer M. Global epidemiology of nonalcoholic fatty liver disease—meta-analytic assessment of prevalence, incidence, and outcomes. Hepatology. 2016 Jul;64(1):73-84.

Younossi ZM. Non-alcoholic fatty liver disease—A global public health perspective. Journal of hepatology. 2018 Nov 9.

Yu GS, Lu YC, Gulick T. Co-regulation of tissue-specific alternative human carnitine palmitoyltransferase Iβ gene promoters by fatty acid enzyme substrate. Journal of Biological Chemistry. 1998 Dec 4;273(49):32901-9.

Yu J, Marsh S, Hu J, Feng W, Wu C. The pathogenesis of nonalcoholic fatty liver disease: interplay between diet, gut microbiota, and genetic background. Gastroenterology research and practice. 2016;2016.

Zárate R, el Jaber-Vazdekis N, Tejera N, Pérez JA, Rodríguez C. Significance of long chain polyunsaturated fatty acids in human health. Clinical and translational medicine. 2017 Dec;6(1):25.

Zelber-Sagi S, Ratziu V, Oren R. Nutrition and physical activity in NAFLD: an overview of the epidemiological evidence. World journal of gastroenterology: WJG. 2011 Aug 7;17(29):3377.

Zheng JS, Sharp SJ, Imamura F, Koulman A, Schulze MB, Ye Z, Griffin J, Guevara M, Huerta JM, Kröger J, Sluijs I. Association between plasma phospholipid saturated fatty acids and metabolic markers of lipid, hepatic, inflammation and glycaemic pathways in eight European countries: a cross-sectional analysis in the EPIC-InterAct study. BMC medicine. 2017 Dec;15(1):203.

Zhou, Liping, et al. "Effects of the dietary protein level on the microbial composition and metabolomic profile in the hindgut of the pig." Anaerobe 38 (2016): 61-69.

Zhu L, Baker RD, Baker SS. Gut microbiome and nonalcoholic fatty liver diseases. Pediatric Research. 2015 Jan;77(1-2):245.

Zhu L, Baker SS, Gill C, Liu W, Alkhouri R, Baker RD, Gill SR. Characterization of gut microbiomes in nonalcoholic steatohepatitis (NASH) patients: a connection between endogenous alcohol and NASH. Hepatology. 2013 Feb;57(2):601-9.

Zhukova NV, Novgorodtseva TP, Denisenko YK. Effect of the prolonged high-fat diet on the fatty acid metabolism in rat blood and liver. Lipids in health and disease. 2014 Dec;13(1):49.

8.0 Appendix

Table 1; Faecal sample concentration sent for 16S rRNA sequencing at Novogene Company Ltd, Cambridge, UK

#	code	ng/ µl	Volume sent-off (µl)
1	CD1	2.92	60
2	CD2	0.95	60
3	CD3	8.36	60
4	CD4	13.8	20
5	CD5	0.94	60
6	CD6	3.86	60
7	CD7	0.97	60
8	CD8	1.2	60
9	CD9	0.93	60
10	CD10	0.89	60
11	HFD1	15.4	15
12	HFD2	5.46	40
13	HFD3	5.36	40
14	HFD4	7.62	35
15	HFD5	15.1	15
16	HFD6	8.2	30
17	HFD7	4.86	40
18	HFD8	11.6	20
19	HFD9	6.38	30
20	HFD10	7.96	30

CD-Control diet, HFD-high fat diet

Table 2: RNA concentrations of Aston LPD

Diet	Date extracted	1st reading ng/ μL	2nd reading ng/ μL	3rd reading ng/ μL	Average ng/ μL
1	07/04/2017	684	677	673	678.0
1	10/04/2017	992	1009	1008	1003.0
1	10/04/2017	1261	1306	1297	1288.0
1	10/04/2017	1370	1339	1311	1340.0
1	11/04/2017	840	847	862	849.7
1	11/04/2017	878	892	891	887.0
1	11/04/2017	880	885	885	883.3
1	11/04/2017	886	899	893	892.7
1	10/04/2017	1274	1296	1289	1286.3
2	10/04/2017	1736	1779	1768	1761.0
2	10/04/2017	1402	1449	1425	1425.3
2	10/04/2017	401	401	438	413.3
2	11/04/2017	1415	1413	1429	1419.0
2	11/04/2017	1205	1209	1233	1215.7
2	11/04/2017	523	530	521	524.7
2	11/04/2017	1575	1573	1578	1575.3
2	12/04/2017	930	934	954	939.3
3	12/04/2017	998	1010	1001	1003.0
3	12/04/2017	1389	1385	1387	1387.0
3	12/04/2017	734	714	719	722.3
3	12/04/2017	988	964	963	971.7
3	12/04/2017	1558	1494	1512	1521.3
3	12/04/2017	1290	1352	1344	1328.7
3	12/04/2017	1381	1393	1354	1376.0

1-NPD, 2-LPD, 3-MD-LPD

Table 3: RNA concentrations of HFD-SPF mice

HIGH FAT DIET RNA EXTRACTION (LIVER TISSUE) 9-10OCTOBER 2018						
Sample code	Weight(mg)	Suspended in (µl)	Conc.(ng/µl)	Conc.(ng/µl)	Conc.(ng/µl)	Average(ug/µl)
CD 1	70.8	50	5664.5	5642.5	5852.4	5719.8
CD 2	63.8	50	6826.5	6752.8	6890.4	6823.233333
CD 3	98.2	50	8899.4	8278	8955.8	8711.066667
CD 4	65.4	50	6637.3	6232.9	6315.1	6395.1
CD 5	80.2	50	6308.8	5945.7	6085.3	6113.266667
CD 6	54.7	50	4627.4	4466.8	4481.9	4525.366667
CD 7	63.3	50	4654.6	4645.9	4745.7	4682.066667
CD 8	63.2	50	5035.5	5192.8	5298.2	5175.5
CD 9	52.5	50	5116.3	5227.6	4912.3	5085.4
CD 10	51.7	50	3803.6	3824.4	3845.4	3824.466667
HFD 1	77.1	50	5597.9	5597.8	5933.1	5709.6
HFD 2	56.1	50	3440.6	3550.8	3522.3	3504.566667
HDF 3	59.9	50	3710.5	3643.3	3747.6	3700.466667
HFD 4	83.7	50	5693.1	5653	5618.4	5654.833333
HFD 5	54.4	50	3043.9	3085.4	3099.1	3076.133333
HFD 6	57.4	50	3731.2	3799.9	3728	3753.033333
HFD 7	59.3	50	4366.9	4189.5	4419.3	4325.233333
HFD 8	60.8	50	4988.6	5105.2	5024.3	5039.366667
HFD 9	62.4	50	4747.4	4886.5	4835.8	4823.233333
HFD 10	52.7	50	4105.4	4094.9	4130.6	4110.3

CD-Control diet, HDF-High fat diet

Table 3b: The absolute serum fatty acid concentrations of short term HFD feeding

Serum FAs (µM)	**CD**		**HFD**		***p*-value**
	Median $\times 10^3$	Minimum $\times 10^3$	Median $\times 10^3$	Maximum $\times 10^3$	
C14:0	2.234	1.71- 3.73	1.124	0.88-1.44	0.0159
C16:0	76.31	63.73-87.09	89.97	83.17-0.10	0.0556
C18:0	18.93	15.99-21.01	46.95	34.82-52.95	0.0079
C15:0	0.34	0.30-0.44	0.26	0.19-0.28	0.0159
C17:0	0.82	0.66-0.96	0.46	0.39-0.64	0.0159
C16:1	5.66	4.82-6.65	20.50	14.90-32.45	0.0079
C18:1	95.95	70.37-109.4	54.61	45.88-65.21	0.0159
C18:2n6	79.59	63.00-85.68	78.77	62.77-89.65	>0.9999
C18:3n3	6.04	5.57-22.34	7.10	6.28-7.52	>0.9999
C20:4n6	5.66	4.24-7.10	5.63	3.22-7.57	0.8413

Table 3.2b: Absolute serum concentrations of a 12-week HFD fed mice at normal husbandry

Serum FAs (µM)	**CD**		**HFD**		***p*-value**
	Median $\times 10^3$	Minimum $\times 10^3$	Median $\times 10^3$	Maximum $\times 10^3$	
C14:0	3.239	1.96-4.11	1.31	1.21-1.59	0.0079
C16:0	87.05	77.52-93.28	96.81	92.69-99.91	0.0556
C18:0	23.97	23.21-25.74	43.54	42.49-53.14	0.0079
C15:0	0.58	0.54-0.69	0.42	0.23-0.43	0.0079
C17:0	0.78	0.61-1.03	0.78	0.72-0.82	>0.9999
C16:1	24.22	19.65-33.33	5.853	5.6-7.62	0.0079
C18:1	97.24	88.66-130.0	63.62	60.19-65.98	0.0079
C18:2n6	81.60	69.39-103.6	97.15	85.97-102.7	0.4206
C18:3n3	0.73	0.66-0.99	0.78	0.73-0.81	0.8413
C20:4n6	25.65	19.48-35.48	54.53	38.87-55.83	0.0159

Control vs HFD, n=5

Table 3.3b: Absolute serum concentrations of a 4-week HFD fed mice at SPF conditions

Serum FAs (µM)	**CD**		**HFD**		***p*-value**
	Median $\times 10^3$	Minimum $\times 10^3$	Median $\times 10^3$	Maximum $\times 10^3$	
C14:0	2.17	1.474-4.74	1.56	1.39-2.94	0.2775
C16:0	56.75	39.24-99.43	53.07	37.93-70.71	0.6607
C18:0	18.00	12.63-26.37	19.29	14.19-25.16	0.8421
C15:0	0.22	0.12-0.47	0.07	0.06-0.11	0.0006
C17:0	0.51	0.44-0.87	0.47	0.33-0.72	0.2511
C16:1	5.74	3.31-12.90	4.140	2.965-7.360	0.2110
C18:1	43.96	28.58-89.19	51.29	38.88-86.82	0.7802
C18:2n6	70.62	44.24-135.4	43.56	31.49- 73.66	0.0947
C18:3n3	0.59	0.45-1.37	0.29	0.25- 0.35	0.0003
C20:4n6	13.55	10.62-16.73	11.11	8.04-22.80	0.4470

Control vs HFD, n=10

Table 3.4b: Absolute liver concentration of a 4-week HFD fed mice at SPF conditions

Liver FAs (µM)	**CD**		**HFD**		***p*-value**
	Median $\times 10^3$	Minimum $\times 10^3$	Median $\times 10^3$	Maximum $\times 10^3$	
C14:0	1.640	1.13-2.63	2.06	1.624-2.83	0.2475
C16:0	99.76	94.61-115.4	111.5	86.85-127.4	0.6842
C18:0	37.96	36.79- 41.47	39.38	36.86- 41.50	0.5787
C15:0	0.72	0.63- 0.98	0.57	0.44-0.74	0.0630
C17:0	1.53	1.37-1.85	1.32	1.19- 1.55	0.0892
C16:1	4.76	3.65- 7.99	4.39	2.835-7.27	0.7394
C18:1	66.02	54.37-105.4	103.1	79.97-126.9	0.0753
C18:2n6	96.54	81.75-141.6	98.57	74.56-119.0	0.7394
C18:3n3	0.83	0.68- 1.35	2.11	1.38- 2.90	0.0029
C20:4n6	26.99	25.55- 30.37	30.89	28.13-34.62	0.0892

Control vs HFD, n=10